

TRANSCRIPTOME ANALYSIS OF *THERMOPLASMA VOLCANIUM* GSS1  
UNDER EXTREME STRESS

A THESIS SUBMITTED TO  
THE GRADUATE SCHOOL OF NATURAL AND APPLIED SCIENCES  
OF  
MIDDLE EAST TECHNICAL UNIVERSITY

BY

SEMA ZABCI

IN PARTIAL FULFILLMENT OF THE REQUIREMENTS  
FOR  
THE DEGREE OF MASTER OF SCIENCE  
IN  
BIOLOGY

FEBRUARY 2015



Approval of the thesis:

**TRANSCRIPTOME ANALYSIS OF *THERMOPLASMA VOLCANIUM* GSS1  
UNDER EXTREME STRESS**

Submitted by **SEMA ZABCI** in partial fulfillment of the requirements for the degree  
of **Master of Science in Biology Department, Middle East Technical University**  
by,

Prof. Dr. Gülbin Dural Ünver  
Dean, Graduate School of **Natural and Applied Sciences**

\_\_\_\_\_

Prof. Dr. Orhan Adalı  
Head of Department, **Biology**

\_\_\_\_\_

Prof. Dr. Semra Kocabıyık  
Supervisor, **Biology Department, METU**

\_\_\_\_\_

**Examining Committee Members:**

Prof. Dr. Emel Arınç  
Biology Dept., METU

\_\_\_\_\_

Prof. Dr. Semra Kocabıyık  
Biology Dept., METU

\_\_\_\_\_

Prof. Dr. Meral Yücel  
Biology Dept., METU

\_\_\_\_\_

Prof. Dr. Fatih İzgü  
Biology Dept., METU

\_\_\_\_\_

Prof. Dr. Rıza Durmaz  
Medical Microbiology Dept., Yıldırım Beyazıt University

\_\_\_\_\_

**Date:** 06.02.2015

\_\_\_\_\_

**I hereby declare that all information in this document has been obtained and presented in accordance with academic rules and ethical conduct. I also declare that, as required by these rules and conduct, I have fully cited and referenced all material and results that are not original to this work.**

Name, Last name: Sema ZABCI

Signature:

## ABSTRACT

### TRANSCRIPTOME ANALYSIS OF *THERMOPLASMA VOLCANIUM* GSS1 UNDER EXTREME STRESS

Zabcı, Sema  
M.S., Department of Biology  
Supervisor: Prof. Dr. Semra Kocabıyık  
February 2015, 165 pages

In this study, to provide new insight into anti-stress mechanisms in archaea, we have carried out genome wide transcriptome analysis of *Thermoplasma volcanium* under severe stress conditions (*i.e.*, heat- shock at 68 °C, sub-lethal and lethal oxidative stress and pH stress at pH 5.0) using whole genome gene expression microarray. The change in the gene expression profile in response to three stressors indicated retardation of cell growth accompanied by down regulation of genes involved in essential cellular processes such as translation, transcription, cell motility, and energy metabolism. In addition, heat- shock resulted in the increased transcription level of genes encoding heat shock proteins (*e.g.*, GroEL, GrpE, DnaK, and DnaJ). The highest number of up-regulated genes was recorded upon pH stress. pH stress response in *T.volcanium* was characterized by activation of several transporter gene products, which are crucial for maintaining intracellular pH homeostasis. Oxidative stress triggered mostly down regulation of gene expression. Up regulation of oxidoreductases, Fe-S oxidoreductases, aldo/keto reductases, and dehydrogenases as a response to oxidative stress provoked by H<sub>2</sub>O<sub>2</sub> can be important for maintaining intracellular redox potential and detoxification of free radicals. On the other hand, activation of the carbohydrate metabolism and transport, as well as some transcriptional regulators was detected in response to three stress signals. The verification of the microarray data with qRT-PCR showed good agreement between results of the two techniques.

Keywords: Archaea, transcriptomics, heat stress, *Thermoplasma volcanium*, stress response

## ÖZ

### ***THERMOPLASMA VOLCANIUM* GSS1'İN EKSTREM STRES ALTINDA TRANSKRİPTOM ANALİZİ**

Zabcı, Sema  
Yüksek Lisans, Biyoloji Bölümü  
Tez Yöneticisi: Prof. Dr. Semra Kocabıyık  
Şubat 2015, 165 Sayfa

Bu çalışmada, arkeabakterilerde stres karşıtı mekanizmaları anlamak için, *Thermoplasma volcanium*'da ağır stres koşulları altında ( ısı stresi 68 °C, oksidatif stres ve pH5.0' te pH stresi) genom boyuntunda transkriptom analizi, tüm genom gen ekspresyon mikrodizinleri kullanılarak yürütülmüştür. Üç stresöre tepki olarak deęişen gen anlatım profile, protein sentezi, gen yazılımı, hücre hareketi ve enerji metabolizması gibi önemli hücresel süreçlerde yer alan genlerin anlatımının azalmasına baęlı olarak hücre gelişiminin yavaşladığını göstermiştir. Buna ek olarak ısı şoku, ısı şoku proteinlerini (örneğin, GroEL, GrpE, DnaK, and DnaJ) kodlayan genlerin transkripsiyon düzeylerinin artmasına neden olmuştur. En fazla sayıda ekspresyonu artan gen sayısı pH stresi sırasında kaydedilmiştir. *T.volcanium*'un pH stres tepkisi, ürünleri hücre içi pH homeostazını sürdürmek için çok önemli olan birçok taşıyıcı geninin indüklenmesi ile tanımlanmıştır. Oksidatif stres genellikle gen anlatımının azalmasını tetiklemiştir. Oksidoredüktazlar, Fe-S oksidoredüktazlar, aldo/keto redüktazlar ve dehidrogenazların yüksek miktarda üretimi H<sub>2</sub>O<sub>2</sub> 'in neden olduğu oksidatif strese tepki olarak, hücre içi redoks potansiyellerini devam ettirmek ve serbest radikallerin detoksifikasyonu için önemli olabilir. Diğer taraftan, üç stres sinyaline tepki olarak, bazı transkripsiyon düzenleyicileri ile karbonhidrat metabolizması ve transportun aktivasyonu da saptanmıştır. Mikrodizin verilerinin qRT-PCR ile doğrulama çalışması, her iki teknikle elde edilen sonuçların uyuştuğunu göstermiştir.

Anahtar kelimeler: Arkeabakteri, transkriptomik, ısı şoku, *Thermoplasma volcanium*, stres tepkisi

To My Parents,

## ACKNOWLEDGMENTS

I would like to express my deep appreciation and respect to my supervisor, Prof. Dr. Semra Kocabıyık for her ceaseless support, encouragement, continued guidance, and patience during my research in our laboratory. It has been a tremendous chance for me to have an advisor like her who taught me not only how to carry out academic research, but also hardworking and using time efficiently. I am also thankful for her guidance during writing of my thesis and providing invaluable comments and revisions. Her strong scientific knowledge, as well as her compassion and respect for others have been a major factor to pursue my academic career in the same field, and carry out Ph.D. study under her supervision. In the future, I would like to be a competent scientist like my supervisor.

I am really indebted to Prof. Dr. Emel Arınç, who believed in my enthusiasm from the very beginning. Her wonderful instructions in the course of Molecular Pharmacology enriched my academic background. I would like to also extend my thanks to her for introducing me my current advisor.

My sincere thanks are also to the committee members, Prof. Dr. Emel Arınç, Prof. Dr. Meral Yücel, Prof. Dr. Fatih İzgü, and Prof. Dr. Rıza Durmaz for their suggestions and critical comments

I would like to thank my great roommate Shahrzad Nikghadam for her kindness and continuous effort for creating a happy and warm atmosphere in our room in dormitory.

My special thanks are to my lab partner Muazzez Çelebi for her assistance and help whenever I needed.

I would like to mention my warmest appreciation to my great friends Seda Çepkenlioğlu, S.Tutku Yıldırım, Dilara Fidan, Reyhan Yaka, Begümhan Yılmaz, Elbay Malikmammadov for their friendships, motivations, who shared many happy and memorable moments with me.

I owe more than thanks to my family members. I am deeply grateful to my mother, Sevil Zabcı, my father, Kadir Zabcı, my uncle, Osman Zabcı and my brother Ertuğrul Zabcı for their love, support and continue encouragement throughout my life. My special thanks are to my dear uncle Assoc. Doc. Dr. Selami Günel for encouraging me for graduate study in METU.

I would like to thank Turkish Scientific and Technical Research Council (TÜBİTAK) (KBAG 113T085) and METU-BAP (BAP-07-02-2014-007-039) for the grants and fellowship to support this work.

## TABLE OF CONTENTS

ABSTRACT .....	v
ÖZ.....	vi
ACKNOWLEDGMENTS.....	viii
TABLE OF CONTENTS .....	x
LIST OF TABLES .....	xv
LIST OF FIGURES.....	xvii
LIST OF ABBREVIATIONS .....	xxi
CHAPTERS	
1. INTRODUCTION .....	1
1.1. Cellular Stress Response .....	1
1.2. Heat-Shock Response and Heat Shock Proteins .....	5
1.2.1. Regulation of Heat- Shock Genes.....	6
1.3. pH Stress .....	8
1.3.1. Adaptive Mechanisms Against Acid Stress.....	8
1.3.2. Adaptive Mechanisms Against Alkaline Stress.....	11
1.4. Cellular Response to Oxidative Stress .....	14
1.5. Life in Hot Acid Environment .....	17
1.5.1. Survival Strategies of Microorganisms in Hot Acidic Niches.....	18
1.6. Stress in <i>Archaea</i> .....	19
1.6.1. Heat Stress in <i>Archaea</i> .....	20
1.6.1.1. Role of Chaperones in Heat- Shock Response in <i>Archaea</i> .....	20
1.6.1.2. Additional Mechanisms for Heat Response in <i>Archaea</i> .....	25
1.6.1.2.1. Protein Degradation.....	25

1.6.1.2.2.	Resistance to Heat Stress via Cell Membrane.....	25
1.6.1.3.	Heat- Shock Response in Different <i>Archaeal</i> Species.....	26
1.6.2.	pH Stress in <i>Archaea</i> .....	28
1.6.2.1.	Acid Stress in <i>Archaea</i> .....	28
1.6.2.2.	Alkaline Stress in <i>Archaea</i> .....	29
1.6.2.3.	Acid /Alkaline Stress Response in Different <i>Archaeal</i> Species.....	30
1.6.3.	Oxidative Stress in <i>Archaea</i> .....	30
1.6.3.1.	Oxidative Stress Response in Different <i>Archaeal</i> Species.....	32
1.6.4.	Other Stresses in <i>Archaea</i> .....	33
1.6.4.1.	Cold Stress in <i>Archaea</i> .....	33
1.6.4.1.1.	Cold-Stress Response in Different <i>Archaeal</i> species.....	34
1.6.4.2.	Osmotic Stress in <i>Archaea</i> and Adaptive Responses.....	36
1.6.4.2.1.	Osmotic Stress Response in Different <i>Archaeal</i> species.....	37
1.6.4.3.	$\gamma$ Gamma Radiation in <i>Archaea</i> .....	38
1.6.4.4.	$\gamma$ Gamma Radiation Resistance in <i>Archaea</i> .....	39
1.7.	Model Organism.....	39
1.8.	Microarray Technology.....	41
1.9.	Aim.....	44
2.	<b>MATERIALS AND METHODS</b> .....	45
2.1.	Materials.....	45
2.1.1.	Chemicals, Enzymes and Kits.....	45
2.1.2.	Buffer Solutions.....	45
2.2.	Media and Culturing Conditions.....	45
2.3.	Growth Under Stress Conditions.....	46
2.4.	Methodology.....	46

2.4.1. RNA Extraction.....	46
2.5. RNA Denaturing Agarose Gel Electrophoresis and Visualization .....	47
2.6. RNA Quality and Quantity Measurements .....	48
2.6.1. Determination of RNA Concentration by Pico Drop.....	48
2.6.2. Qualitative and Quantitative Analysis of RNA Samples by Agilent 2100 Bioanalyzer.....	48
2.7. Microarray .....	49
2.7.1. Array Design and Printing.....	49
2.7.2. cDNA Synthesis, Labelling and Hybridization.....	50
2.7.3. Slide Scanning, Feature Detection and Normalization.....	51
2.7.4. Microarray Data Processing.....	51
2.8. Real Time Quantitative RT- PCR.....	53
2.8.1. First Strand cDNA Synthesis.....	53
2.8.2. Real Time PCR.....	55
3. RESULTS AND DISCUSSION.....	57
3.1. Determination of Growth Restrictive Parameters for Transcriptional Profiling.....	57
3.2. Quantity and Quality Measurements of Isolated RNA Samples .....	60
3.2.1. Pico Drop Measurements.....	60
3.2.1.1. RNA from Untreated Cultures (Controls).....	60
3.2.1.2. RNA from Heat Stress Groups (68°C).....	61
3.2.1.3. RNA from pH Stress Groups ( pH 4.0 and pH 5.0).....	61
3.2.1.4. RNA from Hydrogen Peroxide Treated Groups (0.02 mM and 0.03 mM H <sub>2</sub> O <sub>2</sub> ) .....	62
3.2.2. RNA Quality Assessment.....	63
3.2.2.1. Bioanalyzer Measurements.....	63

3.2.2.2.	Agarose Gel Electrophoresis of RNA.....	68
3.3.	Genome Wide Transcriptional Profiling Under Extreme Stress Conditions.....	71
3.3.1.	Raw Microarray Images.....	71
3.3.2.	Data Pre-Processing .....	72
3.3.2.1.	Normalization & Quality Control.....	72
3.3.3.	Differential Expression of Genes Under The Extreme Heat, pH and Oxidative Stress Conditions .....	79
3.3.3.1.	Genes Responsive to The Heat Shock.....	80
3.3.3.2.	Genes Responsive to pH Stress.....	87
3.3.3.3.	Genes Responsive to Oxidative Stress.....	93
3.3.3.3.1.	Genes Responsive to Mild Oxidative Stress (0.02 mM H <sub>2</sub> O <sub>2</sub> ).....	94
3.3.3.3.2.	Genes Responsive to Lethal Oxidative stress (0.03 mM H <sub>2</sub> O <sub>2</sub> ).....	100
3.3.4.	Comparison of Gene Regulation among Heat Shock, Oxidative Stress and pH Stress Groups .....	108
3.4.	Verification of Microarray Results by qRT-PCR.....	115
3.4.1.	Absolute Quantification of Expression of TVN0830 Gene Under Heat Shock, pH Stress and Oxidative Stress.....	116
3.4.2.	Absolute Quantification of Expression of TVN1426 Gene Under Heat Shock, pH Stress and Oxidative Stress .....	119
3.4.3.	Absolute Quantification of Expression of TVN1285 Gene Under Heat Shock, pH Stress and Oxidative Stress.....	120
3.4.4.	Absolute Quantification of Expression of TVN1343 Gene Under Heat Shock, pH Stress and Oxidative Stress.....	120
3.4.5.	Absolute Quantification of Expression of TVN0401 Gene Under Heat Shock, pH Stress and Oxidative Stress.....	121
3.4.6.	Absolute Quantification of Expression of TVN0835 Gene Under Heat Shock, pH Stress and Oxidative Stress.....	122

3.4.7. Absolute Quantification of Expression of TVN1390 Gene Under Heat Shock, pH Stress and Oxidative Stress .....	123
3.4.8. Absolute Quantification of Expression of TVN1600 Gene Under Heat Shock, pH Stress and Oxidative Stress .....	123
3.4.9. Absolute Quantification of Expression of TVN0021 Gene Under Heat Shock, pH Stress and Oxidative Stress .....	125
3.4.10. Absolute Quantification of Expression of TVN0123 Gene Under Heat Shock, pH Stress and Oxidative Stress .....	125
3.4.11. Absolute Quantification of Expression of TVN1392 Gene Under Heat Shock, pH Stress and Oxidative Stress .....	126
3.4.12. Absolute Quantification of Expression of TVN1466 Gene Under Heat Shock, pH Stress and Oxidative Stress .....	126
3.4.13. Absolute Quantification of Expression of TVN1284 Gene Under Heat Shock, pH Stress and Oxidative Stress .....	128
3.4.14. Absolute Quantification of Expression of TVN0932 Gene Under Heat Shock, pH Stress and Oxidative Stress .....	128
3.4.15. Absolute Quantification of Expression of TVN0164 Gene Under Heat Shock, pH Stress and Oxidative Stress .....	129
3.4.16. Absolute Quantification of Expression of TVN0167 Gene Under Heat Shock, pH Stress and Oxidative Stress .....	130
3.4.17. Absolute Quantification of Expression of TVN0570 Gene Under Heat Shock, pH Stress and Oxidative Stress .....	130
3.4.18. Absolute Quantification of Expression of TVN0875 Gene Under Heat Shock, pH Stress and Oxidative Stress .....	132
4. CONCLUSION .....	133
REFERENCES .....	137
APPENDICES .....	147
A. BUFFER SOLUTIONS AND COMPOSITIONS .....	147
B. MICROARRAY DATA SETS.....	149
C. AMPLIFICATION AND MELTING CURVES.....	159

## LIST OF TABLES

### TABLES

Table 1. 1. The Universal Stress Proteins .....	2
Table 2. 1. Gene specific forward primers (Fp) .....	54
Table 2. 2. Gene specific reverse primers (Rp).....	54
Table 3. 1. Concentrations of total RNA isolated from control groups .....	60
Table 3. 2. Concentration of total RNA isolated from heat shock groups .....	61
Table 3. 3. Concentration of total RNA isolated from pH stress groups .....	61
Table 3. 4. Concentration of total RNA samples isolated from supplemented cultures .....	62
Table 3. 5. Selected RNA samples for microarray analysis.....	70
Table 3. 6. Pairwise correlation coefficients between arrays. Correlation coefficients for each pair of arrays are listed in textual form. ....	74
Table 3. 7. Functional categorization of up regulated <i>Thermoplasma volcanium</i> genes upon heat shock.....	83
Table 3. 8. Functional categorization of the repressed genes upon heat shock .....	86
Table 3. 9. Functional categorization of the induced genes upon pH stress .....	90
Table 3. 10. Functional categorization of repressed genes upon pH stress.....	92
Table 3. 11. Functional categorization of the induced genes upon 0.02 mM oxidative stress.....	97
Table 3. 12. Functional categorization of the repressed genes upon 0.02 mM oxidative stress .....	99
Table 3. 13. Functional categorization of the induced genes upon 0.03 mM H <sub>2</sub> O <sub>2</sub>	103
Table 3. 14. Functional categorization of the repressed genes by 0.03 mM H <sub>2</sub> O <sub>2</sub> .	106
Table 3. 15. Overlapping genes differentially expressed under heat shock and two oxidative stresses.....	110
Table 3. 16. Overlapping genes differentially expressed under pH stress and lethal oxidative stress (0.03 mM H <sub>2</sub> O <sub>2</sub> ) data sets.....	111

Table 3. 17. Overlapping genes differentially expressed under pH stress and two oxidative stress data sets .....	111
Table 3. 18. Overlapping genes differentially expressed under heat shock and lethal oxidative stress groups .....	112
Table 3. 19. Overlapping genes differentially expressed under mild and lethal oxidative stress groups .....	114
Table 3. 20. Analysis of differential expression of selected genes under heat shock by qRT-PCR.....	117
Table 3. 21. Analysis of differential expression of selected genes under pH stress by qRT-PCR.....	117
Table 3. 22. Analysis of differential expression of selected genes under oxidative stress (0.03 mM H <sub>2</sub> O <sub>2</sub> ) by qRT-PCR .....	118
Table B. 1. Up regulated genes upon heat shock .....	149
Table B. 2. Down regulated genes upon heat shock .....	150
Table B. 3. Up regulated genes upon pH stress .....	151
Table B. 4. Down regulated genes upon pH stress.....	152
Table B. 5. Up regulated genes upon 0.02 mM H <sub>2</sub> O <sub>2</sub> .....	152
Table B. 6. Repressed genes genes upon 0.02 mM H <sub>2</sub> O <sub>2</sub> .....	154
Table B. 7. Up regulated genes 0.03 mM H <sub>2</sub> O <sub>2</sub> .....	155
Table B. 8. Repressed genes genes upon 0.03 mM H <sub>2</sub> O <sub>2</sub> .....	157

## LIST OF FIGURES

### FIGURES

Figure 1. 1. Diverse sets of stress signals and their effects on cell metabolism..	4
Figure 1. 2. Regulation of the $\sigma^s$ synthesis and proteolysis in response to the diverse signals.....	4
Figure 1. 3. Regulation of HSF1 in eukaryotic cells.....	7
Figure 1. 4. Overview of pH homeostasis in acidophiles. ....	9
Figure 1. 5. Superoxide and hydrogen peroxide detoxification.....	15
Figure 1. 6. Activation of OxyR. . ....	16
Figure 1. 7. Folding in the GroEL- GroES chaperonin system.....	22
Figure 1. 8. Action of protein refolding with sHSPs. ....	23
Figure 1. 9. Thin section of <i>Thermoplasma volcanium</i> . ....	40
Figure 1. 10. General cycle of oligo synthesis via phosphoramidite chemistry .....	43
Figure 2. 1. Setting up the Chip Priming Station. ....	48
Figure 2. 2. Workflow for microarray processing.....	52
Figure 3. 1. Growth curves of <i>Thermoplasma Volcanium</i> GSS1 strain grow in optimum temperature and suboptimal temperatures 65°C and 68°C.....	57
Figure 3. 2. Growth curves of <i>Thermoplasma Volcanium</i> GSS1 strain grow in optimum pH (2.59) and suboptimal pH values (pH 4.0; pH 5.08) at 60°C. ....	58
Figure 3. 3. Growth curves of <i>Thermoplasma volcanium</i> GSS1 strain in liquid volcanium medium supplemented with 0.03 mM, 0.04 mM and 0.05 mM H <sub>2</sub> O <sub>2</sub> ...	59
Figure 3. 4. Agilent 2100 Bioanalyzer gel like image of first sample set. ....	63
Figure 3. 5. Bioanalyzer electropherograms of RNA samples used in microarray....	64
Figure 3. 6. Agilent 2100 Bioanalyzer gel like image of second sample set. ....	65
Figure 3. 7. Bioanalyzer electropherograms of RNA samples used in microarray..	66
Figure 3. 8. Agilent 2100 Bioanalyzer gel like image of final sample set. ....	67
Figure 3. 9. Bioanalyzer electropherograms of RNA samples used in microarray....	67
Figure 3. 10. Denaturing agarose gel electrophoresis of RNA samples. ....	68

Figure 3. 11. Denaturing agarose gel electrophoresis of RNA samples. ....	68
Figure 3. 12. Denaturing agarose gel electrophoresis of RNA samples. ....	69
Figure 3. 13. Denaturing agarose gel electrophoresis of RNA samples.. ....	69
Figure 3. 14. Illustration of a raw microarray image from 8x60K earrays. ....	71
Figure 3. 15. Box whisker plot of normalized values of the series US11073878 ( samples plus controls) using RMA algorithm. ....	73
Figure 3. 16. Representation of correlation coefficients in a visual form as a correlation plot. ....	75
Figure 3. 17. 3D PCA plot of the normalized signal values of the samples in different conditions. ....	75
Figure 3. 18. Histograms for control and different conditions' data sets. ....	76
Figure 3. 19. Scatter plot for different conditions' data set. ....	77
Figure 3. 20. Volcano plot for different conditions' data sets. ....	78
Figure 3. 21. Differential expression of annotated genes out of 1474 <i>Tpv</i> genes under extreme stress condition. ....	79
Figure 3. 22. Cluster analysis of heat-shock dataset. ....	87
Figure 3. 23. Cluster analysis of pH stress dataset. ....	93
Figure 3. 24. Cluster analysis of Oxi002 stress dataset. ....	100
Figure 3. 25. Cluster analysis of Oxi003 stress dataset. ....	108
Figure 3. 26. Venn diagram generated from all data sets. ....	109
Figure 3. 27. Changes in the abundance of mRNA level of TVN0830 during heat shock, pH stress, oxidative stress. ....	116
Figure 3. 28. Changes in the abundance of mRNA level of TVN1426 during heat shock, pH stress, oxidative stress.. ....	119
Figure 3. 29. Changes in the abundance of mRNA level of TVN1285 during heat shock, pH stress, oxidative stress. ....	120
Figure 3. 30. Changes in the abundance of mRNA level of TVN1343 during heat shock, pH stress, oxidative stress.. ....	121
Figure 3. 31. Changes in the abundance of mRNA level of TVN0401 during heat shock, pH stress, oxidative stress.. ....	122
Figure 3. 32. Changes in the abundance of mRNA level of TVN0835 during heat shock, pH stress, oxidative stress. ....	123

Figure 3. 33. Changes in the abundance of mRNA level of TVN1390 during heat shock, pH stress, oxidative stress.....	124
Figure 3. 34. Changes in the abundance of mRNA level of TVN1600 during heat shock, pH stress, oxidative stress.....	124
Figure 3. 35. Changes in the abundance of mRNA level of TVN0021 during heat shock, pH stress, oxidative stress.....	125
Figure 3. 36. Changes in the abundance of mRNA level of TVN0123 during heat shock, pH stress, oxidative stress.....	126
Figure 3. 37. Changes in the abundance of mRNA level of TVN1392 during heat shock, pH stress, oxidative stress.....	127
Figure 3. 38. Changes in the abundance of mRNA level of TVN1466 during heat shock, pH stress, oxidative stress.....	127
Figure 3. 39. Changes in the abundance of mRNA level of TVN1284 during heat shock, pH stress, oxidative stress.....	128
Figure 3. 40. Changes in the abundance of mRNA level of TVN0932 during heat shock, pH stress, oxidative stress.....	129
Figure 3. 41. Changes in the abundance of mRNA level of TVN0164 during heat shock, pH stress, oxidative stress.....	130
Figure 3. 42. Changes in the abundance of mRNA level of TVN0167 during heat shock, pH stress, oxidative stress.....	131
Figure 3. 43. Changes in the abundance of mRNA level of TVN0570 during heat shock, pH stress, oxidative stress.....	131
Figure 3. 44. Changes in the abundance of mRNA level of TVN0875 during heat shock, pH stress, oxidative stress.....	132
Figure C. 1. Real time PCR amplification and melting curves for TVN0830 gene under heat shock, pH stress and oxidative stress. ....	159
Figure C. 2 Real time PCR amplification and melting curves for TVN1426 gene under heat shock, pH stress and oxidative stress.. ....	159
Figure C. 3. Real time PCR amplification and melting curves for TVN1285 gene under heat shock, pH stress and oxidative stress. ....	160
Figure C. 4. Real time PCR amplification and melting curves for TVN1343 gene under heat shock, pH stress and oxidative stress. ....	160

Figure C. 5. Real time PCR amplification and melting curves for TVN0401 gene under heat shock, pH stress and oxidative stress. ....	160
Figure C. 6. Real time PCR amplification and melting curves for TVN0835 gene under heat shock, pH stress and oxidative stress. ....	161
Figure C. 7. Real time PCR amplification and melting curves for TVN1390 gene under heat shock, pH stress and oxidative stress. ....	161
Figure C. 8. Real time PCR amplification and melting curves for TVN1600 gene under heat shock, pH stress and oxidative stress. ....	161
Figure C. 9. Real time PCR amplification and melting curves for TVN0021 gene under heat shock, pH stress and oxidative stress. ....	162
Figure C. 10. Real time PCR amplification and melting curves for TVN0123 gene under heat shock, pH stress and oxidative stress. ....	162
Figure C. 11. Real time PCR amplification and melting curves for TVN1392 gene under heat shock, pH stress and oxidative stress. ....	162
Figure C. 12. Real time PCR amplification and melting curves for TVN1466 gene under heat shock, pH stress and oxidative stress. ....	163
Figure C. 13. Real time PCR amplification and melting curves for TVN1284 gene under heat shock, pH stress and oxidative stress. ....	163
Figure C. 14. Real time PCR amplification and melting curves for TVN0932 gene under heat shock, pH stress and oxidative stress. ....	163
Figure C. 15. Real time PCR amplification and melting curves for TVN0164 gene under heat shock, pH stress and oxidative stress. ....	164
Figure C. 16. Real time PCR amplification and melting curves for TVN0167 gene under heat shock, pH stress and oxidative stress. ....	164
Figure C. 17. Real time PCR amplification and melting curves for TVN0570 gene under heat shock, pH stress and oxidative stress. ....	164
Figure C. 18. Real time PCR amplification and melting curves for TVN0875 gene under heat shock, pH stress and oxidative stress. ....	165

## LIST OF ABBREVIATIONS

*Tpv*: *Thermoplasma volcanium*

FC: Fold Change

qRT-PCR: quantitative Reverse Transcriptase Polymerase Chain Reaction

T<sub>m</sub>: Melting Temperature

C<sub>p</sub>: Crossing point PCR-cycle

ROS: Reactive Oxygen Species

HSP: Heat-Shock Protein

PCA: Principle Component Analysis

RIN: RNA Integrity Number

DEPC: Diethylpyrocarbonate



## CHAPTER 1

### INTRODUCTION

Stress is an immediate environmental change that leads to damage at molecular, cellular and organismal level (Söti *et al.*, 2007). All form of life can be subjected to stress if the conditions in which they normally sustain their life are drastically changed. Microorganisms have a variety of adaptive mechanisms for maintenance of their existence under fluctuating and most often stressful environmental conditions (Vorob'eva *et al.*, 2013). As a response to diverse sets of stresses, damage in macromolecules mainly proteins, DNA, and lipids occur and organisms develop different strategies in order to prevent such damaging effects of stress.

#### 1.1. Cellular Stress Response

Cellular stress response is a mechanism that is considered as a defense mechanism of cells to respond against stress. Cellular mechanisms are induced by sensing the stress based on macromolecular damage predominantly DNA and protein damage (Kültz, 2005). The latter, leads to unfolding and aggregation of the proteins, and if the stress is intense or long lasting, irreversible precipitates form that impair cell physiology and may even cause cell death.

Stressors are of diverse nature: high/low temperatures, pH, osmolarity changes, pressure shifts, and presence of toxic metal compounds, *etc.* (Sadhale *et al.*, 2007). The common effect of stressors is to alter intracellular homeostasis of the cell. The organisms have developed different ways to cope with a disruption in homeostasis for survival under stress. For example, temporary modifications in gene expression, as well as altering cellular structure and function. Therefore, coping with stress and improving defense mechanisms are indispensable for survival and longevity of the cell. Otherwise, if damage overweighs the tolerance to stress, it compromises the proper functioning of the cell, and almost certainly disrupts cell physiology resulting

in cell death. In this context, all organisms possess stress proteins and “universally stress proteins” are termed as minimal stress proteome (Table 1.1). They highlight important points of cellular stress response, including mechanism for sensing damage on macromolecules, regulation of cell cycle and energy metabolism, redox homeostasis, and repair of damaged macromolecules by chaperone systems (Kültz, 2005).

**Table 1. 1. The Universal Stress Proteins (from Kültz, 2005).**

Redox regulation	DNA damage sensing/repair	Fatty acid/lipid metabolism
Aldehyde reductase	MutS/MSH	Long-chain fatty acid ABC transporter
Glutathione reductase	MutL/MLH	Multifunctional beta oxidation protein
Thioredoxin	Topoisomerase I/III	Long-chain fatty acid CoA ligase
Peroxiredoxin	RecA/Rad51	
Superoxide dismutase		
MsrA/PMSR	<b>Molecular chaperones</b>	<b>Energy metabolism</b>
SeiB	Petidyl-prolyl isomerase	Citrate synthase (Krebs cycle)
Proline oxidase <sup>a</sup>	DnaJ/HSP40	Ca <sup>2+</sup> /Mg <sup>2+</sup> -transporting ATPase <sup>b</sup>
Quinone oxidoreductase <sup>c</sup>	GrpE (HSP70 cofactor)	Ribosomal RNA methyltransferase <sup>d</sup>
NADP-dependent oxidoreductase YMN1 <sup>c</sup>	HSP60 chaperonin <sup>d</sup>	Enolase (glycolysis)
Putative oxidoreductase YIM4 <sup>c</sup>	DnaK/HSP70	Phosphoglucomutase
Aldehyde dehydrogenase <sup>c</sup>		
Isocitrate dehydrogenase <sup>c</sup>	<b>Protein degradation</b>	<b>Other functions</b>
Succinate semialdehyde dehydrogenase <sup>c</sup>	FtsH/proteasome-regulatory subunit <sup>d</sup>	Inositol monophosphatase <sup>b</sup>
6 phosphogluconate dehydrogenase <sup>c</sup>	Lon protease/protease La	Nucleoside diphosphate kinase <sup>e</sup>
Glycerol-3-phosphate dehydrogenase <sup>c</sup>	Serine protease	Hypothetical protein YKP1
2-hydroxyacid dehydrogenase <sup>c</sup>	Protease II/prolyl endopeptidase	
Hydroxyacylglutathione hydrolase	Aromatic amino acid aminotransferase	
	Aminobutyrate aminotransferase	

Furthermore, stress proteins are highly conservative, and present in three kingdoms of life. In this respect, they are significant for understanding molecular mechanisms of cellular adaptation to stress (Söti *et al.*, 2007).

Responses to the stress can be different from one organism to another. Also, defense mechanisms against stress may vary depending on the type of stressors (Sadhale *et al.*, 2007).

The microorganisms deal with the environmental challenges via specific stress response and general stress response mechanisms. In bacterial cells, a single type of stressor usually triggers specific stress response. This response enables the elimination of the stress agent, as well as, repair of the stress-induced damage. For example, in response to the oxidative stress, stress specific responses are activated in order to eliminate reactive oxygen species and repair damage at the DNA, proteins and membrane (Hengge, 2011).

Unlike specific stress response, general stress response is evoked by many different stress signals. General stress response display prevention of the damage rather than repair (Hengge-Aronis, 2002). This response in bacteria revealed is an immediate and sustained adaptation to a variety of stressors. Adaptive strategies employed against multiple stressors involve changing cellular physiology, morphology, membrane composition and DNA supercoiling (Jones, 2012).

In *E.coli* and related proteobacteria, general stress response generally regulated by the master regulator, RpoS ( $\sigma^S$ ) that is a sigma subunit of RNA polymerase. It is established that expression of this gene is induced in response to severe stresses (*i.e.*, sudden starvation, osmotic changes, acidic pH, and suboptimal temperatures) (Hengge-Aronis, 2002). After the accumulation of this sigma factor in *E.coli*, morphological changes (*e.g.* cell becomes shorter), metabolic alterations (shift to anaerobic/fermentative pathways), membrane alterations and stress resistance occurred (Hengge, 2011). These phenotypic alterations are illustrated in Figure 1.1.

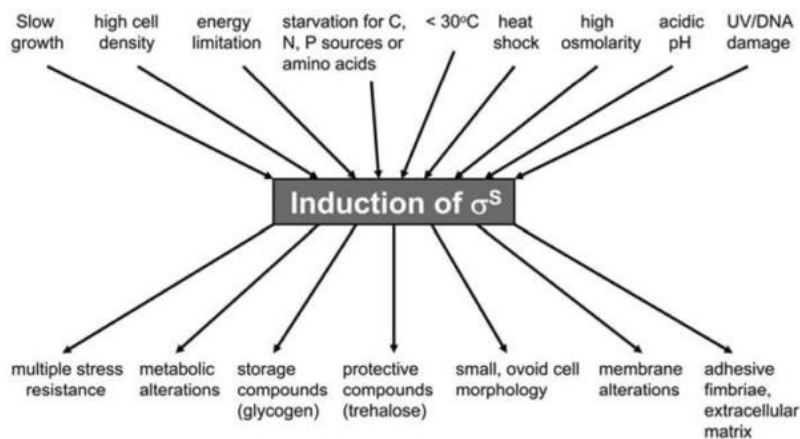


**Figure 1. 1. Diverse sets of stress signals and their effects on cell metabolism.** Variety of stress signals lead to the accumulation of the  $\sigma^S$  that result in the phenotypic alterations (from Hengge, 2011).

Cellular levels of RpoS in *E.coli* are regulated by comprehensive networks that have impacts on transcription, translation, and post-translational stability. Their control mechanisms depend on kind of stressors. Detrimental effects of stressors induce the transcription of the *rpoS* gene and prevent degradation of it by proteases. Furthermore, increased transcription activity of the *rpoS* is well correlated with the decreased in the growth rate (Jones, 2012). General view of control of  $\sigma^S$  synthesis and proteolysis is shown in Figure 1.2.

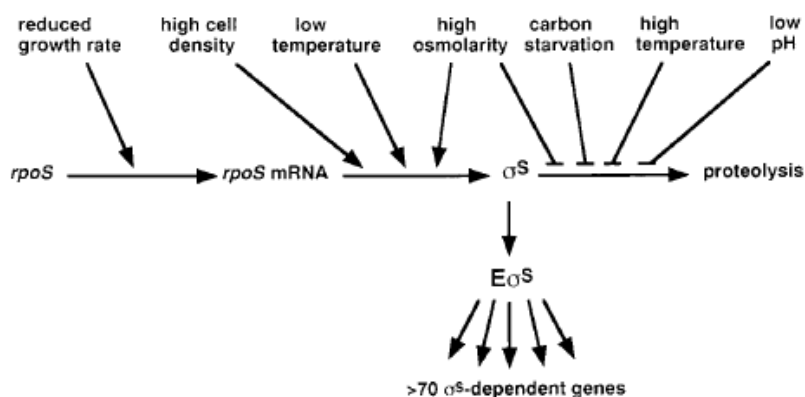


**Figure 1. 2. Regulation of the  $\sigma^S$  synthesis and proteolysis in response to the diverse signals.** Acute stress induces the transcription of *rpoS* and prevents its degradation by proteases.  $\sigma^S$  containing RNAP holoenzyme ( $E\sigma^S$ ) initiates transcription, and more than 70 genes under the control of  $\sigma^S$  (from Hengge-Aronis, 2002).

In addition to the general stress response, stress specific responses are employed by many cells, which are stimulated by unfavourable temperatures, pH, osmolarity, starvation and reactive oxygen species (Jones, 2012). The examples of this response provoked by different stress conditions are discussed in detail in the following sections.

## **1.2. Heat-Shock Response and Heat Shock Proteins**

Temperature elevation above the optimum growth temperature for an organism induces heat shock response. Heat shock response is associated with increased expression of heat shock proteins (HSP). They are induced by a broad spectrum of stresses such as low and high temperatures, osmotic, cold, and salt stresses (Feder *et al.*, 1999). Upon shift in the external temperature, expression of the heat shock proteins in the cell is induced, counteracting the consequences of the heat stress and thus increasing the thermotolerance (Foster, 2007).

It was shown in previous studies that heat shock response is highly evolutionary conserved process in terms of involvement of heat shock proteins. In other words, the genes encoding heat shock proteins are expressed in three kingdom of life (*i.e.*, *eucarya*, *bacteria* and *archaea*). However, they show differences in terms of expression mode of their genes (Feder *et al.*, 1999). Expression of HSPs also depends on induction temperature. For example, in *Drosophila melanogaster*, induction occur between 33-37°C, and in thermophilic bacteria which grows optimally at 50°C, HSP genes are up regulated when temperature rises to 60°C. In mammals, expression of these proteins is induced by small increments in the optimum growth temperature (Lindquist, 1986). In general, threshold temperature for HSP induction is parallel to the optimum temperature at which the organism lives. Therefore, thermophilic species need a higher threshold temperature than psychrophilic to induce HSP gene expressions (Feder *et al.*, 1999). Although heat shock proteins are key elements of anti-stress mechanisms, they have critical physiological roles in the cells, even in the absence of stressors. For example, molecular chaperones have central role to assist proper folding of proteins as they are synthesized, assembly of protein oligomers, and protein secretion. They also aid

refolding of the denatured or improperly folded proteins, and trigger death signal which cause apoptosis or quick necrosis (Pirkkala *et al.*, 2001).

Many of the HSP genes are grouped into families depending on molecular weight and sequence homology like HSP110, HSP100, HSP90, HSP70, HSP40, HSP10, and small HSP families. In order to guard protein conformational homeostasis, cell needs some of the major chaperones such as HSP70, HSP90, and small HSPs (Federe *et al.*, 1999). Also, HSP70 functions related to the stress tolerance. It has ability to aid cellular repair process in response to the heat, oxidative stress and it stimulates proteases, and triggers release of lysosomal and proteolytic enzymes (Kregel, 2002).

### **1.2.1. Regulation of Heat- Shock Genes**

Regulation of genes encoding the heat shock proteins are essential, since rapid response to stress is managed by controlling the synthesis of regulated protein at the transcription level. Regulation of genes at the transcriptional level is more extensively studied in prokaryotes compared to eukaryotic system (Sadhale *et al.*, 2007). In prokaryotic system, different sigma factors that associate with RNA polymerase play role in regulation of genes. In *E.coli* and other bacteria, heat shock response is controlled by sigma factor  $\sigma^{32}$ , which is the product of the RpoH gene. Also, another sigma factor  $\sigma^{24}$  (RpoE) has an important role in regulation of the cellular levels of HSPs (Foster, 2007). Under favorable conditions,  $\sigma^{32}$  expression is low in *E.coli* cells. Following temperature up- shift, translation of the RpoH gene is enhanced and increased stability of  $\sigma^{32}$ . This sigma factor interacts with the core RNA polymerase and allows for the recognition of the heat shock promoters, thus promoting the expression of HSPs. In addition,  $\sigma^{24}$  that is the product of gene RpoE is also heat inducible sigma factor, which is responsible for protecting cells against envelope stress caused by unfolded envelope proteins and heat stress. Distinguishing feature of  $\sigma^{24}$  from  $\sigma^{32}$  is that misfolded or immature extracytoplasmic proteins activate  $\sigma^{24}$  (Jones, 2012).

In eukaryotes, heat shock protein expression is regulated by heat shock factors (HSFs). Transcription of the HSP genes is activated when the HSFs are translocated to nucleus, and then they recognize the modular sequence elements (HSE) within the

HSP promoter region. The mechanisms underpinning the activation of the HSF1 in response to the heat shock are related to the sensing the damage on proteins and increasing the demand for chaperones *i.e.*, Hsp70, Hsp90, and the co chaperone Hdj1. Presence of non native protein and chaperones mediate the translocation of the heat shock factor to nucleus, and its trimerization occur. In the nucleus, this transcription factor is phosphorylated at the serine residue that enable its interaction with HSE that is located upstream of the HSP genes. Thus, induction of the transcription of heat shock genes occurs as a result of stress (Santoro, 2000). Furthermore, according to the recent report, regulation of the gene expression during heat shock occurs by specific interaction of HSF1 with histone deacetylases. This regulation of HSF1 is associated with large scale epigenetic remodeling by histone deacetylation (Vabulas *et al.*, 2010). Overview of this regulation is shown in Figure 1.3.

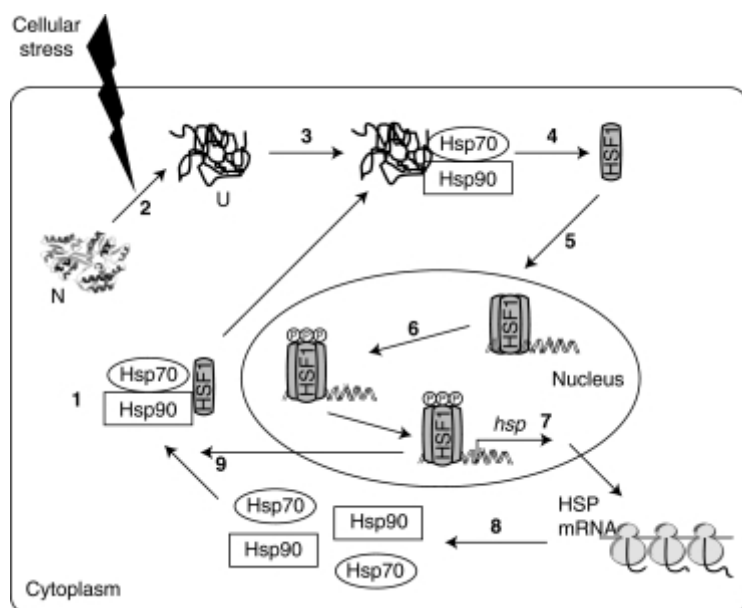


**Figure 1. 3. Regulation of HSF1 in eukaryotic cells.** In unstressful cells, HSF1 is found in cytoplasm as a monomeric form bound to HSP70 and HSP90 (1). Cellular stress triggers the accumulation of deneatured proteins in the cytoplasm (2). Binding of denatured protein to chaperones results in the displacement of the HSF1 (3) (4). This mediates the translocation of HSF1 to nucleus (5). In the nucleus, it is phosphorylated (6). Trimerization of the HSF1 in turn activates the expression of HSP genes (7). Translation of the HSPs occur, including Hsp90 and Hsp70 (8). Increased cellular concentraton of chaperones (HSP70 and HSP90) inactivates the HSF1 (from Vabulas *et al.*, 2010).

In the archaea, mostly in Euarchaeota, heat shock is sensed directly by negatively acting transcription factor Phr. When the temperature is up shifted, transcription factor is dissociated from the DNA and transcription of the heat shock genes are induced (Iqbal *et al.*, 2010). In *Pyrococcus furiosus*, a putative heat shock regulator inhibits the transcription of genes by binding to palindromic sequences covering the transcription initiation site. Heat shock causes the dissociation of the Phr, which allows expression of special group of genes encoding chaperones (*i.e.*, Hsp70/ DnaK and Hsp60/GroEL) (Garrett *et al.*, 2007).

### **1.3. pH Stress**

Regulation of pH homeostasis is fundamental to survival of cells, since functional and structural unity of proteins ensured by maintaining a proper cytoplasmic pH. Otherwise, a shift to acid or alkaline environment is stressful for the cells (Padan *et al.*, 2005). For that reason, a large number of adaptive mechanisms are evolved in order to sustain pH homeostasis in the cells. There are several reports concerning the tolerance to acid stress, but limited reports are available about the adaptation mechanisms to alkaline environments (Saito *et al.*, 2003).

#### **1.3.1. Adaptive Mechanisms Against Acid Stress**

In order to understand protective stress mechanisms under acidic environments, early studies were conducted with acidophiles that are microorganisms with an optimum growth pH is < 3. Their adaptive mechanisms to extreme acid environment are suggested to be associated with cellular bioenergetics, which is the main contributor of proton motive force (Baker-Austin *et al.*, 2007) (Figure 1.4).

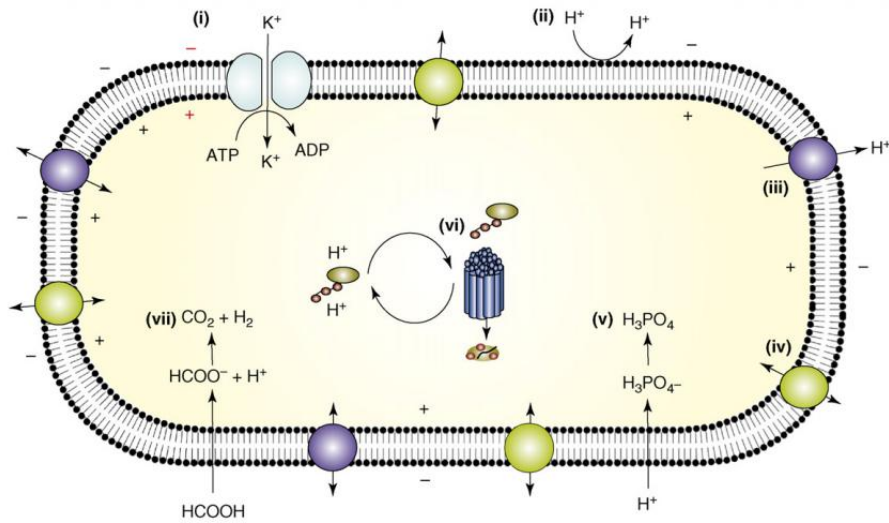


**Figure 1. 4. Overview of pH homeostasis in acidophiles.** Prevention of proton entry by donnan potential (I). Highly impermeable cell membranes retard the influx of protons into the cell (II). pH homeostasis is maintained through active proton export by transporters (blue) (III) and secondary transporters (green) (IV). The presence of buffers help to maintain pH homeostasis (V). DNA and protein repair at low pH (VI) Organic acids degradation (VII) (from Baker-Austin *et al.*, 2007)

According to this mechanism, when protons enter the cell through the FOF1 ATPase, it is equilibrated by extrusion of protons through electron transport chain. This is very important to maintain internal pH of the cell in acidic media. Otherwise, most of the proteins and enzymes that are functional at optimum pH can be damaged by protonation (Jain *et al.*, 2008). For example, *Enterococci* use F type ATPases to extrude protons in order to maintain pH homeostatis in acidic media. Bacteria have numerous type of transport systems *e.g.* H<sup>+</sup>ATPases, antiporters and symporters, which are driven by proton motive force (Saito *et al.*, 2003).

Another acid tolerance response of acidophiles is restricting proton influx by cytoplasmic membrane, which is highly impermeable to protons. An example for impermeable cell membrane is unique archaeal cell membrane, which is made up of tetraether lipids. This lipid structure makes the cell membrane less prone to the acid hydrolysis. Alternatively, restricting proton entry may be linked to the generation of an inside enriched by positive charged molecules by inflow of more potassium ions than efflux of protons. This refers to the Donnan potential, which is potential of positively charged molecules (Baker-Austin *et al.*, 2007).

Another defense mechanism against acidification of the environment is that production of cytoplasmic buffer molecules such as lysine, histidine, and arginine, which have ability to sequester protons. These basic amino acids have predominant roles in acid tolerance. Furthermore, decarboxylase system has central role to sustain life in acidic environment, since they function by consuming hydrogen ions to regulate pH homeostasis. These systems are consisting of decarboxylase enzymes, which function through conversion of their substrates to amine and CO<sub>2</sub>, and antiporters exchange the aminoacids for amine. Therefore, this system protects the cell from acid stress by decarboxylation reactions (Booth *et al.*, 2002). For example, lysine, arginine and glutamate decarboxylases works together with internalized aminoacids and proton, and then exchange the final product like cadaverine, agmatine for another aminoacid substrate (Cotter *et al.*, 2003).

In addition to the cytoplasmic buffer and decarboxylation system, degradation of the organic acids is another way of protecting cells from acid stress. Because organic acids function as uncouplers, and they are detrimental to acidophiles. Furthermore, organic acids affect cytoplasmic pH more than inorganic acids (Booth *et al.*, 2002). It was revealed that extreme heterotropic acidophiles, *P.torridus* and *F.acidarmanus*, use organic acid degradation mechanism to maintain pH homeostatis via organic acid degradation pathways, involving enzymes such as two acetyl CoA synthetases, propionyl CoA synthetase, and lactate -2 monooxygenase. These systems are related to the production of pyruvate from lactate (Baker-Austin *et al.*, 2007).

In addition, acid adaptation requires DNA and protein repair systems since cytoplasmic acidification affects both protein and DNA stability. For that reason, acid induced damage on the macromolecules can be dealt with expressing genes encoding the chaperones and DNA repair proteins. This has been shown in numerous reports which revealed increased expression of both DnaK and GroEL/ES genes as response to acidic pH (Booth *et al.*, 2002). In addition, Rec A takes role in repair mechanism by mediating homologous recombination and regulation of SOS response. Therefore, the absence of Rec A more likely results in death of *S.mutans* cells at pH 2.5 (Cotter *et al.*, 2003).

Another acid tolerance mechanism is the changing membrane lipid composition on the basis of the ratio of unsaturated fatty acid to saturated fatty acid. Decrease in the membrane fluidity is associated with acid resistance, since in this way; the proton influx into the cell is restricted (Jain *et al.*, 2008).

### **1.3.2. Adaptive Mechanisms Against Alkaline Stress**

Like shift to acid environment, a shift to alkaline pH also poses a threat to organisms. Large number of defense mechanisms is deployed to combat with alkaline pH. Some of the adaptive mechanisms are: production of metabolic acids by aminoacid deaminases and sugar fermentation, alteration in the cell membrane composition, induced expression of antiporters such as monovalent cation/proton antiporters and increased ATP synthase activity.

Among these, monovalent cation /proton antiporters have crucial roles in adaptation to the alkaline environments (Padan *et al.*, 2005; Wiegert *et al.*, 2001). Because, under condition of alkaline challenge, proton influx is essential to achieve alkaline pH homeostasis, and it is usually accompanied by transcriptional up regulation of expression of cation/proton antiporters. It was shown that most of the free living bacteria possess numerous  $\text{Na}^+/\text{H}^+$  and  $\text{K}^+/\text{H}^+$  antiporters, and it is proposed that they play crucial roles in not only in pH homeostasis, but also in cation and osmotic homeostasis (Krulwich *et al.*, 2011). Also, it was reported that mutant alkalophilic bacilli which were deprived of sodium/proton antiporter was sensitive to high pH (Saito *et al.*, 2003). In alkaline pH homeostasis, antiporters catalyze electrogenic antiports in which  $\text{Na}^+/\text{H}^+$  antiporters exchange greater number of entering protons than the number of exported sodium ions, which directs the proton ion movement towards inside. Proton entry is provided by proton motive force (PMF) that directs the energization of the exchange. PMF catalyzes accumulation of  $\text{H}^+$ , which is necessary for acidification of cytoplasm at alkaline pH (Padan *et al.*, 2005). For instance, the stoichiometry for *E.coli*  $\text{Na}^+/\text{H}^+$  antiporter is like that two molecules of  $\text{H}^+$  entering the cell is linked to the exchange for one molecule of  $\text{Na}^+$ . Obviously, these  $\text{Na}^+/\text{H}^+$  antiporters have dominant roles in alkaline pH homeostasis of *E.coli* and *Bacillus* strains (Krulwich *et al.*, 2011).

Another strategy for pH challenges involves production of metabolic enzymes with aminoacid deaminase activity. Deaminases provide acid producing mechanisms that underpin important ability to tolerate high cytoplasmic pH values. Expression of deaminases possibly reflecting a need for free ammonia and weak acid by products are released, and homeostasis is ensured by lowering the external pH (Saito *et al.*, 2003). Several enzymes which belong to the aminoacid catabolism are increased to high amount at alkaline pH, including tryptophan deaminase (TnaA), tryptophan transporter (TnaB) and serine deaminase (sdaA) (Padan *et al.*, 2005). Furthermore, enzymes of arginine and glutamate catabolic pathways are expressed in *E.coli* upon alkaline stress (Saito *et al.*, 2003).

Another proposed adaptation of *E.coli* cells for alkaline pH homeostatis is that glycolysis and fermentation of sugars would occur promptly at high pH due to the induction of glycolytic enzymes under alkaline stress. Hence, increased production of fermentation acids and consumption of bases was proposed to support survival in extremely alkaline environments (Saito *et al.*, 2003).

Another remarkable adaptation mechanism is the adjustment of membrane lipid composition. Alkaliphiles have teichuronic acid and S layer protein, SlpA, as the acidic secondary cell wall polymers, which contribute to the alkaline pH homeostasis. It is supposed that positive effect of these acidic secondary cell wall polymers upon alkaline stress is related to the proton binding and enhanced proton uptake together with increasing proton concentration near surface (Krulwich *et al.*, 2011). It was proven that a mutant lacking slpA from alkaliphilic *B.pseudofirmus* OF4 resulted in decreased ability to adapt to alkaline stress. Also, it was presumed that presence of high level of cardiolipin and squalene in the membrane of alkaliphilic *Bacillus* can be associated with one of the adaptation mechanisms to high pH, since cardiolipin has role in trapping protons at membrane surface (Padan *et al.*, 2005).

Additional bacterial responses aimed at regulating pH homeostasis include increased ATP synthase activity in order to minimize loss of H<sup>+</sup>. This is inferred from studies on ATP synthase motif mutations that lead to proton leakiness (Krulwich *et al.*,

2011). In addition, in alkaliphilic *Bacillus* species, proton uptake goes along with ATP synthesis by F1F0 ATP synthase. Therefore, ATP synthesis capacity of *Bacillus* is a remarkable factor in overall pH homeostasis (Krulwich *et al.*, 2011). Furthermore, microarray studies of *E.coli* cells show that among the genes down regulated at the alkaline pH are the genes responsible for pumping protons towards outside; on the other hand, induced genes consists of those encoding F1-F0 ATP synthase that imports protons during ATP synthesis. These observations show that alkaline stress leads to change in the gene expression profile (Padan *et al.*, 2005). As a result, much of the discussion related to the alkaline stress have been focused on mostly on alkaliphilic *Bacillus* species.

However, reports regarding the adaptive mechanisms of eukaryotes to alkaline stress are very limited. In *S.cerevisiae*, transcriptome analysis has revealed a set of responsive genes upon exposure to alkaline stress, and calcium mediated signaling is found as component of this response. It is supposed that alkaline pH could induce a rise in cytoplasmic calcium concentration (Wang *et al.*, 2011). As it is know that calcium mediated signaling mechanisms play crucial roles in gene expression, as well as other wide variety of cellular processes. Therefore, increase in the cytoplasmic calcium leads to activation of various enzymes, such as the protein phosphatase calcineurin (Viladevall *et al.*, 2004).

Adaptation to the alkaline pH in *C.albicans* and *Basidiomycetes* is mediated by conserved transduction pathway, which is regulated by zinc finger DNA binding protein Rim101/PacC. Binding of Rim101p to promoter of genes required for alkaline pH homeostasis stimulates their expression (Wang *et al.*, 2011). Important aspect of Rim101 in adaptive response has been clarified from a study conducted with *S.cerevisiae* Rim101 mutant. This defect results in increased sensivity to high pH (Platara *et al.*, 2006).

Two additional contributions to pH homeostasis have been documented in *S.cerevisiae*. First, cation pumps such as Na<sup>+</sup>-ATPase plays a critical role in growth at alkaline pH. Defect in the cation pumps results in growth retardation even if under mild alkaline conditions (Platara *et al.*, 2006). Second, inorganic polyphosphate

(polyP) representing the diverse range of functions, such as cation sequestration and storage, regulation of gene and enzyme activities, has a remarkable role in stress response, as well. Also, hydrolysis of polyP is associated with the pH-stat mechanism to deal with alkaline stress. Under alkaline stress, accumulation of amines stimulates specific phosphatases to break down polyP to tripolyphosphates (Kulaev *et al.*, 2000). Therefore, polyP has a central role in stress response and stationary phase adaptation.

#### **1.4. Cellular Response to Oxidative Stress**

Cells are vulnerable to the oxidative stress that is caused by the increased levels of reactive oxygen species (ROS) such as hydrogen peroxide ( $\text{H}_2\text{O}_2$ ), superoxide ions ( $\text{O}_2^{\cdot-}$ ), hydroxyl radical ( $\text{OH}^{\cdot}$ ) and alkyl hydroperoxides (ROOH) which severely affect all macromolecules such as proteins, lipids, and DNA (Carmel-Harel *et al.*, 2000). ROS does not only cause oxidative stress, characterized by activation of some stress genes, but they can also repress many genes. Oxidative stress is one of the major mechanisms of aging and cell death. Therefore, it is essential that living organisms should develop defense mechanisms in order to minimize adverse effect of oxidative damage. In this respect, all cells possess ability to remove free radicals from cells in order to reduce the damage and repair the distorted homeostasis (Kültz, 2005).

High level of reactive oxygen species disturb normal redox homeostasis and shift the cells into state of oxidative stress (Finkel *et al.*, 2000). A number of free radical scavenging mechanisms have appeared to combat the oxidative damage, including antioxidants such as glutathione, vitamin A, vitamin E, vitamin C, flavonoids, and various antioxidant enzymes like superoxide dismutase, catalase, glutathione peroxidase, thioredoxin, and metals in storage and transfer proteins (*e.g.* transferrin, ferritin). These enzymes have been found to be induced under various oxidative stress conditions (Martindale *et al.*, 2002). For example, glutathione and thioredoxins at high concentrations establish a strong reducing environment (Kültz, 2005).

The alteration of the cellular redox potential triggers the cellular stress response by activating the expression of redox regulatory genes; products of some of them are

aldehyde reductase, glutathione reductase, thioredoxin, peroxiredoxin, superoxide dismutase, and aldehyde dehydrogenase (Kültz, 2005).

Among them, superoxide dismutase functions as converting superoxide ion to hydrogen peroxide and by help of catalase, and peroxidase, hydrogen peroxide is eliminated from cells yielding water and oxygen (Cabisco *et al.*, 2000). These reactions are shown in Figure 1.5

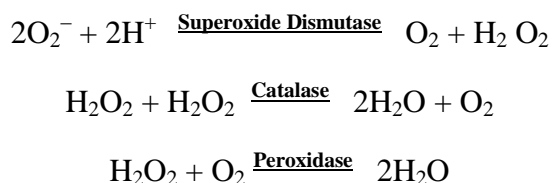


**Figure 1. 5. Superoxide and hydrogen peroxide detoxification** (from Voet *et al.*, 2011).

Furthermore, several oxidoreductases including dehydrogenases could be effective in maintenance of the cellular redox potential. For example, aldehyde dehydrogenases and aldehyde reductases are crucial for scavenging of toxic intermediary metabolites (Kültz, 2005).

In addition to these, oxidative stress activates the proteolytic and lipolytic enzymes, as well as DNA repair enzymes (*e.g.*, endonuclease IV and xanthine oxidase) (Cabisco *et al.*, 2000). Xanthine oxidase is one of the effective enzyme with ability to repair damage on macromolecules. It is capable of recognizing a DNA –oxidized adduct, and then removing it, and adding undamaged base (Kohen *et al.*, 2002).

Furthermore, genetic response to oxidative stress is another distinct feature to maintain the protection against variety of reactive oxygen species. This type of response occurs in bacteria, yeast and mammalian cell lines (Cabisco *et al.*, 2000). For example, *E.coli* cells regulate the transcription factor, OxyR, in response to the  $\text{H}_2\text{O}_2$  and  $\text{O}_2^-$ . Based on the previous DNA footprinting experiments, it is known that OxyR is found in two forms; one is reduced form, and the other is oxidized form. The only oxidized form has ability to induce transcription. Oxidation of this transcription factor by hydrogen peroxide results in disulfide bond formation, enabling the  $\text{H}_2\text{O}_2$  sensing and stimulating the expression of the antioxidant defense

activities (Carmel *et al.*, 2000). The Oxy R gene controls the expression of genes encoding catalase, glutaredoxin, glutathione reductase, NADPH dependent alkyl hydroperoxide reductase, and protective DNA binding protein (Cabisco *et al.*, 2000). Mechanism for the activation of the OxyR in response to the oxidative stress is shown in Figure 1.6.

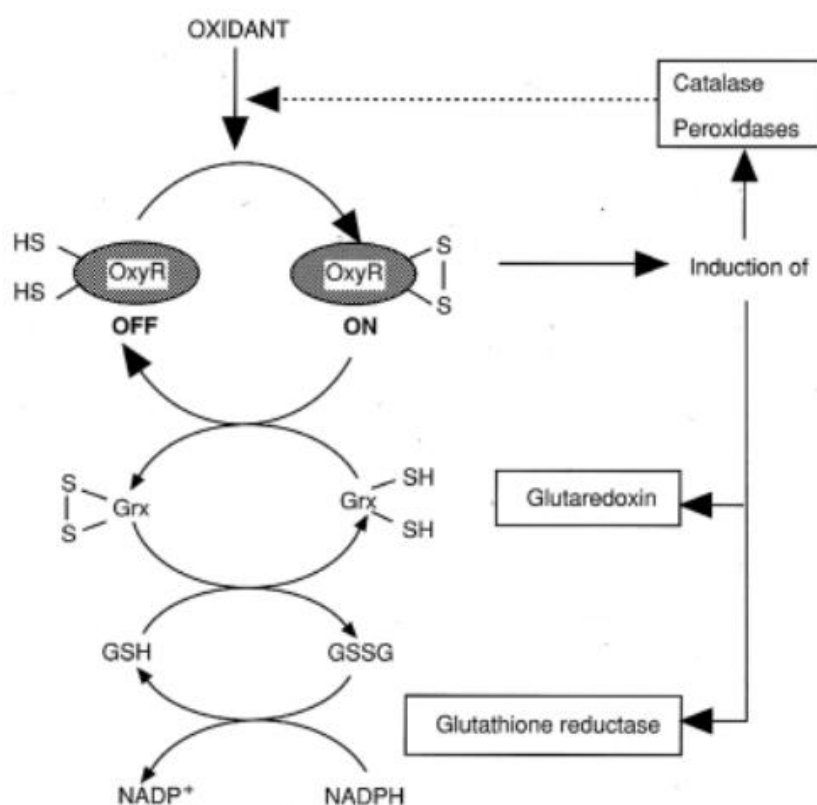


**Figure 1. 6. Activation of OxyR.** Oxidative stress activates OxyR by formation of a disulfide bond, which in turn leads to induction of catalase, peroxidase, glutaredoxin, and glutathione reductase (from Cabisco *et al.*, 2000).

In recent years, role of DNA binding proteins (Dps) have drawn attention due to their crucial roles in severe environmental assaults, mostly in oxidative stress resistance. Dps has been characterized as a ferritin like protein due to its ferroxidase activity that catalyzes oxidation of bound ferrous ion to ferric state. By help of this protein, two molecules of ferrous ions are oxidized for every one molecule of  $H_2O_2$  reduced; thus, preventing hydroxy radical formation via Fenton chemistry. Hence, it plays an

important role in hydrogen peroxide detoxification. Expression of Dps is induced by OxyR which regulates genes including catalase, and alkyl hydroperoxide reductase (Calhoun *et al.*, 2011).

In addition, adaptive response of *E.coli* cells to superoxide ion is modulated by SoxR and SoxS transcription factors. During oxidative stress, SoxR is activated by oxidation of the reduced  $[2\text{Fe-2S}]^{+1}$  form to  $[2\text{Fe-2S}]^{+2}$  form and then active form of SoxR stimulates the transcription of SoxS, resulting in the induced expression of antioxidant activities such as manganese superoxide dismutase (Carmel-Harel *et al.*, 2000).

Similarly, genetic response to hydrogen peroxide occurs in *S.cerevisiae* cells. A number of studies have shown that Yap1p and Skn7p are required for adaptive response of *S.cerevisiae* to hydrogen peroxide. For example, mutational studies showed that single mutation in Yap1p and in Skn7p or double mutation in both transcription factors resulted in the enhanced sensitivity to hydrogen peroxide. Regulatory roles of these transcription factors are poorly understood (Carmel-Harel *et al.*, 2000).

### **1.5. Life in Hot Acid Environment**

Extremophiles are organisms that have adapted to thrive in habitats that are hostile to majority of life on earth. They have specific ability for surviving in extraordinary hot or acidic environments (Gupta *et al.*, 2014). In addition, extreme conditions can be represented by physical extremes such as radiation, pressure, temperature or geochemical extremes (*i.e.*, desiccation, salinity, pH) (Rothschild *et al.*, 2001).

Most known extremophiles are microorganisms belong to the domain of archaea. The major extremophilic groups consist of hyperthermophiles, thermophiles, the psychrophiles, alkaliphiles, acidophiles, halophiles, and piezophiles. Among them, the most well understood extremophilic group is archaeal thermophiles and its distinct subclassified group, namely hyperthermophiles.

Diverse groups of hyperthermophiles are represented in the genera of *Pyrococcus*, *Sulfolobus*, and *Archaeoglobus* (Anitori, 2012). It is found that some extremophiles

like thermoacidophiles are adapted to multiple stresses. *Sulfolobales* and *Thermoplasmatales* are known as extremely thermoacidophilic. These interesting group of microorganisms deal with both extreme pHs (< 4) and temperatures ( $T_{opt}$  >60) (Auernik *et al.*, 2008). Furthermore, it is stated that most of the thermophiles and acidophiles such as *Sulfolobus*, *Picrophilus*, and *Thermoplasma* species share genomic similarities, so phylogenetically they clustered together (Reed *et al.*, 2013).

### **1.5.1. Survival Strategies of Microorganisms in Hot Acidic Niches**

Survival and growth of thermoacidophiles in extreme environments depend on adaptive strategies. Improvements in the molecular genetics tools have facilitated to uncover adaptive mechanisms for survival in hot acidic environments. However, exact reasons for novel growth physiology are not fully understood.

Some of the strategies that contribute to the life in hot acid environments include DNA repair mechanisms, chaperone systems, and metal resistance. First, both acidic and high temperature disrupts the functional integrity of nucleic acids. One of the strategies contributes to the life in hot acid environments centered to the stabilization of nucleic acids and repair mechanisms. In vitro experiments demonstrated the importance of  $\text{Na}^+$ ,  $\text{K}^+$ , and  $\text{Mg}^{2+}$  ions in the stability of dsDNA against damaging effect of heat. Furthermore, it has been shown that aliphatic, noncyclic compounds comprising two or more protonated amino nitrogen atom like polyamines can stabilize DNA or RNA. For example, long polyamines such as spermine and thermine maintain the structural integrity of nucleic acids by fixing phosphate groups (Anitori, 2012).

In addition to the stabilizing strategies for nucleic acids, repair mechanisms also constitute an important and essential feature to cope with challenges posed by extreme environments. As it is known that high temperature and cytosol acidification triggers the susceptibility to DNA damage (Auernik *et al.*, 2008). To cope with such deleterious effects, microorganisms have peculiar components involved in DNA repair.

Components of the repair systems include endonucleases, 5' to 3' exonuclease, DNA ligases, DNA glycosylase and polymerases, which are responsible for elimination of

the damage (Gerday *et al.*, 2007). Also, homologous recombination is an efficient way of repairing DNA (Auernik *et al.*, 2008).

Further insight into adaptation under extreme of pH and temperature is inferred from studies on structures of proteins. However, few identified adaptations for improving protein stability under acidic conditions are available. Since most known acidophiles are thermophiles, their proteins reflect the thermophilic features. Therefore, some principles are common (Reed *et al.*, 2013). It was shown that specific amino acid composition is required for the proteins under extreme environments such that hyperthermophiles and thermophiles have high proline content in their proteins as compared to that of mesophiles. Role of this amino acid is probably related to the thermostability of proteins. It was stated that increased proline content is parallel with a decline of charged amino acids. Thus, lowering charge density probably prevents protein unfolding. In this respect, it is proposed that stability of proteins could be encouraged via increasing internal hydrophobicity (Siddiqui *et al.*, 2008).

In addition to these, survival of extremely thermoacidophilic microorganisms could be achieved by activation of variety of chaperones including thermosome, prefoldin, peptidyl prolyl isomerase, which participates essential roles in cell physiology (Anitori, 2012).

To sum up, even though adaptations of extremophiles to adverse environmental conditions are poorly understood, some of the adaptation strategies give insight into life in hot acid environment (Reed *et al.*, 2013).

### **1.6. Stress in *Archaea***

Archaea, although have evolved to be exceptionally proficient at surviving under extreme conditions, still they must contend with fluctuations in temperature, osmolarity, acidity, salinity in their environment. In this context, in order to survive and grow under challenging environmental conditions, sensing and adapting to environmental stress are essential.

Specifically, the complicated cellular strategies can be developed by different archaea in order to counteract damaging effect of biological, physical, or chemical

stressors. Response of archaea to stressors can vary, which depends on the species itself and its ecosystem.

It is well known that archaea can sustain their life in a variety of environments like very hot, very cold, anoxic, oxygenated. Fluctuations in these environments can cause stress and induce stress response (Pedone *et al.*, 2004).

### **1.6.1. Heat Stress in *Archaea***

Archaea can be exposed to heat stress and they can respond to ambient temperatures through utilizing variety of adaptive mechanisms. Temperature up- shift or down- shift result in heat shock and cold shock respectively (Macario *et al.*, 1999). Heat stress has deleterious effects on macromolecules, membrane structure, and basic cellular functions of cells such as transcription, translation, cell division. Specific heat- shock defense mechanisms within the cells fighting has been found in order to rescue cell from death upon heat stress. A key consequence of heat stress is protein denaturation, and abnormal protein accumulation in the cells. Therefore, there is an increased demand for chaperones and proteases in order to reestablish altered protein homeostasis (Richter *et al.*, 2010).

#### **1.6.1.1. Role of Chaperones in Heat- Shock Response in *Archaea***

Molecular chaperones have a central role in promoting and maintaining the native conformation of proteins in order to counteract aggregated or misfolded proteins. It is revealed that chaperone genes are regulated by heat shock regulon, and although they are transcribed under all conditions, their transcription is induced when they are exposed to heat stress (Lund, 2011).

Universal distribution of chaperone families in archaea is very restricted. Specifically, only small heat shock proteins, chaperonin, AAA ATPase, prefoldin, nascent chain associated complex (NAC) and folding catalyst (peptidyl-prolyl isomerase and disulfide isomerase) are present in all archaea species whose whole genome sequences are determined.

Among them, chaperonins are large double ring complexes which cover substrate proteins for proper folding. Each ring complex encircles a cavity that can change between open or closed conformation and client proteins undergo folding inside the cavity. Chaperonins are divided into two groups *i.e.*, chaperonin I and II (Luo *et al.*, 2011).

Group I chaperones are also termed as HSP60 in eukaryotes and GroEL in bacteria that function with aid of HSP10 factor (GroES in bacteria). Group I chaperones are found in bacteria, mitochondria and chloroplasts. The GroEL-GroES chaperonin system of *E.coli* is well characterized. This complex is composed of two heptameric rings which are stacked end to end. Substrate binds to the apical domain of GroEL, including hydrophobic aminoacid residues for non-native substrate binding. Binding of ATP and GroES to GroEL cause conformational changes within the ring, which in turn close the cavity, and hydrophilic residues are exposed to the internal surface of the cavity as shown in Figure 1.7. Hydrophilic feature of the inner wall traps the protein for folding. Release of the protein depends on the dissociation of the GroES which is allosterically regulated by ATP binding in the opposite ring. This cycle is repeated until the protein is correctly folded (Hartl *et al.*, 2011).

Different from Group I chaperonins, the group II chaperonins in archaea (thermosome) and the eukaryotic cytosol (TRiC) function for protein folding without assistance of Hsp10 factor (Hartl *et al.*, 2011). Basic mechanism for protein folding is quite similar to the group I chaperonins. Structural and functional studies on thermosomes revealed the protein folding process in archaea, as well as thermally inducible subunits (*e.g.*,  $\alpha$  and  $\beta$ ). The first structure analysis on thermosome from *Thermoplasma acidophilum* showed that it consists of two eight membered rings which are arranged with alternating  $\alpha$  and  $\beta$  subunits. Each ring has central cavity. It was proposed that availability of the helical protrusion region in group II chaperone could be associated with the corresponding functional role to GroES subunit by closing the central cavity of chaperone complex (Lund, 2011). Another crystal structure of thermosome from *Thermococcus* KS1 CPN revealed the similar structure to the thermosome of *T.acidophilum*. Moreover, it was shown that temperature affected the subunit composition of the chaperonin complexes in some archaea. For

example, in *Thermococcus* sp. Strain KS-1, expression level of  $\beta$  subunit is enhanced upon heat stress, while  $\alpha$  subunit is not changed. Similarly, *Sulfolobus shibate* contains group II chaperonin made up of three different subunits ( $\alpha$ ,  $\beta$ ,  $\gamma$ ). Expression of the  $\beta$ ,  $\gamma$  subunits are induced following heat shock, and decreased by cold shock (Luo *et al.*, 2011).

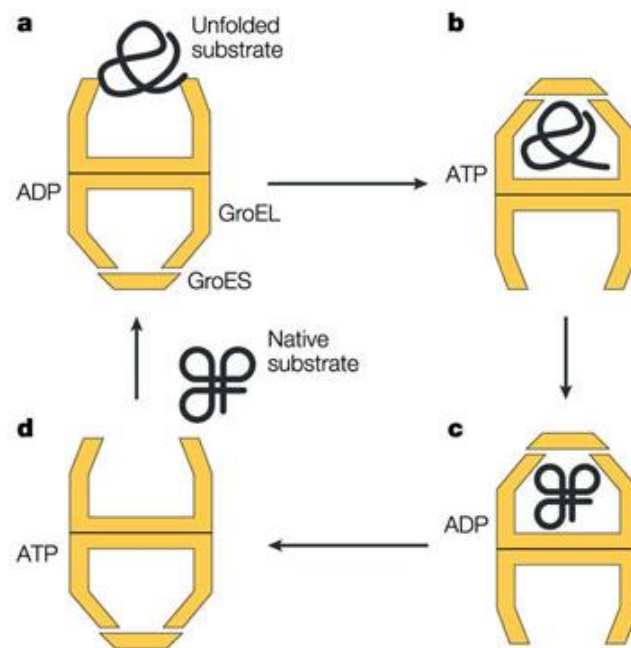


**Figure 1. 7. Folding in the GroEL- GroES chaperonin system.** Substrate and ATP binding to GroEL triggers conformational change in the apical domain (part a). This is continued with binding of GroES and enclosing of the substrate (part b). Then, sequestration of the substrate allows folding (part c). Later, GroES is dissociated after ATP turnover that allows the release of protein (part d) (from Young *et al.*, 2004)

Another class of molecular chaperones is small heat shock proteins (sHSPs). They are a set of small molecular weight proteins (15-30 kDa). They are accumulated in the cells after many different environmental, physiological or pathological stresses (Garrido *et al.*, 2012). Many of them act as molecular chaperones that have remarkable role in protecting proteins against irreversible aggregation (Figure 1.8). Due to this feature, most of the sHSPs are known as holdases. In other words, they prevent the denatured proteins from aggregation (Luo *et al.*, 2011). Besides, they

are ATP independent chaperones that capture large number of partially unfolded proteins, but release of bound substrate and subsequent refolding can be accomplished through interaction with ATP dependent chaperones like HSP70/HSP27 (Kocabiyik *et al.*, 2012).

A previous study on hyperthermophilic archaeon *P.furiosus* showed that denaturated Taq polymerase was refolded by a mixture of sHSP or HSP60 in an ATP dependent pathway. This experiment revealed that denatured proteins due to heat stress or other stresses bind to sHSP to avoid aggregation. Then, the sHSP transfers folding intermediates to chaperonins for subsequent maturation in the ATP dependent cycle (Luo *et al.*, 2009).

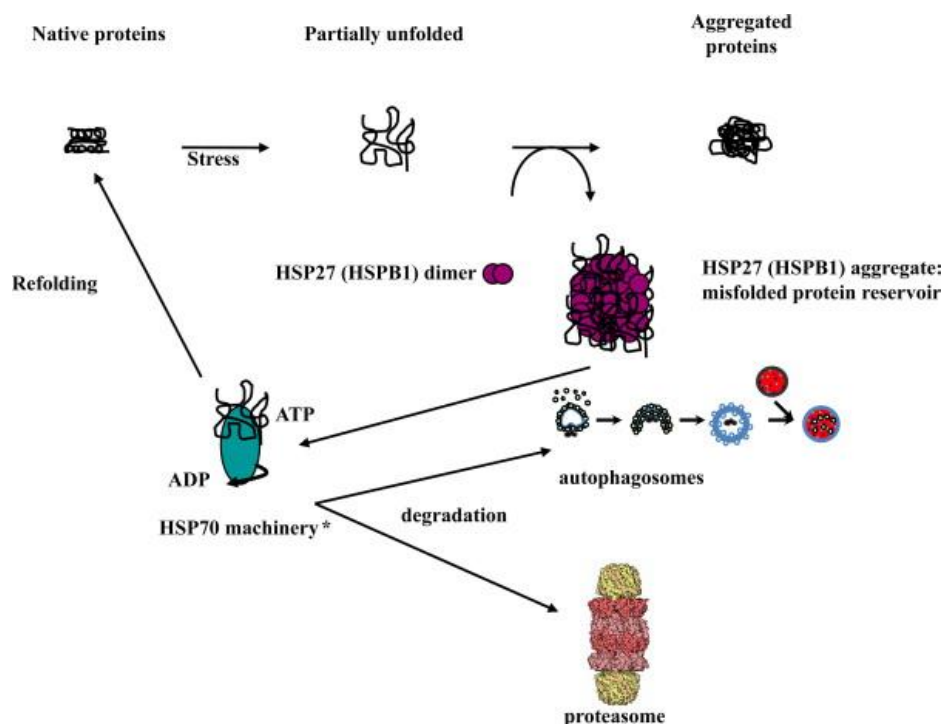


**Figure 1. 8. Action of protein refolding with sHSPs.** Small heat shock proteins act in a coordinated way that enables correct folding of the protein or direct them to proteasome for degradation ( from Garrido *et al.*,2012).

Another chaperone family is AAA ATPase, which represents functional category of protein unfolding or complex disassembly. AAA ATPases with homology to HSP100 are termed as unfoldases and disaggregates. They direct the substrates to

proteases in order to disassemble aggregates (Saibil, 2013). Furthermore, they take role in a variety of important cellular processes such as protein folding, and translocation, DNA replication and repair, membrane fusion and proteolysis (Smith *et al.*, 2006).

Another molecular chaperone in archaea is prefoldin which is also named as GimComplex (GimC). According to the structural studies, archaeal prefoldins are hexamers, which are made up of two  $\alpha$ - subunit and four  $\beta$  -subunits. They function in ATP independent manner and they capture non-native proteins and transfer them to group II chaperonin -thermosome. It was found that *M.jannaschii* has capacity to encode genes for subunits of prefoldin. Gene, pdf, coding for prefoldin subunit  $\gamma$  is heat shock regulated (Luo *et al.*, 2011).

Besides, NAC has dual chaperone function. NAC refers to the " nascent polypeptide associated complex". It is homodimeric complex. It is assumed that function of NAC in archaea is similar to the " bacterial trigger factor". It has variety of functions such as prevention of proteins from aggregation, degradation, premature folding, and incorrect folding during protein synthesis (Preissler *et al.*, 2012).

In addition to the well known molecular chaperone families, peptidyl-prolyl isomerases (PPIases) also have chaperone like activity. PPIases are common in all organisms. Three families of PPIases have been reported such that cyclophilin (CyP), FK506 binding protein (FKBP) and parvulin (Pvn) that have been studied in detail in Eukarya and Bacteria (eubacteria). But little is known about archaeal PPIase. PPIase speed up the rotation of peptidyl-prolyl bonds, which is necessary at the rate limiting step of protein folding. Besides, previous studies showed that the hyperthermophilic and thermophilic archaeal FKBP had aggregation-suppression activity. This was inferred from study on *M. thermolithotrophicus* whose FK506 binding protein accelerated the refolding of urea-denatured RNase-T1 in a dose-dependent fashion. The actual mechanisms about for this process is not known, but it is still questionable that archaeal PPIase can collaborate with other chaperones such as prefoldin, group II chaperonin (Maruyama *et al.*, 2000).

### **1.6.1.2. Additional Mechanisms for Heat Response in *Archaea***

#### **1.6.1.2.1. Protein Degradation**

Elimination of abnormal proteins from cell is vital in order to maintain cell physiology, because abnormal proteins and their fragments are apt to aggregate, precipitate and therefore disrupt the intracellular environment (Maupin-Furlo *et al.*, 2000). Protein degradation occurs inside the 20S proteasome, requiring ATP hydrolysis by associated hexameric AAA ATPase complexes such as proteasome activating nucleotidase (PAN). When the archaeal 20S proteasome interact with PAN in the presence of ATP, the degradation of unfolded proteins are stimulated. PAN has been shown to catalyze ATP dependent unfolding of globular protein, and it is translocation into the 20S proteasome for degradation. Interestingly, not all archaea species possess PAN. For example, in the *T. acidophilum*, VAT is present instead of PAN, which likely function in substrate recognition, unfolding, and translocation of substrates into the 20S proteasome (Smith *et al.*, 2006).

Also, proteases have crucial roles in getting rid of abnormal proteins. Only small group of energy dependent proteins are known. Energy dependent proteases including ClpXP, Lon, and FtsH degrade abnormally folded proteins. Among them, Clp is serine protease, and Clp family includes ClpAP and ClpXP proteases. Also, an archaeal Lon related serine protease is found in the cell membrane. Besides, FtsH family consists of membrane associated zinc dependent metalloproteases (Blum, 2001).

#### **1.6.1.2.2. Resistance to Heat Stress via Cell Membrane**

Temperature has the most well known effect on the viscosity of the membrane. The lipid composition and membrane proteins of archaea with unusual characteristics increase their tolerance to stressful environmental conditions. Distinguishing feature of archaea from bacteria is that hydrophobic part of their membrane is made up of phytanyl chains which are linked to glycerol or other alcohols via ether bonds. This feature provides higher resistance to oxidation and high temperature because both type of the resistance depends on the ether type linkage. It is claimed that high

stability of archaeal membrane lipids restricts the permeability of membrane to protons, which in turn increase resistance to oxidation and to heat stress (Conway de Macario *et al.*, 2000). Furthermore, adaptation to high temperature also is ensured by maintaining membrane fluidity. Keeping the membrane in liquid crystalline state can be achieved by increasing cyclization of the C<sub>40</sub> isoprenoid in the tetraether lipid. Therefore, this alteration results in the tight packing of the lipid, which cause restricted motion of lipid and avoids the membrane becomes too fluid (Albers *et al.*, 2000).

### **1.6.1.3. Heat- Shock Response in Different *Archaeal* Species**

Most of the stress response studies in archaea have centered to heat shock. In *Pyrococcus furiosus*, changes in abundance of transcripts in response to heat stress was determined using a targeted cDNA microarray in conjunction with Northern analysis (Shockley *et al.*, 2003). Up-shift of temperature from 90 °C to 105 °C resulted in the induction of genes encoding heat shock proteins *e.g.*, thermosome (Hsp60) , small heat-shock protein (Hsp 20) and two VAT- related chaperones, which belongs to a branch of AAA<sup>+</sup> family. Other group of genes whose transcript level increased following heat shock are responsible for proteolysis, stabilization of intracellular proteins by compatible solutes, carbohydrate acquisition, and DNA repair. However, expression of some other genes were repressed. For example, genes encoding for the glyceraldehydes- 3 phosphate ferredoxin oxidoreductase, several ATP independent proteases were repressed upon heat shock.

Heat shock response of *Methanococcus jannaschii* have been examined on a genome wide scale using cDNA microarray. Global transcriptome response of *M.jannaschii* to heat stress revealed the differently expressed 76 genes. Among them, the top category of up regulated genes encode  $\alpha$  subunit of putative prefoldin, thermosome, proteases. These represent the functional categories of protein folding and misfolded protein degradation pathways during heat shock. Also, genes encoding transposable elements seem to be up regulated. This indicates that lethal temperature increase the rate of mutagenesis. On the other hand, down regulated genes encoding subunits of

H<sup>+</sup> transporting ATP synthase and genes related to fatty acid processing. (Boonyaratanakornkit *et al.*, 2005).

Another transcriptional study to address the response of archaea to heat stress was conducted with the model organism *Archaeoglobus fulgidus* using a whole genome cDNA microarray. Results indicated that with the temperature shift from 78°C to 89°C, strongly induced genes were representing the functional categories of energy production and conservation, amino acid metabolism. One of the differentially transcribed gene encoded heat-shock regulator, hsr 1. It was shown that this regulator controls an operon of HSP20 and AAA<sup>+</sup> ATPase. Another group of genes whose transcription level increased upon heat shock is related to lipid metabolism (*i.e.*, isoprenoid pathway genes), and organic solute production (*i.e.*, di- mya-inositol phosphate) (Rohlin *et al.*, 2005).

Thermal stress of *Methanosarcina barkeri* was also investigated using whole genome oligonucleotide microarray. Results indicated a group of genes whose transcript level up regulated were encoding proteins such as chaperonin (HSP60), HSP70 (DnaK-DnaJ-GrpE) chaperone system, and AAA<sup>+</sup> ATPase. In addition, a set of genes with regulatory functions were also induced during heat stress, such as putative sensor histidine kinase and transcriptional regulators. Another specific outcome of heat stress is up regulation of genes related to the transposition. On the other hand, transcriptional level of genes involved in amino acid, coenzyme and energy metabolism were strongly repressed following heat- shock. The most strongly down regulated genes were related to protein biogenesis (Zhang *et al.*, 2006).

In an another study heat shock response was investigated in *Sulfolobus solfataricus* by using genome wide scale oligonucleotide microarray. The results obtained from this study were in good correlation with previous transcriptome analyses. Transcriptional profiling following temperature up -shift from 80 °C to 90 °C revealed the induction of genes encoding HSP20, thermosome and transcription regulators. Another significant result obtained was induction of genes encoding DNA binding protein, *i.e.*, Ss07d which maintains negative supercoiling of DNA during heat shock. Heat- stress in *S.solfataricus* also caused differential expression of IS

sequences, transposes and resolvases, which are crucial for transposition and genome plasticity (Tachdjian *et al.*, 2006).

Using whole genome microarray, dynamic differential expression analysis of heat-shock response was also reported for *Halobacterium salinarium* NRC-I. The overall expression profile suggested that heat-shock resulted in the upregulation of several chaperone genes encoding for dnaK, HSP5, thermosome, HSP20, AAA<sup>+</sup> ATPase. Furthermore, gene encoding the DNA repair protein *i.e.*, SMC/Rad50 like was found to be enhanced transcription activity during heat-stress (Coker *et al.*, 2007).

In addition to the transcriptomic approach, proteomic analysis of *Halobacterium salinarium* NRC-I was also carried out in order to identify protein profiles upon heat-stress. Results showed that temperature upshift from 42 °C to 49 °C resulted in up regulation of genes encoding putative chaperons including HSP-5 and sHSP- 2, DnaJ, GrpE, sHSP1, and DNA binding proteins, which were associated with the protection of cell from multiple stresses. Overall results demonstrated that differentially expressed genes belong to the variety of functional categories such as stress response, protein folding, DNA replication and repair, transcriptional and translational regulation, and transporters (Shukla, 2006).

## **1.6.2. pH Stress in Archaea**

### **1.6.2.1. Acid Stress in Archaea**

Acidophilic archaea should develop efficient mechanisms to prevent acidification of their cytoplasm, because maintaining proper cytoplasmic pH is important for enzyme activity, protein stability, structure of nucleic acids as well as other biological molecules. Otherwise, protonation damage proteins and nucleic acids. The ways by which archaea deal with disruption of pH homeostasis are related to the cell membrane structure, regulation of proton efflux, degradation of organic acids and chaperone protection (Baker-Austin *et al.*, 2007).

To begin with, archaea possess diether or tetraether lipids in their cell membranes, and archaea have capacity to arrange degree of tetraether lipid cyclization during pH

stress. By help of this adjustment, hydrocarbon chain mobility is restricted that results in the reduction of membrane permeability to protons (Boyd *et al.*, 2013).

Two *Picrophilus* species (*P.oshimae* and *P.torridus*) are the most extreme acidophilic species that grow aerobically at pH 0-2.2 and temperatures between 45°C -65°C (opt 60°C). *P.torridus* has a very low intracellular pH of 4.6 in contrast to other thermoacidophilic organisms with internal pH close to neutral. These features makes them ideal model organisms to study adaptation mechanisms at thermoacidophilic conditions. For example, *P.torridus* membrane is specifically adapted so that having very low proton permeability and is highly stable in acid. The membrane is made up of polar ether lipids and modified derivatives. S layer proteins in association with polysaccharides from cell wall. To cope with harmful effect of unusually low intracellular pH, not only extracellular proteins, intracellular proteins should be highly acid stable (Baker-Austin *et al.*, 2007).

In addition to these, removal of excess protons is vital for pH balance. Excess protons are removed from cytoplasm through several efflux systems such as H<sup>+</sup> ATPase, antiporters, and symporters. Furthermore, efficient systems to protect and repair nucleic acids are required under the condition of acid stress. Increasing demand for chaperones is a means of protection from damage caused by pH shift. (Baker-Austin *et al.*, 2007).

#### **1.6.2.2. Alkaline Stress in Archaea**

Current knowledge of adaptation to alkaline environment is poorly explained in archaea. This response was extensively investigated in other prokaryotic organisms such as *E.coli* and *B.subtilis*. Adaptive mechanisms utilized by bacteria include increased expression of monovalent cation/proton antiporters, metabolic switching to produce acidic end products by aminoacid deaminase, increased ATP synthase activity and changing membrane composition. Up regulation of pathways that result in production of acids should aid for neutralization of the effect of the external alkaline pH (Slonczewski *et al.*, 2009).

### **1.6.2.3. Acid /Alkaline Stress Response in Different *Archaeal* Species**

There is not much information in the literature about the mechanisms of pH stress in archaea. One report explained the effects of extreme pH on three haloarchaea, *Halorubrum lacusprofundi*, *Haloferax volcanii*, and *Halobacterium sp.NRC-1* by benefiting from DNA microarray technology using whole gene expression oligonucleotide arrays.

Under growth in acidic conditions several gene transcripts were regulated in a similar fashion, including those for stress and motility. In three haloarchaea, transcriptional profiling following pH down shift revealed induction of genes involved in ABC type transport, transposition, periplasmic binding protein, protein folding. On the other hand, other group of genes whose transcript levels decreased were encoding universal stress protein A, transcriptional regulator, oxidoreductases, short chain dehydrogenase and ABC transporter.

In the alkaline stress, common response of three haloarchaea indicated that genes involve in amino acid transport, protein folding (*i.e.*, sHSPs), motility, synthesis of stress proteins (*i.e.*, universal stress proteins) were found to be up regulated. However, genes encoding dehydrogenases, which involve in metabolism, energy conversion and amino acid transport were down regulated. A noteworthy observation of this study has been the regulation of genes encoding transcription initiation factor IIB (TFB), which were thought as general transcription factor for regulating the response to an alkaline pH stress (Moran –Reyna *et al.*, 2014).

### **1.6.3. Oxidative Stress in *Archaea***

Oxidative stress is universal phenomenon experienced by 3 kingdom of life. It is caused by the production of reactive oxygen species such as superoxide ion hydrogen peroxide, hydroxyl radicals, which have detrimental effects on all macromolecules and redox homeostasis. Therefore, prominent protective mechanisms against oxidative stress are consists of free radical scavenging mechanisms, expression of redox regulatory genes, activation of DNA repair system, metal detoxification and induction of genes encoding transporters (Pedone *et al.*, 2004). Accumulation of

reactive oxygen species are highly deleterious to DNA. Therefore, cells respond to oxidative stress by activating DNA repair system. Several DNA glycosylases and dGTPases are specialized in the removal of oxidative damage (Williams *et al.*, 2007). Besides, a number of enzymes including SOD, catalase, peroxiredoxins, thioredoxin, glutathione take role in the elimination of the free radicals. SOD is capable of scavenging superoxide anions by successive oxidation and reduction of the metal ion at the active site. It catalyzes the conversion of the superoxide ion into hydrogen peroxide and O<sub>2</sub> (Cannio *et al.*, 2000).

Catalase decomposes hydrogen peroxide to water and oxygen. It was reported that all archaea do not possess catalase activity. In fact, genomes of *S.solfataricus*, *S.tokodaii*, *A.pernix*, *T.acidophilum*, and *T.volcanium* do not contain catalase orthologous (Pedone *et al.*, 2004).

Peroxidases (prx) are large family of antioxidant enzymes. They have ability to reduce and detoxify hydrogen peroxide and different alkyl hydroperoxides (Nordberg *et al.*, 2001). The gene, which has same homology to thioredoxin peroxidase has been identified in certain archaea such as *S.tokodaii*, *A.pernix*, *T.acidophilum*, and *T.volcanium* (Pedone *et al.*, 2004).

It is known that oxidative stress damage proteins by oxidizing cysteine or methionine. Such reactions most commonly inactivates proteins. However, glutathione and thioredoxin system are capable of keeping catalytical disulfide bonds in reduced form, thus eliminating the damage caused by oxidative stress (Kültz, 2005). Glutathione (GSH) is the thiol based antioxidant and high amount is present in the cells. It is a universal free radical scavenger for cells. Detoxification of free radicals can be achieved by glutathione S transferase. It catalyzes the conjugation of glutathione.

Furthermore, oxidative stress triggers cellular stress response that cause expression of redox regulatory genes. Oxidoreductases have regulatory roles in maintaining redox homeostasis. Most of the oxidoreductases that take role in stress response are dehydrogenases, including aldehyde dehydrogenases, isocitrate dehydrogenases, succinate semialdehyde dehydrogenases. Some of them are constituents of the basic

metabolic pathways like glycolysis, Krebs cycle. They may participate in redox regulation and repair of oxidative damage by producing reducing equivalents for free radical scavenging system (Kültz, 2005). Furthermore, reductases are important family of enzymes that affect cellular redox potential. They function as electron transfer from NADH to several electron acceptors. NADH oxidase is a member of this family. Function of NADH oxidase has been reported as scavenging hydrogen peroxide, so this enzyme is critical with respect to tolerating oxidative stress (Pedone *et al.*, 2004). Another protein taking role in redox homeostasis is Fe-S proteins. They represent the functional category of electron transfer, environmental signal sensing and gene regulation. Ferredoxins and rubredoxins are Fe-S proteins. Thermoacidophilic archaea contain high amount of these proteins (Blum, 2008).

#### **1.6.3.1. Oxidative Stress Response in Different *Archaeal* Species**

Effect of oxidative stress have been studied in certain group of archaea such as *Sulfolobus solfataricus*, *Pyrococcus furiosus*, *Methanosarcina barkeri*.

Behaviour of *Sulfolobus solfataricus* in response to the hydrogen peroxide have been determined by using both transcriptomic and proteomic approaches. Transcriptome and proteome analysis revealed that the most highly up-regulated gene encoded DPSL, which is the ferritin like antioxidant protein, being post transcriptionally modified. DPSL is important to cope with oxidative stress by eliminating hydrogen peroxide and ferrous ion. Other group of genes whose transcript level increased upon oxidative stress were related to the redox potential (*i.e.*, ferredoxins), metal transport (*i.e.*, inorganic ion transporter), and Fe-S cluster biosynthesis. Furthermore, ferric uptake regulator (Fur) seems to be up regulated in response to the oxidative stress. It is a transcription regulator, which functions as activator or repressor. Similar to the transcriptomics, proteome analyses of *Sulfolobus solfataricus* identified the stress related proteins such as small heat shock proteins, thermosome alpha and beta subunits, SOD, peroxiredoxin, and rubrerythrin. General expression profiles from both "omics" data revealed three proteins, DPSL, SOD, and peroxiredoxin that integrate to form a supramolecular complex for removal of ROS (Maaty *et al.*, 2009).

Another reports on oxidative stress associated transcriptome analysis conducted in hyperthermophilic archaeon *Pyrococcus furiosus* ( $T_{opt}$  100°C) using whole genome DNA microarray. Exposure to hydrogen peroxide resulted in the induction of genes encoding DNA repair proteins (*i.e.*, radA), redox proteins (*i.e.*, thioredoxin), Fe-S proteins, Dps like protein and a range of hypothetical proteins. This inducible response is considered as more acute involving primary damage repair rather than protection. The organism also maintains a constitutive protective mechanism involving high levels of oxidoreductase type enzymes such as SOD, thioredoxin, rubrerythrin, alkyl hydroperoxide reductase, Dps like protein and prismae (Strand *et al.*, 2010). Microarray results were verified by qRT-PCR.

Global oxidative stress response was also studied in *Methanosarcina barkeri* using oligonucleotide microarray. Expression of genes related to DNA replication and repair, translation, ribosomal structure and biogenesis function were the most repressed, indicating that protein synthesis was slowed down under oxidative stress. Specific outcome of this study was up regulation of genes encoding transposases, which were involved in mutational divergence. Interestingly, air exposure did not result in increased abundance of transcript levels of superoxide dismutase, catalase, thioredoxin reductase, which are the typical component of oxidative stress response (Zhang *et al.*, 2006).

#### **1.6.4. Other Stresses in Archaea**

##### **1.6.4.1. Cold Stress in Archaea**

Like up-shift of temperature, downshift of temperature is also stressful for archaea. The apparent effect of cold stress are: I) Decline in the essential cellular process such as transcription, translation, replication. II) Decrease in the activity of many enzymes accompanied by slow down of metabolism. III) Decrease in membrane fluidity.

In order to sustain survival and growth under cold stress, archaea utilize several adaptations to cope with damaging effect of this stress (Conway de Macario *et al.*, 2000).

To begin with, cold shock response involves thermal regulation of lipid composition. Fluidity of membrane is restored via various ways such as increasing unsaturated fatty acids, shortening the average chain length of fatty acids and changing the fatty acid branching from iso to anteiso (Cavicchioli, 2006).

In addition to the membrane adaptations, cold shock response restore translation apparatus function, which is compromised at low temperatures, and resolve low-temperature mediated mRNA secondary structures that would otherwise impede the translation machinery. In this respect, RNA helicases have critical functions in cold stress tolerance, since temperature downshift affects DNA related functions such as replication, transcription, and translation. It is proposed that RNA helicase might unwind duplex RNA and remove cold stabilized mRNA structures (Cavicchioli *et al.*, 2000). Another characterized cold inducible proteins are CspA homologs that function as mRNA chaperones. They prevent the formation of inhibitory secondary structures (Weinberg *et al.*, 2005).

Furthermore, protein adaptation is a way of protective mechanisms against adverse effect of cold stress response. Since protein flexibility is crucial for enzyme activity, protein adaptation should have indispensable role in response to cold stress. In this respect, cold adapted proteins have tendency to reduce number of salt bridges, aromatic interactions, charged residues in order to maintain cellular homeostasis at low temperature (Cavicchioli *et al.*, 2000).

#### **1.6.4.1.1. Cold-Stress Response in Different *Archaeal* species**

The transcriptional response of *Pyrococcus furiosus* to cold-shock, by a temperature downshift from 95°C to 72°C, was studied using whole genome DNA microarray. Results showed that *P. furiosus* cells undergo 3 different responses at 72°C: early shock, late shock and adapted responses over a 5 hour lag phase. Early response was characterized by the up regulation of genes whose products participate in translation process, amino acid and carbohydrate metabolisms, solute transport and misfolded protein degradation. Late shock response also involved increased biosynthesis of branched chain amino acids and methionine. The change in DNA topology has been associated with the adapted response of *Pyrococcus furiosus* to cold-shock, since

DNA gyrase activity was up regulated possibly to fulfil less supercoiling structure under non optimal growth condition. As well as microarray analysis and qRT-PCR analysis, 1-D SDS-gel analysis cold induced expression of CipA and CipB proteins which appear to be solute binding. These Cip proteins are homologs of bacterial cold responsive proteins, and contribute to cryoprotection (Weinberg *et al.*, 2005).

Cold adaptation was investigated in Antartatic methanogen *Methanococoides burtonii* (Topt 23°C) using proteome analysis. In order to understand regulatory mechanisms under cold stress, optimum temperature is decreased from 23°C to 4°C, which pointed out key aspects of cold adaptation related to transcriptional regulation, protein folding and energy metabolism For this adaptation, specific roles were attributed to RNA polymerase subunit E, a response regulator, and peptidyl prolyl cis trans isomerase (Goodchild *et al.*, 2004).

Cold shock response was also studied in hyperthermophilic methanarchaeon *Methanococcus jannashii* (Topt 85°C) using complete cDNA microarray by a temperature shock from 85°C to 65°C. The overall expression profile suggested that genes of functional categories such as transcription, translation, transport, protein degradation were found to be up regulated. A gene encoding topoisomerase alpha subunit was also up regulated, which demonstrated the alteration of the DNA topology. Another noteworthy feature occurring in response to cold shock was the increased transcript level of genes encoding ATP dependent RNA helicase with DEAD Box motif, representing important functional categories of translation and ribosome assembly. Also, a gene that codes for FKBP- type PPIase which may facilitate protein folding at low temperature was up regulated. However, expression of some other genes related to the methanogenesis that is the main pathway for energy production from CO<sub>2</sub> were down regulated. Down regulation of these genes implied the slow down of metabolism (Boonyaratanakornkit *et al.*, 2005).

The study of cold shock response has also been conducted with *Halobacterium salinarium* NRC-1 using whole genome DNA microarray. Transcriptional response resulting from temperature downshift from optimum growth temperature, 42°C to 15°C revealed interesting class of responsive genes. It was found that *H.salinarium*

NRC-1 enhanced transcription of genes encoding acyl-coA dehydrogenases, a long chain fatty acid CoA ligase, and acetoacetyl-coA thiolases, which are important for rearrangement of membrane lipid composition in the cold. Furthermore, one of the significantly up regulated genes were found to be cold shock genes, *cspD1* and *cspD2*, and functioning as RNA chaperones, and whose products might interact with ssDNA or RNA allowing the translation initiation under cold. In addition, gas vesicle gene expression and content were also increased in the cold. Moreover, under cold shock stress, cell growth rate significantly decreased due to the repression of genes related to the ATP production, protein synthesis and export, DNA metabolism, and taxis which were the implications of growth arrest (Coker *et al.*, 2007).

#### **1.6.4.2. Osmotic Stress in Archaea and Adaptive Responses**

Adaptation to high salinity and response to osmotic shock involves a set of molecules playing distinctive roles to maintain a physiological concentration of intracellular proteins, electrolytes, cell volume and turgor.

It was established that intracellular accumulation of compatible solutes is a common mechanism for osmotic adjustment (Conway de Macario *et al.*, 2000). Compatible solutes are small, soluble, organic molecules that do not obstruct cellular function in spite of their high concentrations. Some of the compatible solutes in archaea consists of sugars, polyols,  $\alpha$  and  $\beta$  amino acids and methylamines. Most of the archaeal type compatible solutes have a negative charge. These property is associated with their contribution to equilibrate high concentration of intracellular cations, commonly potassium ion. Also, compatible solutes have central role not only in osmotic adjustment, but also play a crucial role in maintenance of protein structure and stability (Müller *et al.*, 2005). The mechanisms for counteracting an increase in external salinity and to avoid dehydration in yeast include also metabolic pathways.

In addition to these, stress proteins can also contribute to the coping with osmotic stress (Kültz, 2003). In this regard, stress proteins or heat shock proteins including molecular chaperones have a protective function such that they prevent protein unfolding and assist refolding of partially unfolded polypeptides (Conway de Macario *et al.*, 2000).

Another protection against osmotic shock is the alteration of membrane lipid composition, which has impact on membrane fluidity, transport, and bilayer thickness. For example, abundance of cardiolipin in cell membrane could protect the cell from adverse effect of osmotic shock, i.e lysis of cell (Corcelli, 2009). Halophilic archaea have adapted to survive at high salinity by selectively up taking  $K^+$  and  $Cl^-$  ions to concentration of  $> 3M$ . Their proteins are kept soluble in this high strength condition since they have adapted to acidic proteome. Proteins contain their negative charges on the surface, thereby help orient water molecules to keep them hydrated and prevent from precipitation.

#### **1.6.4.2.1. Osmotic Stress Response in Different *Archaeal* species**

Osmoregulatory mechanisms have been studied in a number of archaeal species, particularly, *Halobacterium* species and *Methanosarcina mazei*. However, behaviour of archaea in response to osmotic stress has been poorly understood. In fact, very few osmoregulated genes have been identified so far (Gerday *et al.*, 2007).

Most of the reported osmotic stress studies on archaea to date have focused on their adaptation mechanisms to high salinity. The osmotic stress response of halophilic archaeon *Haloferax volcani* was studied at different salt concentrations using two dimensional gel electrophoresis. Under both hypo and hyperosmotic stress conditions, there was a remarkable over expression of general stress proteins and compatible solutes. Synthesis of general stress proteins *i.e.*, 71- and 46 kDa Gsps appeared to be important to generate rapid and strong response. These stress proteins were homologs of HSP70 and DnaJ like chaperones, which function for proper protein folding under hypo/hyper osmotic stress conditions. In addition, it has been pointed out that in response to high external salintiy, intracellular potassium accumulates at higher levels in order to counteract osmotic challenge. On the other hand, intracellular potassium concentration decreases dramatically at low salinity (Mojica *et al.*, 1997).

More comprehensive responses have been detected in the non halophilic archaeon *Methanosarcina mazei* using whole genome DNA microarrays. Results showed that genes that encode hypothetical proteins, metabolic enzymes, transcriptional

regulators, compatible solutes, and heat shock proteins were induced upon exposure to salt stress. Among them, metabolic enzymes such as oxidoreductases, hydrogenases, and heterodisulfide reductases were up regulated, which were accounted for the increased physiological processes. Other group of genes whose transcript level increased encoded transcriptional regulators. This implies that when the environmental changes are sensed by gene expression machinery, proteins with regulatory functions are necessary. Furthermore, putative phosphate permease gene was also up regulated, which might be associated with the increased demand for phosphate binding proteins under high salt concentrations. On the other hand, genes of different functional categories such as those of metabolic enzymes, transporters and ATP synthases have been found to be down regulated, which reflected their functional role in salt adaptation (Pflüger, *et al.*, 2007).

Similar trend was also observed in transcriptional profiling of archaeon *Halobacterium sp. NRC-1* using whole genome DNA microarrays to detect changes in the gene expression under low/high salinity. Results indicated that transcription level of stress genes encoding superoxide dismutase, and glutathione S transferase were up regulated under different osmolarity. In addition, expression of transcription factors and regulators were significantly changed under salt stress. Low salinity enhanced the transcription of basal transcription factors, but transcriptional repressor was up regulated under high salt. Transcription level of a set of genes for cellular metabolism were significantly changed upon exposure to high/low salt. Another notable result from this study was the differential expression of carboxypeptidase gene, which is critical for protein turnover. At low salinity, transcription level of this gene decreased; conversely, abundance of transcript was enhanced at high salinity (Coker *et al.*, 2007).

#### **1.6.4.3. $\gamma$ Gamma Radiation in *Archaea***

Radiation has deleterious effects on DNA due to hydroxyl radical production via radiolysis of water, imparting severe oxidative stress to cell components, mainly nucleic acids. As a response, cellular mechanisms evolved for detoxification of reactive oxygen species, and redox homeostasis are activated. Since exposure to

ionizing radiation induces DNA fragmentation, maintenance of DNA integrity is necessary for cell survival. In response to gamma irradiation the genes that encode DNA repair proteins are induced. Most archaea possess nucleotide excision repair systems (Williams *et al.*, 2007).

#### **1.6.4.4. $\gamma$ Gamma Radiation Resistance in Archaea**

Effect of gamma radiation on hyperthermophilic archaeon *Pyrococcus furiosus* was studied using whole genome DNA microarray. Due to the fact that gamma irradiation enhances oxidative stress, most of genes are regulated in order to participate in oxygen detoxification, redox homeostasis and DNA repair. The genes encoding rubredoxin, rubrerythrin, alkyl hydroperoxide reductase, and oxidoreductases were up regulated in order to eliminate free radicals as well as maintaining intracellular redox balance. Also, the gene encoding ferritin Dps like protein were up regulated. Biological role of this protein is remarkable for limiting hydroxyl radical formation by sequestering free iron atom. Furthermore, expression of some other genes related to protein folding (*i.e.*, small heat shock protein), and DNA repair (*i.e.*, RadA) were up regulated. On the other hand, as in the other stressful conditions, exposure to gamma irradiation also resulted in the repression of the metabolic functions. Down regulation of metabolic functions following gamma radiation was also a trend in *Halobacterium salinarium* strain NRC-I, *Sulfolobus solfataricus* (Williams *et al.*, 2007; Baliga *et al.*, 2004; Salerno *et al.*, 2003).

### **1.7. Model Organism**

*Thermoplasma* is fascinating microorganism that can survive under extreme pH and temperature. Optimum growth conditions are about pH 2.7 and 60 °C (Auernik *et al.*, 2008). *Thermoplasma* species have been described as facultative anaerobes and obligately heterotrophic. The organism can also grow anaerobically in the presence of elemental sulfur (Yasuda *et al.*, 1995). All known organisms belonging to order of Thermoplasmatales require yeast extract for growth (Seegerer *et al.*, 1988).

Interestingly, they are devoid of cell walls and grow as cocci or disk-and sometimes as filaments (Gerday *et al.*, 2007). The cytoplasmic membrane is made up of mainly

tetraether lipids. The availability of a cytoskeleton in *Thermoplasma spp.* is obscure and its structure has not been documented so far. Also, mechanism of cell division in *Thermoplasma spp.* is not understood (Kawashima *et al.*, 2000).

Two species have been reported for the genus of *Thermoplasma*. One is *Thermoplasma acidophilum* and the other is *Thermoplasma volcanium* (Yasuda *et al.*, 1995).

*T.volcanium* belongs to the kingdom of Euryarchaeota, and order of Thermoplasmatales. It was isolated from submarine and continental solfataras on Vulcano Island, Italy (Segerer *et al.*, 1988). Environments suitable for *Thermoplasma volcanium* have pH ranging between 1-4, and growth temperature ranging from 33-67 °C. Especially, they grow best at pH 2.0, 60 °C (Auernik *et al.*, 2008). *T.volcanium* cell shape change from pleiomorphic to spherical, with a diameter of 0.6 to 1.0 µm. They are enveloped by only plasma membrane. They possess multiple flagella that facilitates motility (Faguy *et al.*, 1996) (Figure 1.9)

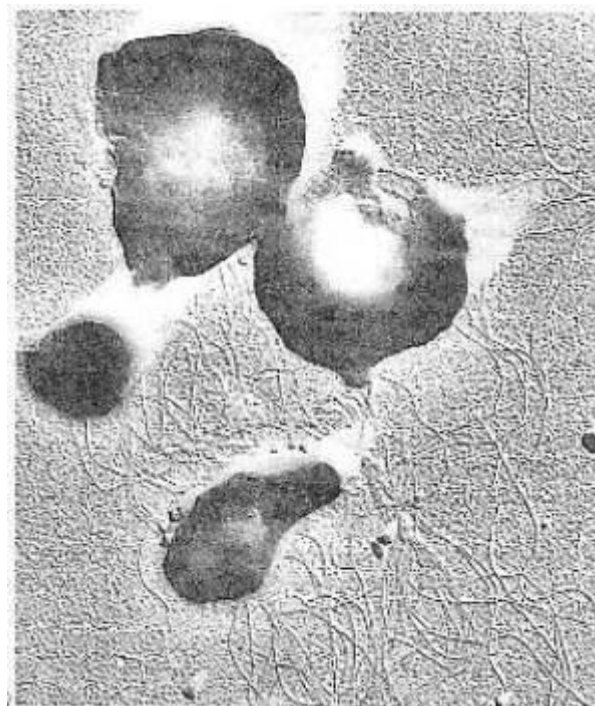


**Figure 1. 9.** Thin section of *Thermoplasma volcanium* (from Seckbach, 2000).

Their genome sequence completed in 2001, and found to be 1.6 Mb in size. Estimated number of encoded proteins were 1,499. Of the matches, 261 were hypothetical proteins and 56 were the insertion elements, including transposase, integrase, or resolvase. The G+C content of the DNA was found to be 39.9 % (Auernik *et al.*, 2008).

### **1.8. Microarray Technology**

Microarray is a technique, which quantifies transcripts levels on a global scale by quantifying the mRNA expression level of thousands of genes simultaneously (Nguyen *et al.*, 2002). In recent years, microarray technology has been widely used in several field of molecular biology due to its sensitivity and selectivity. This technology opens new horizons to determine the function of genes, proteins and new metabolic pathways (Hoheise, 2006). Furthermore, the technology is also used in diverse fields such as forensic science, cancer research, and genetic diseases.

Among these fields, DNA microarray hybridization analysis most commonly employed in gene expression analysis and detection of single nucleotide polymorphisms. This technology enables monitoring changes in the expression of the thousands of genes and genome wide gene expression data obtained by this technology are increasingly accumulating in literature (Heller, 2002). Recently, microarray was used as a transcriptomic tool to study stress response in different organisms including archaea (Blum, 2008).

DNA hybridization microarrays generally manufactured on glass, silicon or plastic substrates. Among them, glass slide microarrays are now widely used, due to its cost effective feature. DNA targets which can be synthetic oligonucleotides (oligoarrays), large DNA/RNA fragments, PCR amplicons or cDNAs (cDNA array) are selectively printed to test sites by different techniques (Falciani, 2007).

There are two major technologies used for printing glass slide microarrays: Noncontact printing and contact printing. Noncontact printing technologies use ink-jet printing technologies to spot small volume of liquid onto a solid surface. Deposition of the liquid depends on the electrical pulse that tighten the hose in such a

way the liquid is released on to the surface. Each time a nucleic acid is printed, the spot is termed as a feature. Following printing, the microarrays are permanently bound to the printed DNA and then surface of the array is deactivated in order to minimize high back ground signal caused by non specific interactions. Then, microarray wafers are separated into individual microarrays and are bar coded for identification. This technology is suitable for printing of *in-situ* synthesis of oligonucleotides or presynthesized oligonucleotides. This printing method was develop from commercial organizations, of which Agilent is very well known. On the other hand, in contact printing, transferring of solution depends on the capillary force. This is achieved by dipping pins into the DNA solution and transferring the fluid by direct contact with array using robotic spotting machines (Mèuller *et al.*, 2006).

In order to produce hybridization probe, total RNA is isolated from control and test groups. In vitro synthesized cDNAs or cRNAs, then are fluorescently labelled with either cyanine dyes (*i.e.*, Cy2, Cy3 and Cy5) or their analogs. Hybridization reaction occurs between fluorescently labelled reporter probes and target DNA on the chip under high salt concentrations that enhance the intermolecular base pairing. After hybridization, several washings are performed in order to eliminate nonspecifically bound probes. Slides are then dried prior to the scanning (Falciani, 2007)

Scanning is employed to generate microarray images. During scanning process, intensity of each spot is determined and foreground and background intensities are calculated for each spot, and then quality measurements are done in order to check how good and reliable intensities are measured. Comprehensive data analysis is achieved by using variety of bioinformatic tools (Heller, 2002).

One of the best known oligo array is Affymetrix array. They have been widely used in genome wide transcriptional profiling. Affymetrix arrays use multiple, short oligonucleotides specifically 25-mer for the detection of a given transcript (Falciani, 2007). Probes are designed for each gene, both as perfect match probes and mismatch probes containing a nucleotide mismatch to detect the unspecific signal

and background signal. Oligomers on the solid substrate (-a quartz wafer) is directly synthesized using DNA synthesis chemistry and an adaptation of photolithography masking technique. Photolithographic masks are taking role in either blocking or let light to pass different sections of solid surface. Once the specific regions of surface that is modified with protective groups is exposed to UV light, oligonucleotides are synthesized. This illumination results in the reactive hydroxyl group production that is coupled with the addition of phosphoramidites, which are also protected at their 5'-hydroxy position, to the substrate. In this way, different oligonucleotides are synthesized on the surface (Falciani, 2007). Agilent Technologies also provides *in situ* synthesized oligonucleotide microarrays in which oligos are synthesized directly on the glass microarray surface based on standard phosphoramidite chemistry (Figure 1.10). The best set of the probes are designed based on such criteria as  $T_m$ , base composition, basic probe suitability, and low potential for cross hybridization (Agilent Microarray Technology manual).

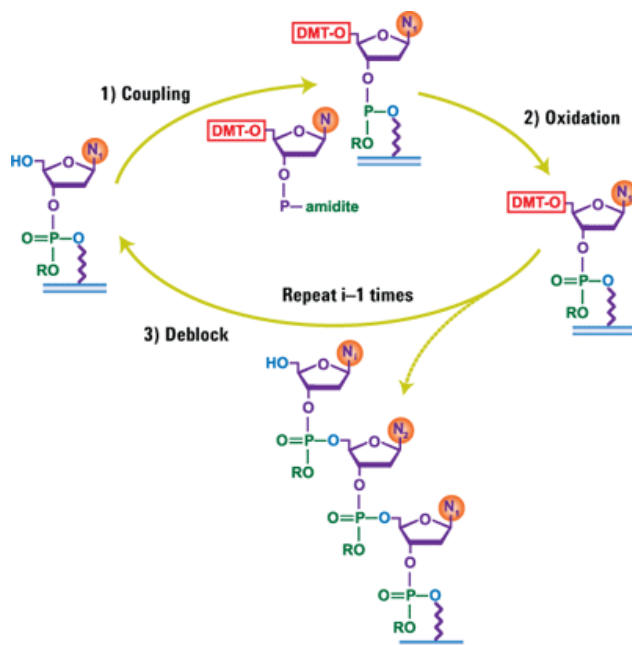


**Figure 1. 10. General cycle of oligo synthesis via phosphoramidite chemistry** (from Agilent Microarray Technology manual).

## 1.9. Aim

In this thesis, to analyze the global gene expression of *Thermoplasma* spp. in response to environmental stress, we have used whole genome oligonucleotide microarray. Transcriptome analyses were conducted using three conditions including severe heat-shock (at 68° C), pH stress (pH 5.0) and oxidative stress (0.03 mM H<sub>2</sub>O<sub>2</sub>) relative to cultures grown under optimal conditions. Verification of the microarray results for a set of *Tpv* genes was achieved by using qRT-PCR technique. The resulting data set allowed us to advance our understanding of the stress response of *T. volcanium* that has been previously investigated under mild stress conditions in our laboratory. In addition, novel stress specific candidate genes and regulatory pathways, as well as potential mechanisms for stability of biomolecules were documented.

## CHAPTER 2

### MATERIALS AND METHODS

#### 2.1. Materials

##### 2.1.1. Chemicals, Enzymes and Kits

Agarose, lysozyme, Tris, MOPS, glycerol, formamide, DEPC, ethidium bromide were bought from Sigma Aldrich ® (Missouri, USA). Glucose and hydrogen peroxide were bought from Applichem, Inc. (Missouri, USA). NaOH, Bromophenol Blue, 2 mercaptoethanol, sodium acetate anhydrous, EDTA, formaldehyde were purchased from MERCK (Germany, Darmstadt). Yeast extract was bought from Difco (Detroit, USA). Absolute ethanol was purchased from Riedel-de Haën (Germany)

RNA 6000 Nano Kit, Low-Input QuickAmp WT labeling kit, RNA Spike - In Kit were purchased from Agilent Technologies Inc. (Santa Clara, California, USA). Revertaid H minus First strand cDNA synthesis kit was bought from Thermo Scientific (Waltham, MA). LightCycler Fast Start DNA Master Plus SYBR Green I Kit was bought from Roche (Switzerland). RNeasy Mini Kit and RNA Protect Bacterial Reagent were supplied by Qiagen (Valencia, USA)

##### 2.1.2. Buffer Solutions

All buffer solutions and their components are listed in Appendix A.

#### 2.2. Media and Culturing Conditions

*Thermoplasma volcanium* GSS1 strain was grown in standard Volcanium Medium (pH 2.6), containing 0.5 % glucose and 0.1 % yeast extract at 60°C without shaking for routine uses (Kocabiyik *et al.*, 2007). According to the experimental needs either 100 mL or 1000 mL cultures were prepared.

### **2.3. Growth Under Stress Conditions**

For the each stress experiments, growth kinetics of *T.volcanium* cultures were studied to identify growth limiting temperature, pH, or H<sub>2</sub>O<sub>2</sub> concentrations for microarray experiments. For this purpose, cell cultures were prepared in 250 mL Erlenmeyer flasks containing 75 mL of Volcanium medium (pH 2.6) supplemented with glucose and yeast extract. After inoculation, cultures were incubated at 60 °C for 2-3 days until reaching mid-exponential phase with an optical density of 0.2-0.4 at 600 nm, as detected by UV visible spectrophotometer (UV-1601, Shimadzu, Japan). For heat shock experiments, *T.volcanium* cultures were grown at 60 °C until mid log phase, then subjected to heat shock by temperature up shift to 68 °C for 1 hour. For pH stress experiment, *T.volcanium* cultures was grown in liquid Volcanium medium (pH 2.6) until mid log phase, then pH of the medium was raised to 5.0 for 1 hour. For the oxidative stress experiments, mid log cultures were supplemented with 0.02 mM H<sub>2</sub>O<sub>2</sub>, and 0.03 mM H<sub>2</sub>O<sub>2</sub> and cell growth was continued for an additional 1 hour at 60 °C. The control cultures were grown under optimum conditions (60 °C, pH 2.6), without any H<sub>2</sub>O<sub>2</sub> supplementation. Following 1 hour induction, from test cultures and from control cultures, cells were harvested by centrifugation at 5.000 g for 10 min (Sigma 3K30 Centrifuge (Germany)).

### **2.4. Methodology**

#### **2.4.1. RNA Extraction**

Prior to the RNA isolation, Diethylpyrocarbonate (DEPC) treatment was applied to inhibit RNase activity and cleaning of the glasswares used during RNA isolation. The millique water that was used for buffer preparation and cleaing of the glassware is supplemented with DEPC at a ratio of 0.1% (v/v). Then, together with rinsed glasswares, they were autoclaved or sterilized in the oven to destroy the residual chemical.

Total RNA was isolated from both stress exposed and untreated cells by following the Qiagen RNeasy mini kit protocol. RNprotect® Bacteria Reagent was added to the *T.volcanium* cell pellet and dissolved immediately by vortexing for 5 s. After

incubation for 5 min at room temperature, the suspension was centrifuged for 10 min at 5000 g. The supernatant was discarded and the cells were lysed in 100  $\mu$ L TE buffer containing 1 mg lysozyme by vortexing. After incubation for 10 min at room temperature, 350  $\mu$ L of RLT buffer containing beta-mercapto-ethanol was added and vortexed vigorously. Then, 250  $\mu$ L of ethanol (96-100 %) was added into mixture, and solution was mixed well by pipetting. The cell lysate was transferred to the RNeasy Mini spin column placed into 2 ml collection tube and centrifuged for 15 s at 12.000 rpm. Then, flow through was discarded and 700  $\mu$ L of RW1 buffer was added to the spin column and centrifuged for washing membrane at 12.000 rpm for 15 s. Later, collection tubes with flow through were discarded. The spin column was put onto new 2 ml collection tube and 500  $\mu$ L of buffer RPE was added and centrifuged for 15 s at 12000 rpm. The flow through was discarded and centrifugation was performed once more. Finally, spin columns were transferred to new 1.5 ml collection tube, and 30  $\mu$ L RNase free water was added. After incubation at room temperature for 2 min, the tubes were centrifuged for 1 min at 12.000 rpm to elute the RNA. The RNA samples were stored at -80°C until use.

## **2.5. RNA Denaturing Agarose Gel Electrophoresis and Visualization**

Initial checks for the RNA samples were done by agarose gel electrophoresis. To get rid of the secondary structures, electrophoresis was performed under denaturing conditions.

Agarose gel (1.2 % w/vol) was prepared using 10 X FA gel buffer (supplemented with formaldehyde) that was prepared with RNase free water. Then, agarose gel was poured to the gel tray and after it solidified, the gel was placed in the gel tank, and 1X FA running buffer was poured for equilibration before sample loading. For the sample preparation, RNA sample (10  $\mu$ L) was mixed with 3  $\mu$ L of 5X loading buffer. Then, samples were heated on water bath at 65 °C for 5 min and chilled on ice for 2 min. Then, electrophoresis was carried out using the Bio –Rad power supply, at a constant voltage and current for 1.5 hour. After run was completed, the gel was examined under UV light and photography was taken by Vilber Lourmat gel imaging system (Marne La Vallee Cedex 1, France).

## 2.6. RNA Quality and Quantity Measurements

Following total RNA isolation, the quantity and quality of the RNA samples were assessed for transcriptome analysis. To this end, RNA concentrations were determined by picodrop measurements (Picopet 01, Picodrop Ltd. UK). Also, quality checks were done using an Agilent RNA 6000 Nano kit using Agilent 2100 Bioanalyzer (Agilent Technologies Inc. Santa Clara, California, USA).

### 2.6.1. Determination of RNA Concentration by Pico Drop

Picodrop was used for determination of RNA concentration directly with help of UVpette tips by pipetting 3  $\mu\text{L}$  of RNA sample. Picodrop measurement yielded the RNA concentration as  $\text{ng}/\mu\text{L}$ , as well as, optical density ratios of A260/A280 and A260/A230.

### 2.6.2. Qualitative and Quantitative Analysis of RNA Samples by Agilent 2100

#### Bioanalyzer

Agilent RNA 6000 Nano Kit together with supplied chips and reagents were used for quality and quantity analysis of isolated RNA samples following the Agilent RNA 6000 Nano Kit Quick Start Guide protocol. First, RNA samples were denatured at 70°C for 2 min to relieve secondary structure of RNA and to make it single stranded. Then, chip priming station was set up as shown in the Figure 2.1.



**Figure 2. 1. Setting up the Chip Priming Station** Firstly, new syringe is inserted into clip, and it is slid into the hole of luer lock adapter, and it is tightly screwed to chip priming station. Secondly, base plate is adjusted, which is lifted and inserted into position C. Thirdly, the syringe clip is adjusted by releasing the lever of the clip, and then it is slid up to top position ( from Agilent RNA Nano Kit Guide, 2013).

Then, gel was prepared such that 550  $\mu\text{L}$  of RNA 6000 Nano gel matrix was pipetted and transferred to the spin column. Then, it was centrifuged at 15,000 g for 10 min. Later, 65  $\mu\text{L}$  of filtered gel aliquot was delivered into the 0.5 mL RNase free micro centrifuge tubes. Next, 1  $\mu\text{L}$  of dye was added into the 65  $\mu\text{L}$  aliquot of filtered gel. After then, solution was mixed well via vortex and it was spinned at 1300 g for 10 min at room temperature. Next, nano chip was placed on the chip priming station. Then, 9  $\mu\text{L}$  of gel-dye mix was put into the dark circle G well. After closing the chip priming station, plunger was pressed down, and waited for 30 sec for moving gels through channels, then clip was released. After waiting for 5 s, plunger was pulled back slowly, and 9  $\mu\text{L}$  of gel-dye mix was put into the wells marked light circle G. Next, 5  $\mu\text{L}$  of RNA 6000 Nano marker (green ) was loaded into 12 samples wells as well as ladder well, and 1  $\mu\text{L}$  of ladder was loaded to the ladder well. Then, 1  $\mu\text{L}$  of samples were loaded to the 12 sample wells. After ladder and samples were loaded, the chip was placed horizontally in the adapter of IKA vortexer, and vortexed for 1 min at 2400 rpm. Finally, the assay was run on the Agilent 2100 Bioanalyzer instrument. Results were obtained and analyzed by the help of the Agilent 2100 Expert Software.

## **2.7. Microarray**

Genome wide transcriptional profiling under extreme stress conditions have been investigated using Agilent Custom Expression Oligo microarray.

### **2.7.1. Array Design and Printing**

*T.volcanium* custom microarrays 8x60K (SurePrint HD format) were designed by SEM Ltd., (Turkey) using Agilent eArray in two slides (8 array per single slide). The arrays were prepared for three biological replicates for each stress condition, and four biological replicates for control (total 16 arrays). Custom arrays were constructed by designing all possible oligonucleotide primers to cover all expressed open reading frames of *Tpv* genes. While designing probes, the most important criteria that were considered are melting temperature (80°C), low potential for cross hybridization, and base composition. In the design, repeated regions were masked. Overall, the array

contained total 7,458 probes, out of which 1,474 matched-up with *T. volcanium* specific expressed ORFs. Also, in the design 1,319 Agilent control probes were included in each array. Eight copies of each probe were spotted on the array by inkjet printing. Designed microarray slides were manufactured by Agilent Technologies Inc (Santa Clara, California, USA).

### **2.7.2. cDNA Synthesis, Labelling and Hybridization**

The cDNA synthesis, amplification, cRNA synthesis and labeling were achieved by using Agilent's Low-Input QuickAmp WT labeling kit and RNA Spike - In Kit.

More specifically, cDNA was prepared with equal amount of RNA from four biological replicates of untreated samples and three replicates of the each one of the stress exposed samples. RNA concentrations were adjusted by dilutions to approximately 50 ng. Primer master mix was prepared using Agilent's Low-Input QuickAmp WT labeling kit in such a way that 3  $\mu\text{L}$  of the WT primer master mix was added to the tube containing 2.3  $\mu\text{L}$  of total RNA so as to denature primer and template. Then, the mixture was incubated at 65°C for 10 min using thermocycler (Techgene, UK). The cDNA master mix was prepared by addition of 40  $\mu\text{L}$  of 5X first strand buffer, 20  $\mu\text{L}$  of 0.1 M DTT, 10  $\mu\text{L}$  of 10 mM dNTP mix and 24  $\mu\text{L}$  of AffinityScript RNase Block Mix.

An aliquot of cDNA master mix (4.7  $\mu\text{L}$ ) was distributed to the each sample tube and incubated for 2 hours at 40°C, and then for 15 min at 70°C in thermocycler. (Techgene, UK). Later on, samples were incubated for 5 min on ice and they were spinned in a microcentrifuge to drive down tube contents from the tube walls and lid.

Thereafter, cRNA synthesis including labeling were done by preparing transcription master mix. Following components were added in the given order 15  $\mu\text{L}$  of nuclease free water, 64  $\mu\text{L}$  of 5X transcription buffer, 12  $\mu\text{L}$  of 0.1 M DTT, 20  $\mu\text{L}$  of NTP mix, 4.2  $\mu\text{L}$  of T7 RNA polymerase Blend and 4.8  $\mu\text{L}$  of Cyanine 3-CTP were mixed. A 6  $\mu\text{L}$  volume of transcription master mix was added to the each sample tube and mixed by pipetting. Later, samples were incubated at 40°C for 2 hour using thermocycler. Labelled cRNAs were cleaned up with Qiagen's RNeasy mini spin

columns, according to the manufacturer's instructions (Valencia, USA). Before proceeding with hybridization, quantity of purified cRNAs was assessed using NanoDrop ND-1000 UV-VIS spectrophotometer version 3.2.1. Accordingly, cRNA yields and specific activity values were calculated for hybridization. Then, samples were prepared for the hybridization. Specific volume of labeled cRNA, 10X blocking agent, nuclease free water, and 25X fragmentation buffer were added for each microarray, and incubated at 60°C for 30 min. After then, hybridization mix including cRNA and hybridization buffer was prepared to stop fragmentation reaction. Then, correct volume of hybridization mixture was loaded onto the gasket flask. Hybridizations were performed under optimized conditions with Agilent Microarray Hybridization Chamber at 65°C for 17 hour. Afterwards, microarray slides were washed to ensure high quality microarray data. A flowsheet for microarray processing is given in Figure 2.2.

### **2.7.3. Slide Scanning, Feature Detection and Normalization**

Slides were scanned using Agilent High Resolution (G2565CA) Scanner System. 61 x21.6 mm area was scanned with 3 µm resolution and raw data image files were generated. Then, information regarding probe features was extracted from microarray scan data with Agilent Feature Extraction Image Analysis software. Quantile normalization method was used to normalize Agilent one color microarray signals.

### **2.7.4. Microarray Data Processing**

The data visualization and analysis was performed using Agilent's Genespring GX software (Demo Ver. 12.6). In quantile normalization, for each probe, the median of log summarized values of control samples were calculated, and then this was used for baseline transformation of all samples. Moderated t- test statistic was applied in order to calculate difference in gene expression compared to the within group variation. For the p- value calculation, asymptotic analysis was used which assumes that genes are normally distributed and variances within the groups are the same. Then, Benjamini- Hochberg false discovery rate (FDR) analysis, (a kind of multiple testing correction method) was applied to adjust the p value. Based on these

statistical analysis, changes in the gene expression at a magnitude of 2- fold or more, and 95 % confidence level ( $p < 0.05$ ) were considered statistically significant. Software based quality control on samples was assessed by generating three dimensional Principle Component Analysis (3D PCA) plots , correlation plots, correlation coefficients, and heat maps together with hierarchical clustering. For the calculation of the correlation coefficients, Pearson Similarity Metric was used. Cluster analysis was performed using hierarchical algorithm that generates a tree where the branches contain similar samples. Similarity of genes was determined by using Euclidean distance measures. Centroid linkage rule was used to assess the average distance between two clusters. Furthermore, volcano plots, histograms, box-whisker plots and scatter plots were also generated in order to visualize the processed microarray data, as well as to facilitate the data interpretation.

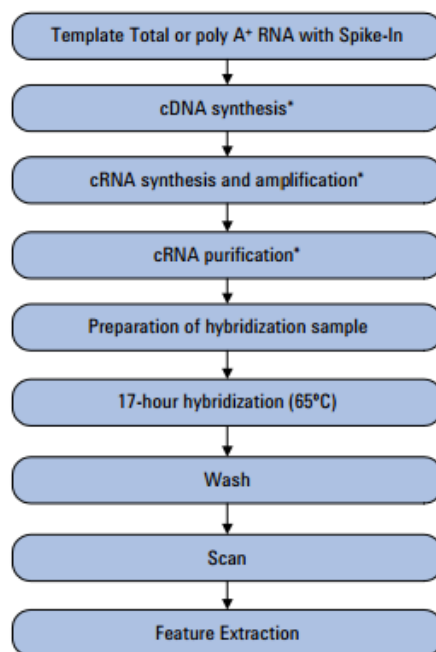


**Figure 2. 2.Workflow for microarray processing** (from Microarray-Based Gene Expression Analysis Low Input Quick Amp Labeling V6.6. Protocol, 2014).

## **2.8. Real Time Quantitative RT- PCR**

Gene expression results obtained from oligoarray platform were verified by Quantitative Real Time Reverse Transcription PCR (qRT-PCR). Some set of genes which were found to be significantly up- or down- regulated as deduced by microarray analysis were selected for further analysis by qRT-PCR technique. This analysis was performed by following two step protocol:

First step involves the reverse transcription of RNA into cDNA. In the second step, amplification of the PCR products were detected in real time. Then, a quantitative analysis was performed by the help of an on-line software programme.

### **2.8.1. First Strand cDNA Synthesis**

First strand cDNA was synthesized following the Revertaid H minus First Strand cDNA Synthesis Kit's protocol. To begin with, 0.2 µg of RNA samples and 20 pmol gene specific reverse primers were mixed in sterile PCR tubes. The list of primers used in cDNA synthesis and RT-PCR is shown in Table 2.1 and Table 2.2. Afterwards, total volume was completed to the 12 µL by addition of RNase free double distilled water. Then, mixture was denatured at 65 ° C for 5 min in a thermal cycler (Techgene, UK). After denaturation, other components of the kit were added in the following order: 4 µL of 5X reaction buffer, 1 µL of RNase inhibitor, 2 µL of 10 mM dNTP mix and 1 µL of Reverse Transcriptase were mixed well by pipetting. Next, incubation was carried out for 60 min at 42 ° C and reaction was stopped by heating at 70 ° C for 5 min in thermal cycler (Techgene, UK). The cDNA samples were stored on ice or at -20° C until use.

**Table 2. 1. Gene specific forward primers (Fp)**

<b>Fp-TVN0932</b>	5' ACCAGAGCTATACAGGGACTCAA 3'
<b>Fp-TVN1392</b>	5' GCGGCTACGTATCCTCATATTT 3'
<b>Fp-TVN1466</b>	5' CGGAAAATCAATTGTGATACTAGATG 3'
<b>Fp-TVN1284</b>	5' CTATGGGGGCAAGCATAGC 3'
<b>Fp-TVN0164</b>	5' ATGAAGATATCGCCAAACAGC 3'
<b>FP-TVN1343</b>	5'-AAGCTCTTCCATTTGTATGCTGA-3'
<b>FP-TVN0875</b>	5'-GGCCAAATCCAGATGTACTCA-3'
<b>FP-TVN0570</b>	5'-CCTCGCAAGTAAGCCTTATGA-3'
<b>FP-TVN1426</b>	5'-TCCGTGCTCATAACACACAGC-3'
<b>FP-TVN1600</b>	5'-TCCCAAACGCAGATCCTATC-3'
<b>FP-TVN0123</b>	5'-ACAAAAGGAGTTTCTAATTACCCTTG-3'
<b>FP-TVN0835</b>	5'-CAGTGGCGGCCCTACTTAC-3'
<b>FP-TVN0167</b>	5'-GAAGCTTGATGTCCCTGGAA-3'
<b>FP-TVN1390</b>	5'- AGGCGACAGTTGGCAAGATA-3'
<b>FP-TVN0830</b>	5'- TTGTGGATTTTGATCCTATTGATTT-3'
<b>FP-TVN0021</b>	5'-CCGTTCTCTCCCTGTATCTCC-3'
<b>FP-TVN0401</b>	5'-GGAAATTCGTTATAGCCGGTTC-3'
<b>FP-TVN1285</b>	5'-AGTACGATGTGGAGGCGAAG-3'

**Table 2. 2. Gene specific reverse primers (Rp)**

<b>Rp-TVN0932</b>	5' TCGTATACTTTTGCAGGTATCGAG 3'
<b>Rp-TVN1392</b>	5' AAAGCGATATGCCCTTATCTGTA 3'
<b>Rp-TVN1466</b>	5' TGCCTCGTTATATGATAGAGGACAT 3'
<b>Rp-TVN1284</b>	5' TCGCATGCGGTATATGGAC 3'
<b>Rp-TVN0164</b>	5' ACAATTGATATATTTGCGATCTGG 3'
<b>RP-TVN1343</b>	5'-TCGATGCCCTATAAACCAGAG-3'
<b>RP-TVN0875</b>	5'-TTGCCCTCGTCCATTAATTC-3'
<b>RP-TVN0570</b>	5'-GCCAAATAAAGAGCCGAAATC-3'
<b>RP-TVN1426</b>	5'-GTAGTAGTTCCGGTGCTAGATGC-3'
<b>RP-TVN1600</b>	5'-TCATTGTTTACTCGAGACCCTTT-3'
<b>RP-TVN0123</b>	5'-AGCCCAATCCATTAGGAACC-3'
<b>RP-TVN0835</b>	5'-TGGCACATTTAGCTTTCGTA-3'
<b>RP-TVN0167</b>	5'-ATGAGGTGCTCCCAATGGT-3'
<b>RP-TVN1390</b>	5'- AGAGGCCCTGGACCTTAG-3'
<b>RP-TVN0830</b>	5'-GGGCATTGCAGAAATACGA-3'
<b>RP-TVN0021</b>	5'-TGAGGTTATGGCAGCGAATA-3'
<b>RP-TVN0401</b>	5'-CGTACACTATGTAGGATATGAATGACG-3'
<b>RP-TVN1285</b>	5'-TATAGGAGTCCATTCCGTAGCA-3'

### 2.8.2. Real Time PCR

For the real time PCR, LightCycler Fast Start DNA Master Plus SYBR Green I Kit (Roche Diagnostics, Switzerland) was used. In a 1.5 mL reaction tube, master mix per 20  $\mu\text{L}$  was prepared including 9  $\mu\text{L}$  double distilled water, 1  $\mu\text{L}$  of reverse primer, 1  $\mu\text{L}$  of forward primer and 4  $\mu\text{L}$  of Master mix. Then, 15  $\mu\text{L}$  of the master mix was put into each pre-cooled light cycler capillary and to each 5  $\mu\text{L}$  of cDNA samples was added. For the negative control groups, instead of cDNA, 5  $\mu\text{L}$  of water was added. After brief centrifugation, the capillaries were transferred into instrument (LightCycler®1.5, Roche).

The analysis of the experiment results was done by using LinReg PCR software program. PCR efficiencies for each sample was calculated via this program. The  $\Delta C_p$  values and fold changes were calculated as follows:

$$\text{FC} = \text{Efficiency}^{-\Delta C_p} \quad \Delta C_p = C_p \text{ test} - C_p \text{ control}$$



## CHAPTER 3

### RESULTS AND DISCUSSION

#### 3.1. Determination of Growth Restrictive Parameters for Transcriptional Profiling

The most restrictive growth conditions in terms of temperature, pH, and H<sub>2</sub>O<sub>2</sub> were determined by plotting growth curves.

To find out the growth limiting temperature, *Tpv* cultures were grown at different temperatures and growth curves were plotted as shown in Figure 3.1. As the temperature increased, the growth rates of cultures were decreased. Specific growth rate ( $\Delta\text{Abs}_{600} \cdot \text{h}^{-1}$ ) of *T.volcanium* cells grown at optimum temperature (60°C) was decreased dramatically from  $3.2 \times 10^{-3}$  to zero when the growth temperature was increased to 68°C. One hour after temperature up shift to 65°C, growth rate was  $2.4 \times 10^{-3}$ . Based on this result, the most growth inhibiting temperature for *Tpv* was found to be 68°C and this temperature was used for heat shock in transcriptional profiling studies.

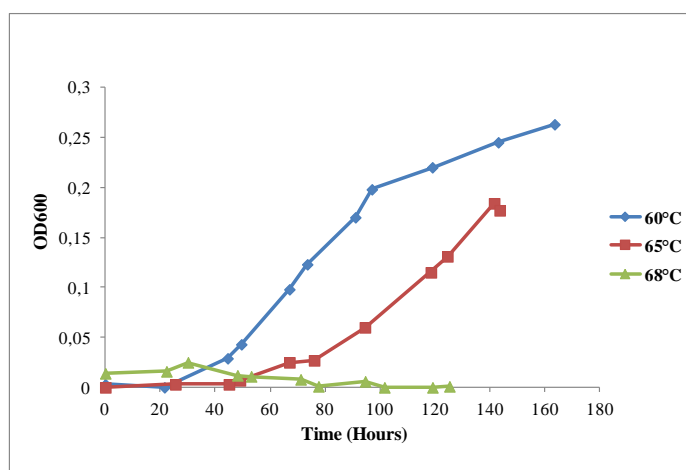
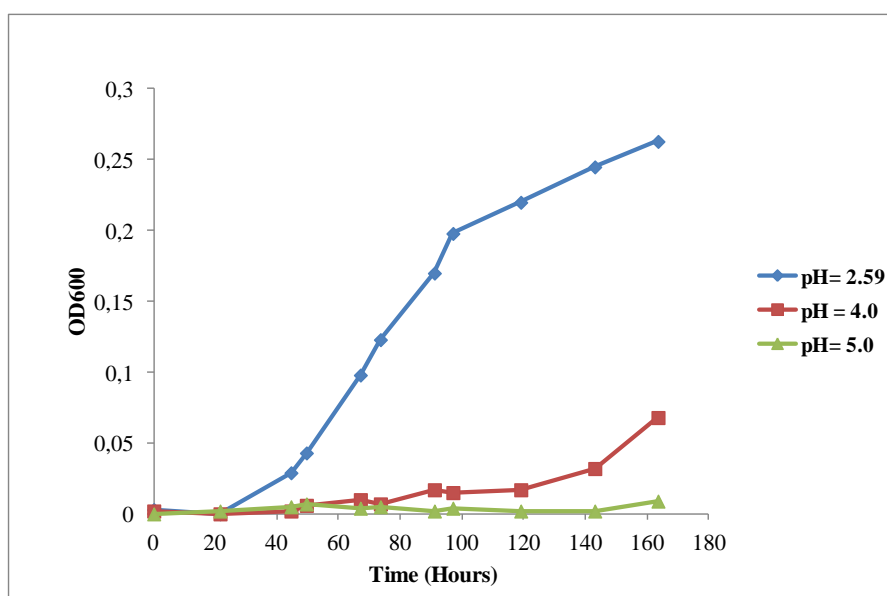


Figure 3. 1. Growth curves of *Thermoplasma volcanium* GSS1 strain grow in optimum temperature and suboptimal temperatures 65°C and 68°C.

Secondly, growth profile of *T.volcanium* at optimum pH (pH 2.59) was compared to that of suboptimal pH values. From growth curve, slope of exponential phase line gives the specific growth rate ( $\Delta\text{Abs}_{600}\cdot\text{h}^{-1}$ ). At the optimal condition of pH 2.59, specific growth rate was found to be  $3 \times 10^{-3}$ . On the other hand, growth rates of other cultures under the suboptimal conditions (at pH 4.0 and 5.0) are approaching zero (Figure 3.2). It was noticed that the growth was significantly impaired when the pH was shifted to the pH 5.08. Therefore, this pH was chosen as a growth limiting stress factor to be considered in gene expression profiling. The RNA was harvested from *T.volcanium* cultures at mid-exponential phase following pH shift from 2.6 to 5.0 for 1 h.



**Figure 3. 2. Growth curves of *Thermoplasma volcanium* GSS1 strain grow in optimum pH (2.59) and suboptimal pH values (pH 4.0; pH 5.0) at 60°C.**

Lastly, the effect of  $\text{H}_2\text{O}_2$  at different concentrations on growth was investigated by growing *T.volcanium* cells separately in liquid media containing 0.02 mM  $\text{H}_2\text{O}_2$ , or 0.03 mM  $\text{H}_2\text{O}_2$ , or 0.04  $\text{H}_2\text{O}_2$ , or 0.05 mM  $\text{H}_2\text{O}_2$ . Growth kinetics of supplemented cultures were followed as shown in Figure 3.3.

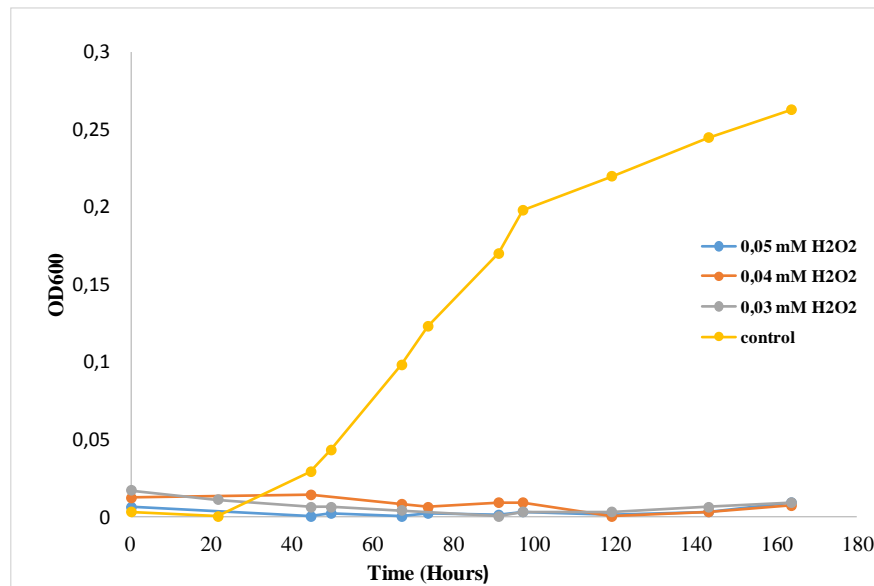


**Figure 3. 3. Growth curves of *Thermoplasma volcanium* GSS1 strain in liquid volcanium medium supplemented with 0.03 mM, 0.04 mM and 0.05 mM H<sub>2</sub>O<sub>2</sub>**

According to the growth profile, cell density was decreased as the H<sub>2</sub>O<sub>2</sub> concentration increased when compared to the untreated cultures (Figure 3.3). The growth was remarkably arrested when cultures were exposed to > 0.025 mM H<sub>2</sub>O<sub>2</sub>. Data for concentration ≤ 0.025 mM H<sub>2</sub>O<sub>2</sub> was evaluated from a previous study conducted in our laboratory (Doldur, 2008) and 0.02 mM H<sub>2</sub>O<sub>2</sub> was selected as sub-lethal concentration to induce mild oxidative stress in this project.

Growth profiles of *T.volcanium* cells grown in the presence of 0.03 mM H<sub>2</sub>O<sub>2</sub> and 0.04 mM were almost indistinguishable, and cell death occurred when H<sub>2</sub>O<sub>2</sub> at that concentrations was added to the medium at mid log stage. Therefore, 0.03 mM H<sub>2</sub>O<sub>2</sub> was selected as lethal concentration to provoke severe oxidative stress for our transcriptional profiling experiments. After the determination of the critical concentrations of H<sub>2</sub>O<sub>2</sub>, total RNA was isolated from multiple biological replicates and technical replicates of the 1 hour oxidative stress exposed cultures as well as untreated cultures. Reason for RNA isolations from several replicates is that high quality RNA is required for gene expression profiling studies.

## 3.2. Quantity and Quality Measurements of Isolated RNA Samples

### 3.2.1. Pico Drop Measurements

#### 3.2.1.1. RNA from Untreated Cultures (Controls)

RNA concentrations were determined by using Pico Drop. Purity of RNA samples was assessed based on ratios of  $A_{260/280}$  and  $A_{260/230}$ . Nucleic acids absorb UV light at 260 nm, and proteins absorb UV light at 280 nm. Accordingly, if the ratio of absorbance at 260 nm and 280 nm is 2.0, it indicates a pure RNA (Wilfinger *et al.*, 1997). Expected  $A_{260/230}$  ratio for pure RNA is close to the 2.0. For Pico drop measurements of RNA samples isolated from untreated cells (controls) are listed in Table 3.1. Most of the  $A_{260}/A_{280}$  results were compatible with the expected values. However, some of the RNA samples yielded low ratio of absorbance at 260 nm and 230 nm. This could be due to contamination with guanidine isothiocyanate found in the lysis buffer (Qiagen Newsletter, 2010). For the microarray analysis, selection of RNA samples were not only based on Pico Drop measurements, but for more sensitive RNA quality checks, Agilent Bionalyzer system was used.

**Table 3. 1. Concentrations of total RNA isolated from control groups**

<b>Samples</b>	<b>Isolation date</b>	<b>Concentration (ng /<math>\mu</math>L)</b>	<b>A260/A280</b>	<b>A260/A230</b>
C1.1	4.12.13	57.7	1.915	1.080
C1.2	4.12.13	75.1	1.95	1.974
C2.1	4.12.13	134.2	2.541	0.698
C2.2	4.12.13	113.2	2.378	0.817
C1	11.12.13	382.1	2.059	2.48
C2	11.12.13	332.5	2.059	1.958
C1	31.01.14	163.0	2.139	1.578
C2	31.01.14	250.5	2.152	1.163

### 3.2.1.2. RNA from Heat Stress Groups (68°C)

Pico Drop measurements of RNA isolated heat shock groups revealed that the ratio of absorbance at 260 nm and 280 nm was consistent with the expected ones. The measurements for selected samples are given in Table 3.2. A low  $A_{260}/A_{230}$  ratio was also experienced with RNA samples from heat stress groups. Therefore, bioanalyzer results and gel images were also used while evaluating the RNA samples of all stress conditions for microarray experiments.

**Table 3. 2. Concentration of total RNA isolated from heat shock groups**

Samples	Isolation Date	Time (Hour)	T (°C)	Concentration (ng/ $\mu$ L)	A260/280	A260/230
HS1	11.12.13	1	68°C	205.6	2.144	0.787
HS2	11.12.13	1	68°C	33.2	1.703	1.416
HS1	20.12.13	1	68°C	170.8	2.027	0.680
HS2	20.12.13	1	68°C	192.4	1.961	1.525

### 3.2.1.3. RNA from pH Stress Groups ( pH 4.0 and pH 5.0)

RNA concentrations of several samples isolated after up-shift of the pH of the growth medium were measured using Pico Drop. A summary of measurements for selected RNA samples is shown in Table 3.3. According to the results, ratio of absorbance at 260 nm and 280 nm was ideal from the point of RNA purity. However, as in the control groups, increased absorbance at 230 nm was observed for most of the pH samples. It was especially noticed when the yields of RNA samples were low (*e.g.*, samples pH 2, and pH2.2) caused this problem. Quality assessment of these samples was also performed using Agilent Bioanalyzer System.

**Table 3. 3. Concentration of total RNA isolated from pH stress groups**

Samples	Isolation Date	Time (Hour)	pH	Concentration (ng / $\mu$ L)	A260/280	A260/230
pH 2.1	20.12.13	1	5.0	139.1	2.03	1.20
pH2.2	20.12.13	1	5.0	94.5	2.07	0.70
pH1	31.01.14	1	5.0	204.8	2.18	1.39
pH2	31.01.14	1	5.0	75.1	2.16	0.22

### 3.2.1.4. RNA from Hydrogen Peroxide Treated Groups (0.02 mM and 0.03 mM H<sub>2</sub>O<sub>2</sub>)

RNA samples isolated from cultures induced by were quantified using Pico Drop. Results were presented in Table 3.4. It was noticed that high yield of RNA together with appropriate ratio of A<sub>260</sub>/A<sub>280</sub> was obtained for almost all of the samples. However, still a low ratio of absorbance at 260 nm and 230 nm has been observed for these samples. Previously mentioned reasons should be valid for this result.

**Table 3. 4. Concentration of total RNA samples isolated from supplemented cultures**

Samples	Isolation date	Time (Hour)	H <sub>2</sub> O <sub>2</sub> Concentration	Concentration (ng/μL)	A <sub>260/280</sub>	A <sub>260/230</sub>
Oxi.1.1	4.12.13	1	0.03 mM	302.9	2.06	2.50
Oxi.1.2	4.12.13	1	0.03 mM	185.1	2.09	1.68
Oxi.2.1	4.12.13	1	0.03 mM	213.4	2.07	1.85
Oxi.2.2	4.12.13	1	0.03 mM	217.6	2.10	1.13
Oxi.1.1	11.12.13	1	0.02 mM	370.2	2.07	2.07
Oxi.1.2	11.12.13	1	0.02 mM	400.1	2.08	2.33
Oxi.2.1	11.12.13	1	0.03 mM	199.1	2.10	1.27
Oxi.2.2	11.12.13	1	0.03 mM	330.7	2.13	2.13
Oxi 2.1	18.12.13	1	0.03 mM	28.9	2.19	0.14
Oxi 2.2	18.12.13	1	0.03 mM	162.1	2.16	1.57
Oxi 1	20.12.13	1	0.02 mM	75.1	1.62	0.66
Oxi 2	20.12.13	1	0.02 mM	66.2	1.91	0.11
Oxi 1.2	13.01.14	1	0.02 mM	305.1	2.07	1.76
Oxi 1.2*	13.01.14	1	0.02 mM	215.8	2.10	1.99
Oxi 2.2	13.01.14	1	0.03 mM	233.6	2.17	1.28
Oxi 2.2*	13.01.14	1	0.03 mM	245.9	2.08	1.92
Oxi 1	31.01.14	1	0.03 mM	309.0	2.11	1.79
Oxi 2	31.01.14	1	0.03 mM	344.1	2.08	1.62

### 3.2.2. RNA Quality Assessment

#### 3.2.2.1. Bioanalyzer Measurements

On- chip gel electrophoresis was used for the analysis of extracted RNA samples in terms of intactness and purity. In addition to the gel electrophoresis, RNA integrity number (RIN), calculated as a numerical estimate of RNA integrity by a software, algorithm was also considered in quality control of RNA samples. RIN changes from 1 to 10 indicate the classification of total RNA from most degraded to the most intact one. To begin with, for selecting RNA samples to be used in microarray, gel like images were helpful. Electrophoresis run summary of a sample set is given in Figure 3.4. Presence of two distinct bands corresponding for 16S and 23S RNA is an indication of the intact total RNA. In the figure, two clear distinct bands show intact total RNA samples in the wells 1, 2, 3, 4, 7, and 8). Multiple bands are indicating the fragmentation of total RNA samples in the wells 9, 10, 11, 12.

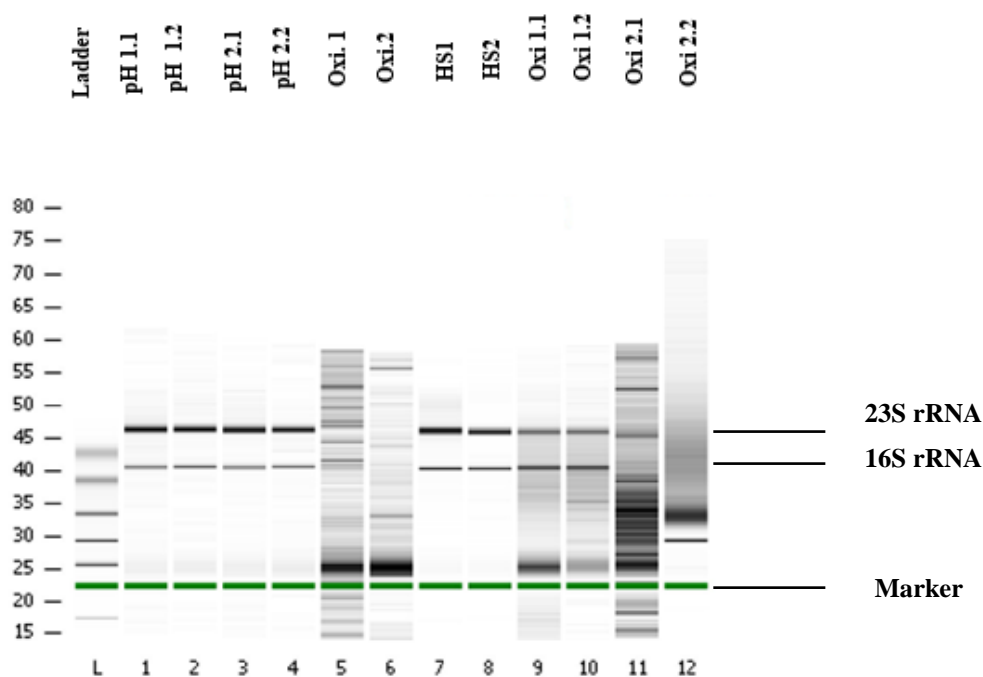


**Figure 3. 4. Agilent 2100 Bioanalyzer gel like image of first sample set.** Wells from 1<sup>st</sup> to 8<sup>th</sup> refer to the RNA samples isolated on 20.12.13 and rest of the samples isolated on 18.12.13. RNA ladder is included in each run as a reference for data analysis.

From the sample set given in Figure 3.4, the RNA samples labeled as pH 2.1, pH 2.2, HS1 and HS2 were chosen for microarray. Their RIN values ( $>9.0$ ) also indicated perfect, high quality RNA. Intact total RNA peaks belonging to these sample groups are shown in the electropherograms given in the Figure 3.5. Intact samples exhibit two distinct ribosomal RNA peaks equivalent to 23S and 16S RNA. Small molecular weight RNAs (5S RNA) can be seen after the marker peak (first peak) as seen in Figure 3.5.a and b. On the other hand, flat baseline is observed after marker peak in the samples of heat induced groups that might be due to success of second wash step during RNA isolation interms of elimination of all small RNAs (Figure 3.5.c and d).

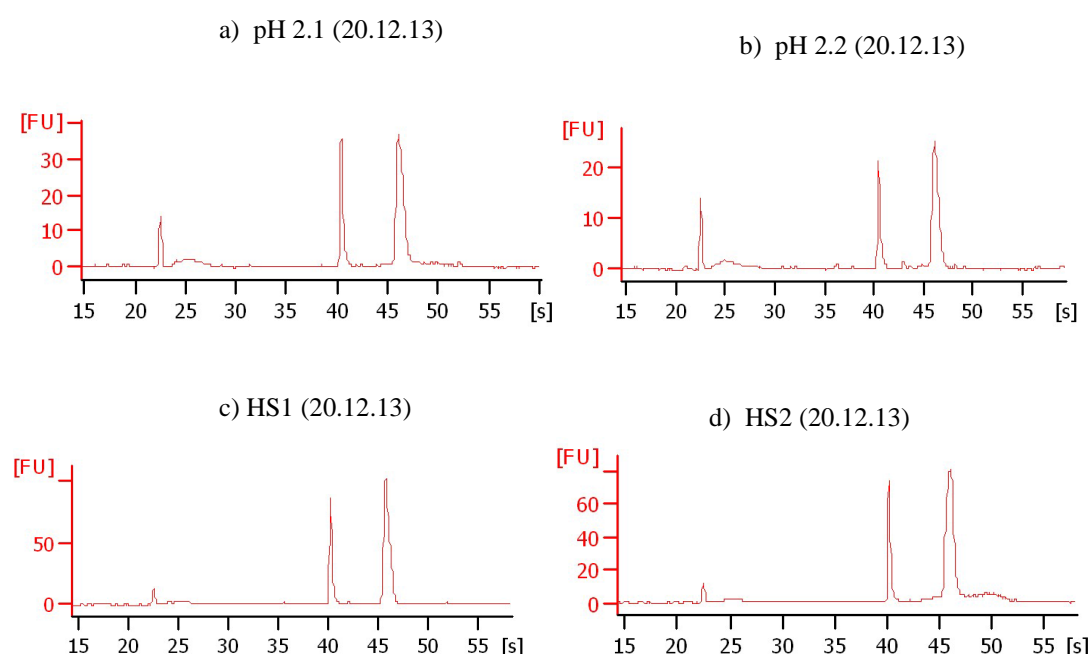


**Figure 3. 5. Bioanalyzer electropherograms of RNA samples used in microarray.** First peak belong to the marker, second peak and third peak refer to the 16S and 23S RNA respectively. Ratio of 23S/16S is greater than 2 (a, b, c, d). Small peaks after the marker (a, b) indicate the presence of small RNAs

Similarly, analysis of second sample set for RNA quality was performed considering the same criteria as the first sample set. Agilent gel like image of total RNA is shown in Figure 3.6. In this figure, 16S and 23S RNA bands are clearly identified for all isolated RNA samples.

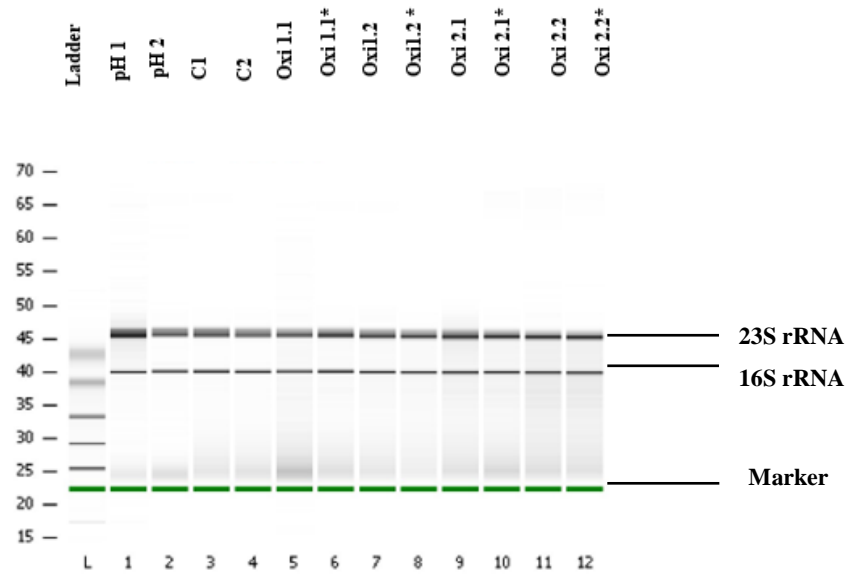


**Figure 3. 6. Agilent 2100 Bioanalyzer gel like image of second sample set.** Samples well from 1<sup>st</sup> to 2<sup>nd</sup> refer to the RNA samples isolated on 18.12.13, and samples well from 3<sup>rd</sup> to 4<sup>th</sup> refer to samples isolated on 11.12.13, and rest of samples were isolated on 13.01.14. RNA ladder is included in each run as a reference for data analysis. The 23S and 16S distinctive ribosomal RNA bands are observed for all samples.

The RIN scores of these samples were ranged from 7.2 to 9.8, but RIN scores of few samples could not be determined for technical reasons. This could be caused by either too high or too low concentration of RNA.

Out of 12 samples from this set, those labeled as C1, C2, Oxi1.2\*, Oxi2.2 and Oxi2.2\* were selected for microarray experiments considering their RIN scores (>7.2) and concentrations. Also, their electropherogram profiles are indicating high RNA quality (Figure 3.7).

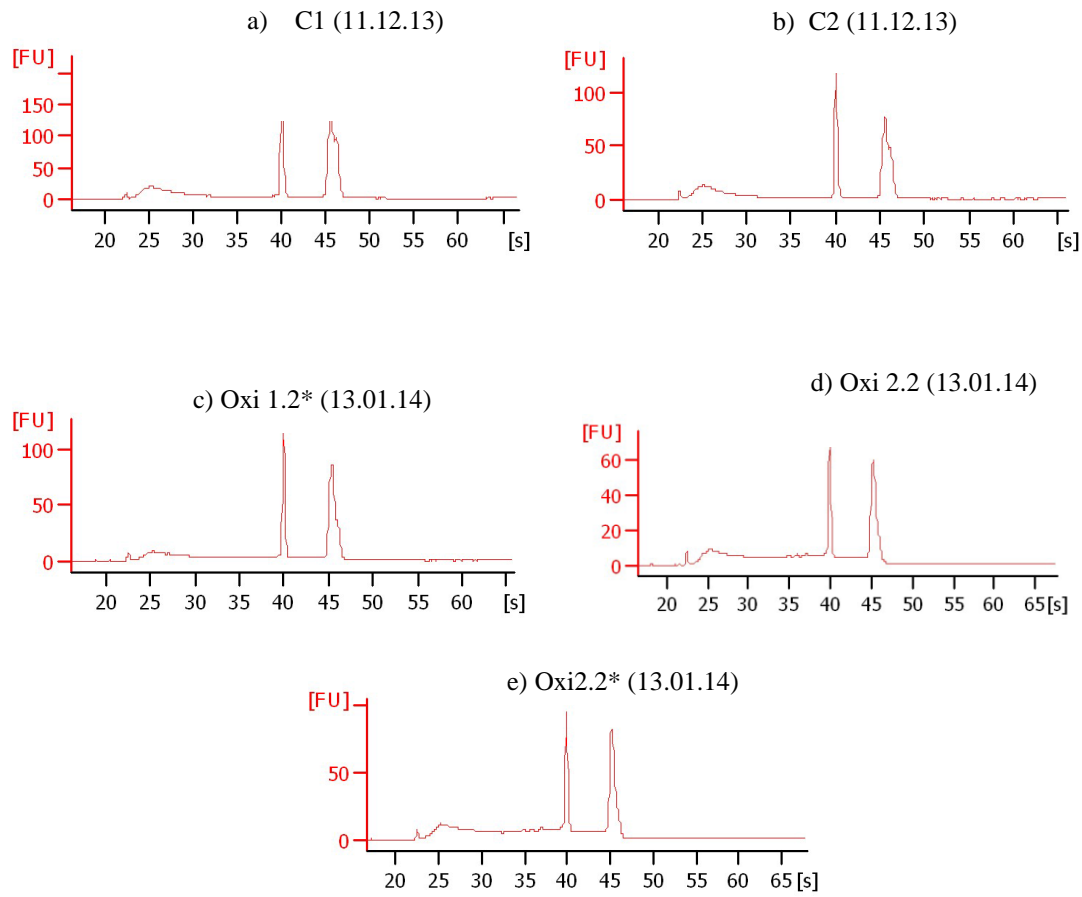


**Figure 3. 7. Bioanalyzer electropherograms of RNA samples used in microarray.** First peak belong to the marker, second peak and third peak refer to the 16S and 23S RNA respectively. Ratio of 23S/16S is approximately equal to 2 (a, b, c, d, and e). Small peaks after the marker peaks indicate the presence of some small RNAs (*i.e.*, 5S rRNA) in all samples.

Finally, quality control results of the last set of RNA samples are given in Figure 3.8. According to the on-chip electrophoresis result, distinct 23S and 16S RNA bands were seen for all samples. However, some RNA fragmentation was detected in samples 2, 5, 6.

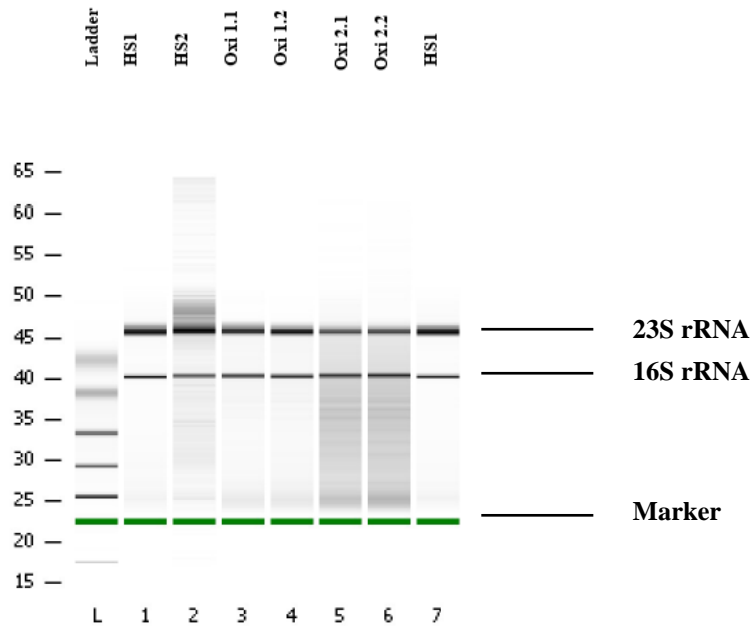


**Figure 3. 8. Agilent 2100 Bioanalyzer gel like image of final sample set.** RNA samples isolated on 11.12.13. The 23S and 16S distinctive ribosomal RNA bands are observed for all samples. A low molecular weight fragments are seen in ladder 2, 5, 6.

Out of seven analyzed samples, three of them were selected for microarray processing *i.e.*, HS1, Oxi1.1, and Oxi 1.2. RNA integrity value of these samples ranged between the 8.5- 9.6. Their electropherogram profiles also showed the intact and high quality characteristics of these samples (Figure 3.9).

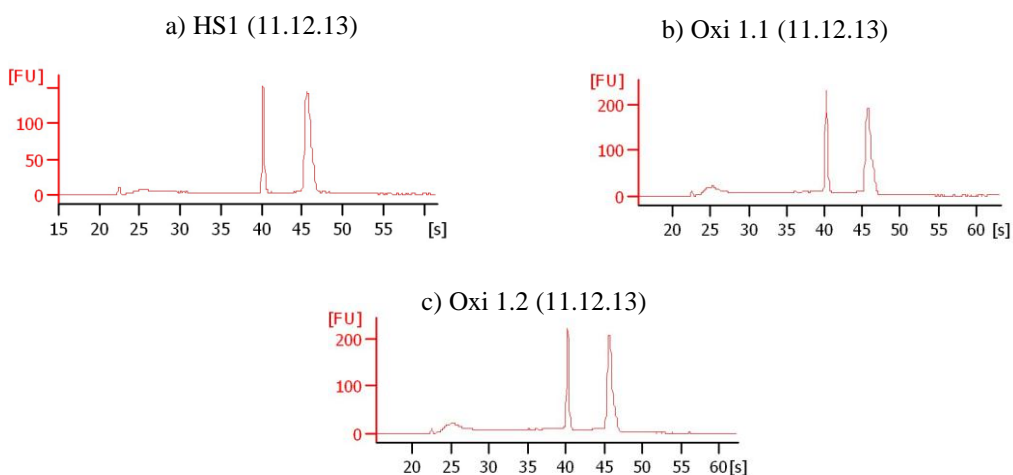


**Figure 3. 9. Bioanalyzer electropherograms of RNA samples used in microarray.** First peak belong to the marker, second peak and third peak refer to the 16S and 23S RNA respectively. Small peaks after the marker peaks indicate the presence of small RNAs (b and c)

### 3.2.2.2. Agarose Gel Electrophoresis of RNA

Intactness and purity of RNA samples following isolation were initially checked by denaturing agarose gel electrophoresis. Results are consistent with the bioanalyzer gel like images. Two sharp bands observed in all samples are indicating the 23S rRNA and 16S rRNA. No genomic DNA contamination was observed in the images. Electrophoresis gel images are given below (Figure 3.10, 3.11, 3.12, 3.13).

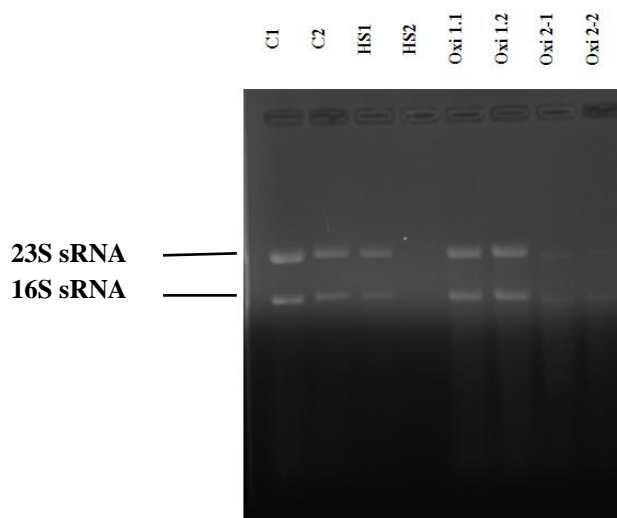


**Figure 3. 10. Denaturing agarose gel electrophoresis of RNA samples.** RNA samples were isolated on 11.12.13.

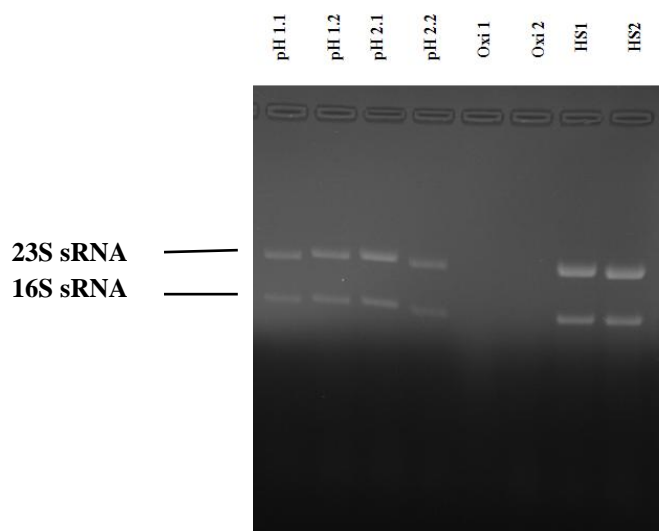


**Figure 3. 11. Denaturing agarose gel electrophoresis of RNA samples.** RNA samples were isolated on 20.12.13.

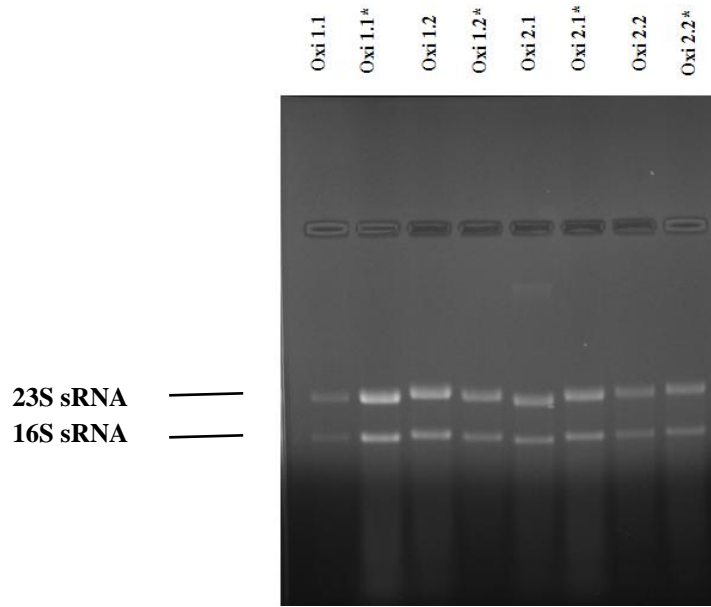


**Figure 3. 12. Denaturing agarose gel electrophoresis of RNA samples.** RNA samples were isolated on 13.01.14.

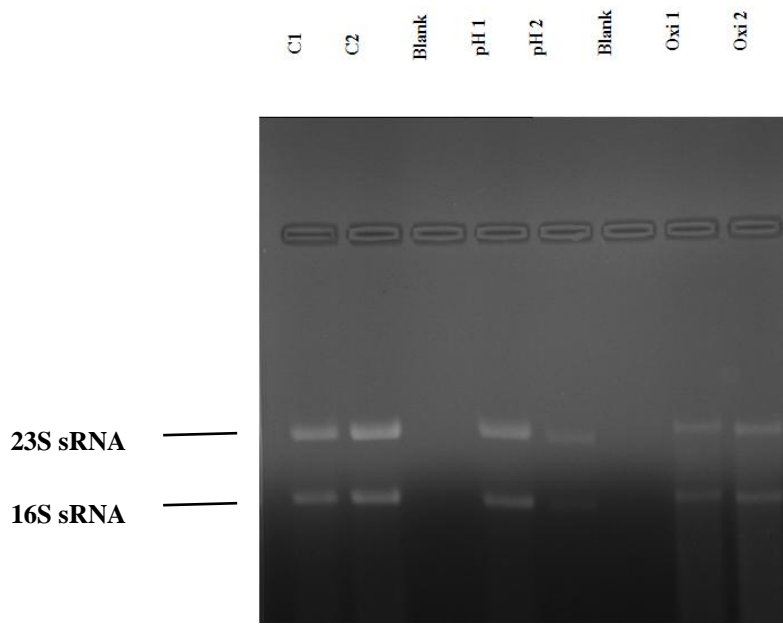


**Figure 3. 13. Denaturing agarose gel electrophoresis of RNA samples.** RNA samples were isolated on 31.01.14.

When selecting RNA samples for microarray, results obtained from pico drop measurements, bioanalyzer gel like images, electropherograms and images of denaturing agarose gel electrophoresis were all together taken into consideration. RNA samples from four biological replicates of control group and RNA samples from three biological replicates of stress exposed groups were chosen to be used in microarray experiments. The selected RNA samples are listed in Table 3.5.

**Table 3. 5. Selected RNA samples for microarray analysis**

<b>Sample</b>	<b>Date of isolation</b>	<b>Concentration (ng/ µl) (Bioanalyzer)</b>	<b>Concentration (ng/ µl) (Pico Drop)</b>	<b>RIN</b>	<b>A<sub>260/280</sub></b>	<b>A<sub>260/230</sub></b>
C1	11.12.13	360	382.1	9.3	2.059	2.48
C2	11.12.13	201	332.5	N/A	2.059	1.958
C2	31.01.14	-	250.5	-	2.152	1.163
C1	31.01.14	-	163.0	-	2.13	1.578
HS1	11.12.13	233	205.6	9.6	2.144	0.787
HS1	20.12.13	138	170.8	9.9	2.027	0.680
HS2	20.12.13	121	192.4	N/A	1.961	1.525
pH 2.1	20.12.13	69	139.1	10	2.027	1.203
pH 2.2	20.12.13	42	94.5	9.9	2.073	0.697
pH 1	31.01.14	-	204.8	-	2.175	1.387
Oxi 1.1	11.12.13	440	370.2	8.7	2.072	2.068
Oxi1.2	11.12.13	447	400.1	8.5	2.083	2.33
Oxi 1.2*	13.01.14	197	215.8	8.7	2.096	1.990
Oxi 2.2	13.01.14	185	233.6	7.2	2.169	1.280
Oxi 2.2*	13.01.14	248	245.9	7.2	2.077	1.923
Ox 2	31.01.14	-	344.1	-	2.071	1.621

N/A: Not available RIN number.

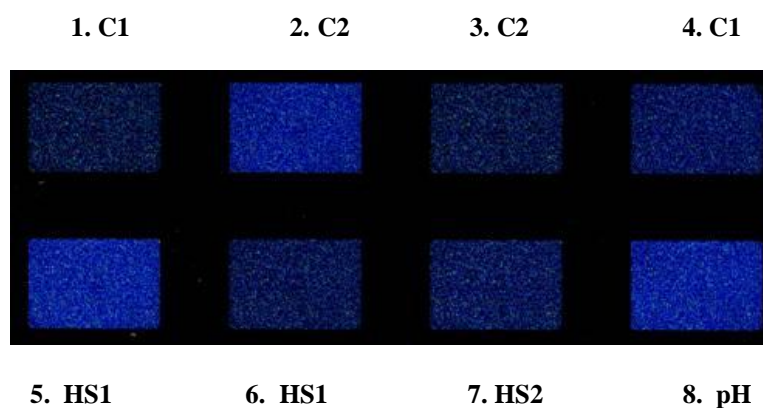
### 3.3. Genome Wide Transcriptional Profiling Under Extreme Stress Conditions

Whole genome transcriptional profiling under extreme stressful conditions *i.e.*, heat shock at 68°C, oxidative stress at 0.02 mM H<sub>2</sub>O<sub>2</sub> (mild) and 0.03 mM H<sub>2</sub>O<sub>2</sub> (severe), and pH stress at pH 5.0 were investigated using Agilent Custom Expression Oligo Microarray.

#### 3.3.1. Raw Microarray Images

As it was mentioned previously in section 2.7, microarray raw image files were generated using Agilent's high resolution scanner that scans very small areas with laser and measures fluorescence intensity of one color labeled nucleic acids. Raw microarray images together with sample order are shown in Figure 3.14.

##### Slide 1.



##### Slide 2.

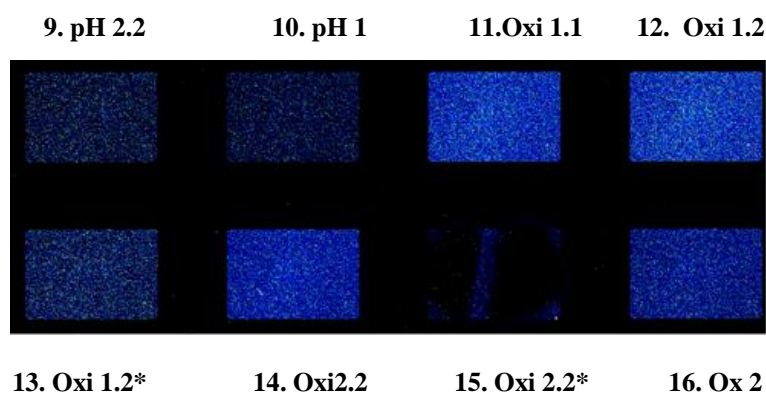


**Figure 3. 14. Illustration of a raw microarray image from 8x60K earrays.** One glass slide contains 8 arrays, each containing total 7458 probes and 1319 Agilent control probes.

Scanned single color image of 8x60K custom arrays revealed the medium and high level fluorescence intensities which might be related to washing efficiency. In Slide 1, array number 1, 3, and 4 exhibit the correlated fluorescence intensities. Similarly, fluorescence intensities of the array number 6 and 7 are similar. In the Slide 2, there is a correlation in fluorescence intensities of pH stress group (9 &10), 0.02 mM oxidative stress group (11&12) as well as 0.03 mM oxidative stress group (14&16). Unfortunately, due to a technical error, array named as Oxi 2.2\* was destroyed during hybridization. Therefore, it was excluded from analysis.

### **3.3.2. Data Pre-Processing :**

#### **3.3.2.1. Normalization & Quality Control**

For normalization and quality control of array data, Agilent's Genespring GX software (Ver 12.6) was used. Prior to the data processing, normalization of one color signals are required for comparison of different experimental samples and elimination of technical artifacts in the data (Gèohlmann *et al.*, 2009). By help of the normalization, variation in the signal intensities which causes different brightness in the raw microarray images (Figure 3.14) are eliminated. The 16 samples of the series of US11073878 were imported to Genespring GX software 12.6 data analysis tool. Using Robust Multi- array Average (RMA) algorithm, the raw signal values of each probe set in the samples were normalized by baseline to median of the control samples. RMA algorithm involves background correction of raw signal values, log<sub>2</sub> transformation of the back corrected values followed by quantile normalization (Irizarry *et al.*, 2003). It was used in order to equalize distribution of probe intensities for all microarrays in the experiment. After the quantile normalization, distribution of the data per sample was visualized by creating Box-Whisker plot, which shows the normalized intensities of the transcript around the median. This box plot is convenient way of examining data sets graphically. Lower end of the box represents the intensities at the 25<sup>th</sup> percentile and upper end of the box shows the intensities at 75<sup>th</sup> percentile. (Gèohlmann et al 2009). Whiskers are the extensions of the box and shown in a different color. The points that lie outside the 25<sup>th</sup> percentile value (*i.e.*,

first quartile) and 75<sup>th</sup> percentile (*i.e.*, third quartile) value are considered outliers (Figure 3.15).

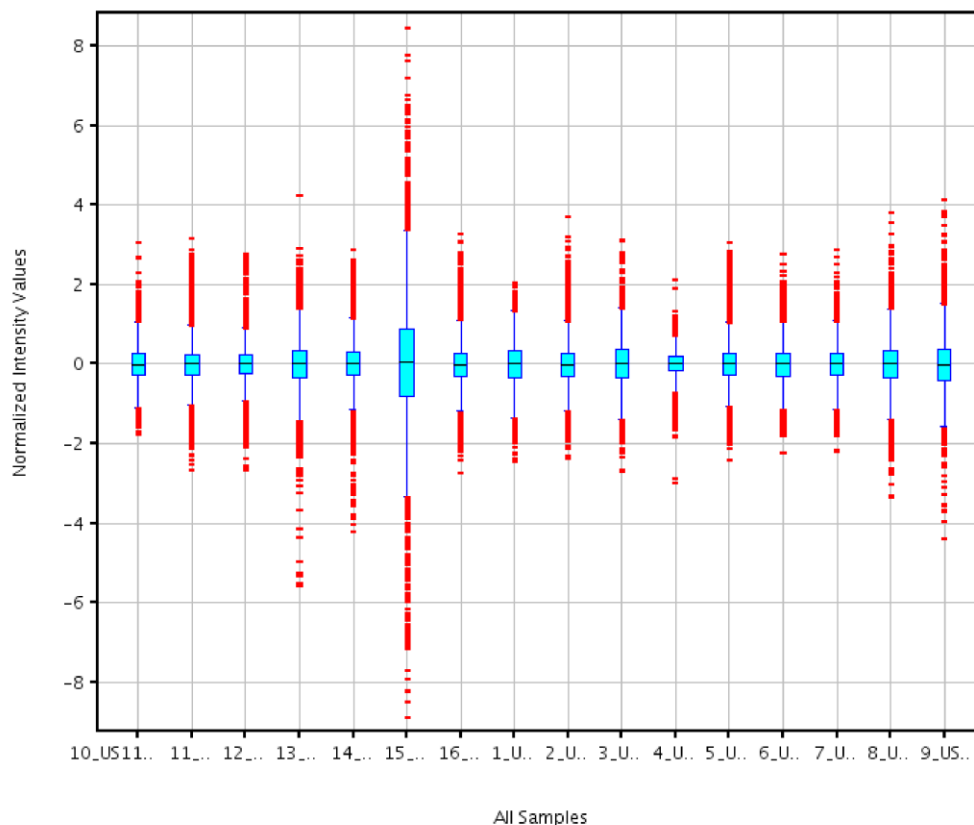


**Figure 3. 15. Box whisker plot of normalized values of the series US11073878 (samples plus controls) using RMA algorithm.**

Quality control (QC) on samples allows to decide which samples are ambiguous and which are passing the quality criteria. According to QC results, the unreliable samples can be removed from the analysis. Software based quality control on samples (sample means data obtained from an array for a single biological source) was achieved by generating Principle Component Analysis (PCA) plots (as a 3D scatter plot), heat maps across arrays, scatter plots, volcano plots, histograms, correlation plots. By correlation analysis, correlation coefficients for each pair of arrays are calculated using Pearson Similarity Metric. Highly correlated samples (*i.e.*, with the same parameter values) have correlation coefficients around 1.0.

From the correlation scores given in Table 3.6, high correlation within the replicates of each experimental group as well as control group is obvious. Top ranking score

belongs to the heat-shock induced samples. Pairwise correlation coefficient between samples 6 and 7 was 0.999.

**Table 3. 6. Pairwise correlation coefficients between arrays.** Correlation coefficients for each pair of arrays are listed in textual form.

Array name	10	11	12	13	14	16	1	3	4	5	6	7	8	9
9	0.952	0.9299	0.9211	0.9515	0.933	0.9366	0.9238	0.9412	0.9472	0.9119	0.9271	0.922	0.9871	1
8	0.933	0.9337	0.9252	0.9407	0.93	0.9282	0.9107	0.9292	0.9408	0.9157	0.92	0.917	1	0.9871
7	0.891	0.9293	0.9333	0.9428	0.894	0.9016	0.9622	0.9695	0.9646	0.9764	0.9989	1	0.9169	0.9217
6	0.903	0.9336	0.9345	0.9442	0.904	0.9106	0.9639	0.9701	0.9673	0.9784	1	0.999	0.92	0.9271
5	0.909	0.9513	0.9488	0.9293	0.915	0.9214	0.9589	0.9599	0.9646	1	0.9784	0.976	0.9157	0.9119
4	0.953	0.9571	0.9524	0.9655	0.951	0.9545	0.9778	0.9952	1	0.9646	0.9673	0.965	0.9408	0.9472
3	0.935	0.9469	0.9484	0.9686	0.93	0.9368	0.9799	1	0.9952	0.9599	0.9701	0.969	0.9292	0.9412
1	0.926	0.9479	0.9492	0.9451	0.921	0.9306	1	0.9799	0.9778	0.9589	0.9639	0.962	0.9107	0.9238
16	0.968	0.9674	0.9528	0.9538	0.99	1	0.9306	0.9368	0.9545	0.9214	0.9106	0.902	0.9282	0.9366
14	0.975	0.9524	0.9335	0.9487	1	0.9904	0.921	0.9304	0.9512	0.9153	0.9039	0.894	0.9296	0.9331
13	0.931	0.9581	0.9616	1	0.949	0.9538	0.9451	0.9686	0.9655	0.9293	0.9442	0.943	0.9407	0.9515
12	0.902	0.995	1	0.9616	0.934	0.9528	0.9492	0.9484	0.9524	0.9488	0.9345	0.933	0.9252	0.9211
11	0.924	1	0.995	0.9581	0.952	0.9674	0.9479	0.9469	0.9571	0.9513	0.9336	0.929	0.9337	0.9299
10	1	0.9239	0.9024	0.9314	0.975	0.9676	0.9256	0.9354	0.9527	0.9089	0.9032	0.891	0.9329	0.9516

Based upon the correlation coefficient results, data was visualized by generating correlation plots. Relationship between samples can be interpreted from the color scale. Highly correlated samples across arrays are shown in a red color. Less correlated ones shown in black color (Figure 3.16). Based on QC results unreliable samples were removed from analysis. The samples passed quality criteria were grouped as : heat shock induced group (*i.e.*, samples 6 and 7), pH induced group (*i.e.*, samples 8 and 9), 0.02 mM H<sub>2</sub>O<sub>2</sub> induced group (*i.e.*, samples 11 and 12), 0.03 mM induced group (*i.e.*, samples 14 and 16) and control-uninduced group (*i.e.*, samples 3 and 4).

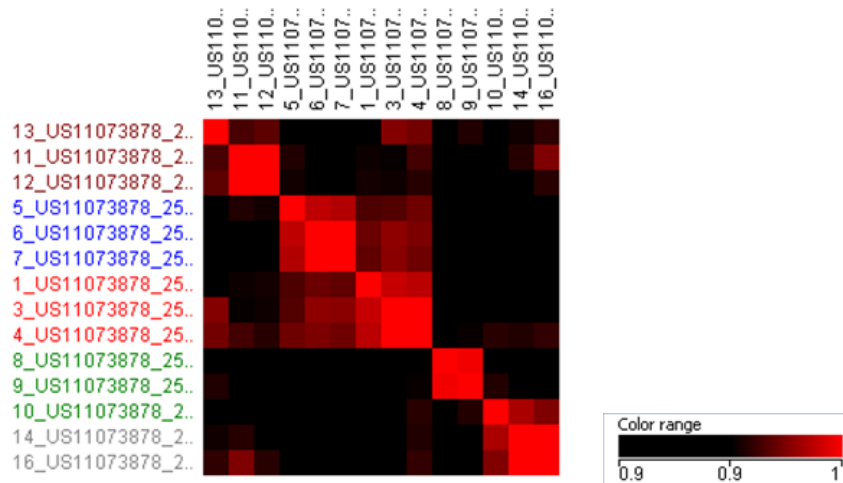


**Figure 3. 16. Representation of correlation coefficients in a visual form as a correlation plot.** Highly correlated samples within the replicates are associated with the red color. Less correlated ones shown as black color.

In quality control on samples by Principle Component Analysis (PCA) generated 3D scatter plot that helps to check whether replicates within a group distinguishable from other groups. PCA scores were calculated by using an algorithm of PCA, and the scores were summarized in three-dimensional PCA scatter plot. Discrete groups within the replicates can be seen in Figure 3.17.

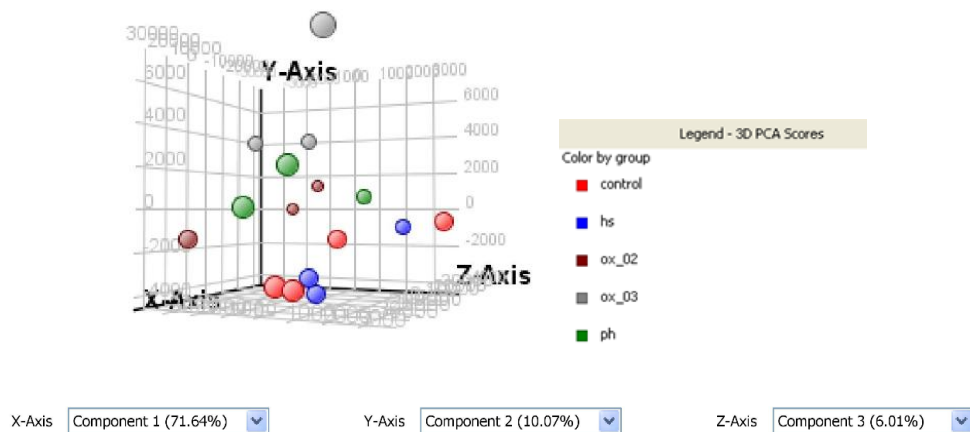


**Figure 3. 17. 3D PCA plot of the normalized signal values of the samples in different conditions.**

In addition to these, frequency of the normalized signal values for control groups and test groups are graphically depicted by plotting histograms as shown in Figure 3.18. The presented histograms correspond to averaged normalized signal values of the samples in different conditions. Histograms are used to visualize the spread of data

and compare and contrast probe intensity between arrays of the data set. Histograms check the quality of the data as well as shape of the distribution. For whole genome experiments, the histogram is expected to be symmetrical. Otherwise, large shift from the normal like shape is connected to the problem with data or normalization process (Drăghici, 2012). In this respect, histograms of test and control data sets are found to be consistent with the expectations.

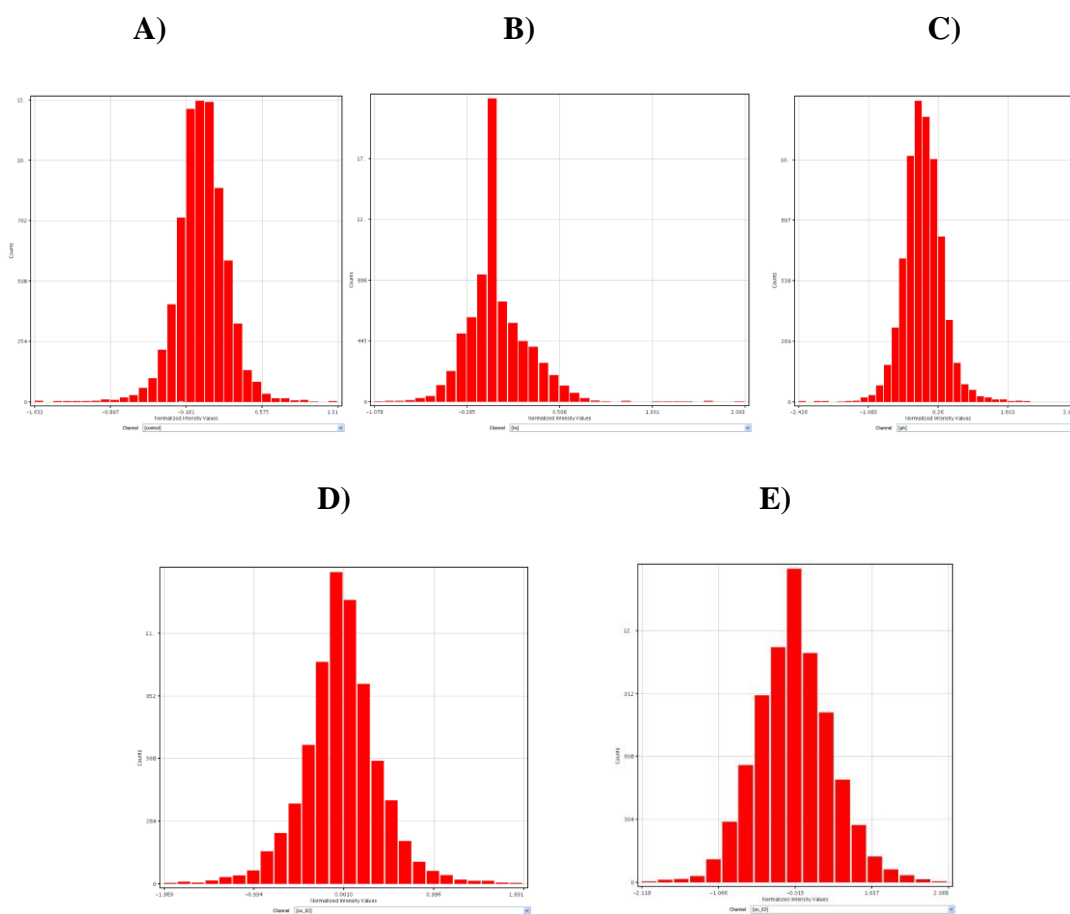


**Figure 3. 18. Histograms for control and different conditions' data sets.** Frequency of the normalized signal values for control (A), heat-shock data set (B), pH stress data set (C), 0.02mM H<sub>2</sub>O<sub>2</sub> oxidative stress data set (D) and 0.03mM H<sub>2</sub>O<sub>2</sub> oxidative stress data set(E) are shown. X axis represents probe density level and Y axis indicates probe intensity.

Furthermore, in order to assess quality of normalization, scatter plots are generated for the determination of the gene expression level and for facilitating visualization of the data (Drăghici, 2012). In the scatter plot, each point represents the expression value of a gene in control and test experiments. One plotted on the X-axis and the other one on the Y-axis. The identity line *i.e.*,  $y=x$  line is drawn as a reference. In

such a plot, genes with equal expression values would line up on the identity line (diagonal) of the coordinate system; with higher expression values further away from the origin. A gene that has an expression level that is very different between the control and test experiments will appear far from the diagonal. The data points fall above or below the fold change lines are indicating 2 fold up- or down- regulated genes. Scatter plots for experimental data sets are given in Figure 3.19.

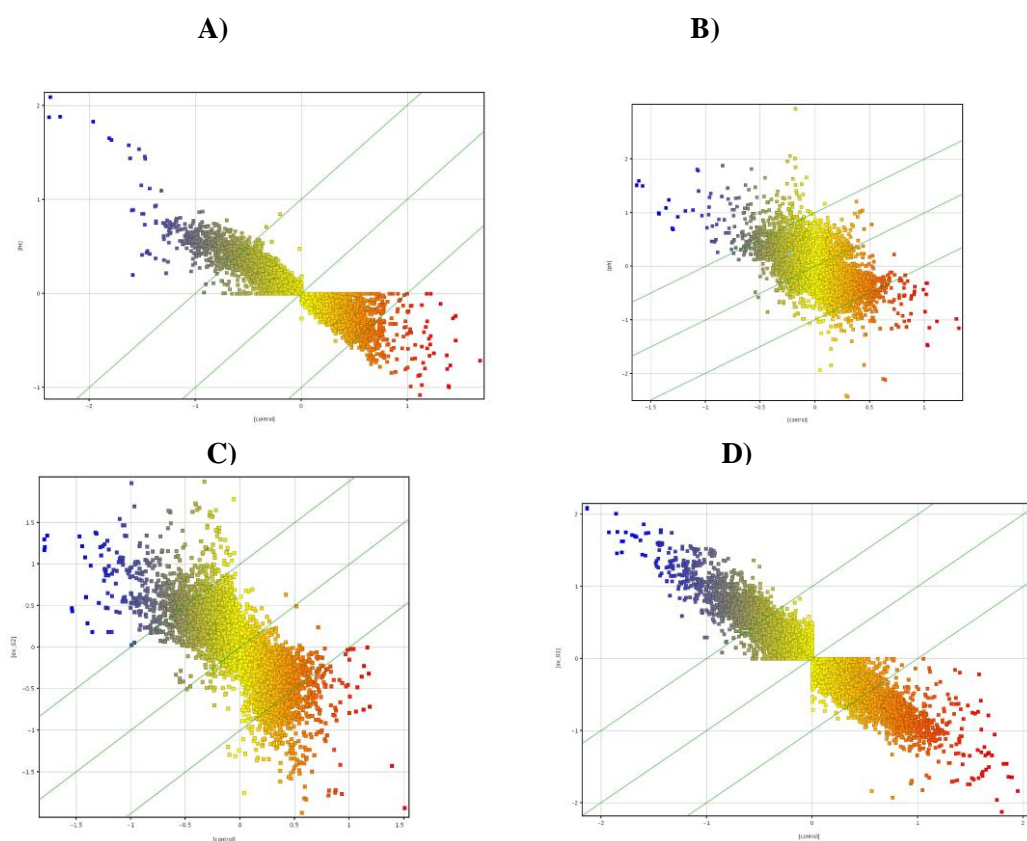


**Figure 3. 19. Scatter plot for different conditions' data set.** Every gene is represented by a point in the graph, showing 2-D scatter of all entities with averaged normalized signal values at the samples. Control is plotted on the horizontal axis, while heat shock (A), pH stress(B), mild oxidative stress (0.02 mM H<sub>2</sub>O<sub>2</sub>) (C) and severe oxidative stress (0.03 mM H<sub>2</sub>O<sub>2</sub>) (D) are plotted on the vertical axis. Blue and red dots represent the higher and lower expression of genes.

Differentially expressed genes can also be quickly detected by another type of scatter plot which is volcano plot. It is widely used for ranking the genes depending on both fold change and t test criteria and used to visualize p-values and fold changes of data points (*i.e.*, genes) (Gèohlmann *et al.*, 2009). "p value" computation was done asymptotically using moderated T-test. The volcano plots were generated using

GeneSpring software displays  $-\log_{10}$  (p -value) versus  $\log_2$  (fold change) scatter plot of genes. Two vertical fold change lines at a fold change level of 2 which corresponds to +1 and -1 on a  $\log_2$  scale. The horizontal line at the 0.05 p-value level is equivalent to 1.3 on the  $-\log_{10}$  (p -value) scale. Data points for the genes that are considered both statistically significant (above the p -value line) and differentially expressed (outside the fold change lines) appear in red and the rest appear in grey. The volcano plots of heat-shock, pH stress, and oxidative stress (0.02 mM and 0.03 mM H<sub>2</sub>O<sub>2</sub>) are given in Figure 3.20.

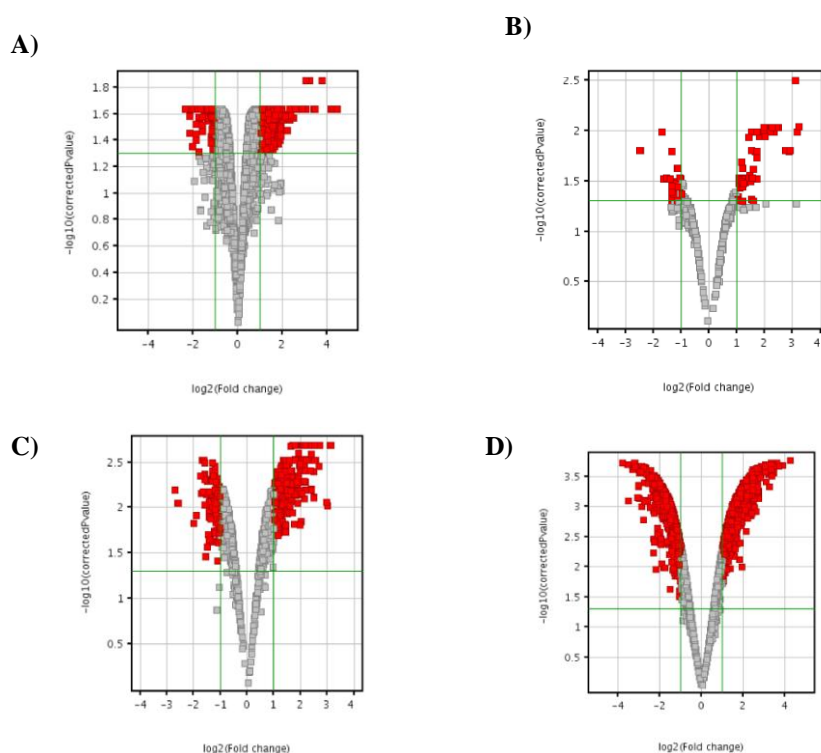


**Figure 3. 20. Volcano plot for different conditions' data sets.** The horizontal line shows where  $p=0.05$  with points above the line having  $p<0.05$  and points below the line having  $p>0.05$ . The vertical lines indicate the fold change lines. Those data points display both large magnitude fold changes ( $\geq 2$ fold) as well as high statistical significance ( $p < 0.05$ ) are red colored. Those points having a fold change  $< 2$  and p values  $> 0.05$  are shown in grey. (A: Heat shock, B: pH stress, C: mild oxidative stress (0.02 mM H<sub>2</sub>O<sub>2</sub>), D: severe oxidative stress (0.03mM H<sub>2</sub>O<sub>2</sub>).

### 3.3.3. Differential Expression of Genes Under The Extreme Heat, pH and Oxidative Stress Conditions

The regulation of the expression of genes is an essential mechanism for cell viability as a response to environmental fluctuations. These challenges are predominantly dealt with by activating protective cellular components. In this sense, whole genome transcriptional profiling of *Thermoplasma volcanium* revealed high number of up and down regulation of annotated genes (*i.e.*, in total 1474 *Tpv* genes) upon exposure to the high temperature, alkaline pH and oxidative stress. Most of the regulated genes are responsible for maintenance of cellular homeostasis.

A summary of the results showing up- and down - regulated gene numbers under each stress as is given in Figure 3.21.

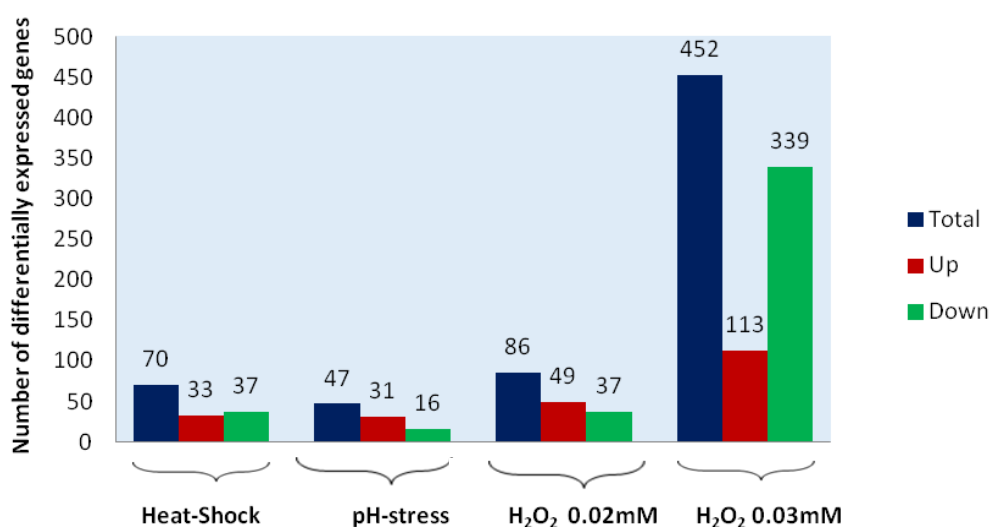


**Figure 3. 21. Differential expression of annotated genes out of 1474 *Tpv* genes under extreme stress condition.**

In the following sections, to provide a new insight into the complicated regulation of cellular homeostasis in archaea, differentially expressed genes are grouped according

to their potential functions and their possible roles under specific stress conditions were discussed.

### **3.3.3.1. Genes Responsive to The Heat Shock**

*Thermoplasma volcanium* grows optimally at 60°C and an increase in temperature above the optimum temperature provokes stress response for the survival of the cells. In this study, gene expression profiling of *T.volcanium* upon heat stress was investigated using whole genome oligo array and transcriptional responses of stress exposed groups and control groups were compared in order to elucidate physiology of stress response and specific behavior of *T.volcanium* under the condition of heat stress. Microarray analysis using GeneSpring Software showed that in order to counteract damaging effect of heat stress, several *T.volcanium* genes were induced and corresponding gene products may take role in maintaining cellular homeostasis. Temperature shift of 60° C to 68° C resulted in a significant change (moderated T-test FC  $\geq$ 2-fold, cut off value  $p < 0.05$ ) in the expression of 70 genes out of 1,474 annotated *TPV* genes. Among the differentially expressed genes, 33 genes were up regulated and 37 genes were down regulated. A list of differentially expressed genes upon heat shock is given in Appendix B.

The functional categorization of the differentially expressed genes was performed by a search in the National Center for Biotechnology Information (NCBI) data base. The functional categories of the differentially expressed genes are listed in Table 3.7. According to the increased or decreased mRNA levels, the major categories effected include heat shock proteins (*e.g.*, molecular chaperones), proteins associated with energy production /conversion, membrane transport systems, motility, cell/wall membrane biosynthesis, replication and recombination, lipid metabolism and detoxification.

Transcription levels of genes encoding the heat shock proteins *e.g.*, molecular chaperones GroEL ( $\alpha$  and  $\beta$  subunits), GrpE, DnaJ and DnaK seem to be significantly up regulated. These proteins are involved in maintaining the native conformation of newly synthesized proteins and in the protein refolding process to prevent aggregation of misfolded or denatured proteins. This response to heat shock

was also observed in other archaea *i.e.*, *P. furiosus*, *M.jannaschii*, *A.fulgidus*, *Sulfolobus solfataricus*, *M.barkeri* and *Halobacterium salinarium* (Shockley *et al.* , 2003; Boonyaratanakornkit *et al.*, 2005 ; Rohlin *et al.*, 2005; Tachdjian *et al.*, 2006; Zhang *et al.*, 2006; Shukla, 2006). Therefore, there should be increased demand for chaperones among different archaeal species upon heat stress.

Another significant outcome of our microarray analysis was the induction of the *Tpv* genes encoding sugar transporters *i.e.*, TVN0721, TVN0206, TVN0021, TVN0216 and amino acid transporters such as TVN1423, TVN1221 and TVN1224. Out of 33 differentially up regulated genes, 21 % of them were classified in this group. Little is known about the biological significance of the increase expression levels of various transporters upon heat stress. In parallel to the similar reports of the transcriptomic analysis in *Archaeoglobus fulgidus* and *Pyrococcus furiosus* under heat stress, increased expression of sugar transporters in *T.volcanium* can be related to metabolic adaptation e.g., demand for ATP to restore energy balance under stress (Shockley *et al.* , 2003 ; Rohlin *et al.*, 2005).

Another group of up-regulated *Tpv* genes under heat stress are responsible for maintaining cellular redox homeostasis. Activation of some redox proteins such as alcohol dehydrogenase (TVN1284; 2.66 fold), aldehyde dehydrogenase (TVN1283; 2.14 fold) and aldo/keto reductase (TVN0875; 2.07 fold) may imply the regulation of redox homeostasis as well as basic metabolic functions under heat shock (Kültz 2005). Previous transcriptome analyses associated with heat stress did not report any role for the redox proteins during thermal stress, rather their roles were more evident in oxidative stress. It is likely that these redox regulatory proteins could take adaptive role in cellular stress response by sensing the heat stress, and then restoring the homeostasis by producing reducing equivalent necessary for cell functions.

It is known that heat affects the fluidity of the membrane and at high temperature membrane can become too fluid. Therefore, one can expect differential expression of genes that can change or modify membrane lipid composition under heat stress. Transcription of genes encoding acyl-CoA dehydrogenase (TVN0670; 2.034 fold),

long chain fatty acid CoA ligase (TVN1309; 2.57 fold) and acetyl-CoA acetyltransferase (TVN1260; 2.28 fold) increased significantly.

It is likely that products of those genes are involved in the alteration of the membrane lipid composition by reducing fluidity in order to protect the cells from damaging effect of the heat stress. Similarly, membrane composition of *Archaeoglobus fulgidus* changed significantly following heat shock. Increased expression of genes in this archaeon related to the isoprenoid pathway could be an indication of the same response (Rohlin *et al.*, 2005).

When exposed to the heat shock, in *S. solfataricus*, *M.barkeri* and *M.jannaschii*, mRNA transcript levels of the genes encoding transposable elements which have crucial role in transposition and genome plasticity were up regulated (Tachdjian *et al.*, 2006; Zhang *et al.*, 2006; Boonyaratanakornkit *et al.*, 2005. Our results are in consistent with this report. In *T.volcanium*, transcript level of integrase (TVN0823) increased by a factor of 2.80 fold upon heat shock. Function of this protein could be linked to generation of genetic diversity in order to regulate genes immediately upon heat shock. In addition, 31 % of the up regulated genes (total 33 genes) were identified as hypothetical proteins. Expression level of some of them (*i.e.*, TVN0161; 3.56 fold, TVN0204; 3.19 fold) remarkably increased upon heat shock. Characterization can give insights on their roles in adaptation to the high temperatures.

A suprising outcome of this study is that transcript level of genes responsible for de novo purine biosynthesis is enhanced greatly by a factor of 6.34 following heat shock. However, nothing is known so far about the functional role of archaeal phosphoribosylaminoimidazole synthetase during heat stress. Nevertheless, a recent study conducted with hyperthermophilic archaeon *Pyrococcus horikoshii* OT3 pointed out that phosphoribosylaminoimidazole-succinocarboxamide synthetase takes role in thermostability of proteins (Manjunath *et al.*, 2013). In accordance with this notion, *T.volcanium* could adopt a similar adaptive strategy to cope with heat stress.

**Table 3. 7. Functional categorization of up regulated *Thermoplasma volcanium* genes upon heat shock**

<b>Functional classes of proteins</b>	<b>Gene symbol</b>	<b>P values</b>	<b>Fold change</b>
<b>Protein Folding</b>			
Molecular chaperone GroEL (HSP60 alpha subunit)	TVN1128	0.023	2.74
Molecular chaperone GroEL (HSP60 beta subunit)	TVN0507	0.023	2.57
Molecular chaperone GrpE	TVN0489	0.023	2.45
DnaJ	TVN0487	0.023	1.83
DnaK	TVN0488	0.023	1.74
<b>Sugar Transport</b>			
Major facilitator superfamily permease	TVN0721	0.031	3.04
ABC type sugar transporter	TVN0206	0.033	2.35
Permease	TVN0021	0.023	2.12
Major facilitator superfamily permease	TVN0216	0.040	2.11
<b>Aminoacid Transport</b>			
Amino acid transporter	TVN1423	0.025	3.86
Cationic aminoacid transporter	TVN1221	0.039	2.72
Aminoacid transporter	TVN1224	0.029	2.074
<b>Oxidation –reduction process</b>			
Alcohol dehydrogenase	TVN1284	0.029	2.66
NAD dependent aldehyde dehydrogenase	TVN1283	0.023	2.14
Aldo/Keto reductase	TVN0875	0.049	2.07
<b>Lipid metabolism</b>			
Long chain fatty acid coA ligase	TVN1309	0.025	2.57
Acetyl-coA acetyltransferase	TVN1260	0.034	2.28
Acyl-coA dehydrogenase	TVN0670	0.029	2.03
<b>Integration / recombination</b>			
Integrase /recombinase	TVN0723	0.035	2.80
Integrase/recombinase	TVN0678	0.023	2.56
<b>Purine Metabolism</b>			
Phosphoribosylaminoimidazole synthetase	TVN0164	0.023	6.34
<b>Coenzyme metabolism</b>			
ATP:corrinoic adenosyltransferase	TVN1190	0.025	2.16
<b>Hydrolysis</b>			
Zn dependent hydrolase	TVN0167	0.023	5.86
Zn dependent hydrolase (AttM related)	TVN1285	0.023	3.16
<b>Others</b>			
Hypothetical proteins	TVN0161	0.023	3.56
Hypothetical proteins	TVN0204	0.025	3.19
Nucleic acid binding protein	TVN1259	0.029	2.06

Following a stressful environmental transition, expression of the 37 genes out of 1474 annotated *Tpv* genes were down regulated (Moderated T- test FC  $\geq 2$ -fold, cut off value  $p < 0.05$ ) upon heat shock. The major effect of the heat shock response in *Thermoplasma volcanium* is retardation of the cell growth rate, as a result of the general stress response. This response is well correlated with the transient drop in overall protein synthesis and transcription under stress. Transcription levels of genes encoding transcriptional regulators (TVN1422, TVN0624), RNA helicase (TVN1303; -2.31 fold) were found to be down regulated, which could be implication of this response. Previous transcriptome studies conducted with *M.barkeri*, *A.fulgidus* also yielded similar results (*i.e.*, aminoacid, coenzyme and energy metabolisms) were strongly repressed following heat shock (Rohlin *et al.*, 2005; Zhang *et al.*, 2006). These results from different archaeal species might be indicating importance of some critical metabolic adaptations in heat shock response.

Microarray analysis results also indicated that genes grouped in functional categories of cell motility, protein secretion, amino acid and pyruvate metabolism, nucleotide biosynthesis are repressed remarkably ( Table 3.8). Combined effect of this response may be to conserve mass and energy while the cell adapts itself to new condition.

Another group of down regulated genes are related to cell wall biosynthesis. These genes could be functionally related to the posttranslational modifications such as protein glycosylation. Biological significance of protein glycosylation was observed in protein assembly. It is also known that glycosylation has important role in coping with harsh environmental conditions by increasing stability of proteins (Eichler *et al.*, 2005). Therefore, repression of the *Tpv* genes whose products take role in glycosylation upon heat shock could be in part responsible for the reduced thermal stability of proteins.

Another intriguing result from microarray experiments was down regulation of the genes encoding DNA repair proteins (*i.e.*, Type III restriction modification enzyme (TVN1463; -2.90). It would be expected that DNA repair system should be induced during heat shock to repair heat induced damages in DNA. Our results are not consistent with data from previous reports of transcriptomic and/ or proteomic

analysis of *Pyrococcus furiosus* and *Halobacterium salinarium* that revealed the induction of genes responsible for DNA repair and protection (Coker *et al.*, 2007; Shukla, 2006; Shockley *et al.*, 2003).

In addition, mRNA transcript levels of some genes responsible for coenzyme metabolism and carbohydrate metabolism were also down regulated (with p values < 0.05 and at least 2 fold change in gene expression), possibly as result of drop in the rate of biosynthetic processes under heat stress (Table 3.8). Their products are involved in oxidation- reduction reactions.

Another noteworthy result from microarray analysis was the down regulation of a gene encoding rhodanase related protein by a factor of -2.29. Rhodanases are enzymes that carriers the sulfur in a variety of metabolic process. Although their exact roles in biologic processes are not known well, some of the proposed functions are related to selenium metabolism, thiamine biosynthesis, and formation of prosthetic groups in Fe-S proteins (Bordo *et al.*, 2002). Recently, it was shown that rhodanases are involve in tRNA modification pathway, which is crucial for efficient translation (Shigi *et al.*, 2014). The latter appears to be more reasonable, since heat shock causes global decrease in the overall protein synthesis of *T.volcanium* when our results are considered.

**Table 3. 8. Functional categorization of the repressed genes upon heat shock**

<b>Functional classes of proteins</b>	<b>Gene symbol</b>	<b>P values</b>	<b>Fold change</b>
<b>Motility</b>			
Flagellin ;K07325 archaeal flagellin FlaB	TVN1426	0.023	-4.05
Flagellar protein G	TVN0611	0.024	-2.15
<b>Transcription</b>			
Transcription regulator	TVN1422	0.026	-2.42
Transcription regulator	TVN0624	0.026	-2.11
<b>Translation</b>			
RNA helicase	TVN1303	0.024	-2.31
<b>Cell wall biosynthesis</b>			
Glycosyltransferase	TVN0430	0.023	-2.18
dTDP-4dehydrorhamnose reductase	TVN0900	0.025	-2.14
Cell wall biosynthesis glycosyltransferase	TVN0547	0.029	-2.08
Cell wall biosynthesis glycosyltransferase	TVN0869	0.023	-2.07
<b>DNA replication, repair and recombination</b>			
Single stranded DNA binding protein	TVN1236	0.023	-3.23
Type III restriction modification enzyme , helicase unit	TVN1463	0.025	-2.90
<b>Sugar transport</b>			
Major facilitator superfamily permease	TVN0436	0.023	-2.55
Major facilitator superfamily permease	TVN0226	0.035	-2.25
Major facilitator superfamily permease	TVN0255	0.026	-2.05
<b>Aminoacid transport</b>			
Aminoacid transporter	TVN0898	0.023	-2.42
<b>Coenzyme metabolism</b>			
GTP:adenosylcobinamide–phosphateguanyly transferase	TVN1428	0.023	-2.07
<b>Pyrimidine metabolism</b>			
Carbamoylphosphate synthase small subunit	TVN0802	0.023	-2.22
<b>Carbohydrate metabolism</b>			
phosphoenolpyruvate carboxykinase	TVN0200	0.023	-2.23
<b>Aminoacid export</b>			
7S Ribosomal RNA	TVNr03	0.023	-3.94
<b>Oxidation –reduction process</b>			
NAD(FAD) dependent dehydrogenase	TVN0473	0.023	-2.25
Ubiquinone/menaquinone biosynthesis methylase	TVN1030	0.023	-2.15
<b>Multi regulatory function</b>			
Rhodanese related protein	TVN0830	0.030	-2.29
<b>Others</b>			
Hypothetical protein	TVN0147	0.033	-3.07
Hypothetical protein	TVN0365	0.024	-2.10
Metal binding protein	TVN0073	0.023	-2.15

Heat maps are used in order to visualize expression level of stress exposed cultures as well as hierarchical clustering. Every row refers to the gene expression profile among samples, and abundance of transcripts are interpreted by color legends Gèohlmann *et al.*, (2009). Differentially expressed *Tpν* genes under heat stress were clustered using hierarchical algorithm and the Heat maps generated are shown in Figure 3.22. Euclidean distance measures were used in order to cluster genes with similar absolute expression levels together.

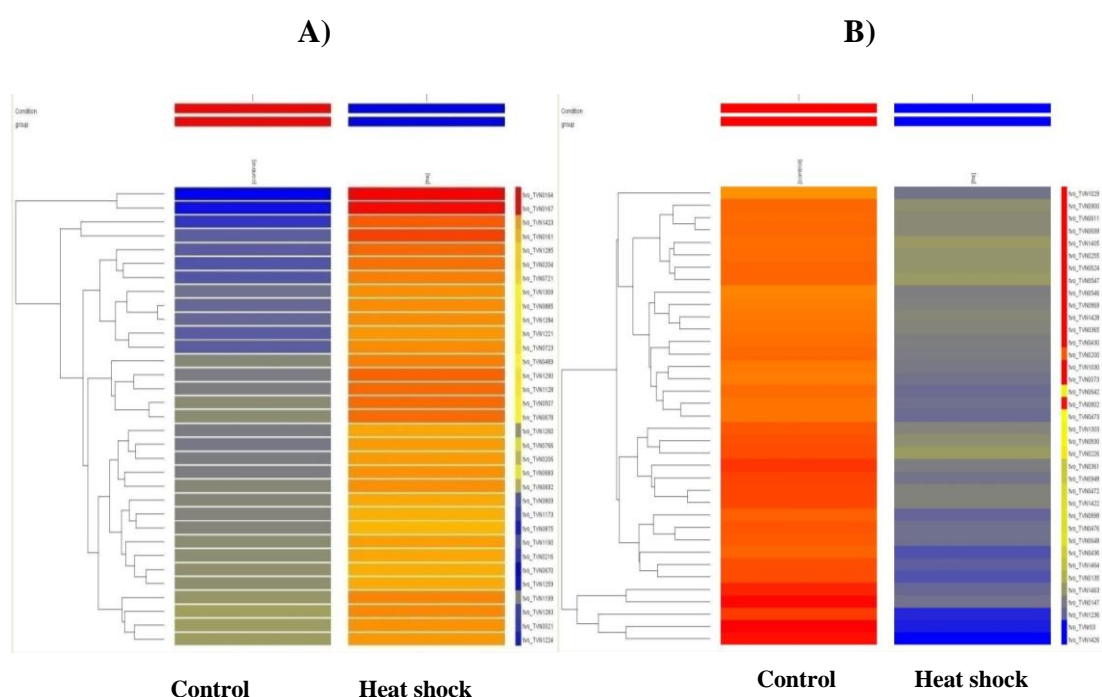


**Figure 3. 22. Cluster analysis of heat-shock dataset.** Expression levels are indicated by colors. The shades of blue and red refer to the different expression levels. The dark red indicates the higher expression level, while the dark blue shows the lower expressions. The heat maps cover 47.14 % of the differentially expressed genes that are up regulated (A) and the remaining 52.86 % that are down regulated (B).

### 3.3.3.2. Genes Responsive to pH Stress

*Thermoplasma volcanium* is very interesting microorganism that can deal with two extreme conditions (*i.e.*, extremely low pH ranging from 1 to 4 and  $T_{opt}$  60 ° C). The adaptive mechanisms they use for sustaining their life at low pH depend on the cellular bioenergetics. Shift to alkaline pH poses a threat to *T.volcanium*. Protective mechanisms against alkaline stress is poorly understood in archaea. Only one report

on alkaline stress has been available until now. In this sense, in order to characterize anti-stress mechanisms developed by *T.volcanium*, the pH of the mid log culture was up shifted from 2.6 to 5.0 for 1 hour and changes in the abundance of transcripts as compared to control culture were determined. Using the same cut off criteria of 2.0 fold change and p value less than 0.05, a total of 47 genes out of 1474 annotated *TPV* genes were found to be differentially expressed as revealed by genome wide transcription profiling. Out of 47 differentially expressed genes, 66 % genes were up regulated and 34% of the genes were down regulated. Among induced genes, 26% were annotated as hypothetical proteins as listed in Appendix B. For example, TVN0679, TVN0300 fall into top category of up regulated genes with fold change values of 9.26 and 8.87 respectively (Table 3.9). These hypothetical proteins might have crucial roles in adaptation of *T.volcanium* to pH stress. A group of genes encoding several transporters including phosphate ABC transporter (TVN0123; 8.4-Fold), iron regulated ABC transporter (TVN1391, 4.69-fold., TVN1389, 4.54-fold) were found to be significantly induced following pH shift. Biological roles of these proteins are mainly implicated in maintenance of intracellular ionic balance. They are thought to play central role in pH homeostasis in many bacteria, as well (Padan *et al.*, 2005). The gene (TVN0494) encoding ATP dependent protease Lon was also up regulated (by 2.24-fold), which is known to have role in selective degradation of abnormally folded protein or short lived regulatory proteins. This result was expected one, because disruption of the cellular pH homeostasis adversely affects unity of proteins (Padan *et al.*, 2005). It is likely that it causes denaturation of proteins, which then tend to precipitate, aggregate and eventually exert cytotoxic effects. Therefore, up regulation of genes encoding proteases can rescue cell from damaging effect of unfolded proteins and their precipitates by degrading them.

Alternatively, in response to the pH stress, when Lon homolog was activated, it may subsequently alter function of another protein by cleavage to trigger a regulatory pathway.

A group of genes related to the oxidation reduction processes (*e.g.*, formate dehydrogenase major subunit, TVN0243, 2.9-fold and Fe-S oxidoreductase, TVN0932; 2.7-fold) were also significantly up regulated at high pH. These proteins

have important roles in maintaining intracellular redox balance and in environmental sensing as well as gene regulation (Blum, 2008). Their increased activities might be a species specific strategy in response to the elevated pH, since gene expression profiling of halophilic archaea revealed that transcription levels of genes encoding dehydrogenases were decreased upon pH up shift (Moran –Reyna *et al.*, 2014).

Another noteworthy observation from transcriptional profiling was up regulation of genes encoding transcription initiation factor IIB by a factor of 7.41 fold. It has been known that eukaryal TFIIB is homologues of the archaeal TFB. This finding could imply that a set of genes are regulated by *Thermoplasma volcanium* in response to pH stress in a similar fashion to eukaryotic organisms (Lu *et al.*, 2008). This result is in agreement with data documented for halophilic archaea i.e., *Halorubrum lacusprofundi*, *Haloferax volcanii*, and *Halobacterium sp.NRC-1* (Moran –Reyna *et al.*, 2014). It is more likely in general that there is involvement of major transcription factors of Archaea in stress response including the one against elevated pH.

The gene (TVN0502) encoding for the nucleotide binding protein universal stress protein (Usp-A) was found to be up regulated (by 4.47) during pH stress. According to previous reports, following environmental transitions to stressful conditions, universal stress proteins are overproduced and they help organisms to survive under fluctuational environments. It was illustrated that UspA gene from *Salmonella typhimurium* LT2 is induced upon oxidative, metabolic and temperature stress (Tkaczuk *et al.*, 2013). Consistent results are also observed in the study of Moran's group (Moran –Reyna *et al.*, 2014).

The *Tpv* gene (TVN1600), that code for KEOPS complex cgi121 like subunit were found to be up regulated by a factor of 2.88 fold.

KEOPS refers to the Kinase Endopeptidase and other proteins of small size. The complex is made up of protein kinase, predicted endonuclease and three uncharacterized proteins such as Cgi121. This complex is highly conserved throughout archaea and eukaryotic domains, and represents functional categorization of tRNA modification, which is crucial for normal cell growth and precise

translation (Perrochi *et al.*, 2013). There is no information regarding functional role of this complex in counteracting pH stress, but it can be possible that in *Thermoplasma volcanium*, its elevated expression upon pH shift could be species specific response rather than a general one.

**Table 3. 9. Functional categorization of the induced genes upon pH stress**

<b>Functional classes of proteins</b>	<b>Gene symbol</b>	<b>P values</b>	<b>Fold change</b>
<b>Transcription</b>			
Transcription initiation factor IIB	TVN0570	0.015	7.41
Transcription regulator	TVN0406	0.018	3.26
Transcription regulator	TVN1392	0.010	3.22
Transcription regulator	TVN1272	0.049	2.26
<b>Oxidation-Reduction process</b>			
Formate dehydrogenase major subunit	TVN0243	0.024	2.95
Fe-S oxidoreductase	TVN0932	0.028	2.71
<b>Transport</b>			
Phosphate ABC type transporter	TVN0123	0.003	8.44
Iron-regulated ABC transporter ATPase subunit	TVN1391	0.009	4.68
Iron-regulated ABC-type transporter	TVN1389	0.010	4.54
Iron-regulated ABC-type transporter	TVN1390	0.011	3.96
Amino acid transporter	TVN1238	0.047	2.039
<b>Proteases</b>			
ATP dependent protease Lon	TVN0494	0.031	2.24
<b>Protein export</b>			
Protein translocase subunit Sss1	TVN1444	0.029	2.10
Signal recognition particle protein Srp54	TVN0992	0.036	2.12
<b>Stress endurance activity</b>			
Nucleotide binding protein (UspA- related)	TVN0502	0.009	4.47
<b>Protein modification</b>			
Lipoate-protein ligase A	TVN0990	0.016	3.27
<b>Others</b>			
KEOPS complex cgi121 like subunit	TVN1600	0.015	2.88
<b>General function prediction only</b>			
Aromatic ring hydroxylating enzyme	TVN1393	0.010	2.83
H/ACA RNA-protein complex component Gar1	TVN1084	0.049	2.14
<b>Hypothetical proteins</b>			
Hypothetical protein	TVN0300	0.010	8.87
Hypothetical protein	TVN0679	0.009	9.26

Transcriptional profiling following pH up shift revealed the repression of the 34 % of the genes out of 1474 annotated *Tpv* genes. Down regulated genes include members from functional categories of transcription, translation, signal transduction, lipid metabolism, biosynthesis processes and general function predicted ones. Among them, about 19% of gene products are involved in the translation process *i.e.*, ribosomal proteins TVN1247 (30s ribosomal protein S3); -2.01 fold, TVN0555 (30s ribosomal protein S8; -2.06 fold) and Leucyl-tRNA synthetase (TVN0761; -2.24 fold).

Products of an another down regulated gene set are related to lipid metabolism (*e.g.*, enoyl-coA hydratase, TVN0363, -2.19 fold), purine biosynthesis (*i.e.*, GMP synthase subunit A, TVN1088, -2.064 fold), signaling (*i.e.*, GTPase, TVN0401,-2.06). These results show metabolic activity of *Tpv* cells is decreased in parallel to the cessation of growth under stressful conditions. The combined effect of this response may help to save energy. Similar trend was also found in the microarray analysis of *E.coli*; genes involving cell division and nucleotide biosynthesis were down regulated as response to pH stress (Padan *et al.*, 2005). In addition, expression of the gene (TVN0784) encoding benzoyl formate decarboxylase was repressed by a factor of 3.09 fold. Previous studies conducted with *E.coli* and *B.subtilis* also indicated that decarboxylase system is used for adaptation to pH stress. The role of this system might be regulation of pH homeostasis by consuming hydrogen ions, which promotes alkalization. In these respects, down regulation of the decarboxylase gene in *T.volcanium* prevented further alkalization of the cytoplasm.

Among the differentially regulated genes, 19% of them were annotated as encoding hypothetical proteins (Figure 3.24). In order to understand their adaptive roles in alkaline stress, further characterization is needed. This is also valid for the predicted proteins as listed in Table 3.10.

**Table 3. 10. Functional categorization of repressed genes upon pH stress**

<b>Functional classes of proteins</b>	<b>Gene symbol</b>	<b>P values</b>	<b>Fold change</b>
<b>Transcription</b>			
Transcription regulator (HTH)	TVN1447	0.029	-2.89
<b>Translation</b>			
30 s ribosomal protein S3	TVN1247	0.042	-2.01
30 s ribosomal protein S8	TVN0555	0.049	-2.06
Leucyl-tRNA synthetase	TVN0761	0.049	-2.24
<b>Signal transduction</b>			
GTPase	TVN0401	0.036	-2.06
<b>Lipid metabolism</b>			
Enoyl-coA hydratase	TVN0363	0.036	-2.19
Acyl-coA dehydrogenase	TVN1343	0.024	-2.24
<b>DNA repair</b>			
Endonuclease IV	TVN0971	0.035	-2.57
<b>Catalytic activity</b>			
Benzoylformate decarboxylase	TVN0784	0.030	-3.09
<b>Purine Biosynthesis</b>			
GMP synthase subunit A	TVN1088	0.029	-2.064
<b>NAD Biosynthesis</b>			
Nicotinate phosphoribosyltransferase	TVN1243	0.049	-2.063
<b>Hypothetical proteins</b>			
Hypothetical proteins	TVN0188	0.049	-2.55
Hypothetical proteins	TVN0549	0.015	-2.55
Hypothetical proteins	TVN0643	0.023	-2.16
<b>Predicted and uncharacterized proteins</b>			
GTPase	TVN1085	0.049	-2.16
SAM dependent methyltransferase	TVN0896	0.047	-2.52

Differentially expressed *Tpv* genes under pH stress were clustered using hierarchical algorithm and the Heat maps generated are shown in Figure 3.23.

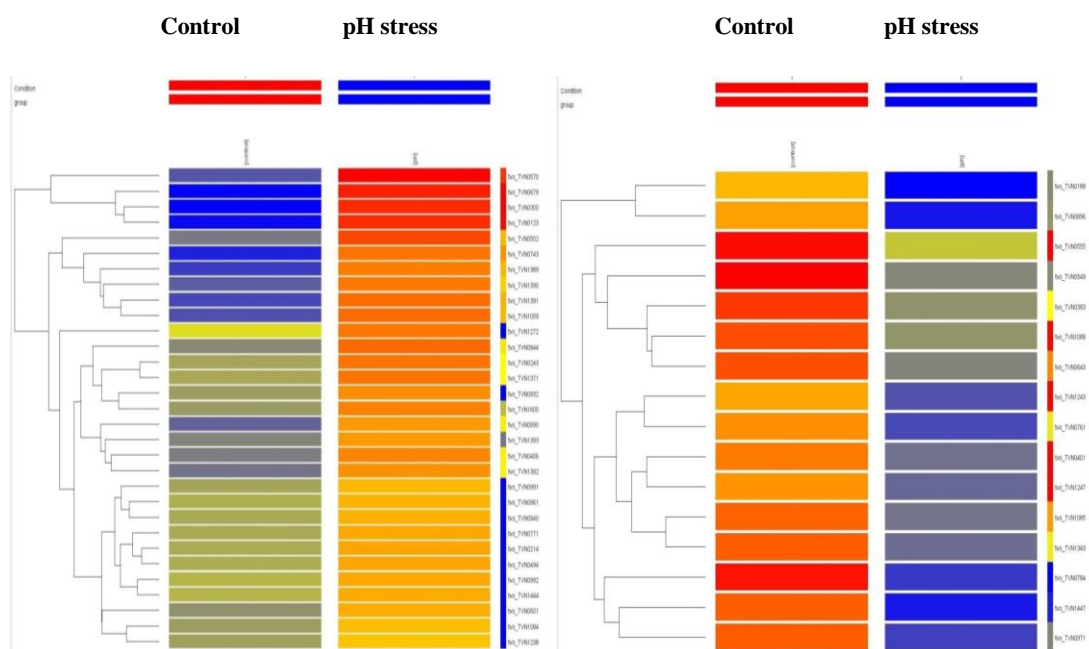


**Figure 3. 23. Cluster analysis of pH stress dataset.** Expression levels are indicated by colors. The shades of blue and red refer to the different expression levels. The dark red indicates the higher expression level, while the dark blue shows the lower expressions. The heat maps cover 66 % of the differentially expressed genes that are up regulated (A) and the remaining 34 % of the genes that are down regulated (B).

### 3.3.3.3. Genes Responsive to Oxidative Stress

Oxidative stress is caused by the production of reactive oxygen species (ROS) such as superoxide ion, hydrogen peroxide, hydroxyl radicals, which have detrimental effects on all cellular macromolecules and redox homeostasis. There are several reports on specific detoxification enzymes, ion scavengers, and their regulators. Activation of many these regulators by different stressors indicating that diverse environmental factors can directly or indirectly enhance production of ROS.

All microorganisms can be exposed to oxidative stress if the pro-oxidants outweigh the anti-oxidants in the cell, which eventually causes deleterious effects on the growth of many organisms. However, cells utilize different defense mechanisms against oxidative stress.

Understanding of the mechanisms can open new horizons in identification of the new metabolic pathways, enzymes, and their regulations. Based on this idea, transcriptional behavior of *Thermoplasma volcanium* when exposed to the oxidative stress was investigated by supplementing cultures with 0.02 mM and 0.03 mM H<sub>2</sub>O<sub>2</sub>. Subsequently, cells exposed to the mild (sub-lethal) oxidative stress (0.02 mM H<sub>2</sub>O<sub>2</sub>) and cells exposed to severe (lethal) oxidative stress (0.03 mM H<sub>2</sub>O<sub>2</sub>) were studied separately by using genome wide expression microarrays. The number of differentially expressed genes under severe oxidative stress were higher than the genes regulated under mild oxidative stress condition. Although different set of proteins were induced in each conditions, some common features found in both oxidative stress groups.

#### **3.3.3.3.1. Genes Responsive to Mild Oxidative Stress (0.02 mM H<sub>2</sub>O<sub>2</sub>)**

The change in the expression of a total of 86 genes were found to statistically significant during oxidative stress based on cut off criteria of p-values less than 0.05 and fold change  $\geq 2$ . Among these genes, 49 of them were up regulated as listed in Appendix B. It was important to note that the expression of aldo/ keto reductase (TVN0875; 6.33 fold), and Fe-S oxidoreductase (TVN0932; 4.33 fold) genes were remarkably increased. The products of these genes have critical roles in electron transfer and redox balance.

Aldo/keto reductases belong to the large superfamily of oxidoreductases involved in oxidation/ reduction of variety of compounds (Hyndman *et al.*, 2003). Most of the oxidoreductases produce reducing equivalents for free radical scavenging system (Kültz, 2005). Therefore, induced expression of TVN0875 and TVN0932 could be correspond for detoxifying lipid per oxidation products and maintaining intracellular redox balance. Moreover, data from previous transcriptome study also revealed that aldo/ keto reductase was up regulated upon exposure to oxidative stress in 3 kingdom of life. This was inferred from the network analysis performed using data from transcriptomics and proteomics study on *S.solfataricus*, *Bacillus*, *E.coli* and Yeast (Maaty *et al.*, 2009). These common response might suggest that aldo/keto reductase has central role in oxidative stress management in different organisms.

Transcript level of gene encoding thioredoxin reductase (TVN0470) enhanced by 2.15 fold in response to mild oxidative stress that has been previously reported for hyperthermophilic archaeon *Pyrococcus furiosus*, as well (Strand *et al.*, 2010). However, under oxidative stress *Methanosarcina barkeri* did not induce expression of the gene encoding thioredoxin reductase that was explained by inefficient induction condition (Zhang *et al.*, 2006).

In addition, product of 29% of the genes expression of which changed were described as hypothetical proteins and they were also up regulated. In fact, two genes TVN0700, TVN0933 were found to be highly up regulated > 4.0 fold (Appendix B) . Although their role in adaptive or regulatory response to oxidative stress is not known, further characterization might provide new insights onto the mechanisms of oxidative stress response.

Oxidative stress response in *T.volcanium* also resulted in the induction of some genes related to the transcription and translation process. This might indicate that *Tpv* cells are still capable of proceeding basic metabolic functions which are required for their survival. Therefore, increased transcript levels of genes encoding transcription anti termination protein NusG (TVN1443- 3.25 fold), two transcriptional regulators (TVN0567- 2.52; TVN0938-2.46), and two translation initiation factors (TVN0011- 2.42 fold; TVN1178-2.41) could be a consequence of that response. Under mild oxidative stress, adaptation of the *Thermoplasma volcanium* can also be helped by increased expressing the genes related to the carbohydrate metabolism.

It is quite possible that increased ATP demand during stress could be satisfied by activation of the certain carbohydrate metabolic pathways. Another important result from our microarray analysis is about 10% of the induced *Tpv* genes (total 49) in response to the mild oxidative stress belongs to the functional category of transport (including arsenite transport permease (TVN0285; 2.28 fold), Kef-type K<sup>+</sup> transporter (TVN0097; 2.011), major facilitator superfamily permease (TVN1245; 2.03 fold, TVN1053; 3.37 fold) and phosphate permease( TVN0063; 2.21 fold). genes. Induced expression of transporters might have role in maintaining the intracellular ionic concentration during oxidative stress, since *T.volcanium* has an

unusually high positive charge distribution inside the cell (Gerday *et al.*, 2007). Also, induced expression of genes encoding secondary transporters (permeases) could be associated with increased demand for uptaking of organic molecules during stress, as in other stresses. These results are consistent with the transcriptional analysis in *P.furiosus* and *S.solfataricus* to peroxide shock where ABC transporters and permeases were up regulated in response to H<sub>2</sub>O<sub>2</sub> induced oxidative stress (Strand *et al.*, 2010; Maaty *et al.*, 2009).

Of the 49 up regulated *Tpv* genes upon mild oxidative stress, about 8% of them fall into the functional categories of integration/recombination (*e.g.*, TVN0587, (transposase; 2.14 fold), TVN0695 (site specific recombinase; 3.69 fold), TVN0137 (integrase/recombinase; 3.15 fold)). Orthologs of these genes in *Methanosarcina barkeri* were also induced in response to the oxidative stress. Proteins of these genes related to the transposition with a proposed role in mutational divergence (Zhang *et al.*, 2006). Enhanced transposition activity in *Pseudomonas putida* upon starvation was thought as a strategy to raise overall mutation rate and create new and useful mutations under stress (Ilves *et al.*, 2001). One of the up-regulated *Tpv* genes encodes an ATPase AAA (TVN0696), which is a member of a large superfamily of proteins having a diverse range of functions, (for example as subunits of proteases or as molecular chaperones involved in the unfolding and disaggregation of macromolecules) (Saibil, 2013). This result is in agreement with the data from a previous report on oxidative stress associated transcriptional profiling of *Pyrococcus furiosus* (Strand *et al.*, 2010).

The PF1321 gene of *P.furiosus* encoding AAA ATPase was found to be up regulated by a factor of 6.0 within 30 min following exposure to 0.5 mM H<sub>2</sub>O<sub>2</sub>. These results imply that AAA ATPases might have critical role in protection of proteins against damaging effects of oxidative stress in archaea. Effect of oxidative stress on protein export was also implicated in *Thermoplasma volcanium* since the gene (TVN1444) encoding protein translocase subunit Sss1 (SEC61 subunit gamma) was found to be up regulated about 3.60 fold (Table 3.11). However, in *M.barkeri*, protein translocase subunit SecY production was repressed as a result of air exposure (Zhang *et al.*,

2006). This inconsistency may indicate involvement of different pathways by different species while adapting to stress.

**Table 3. 11. Functional categorization of the induced genes upon 0.02 mM oxidative stress**

<b>Functional classes of proteins</b>	<b>Gene Symbol</b>	<b>P values</b>	<b>Fold change</b>
<b>Complex disassembly</b>			
ATPase AAA	TVN0696	0.018	2.23
<b>Electron transfer and redox balance</b>			
Aldo/ Keto reductase	TVN0875	0.003	6.33
Fe / S Oxidoreductase	TVN0932	0.003	4.33
Hydrogenase 4 subunit F	TVN1455	0.008	2.54
Hydrogenase 4 subunit B	TVN1458	0.008	2.17
Thioredoxin reductase	TVN0470	0.010	2.15
<b>Transcription</b>			
Transcription antitermination protein NusG	TVN1443	0.002	3.25
LysR family transcriptional regulator	TVN0567	0.005	2.52
Metal dependent transcriptional regulator	TVN0938	0.008	2.46
<b>Translation</b>			
Translation initiation factor IF-6	TVN0011	0.005	2.42
Translation initiation factor IF-1A	TVN1178	0.004	2.41
<b>Carbohydrate metabolism</b>			
Pyruvate: ferredoxin oxidoreductase	TVN0835	0.005	2.37
2-oxoisovalerate-ferredoxin oxidoreductase	TVN0834	0.009	2.35
<b>Transporters</b>			
Kef-type K <sup>+</sup> transporter	TVN0097	0.01	2.011
Arsenite transport permease	TVN0285	0.006	2.28
Major facilitator superfamily permease	TVN1245	0.009	2.03
Phosphate permease	TVN0063	0.006	2.21
<b>Integration/Recombination</b>			
Site specific recombinase	TVN0695	0.005	3.69
Integrase/recombinase	TVN0137	0.004	3.15
Transposase	TVN0587	0.006	2.14
<b>Protein secretion</b>			
Protein translocase subunit Sss1	TVN1444	0.002	3.60
<b>Hypothetical Proteins</b>			
Hypothetical Protein	TVN0930	4.14	0.004
Hypothetical Protein	TVN0700	5.11	0.001

Among 86 *Tpv* genes that are exclusively responsive to oxidative stress, 37 were found to be down regulated (Appendix B). Functional analysis showed that down regulated genes fell into a variety of functional groups such as cell division, motility, signaling, biosynthetic process, electron transfer, and proteolysis as listed in Table 3.12. This shows that oxidative stress hits the basic functions of cells. Out of 37 repressed genes, 19% of them are encoding the electron transfer proteins *i.e.*, dehydrogenase (TVN1278), Rieske Fe-S protein (TVN0366), alcohol dehydrogenase (TVN0944), ferredoxin like protein (TVN1279). Decreased expression of electron transfer proteins which is required for central metabolic pathways imply that when confronted with oxidative stress, metabolic activity of *Thermoplasma volcanium* declines. Our result is supported by previous reports on *M.barkeri* and *P.furiosus* that showed reduced expression of genes coding for hydrogenases, oxidoreductases in response to the oxidative stress (Zhang *et al.*, 2006; Maaty *et al.*, 2009).

Another group of repressed *Tpv* genes in response to the mild oxidative stress are those related to the aminoacid, lipid and cofactor biosynthesis, which constitute 19% of the down regulated genes. Decrease in the expression level of these genes associated with a range of biosynthesis processes suggest that *Tpv* cells respond to the oxidative stress by slowing down their metabolism. Same trend was also observed in *M.barkeri* upon air exposure (Zhang *et al.*, 2006). As in other stressfull conditions, oxidative stress also resulted in arrest of the cell growth. Repression of the expression of cell division protein FtsZ (TVN0027;-2.31 fold) can be an implication of this response. Furthermore, *Tpv* genes encoding flagellins (FlaH and FlaF) were suppressed upon oxidative stress. In addition, about 22% of down regulated genes were annotated as hypothetical proteins. Further characterization of those hypothetical proteins are required in order to understand whether these responses are specific to H<sub>2</sub>O<sub>2</sub> induced stress or not.

**Table 3. 12. Functional categorization of the repressed genes upon 0.02 mM oxidative stress**

<b>Functional classes of proteins</b>	<b>Gene Symbol</b>	<b>P values</b>	<b>Fold change</b>
<b>Electron transfer and redox balance</b>			
Dehydrogenase	TVN1278	0.012	-3.73
5,10 methylene tetrahydrofolate reductase	TVN1125	0.003	-3.21
Rieske Fe-S protein	TVN0366	0.004	-3.11
Ferredoxin like protein	TVN1279	0.035	-2.93
Alcohol dehydrogenase	TVN0944	0.001	-2.47
Electron transfer flavoprotein subunit alpha	TVN1281	0.024	-2.46
NAD(FAD) dependent dehydrogenase	TVN1432	0.017	-2.04
<b>Cell division</b>			
Cell division protein FtsZ	TVN0027	0.004	-2.31
<b>Motility</b>			
Archaeal flagellar protein FlaF	TVN0610	0.004	-2.31
Archaeal flagellar protein FlaH	TVN0612	0.007	-2.08
<b>Aminoacid metabolism and biosynthesis</b>			
Aspartate aminotransferase	TVN0848	0.015	-4.01
Methionine synthase	TVN1123	0.008	-2.70
Glutamine synthase	TVN1492	0.024	-2.14
3-dehydroquininate synthase	TVN1316	0.014	-2.28
<b>Lipid metabolism</b>			
Enoyl-CoA hydratase	TVN0363	0.009	-2.26
<b>Cofactor Biosynthesis</b>			
Cobalamin synthase	TVN0495	0.005	-2.15
Pyridoxal biosynthesis lyase	TVN0998	0.01	-2.11
<b>Proteolysis</b>			
Metal dependent carboxypeptidase	TVN0740	0.007	-2.71
<b>Uncharacterized proteins</b>			
Inner membrane protein	TVN0965	0.022	-2.57
SAM dependent methyl transferase	TVN0574	0.007	-2.27
<b>Signalling</b>			
GTPase	TVN0401	0.004	-2.29
<b>Hypothetical proteins</b>			
Hypothetical protein	TVN0941	0.007	-3.33
Hypothetical protein	TVN0360	0.003	-3.0

Differentially expressed *Tpv* genes under mild oxidative stress were clustered using hierarchical algorithm and the Heat maps generated are shown in Figure 3.24.

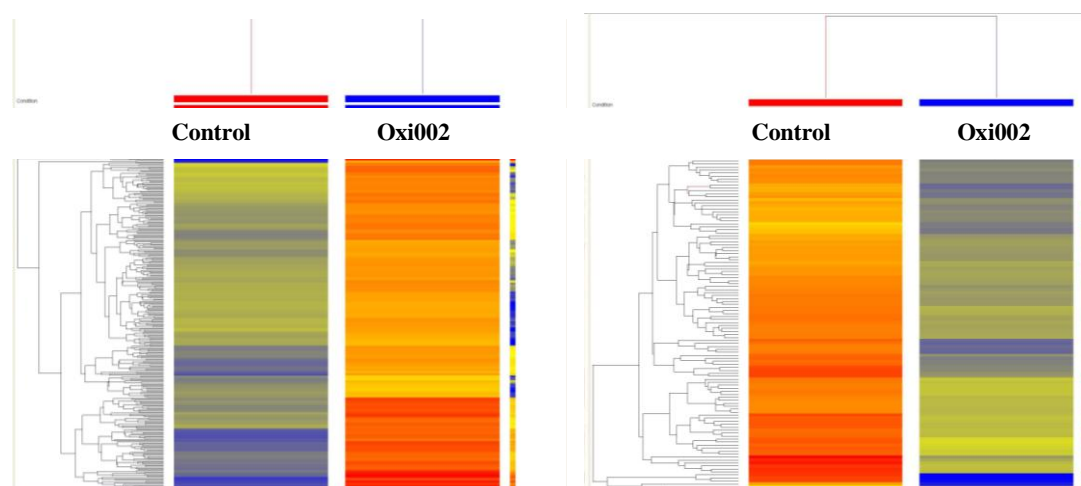


**Figure 3. 24. Cluster analysis of Oxi002 stress dataset.** Expression levels are indicated by colors. The shades of blue and red refer to the different expression levels. The dark red indicates the higher expression level, while the dark blue shows the lower expressions. The heat maps cover 57 % of the differentially expressed genes that are up regulated (A) and the remaining 43 % of the genes that are down regulated (B).

### 3.3.3.3.2. Genes Responsive to Lethal Oxidative Stress (0.03 mM H<sub>2</sub>O<sub>2</sub>)

Under lethal oxidative stress condition, expression of 339 genes out of 1474 annotated *Tpv* genes (moderated T- test FC  $\geq 2$ -fold, cut off value  $p < 0.05$ ) were down regulated while 113 genes were up regulated. Majority of the induced genes are associated with electron transfer, redox potential and detoxification of the reactive oxygen species. Among these, Fe-S oxidoreductases (TVN0932; 5.29-fold), hydrogenase 4 subunit F (TVN1455; 3.40 fold) are likely to be involved in maintenance of intracellular redox balance. Increased expression of aldo/keto reductases (TVN0875; 12.84 fold) and mercuric reductase (TVN0251; 3.44 fold) may be related to the detoxification of the lipid peroxidation products and scavenging of the toxic metals. Some of these genes were also found to be up regulated under mild oxidative stress caused by 0.02 mM hydrogen peroxide *i.e.*, TVN0875 (aldo/keto) reductase and TVN0932 (oxidoreductase). This result suggests that maintaining redox homeostasis and elimination of free radicals are of central

importance for dealing with oxidative stress. Interestingly, although *T.volcanium* has capacity to encode superoxide dismutase, glutaredoxin, thioredoxin peroxidase, their transcription levels did not change in response to the oxidative stress. In contrast to transcriptional profiling of *T.volcanium*, transcriptome analysis of *Sulfolobus solfataricus* upon oxidative stress revealed the largest changes in the abundance of genes encoding Archaeal Rieske-type ferredoxin, and peroxiredoxin. The proteomic data from *Sulfolobus solfataricus* also showed the induced expression of genes encoding superoxide dismutase, rubrerythrin, peroxiredoxin under oxidative stress (Maaty *et al.*, 2009). Response of hyperthermophilic archaeon *Pyrococcus furiosus* to hydrogen peroxide was similar to the *S.solfataricus*. qRT-PCR results showed the increased expression of genes encoding thioredoxin, rubrerythrin, alkyl hydroperoxide reductase, and Dps like protein in *P.furiosus*. Enhancement of their expression should contribute to maintenance of redox homeostasis and elimination of reactive oxygen species (Strand *et al.*, 2010). It is questionable why none of those genes was differentially expressed in *T.volcanium* under the oxidative stress condition, and might be explained by use of alternative adaptive mechanisms which are species- specific. On the other hand, the gene (TVN1466) encoding AAA ATPase was highly induced by a factor of 14.65 fold. The same mRNA level was also increased about 2.33 fold in 0.02 mM hydrogen peroxide treated *Tpv* cells. As it is known AAA ATPase has roles in a variety of cellular process such as protein folding, and translocation, DNA replication and repair, membrane fusion and proteolysis (Smith *et al.*, 2006). It is more likely that AAA ATPase should have central role in *T.volcanium* to cope with oxidative stress provoked by hydrogen peroxide. Transcriptional profiling indicated that under severe oxidative stress expression of the genes responsible for carbohydrate metabolism and transport activity were also induced. The genes TVN0834 and TVN0835 encoding 2-oxoisovalerate oxidoreductase and pyruvate: ferredoxin oxidoreductase, respectively were significantly up regulated (> 3 fold) (Table 3.13). Induced expression of these genes, and those encoding several type of transporters *e.g.*, inorganic ion transporters (TVN0997, TVN0303, TVN0828), aminoacid transporter (TVN1130), carbohydrate transporters (TVN1143, TVN1053, TVN0594) should contribute to the energy production and conservation. Same sets of genes are also up regulated in response to

mild oxidative stress generated by 0.02 mM hydrogen peroxide as mentioned previously.

Unlike 0.02 mM H<sub>2</sub>O<sub>2</sub>, exposure to the 0.03 mM H<sub>2</sub>O<sub>2</sub> increased mRNA levels of the genes (*i.e.*, TVN1389; 4.67 fold, TVN1390; 4.07 fold, TVN1391; 3.80 fold) responsible for Fe-S cluster biosynthesis. This cluster is made up of non-heme iron atom and an acid labile sulfur atom and found in variety of ferredoxins and Fe-S metalloenzymes. They have important roles in substrate binding/activation, environmental sensing and gene regulation. Fe-S cluster is vulnerable to oxidative stress. Therefore, in order to compensate damage induced by oxidative stress, synthesis of Fe- S cluster occurs by mobilization of sulfur and iron atoms to scaffold protein, which provide an intermediate assembly site (Iwasaki, 2010). Thus, enhancement of iron uptake by *T.volcanium* under oxidative stress is more likely to *restore* the Fe-S cluster. Our results are in agreement with the data from gene expression profiling of *S.solfataricus* under oxidative stress. The up regulated genes such as sufB, sufD also participate in Fe-S cluster biosynthesis in this archaeon (Maaty *et al.*, 2009). Moreover, homology domain search shows that TVN1389 and TVN1390 proteins have sufB domain. This result may imply that biosynthesis of Fe-S cluster can be important for protection from oxidative damage in archaea.

Moreover, under severe oxidatives stress condition, *Tpv* genes coding for transcription regulators (*i.e.*, TVN0938, TVN0567, TVN1392) and translation initiation factors were found to be up regulated, as well (Table 3.13). These results indicate that *T.volcanium* still synthesize some proteins, which are vital for its survival to combat with severe oxidative stress.

Severe oxidative stress, like mild stress induced by 0.02 mM H<sub>2</sub>O<sub>2</sub> enhanced the expression of *Tpv* genes (*i.e.*, TVN0137; 5.16 fold, TVN0687; 3.06 fold, TVN0695; 2.93 fold, TVN0136; 2.61 fold, TVN0587; 2.15 fold ) whose products involve in integration/recombination processes. Besides, about 27% of the induced genes were found to be annotated as genes for hypothetical proteins. Among them, transcript levels of TVN1417, TVN0150, and TVN1418 were strongly induced by a factor of

9.28, 8.42, and 8.15 fold, respectively. Whether those hypothetical proteins play important regulatory role during oxidative stress is awaiting for further research.

In addition to the hypothetical proteins, some uncharacterized proteins are also found to be differentially expressed. For example, function of HD family phosphatase (encoded by TVN1403 gene) is not known. Similarly, transcriptome analysis of *S.solfataricus* in response to the hydrogen peroxide also showed induced expression of the SSO2355 gene encoding a putative phosphatase (Maaty *et al.*, 2009). Further characterization is required to fully understand the involvement of phosphatases to counteract with oxidative stress in the archaea.

**Table 3. 13. Functional categorization of the induced genes upon 0.03 mM H<sub>2</sub>O<sub>2</sub>**

Functional classes of proteins	Gene symbol	P values	Fold change
<b>Carbohydrate metabolism</b>			
Pyruvate:ferredoxin oxidoreductase	TVN0835	5.06E-04	3.83
2-oxoisovalerate-ferredoxin oxidoreductase	TVN0834	0.007	3.12
<b>Transporters</b>			
Major facilitator superfamily permease	TVN1053	2.88E-04	6.11
Threonine dehydratase	TVN1130	6.99E-04	6.04
Mn <sup>2+</sup> transporter	TVN0828	0.001	4.12
Major facilitator super family permease	TVN1245	9.75E-04	3.47
Kef type K+ transporter NAD binding	TVN0997	7.84E-04	3.44
Sugar binding protein	TVN1143	9.95E-04	3.16
Phosphate ABC transporter permease	TVN0303	0.01	3.78
Major facilitator superfamily permease	TVN0594	0.001	2.68
ABC transporter permease	TVN0936	0.002	2.60
<b>Iron sulfur cluster assembly</b>			
Iron regulated ABC type transporter	TVN1389	8.18 E-04	4.67
Iron –regulated ABC type transporter	TVN1390	8.01E-04	4.07
Iron regulated ABC transporter ATPase subunit	TVN1391	9.75E-04	3.80
<b>Electron transfer and redox balance</b>			
Aldo/keto reductase	TVN0875	2.15E-04	12.84
Fe-S oxidoreductase	TVN0932	3.96E-04	5.29
Mercuric reductase	TVN0251	7.88E-04	3.44
Hydrogenase 4 subunit F	TVN1455	6.49E-04	3.40
<b>Transcription</b>			
Metal dependent transcription regulator	TVN0938	6.29E-04	3.99
LysR family transcriptional regulator	TVN0567	6.98E-04	3.69
RNA processing exonuclease	TVN0437	6.82E-04	3.56
Transcriptional regulator	TVN1392	0.001	3.30
Transcription initiation factor IIB	TVN1083	0.001	3.29
nusG;transcription antitermination protein	TVN1443	7.43E-04	3.01

"Table 3.13 (Cont'd)"

Functional classes of proteins	Gene symbol	P values	Fold change
<b>Translation</b>			
Translation initiation factor IF-1A	TVN1178	0.002	2.58
Translation initiation factor IF-6	TVN0011	0.003	2.18
<b>Integration/Recombination</b>			
Integrase /recombinase	TVN0137	0.018	5.16
Hypothetical protein;K07485 transposase	TVN0687	0.001	3.06
Site specific recombinase .DNA invertase Pin related	TVN0695	0.001	2.93
Integrase /recombinase	TVN0136	0.002	2.61
Transposase	TVN0587	0.008	2.15
<b>Protein unfolding and complex disassembly</b>			
ATPase AAA	TVN1466	2.06E-04	14.65
ATPase AAA	TVN0696	0.002	2.77
<b>Hypothetical proteins</b>			
Hypothetical protein	TVN1417	4.75E-04	9.28
Hypothetical protein	TVN0150	2.43E-04	8.42
<b>Uncharacterized Protein</b>			
HD family phosphatase	TVN1403	2,44E-04	5.40

On the other hand, under severe oxidative stress, out of 452 differentially expressed *Tpv* genes, 75% of them were down regulated. The major group of down regulated genes is related to the ribosomal structure (*i.e.*, TVN0355; -3.82 fold, TVN0399; -3.35 fold, TVN0423; -2.81 fold). This stress also adversely affected transcription/translation processes. This is evident from down regulation of several transcriptional regulators (*i.e.*, TVN0603; -5.78 fold, TVN1186; -4.86 fold, TVN0498; -3.79 fold, TVN0292; -3.47 fold), and translation initiation factors (*i.e.*, TVN0655; -4.32 fold, TVN1252; -3.11 fold, TVN1274; -3.28 fold, TVN1298; -2.43 fold). This combined effect of decreased transcription and translation is impairment of protein synthesis during oxidative stress. In addition, transcription of some genes related to the purine metabolism (*e.g.*, carbamoyl phosphate synthase small subunit, TVN0802; -4.20 fold) and signal transduction (*e.g.*, GTPase; TVN0401; -6.15 fold) were also repressed. These results are consistent with the previous report on *M.barkeri* (Zhang *et al.*, 2006). In this study, it was found that most of the down regulated genes are belonged to the functional categories of translation, ribosomal structure, aminoacid transporter, and signal transduction. Our results also showed that *Tpv* cell growth was arrested under oxidative stress as in other stressfull conditions. Repression of the

expression of cell division protein FtsZ (TVN0027;-4.84 fold) can be an implication of this response (Table 3.14). In addition, growth arrest can be related to the decrease in the ATP synthesis activity. The *Tpv* genes encoding V-type ATP synthase subunits F and C were found to be down regulated. As an extension of such general stress response, carbohydrate and lipid metabolisms should be shut down, since abundance of TVN1141 and TVN1091 transcripts (encoding glycerol kinase and 3-hydroxyacyl-CoA dehydrogenase, respectively) were found to be dropped significantly. According to our microarray analysis, *Tpv* gene encoding DNA repair proteins *i.e.*, DNA repair exonuclease (TVN0228, -2.24 fold), and radB (TVN0559,-2.0 fold) were down regulated. However, the report on oxidative stress associated transcriptome analysis conducted in hyperthermophilic archaeon *Pyrococcus furiosus* revealed that exposure to hydrogen peroxide resulted in the induction of genes encoding DNA repair proteins (*i.e.*, radA) (Strand *et al.*, 2010). This might be an another manifestation of species- specific difference between members of archaea in terms of stress response mechanisms.

In addition to these, transcript levels of the genes related to the electron transfer and redox balance were also down regulated (*i.e.*, TVN1280 (electron transfer flavoprotein subunit beta; -4.80 fold), TVN0473 (NAD-FAD dehydrogenase; -4.73 fold), TVN1004 (Fe-S oxidoreductase; -4.002 fold), TVN1157 (Oxidoreductase; - 3.52 fold), TVN0777 (Thioredoxin; -2.61 fold), TVN1279 (Ferredoxin like protein; -3.61 fold)). Thus, in the cases of mild and severe oxidative stress, general metabolic processes such as carbohydrate, lipid, cofactor metabolisms slow down, possible for the reason of reducing the electron transfer activity. However, down regulation of genes encoding thioredoxin and ferredoxin like proteins was not expected, since these two proteins have critical roles in coping with oxidative stress by maintaining the redox balance. For example, genes encoding ferredoxins were up regulated as revealed by the microarray data of transcriptome analyses in *Sulfolobus solfataricus*, and *Pyrococcus furiosus* under oxidaitve stress (Maaty *et al .*, 2009; Strand *et al.*, 2010).

Another unexpected result of our study is the gene TVN0578 encoding FKBP-type peptidylprolyl isomerase was highly down regulated (about 6.5 fold). It is known

that oxidative stress damages proteins by oxidizing cysteine or methionine and disturbing the native structure of proteins that is essential for their proper functioning (Kültz, 2005). Biological significance of this protein is related to its role in rate limiting step of protein folding besides its the chaperone like activity (Ideno *et al.*, 2002). Also, this protein is one of the highly conserved stress proteins (Kültz, 2005). In accordance with this notion, we would like to expect increased expression of TVN0578 during oxidative stress. Unlike our results, proteome analysis of *Sulfolobus solfataricus* after hydrogen peroxide treatment revealed that genes related to protein folding (*i.e.*, the small heat shock protein, thermosome alpha and beta subunit) were up regulated (Maaty *et al.*, 2009).

In addition to these, large number of genes (approximately 21% out of 339 down regulated genes) were annotated as hypothetical proteins. Among them, TVN0946, TVN1405, TVN0860 are in the top category of highly repressed genes (Appendix B).

**Table 3. 14. Functional categorization of the repressed genes by 0.03 mM H<sub>2</sub>O<sub>2</sub>**

Functional classes of proteins	Gene Symbol	P-Value	Fold change
<b>Transcription</b>			
Transcription regulator	TVN0603	3,31E-04	-5.78
Transcription regulator	TVN1186	3,04E-04	-4.86
RNA polymerase II complex ELP3 subunit	TVN0498	7,24E-04	-3.79
Metal dependent transcription regulator	TVN0945	4,10E-04	-3.98
Transcription regulator	TVN1162	7,32E-04	-3.85
Transcription regulator	TVN0624	8,26E-04	-3.33
Transcription regulator	TVN1127	8,48E-04	-3.05
Transcription regulator	TVN0185	0,003	-2.19
Transcription activator	TVN0084	0,004	-2.04
Transcription activator	TVN0406	0,006	-2.04
Fur family transcriptional regulator	TVN0292	6,49E-04	-3.47
<b>Translation</b>			
Translation initiation factor IF-2 subunit beta	TVN0655	3,60E-04	-4.32
rpl37e; 50S ribosomal protein L37	TVN0355	4,75E-04	-3.82
rps2P; 30S ribosomal protein S2	TVN0399	9,66E-04	-3.35
rpl11p; 50S ribosomal protein L17	TVN0423	0,001	-2.81
Translation initiation factor IF-2B subunit alpha	TVN1252	9,50E-04	-3.11
Translation initiation factor IF-2B subunit gamma	TVN1274	9,33E-04	-3.28
50S ribosomal protein L17	TVN0423	0,001	-2.81
Translation factor(SUA-5 related)	TVN1298	0,002	-2.43
<b>Purine/Pyrimidine metabolism</b>			
Carbamoyl phosphate synthase small subunit	TVN0802	3,64E-04	-4.20
Folate dependent phosphoribosyl glycine	TVN0171	3,65E-04	-4.35

"Table 3.14 (Cont'd)"

Functional classes of proteins	Gene Symbol	P-Value	Fold change
<b>Cell division</b>			
Cell division GTPase	TVN0657	7,02E-04	-4.45
Cell division protein FtsZ	TVN0027	3,99E-04	-4.84
<b>Electron transfer and Redox balance</b>			
Dehydrogenase (flavoprotein)	TVN1278	0,01	-3.41
Thioredoxin	TVN0777	0,002	-2.61
Ferredoxin like protein	TVN1279	0,010	-3.61
Electron transfer flavoprotein subunit beta	TVN1280	0,004	-4.80
NAD(FAD)-dependent dehydrogenase	TVN0473	3,20E-04	-4.73
Fe-S oxidoreductase	TVN1004	4,75E-04	-4.02
Oxidoreductase	TVN1157	0,002	-3.52
Electron transfer flavoprotein subunit beta	TVN1383	0,002	-2.53
<b>DNA repair</b>			
DNA repair exonuclease	TVN0228	0,005	-2.24
radB; DNA repair and recombination protein RadB	TVN0559	0,006	-2.00
<b>ATP synthesis</b>			
V-type ATP synthase subunit F	TVN0051	0,004	-2.33
V-type ATP synthase subunit C	TVN0050	0,003	-2.10
Kef-type K <sup>+</sup> transporter	TVN0988	7,03E-04	-3.31
ABC-type multidrug transport system. ATPase component	TVN1367	0,001	-3.11
H <sup>+</sup> -ATPase subunit K	TVN0048	9,33E-04	-3.08
Cation transport ATPase	TVN1240	5,06E-04	-3.95
Aminoacid transporter	TVN0911	0,001	-5.59
Proline/betaine transport permease	TVN1160	6,29E-04	-4.28
Cation transport ATPase	TVN1240	5,06E-04	-3.95
Kef-type K <sup>+</sup> transporter	TVN0988	7,03E-04	-3.31
<b>Carbohydrate metabolism</b>			
Glycerol kinase	TVN1141	6,53E-04	-3.72
Pyruvate kinae	TVN1020	0,006	-2.04
<b>Lipid metabolism</b>			
3-hydroxyacyl-CoA dehydrogenase	TVN1091	0,001	-3.16
Glycerol 1 phosphate dehydrogenase	TVN1227	0,001	-2.83
<b>Cofactor Biosynthesis</b>			
Riboflavin kinase	TVN0519	0,002	-2.29
Molybdopterin/thiamine biosynthesis	TVN0943	5,06E-04	-3.55
Molybdopterin biosynthesis protein	TVN0751	0,006	-2.06
<b>Protein folding</b>			
FKBP type peptidylproyl isomerase	TVN0578	8,18E-04	6.5
<b>Signalling</b>			
GTPase	TVN0401	2,91E-04	-6.15

Differentially expressed *Tpv* genes under lethal oxidative stress were clustered using hierarchical algorithm and the Heat maps generated are shown in Figure 3.25.

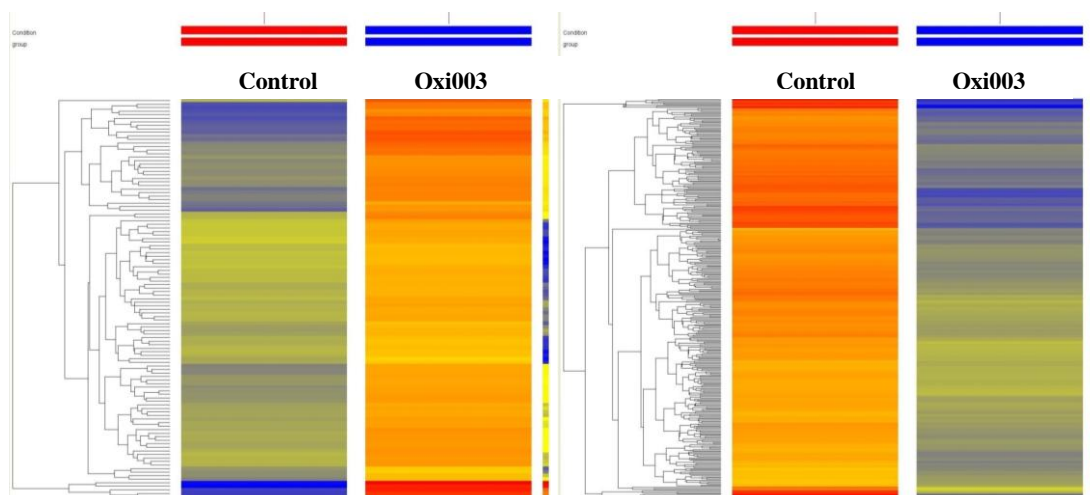


**Figure 3. 25. Cluster analysis of Oxi003 stress dataset.** Expression levels are indicated by colors. The shades of blue and red refer to the different expression levels. The dark red indicates the higher expression level, while the dark blue shows the lower expressions. The heat maps cover 25 % of the differentially expressed genes that are up regulated (A) and the remaining 25 % of the genes that are down regulated (B).

### 3.3.4. Comparison of Gene Regulation among Heat Shock, Oxidative Stress and pH Stress Groups

In order to compare gene expression profiles in 4 different stress groups, Venn Diagrams are generated using GeneSpring software program. Venn diagram illustrates differentially expressed genes which are stress specific or shared between different stress groups (Figure 3.26).

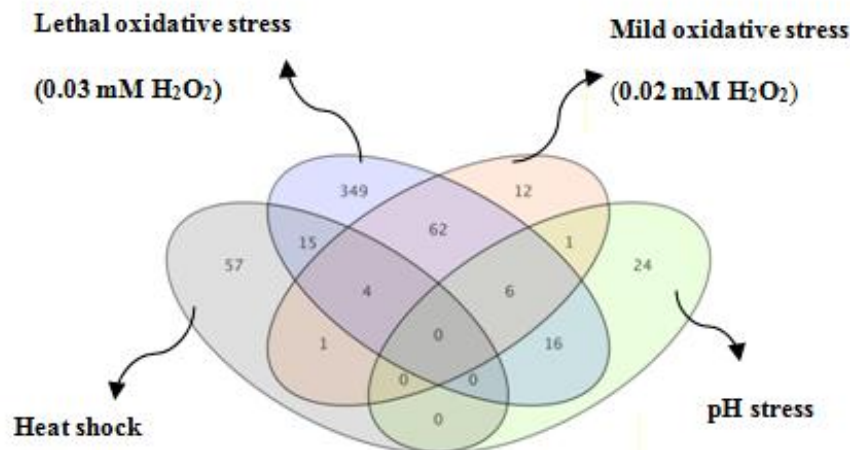


**Figure 3. 26. Venn diagram generated from all data sets.** The numbers inside the areas show the differentially expressed genes based on cut of criteria criteria ( $p$  value  $< 0.05$ ;  $FC \geq 2$  fold). Intersections between circles show overlapping genes (up/down regulated) under different stress conditions.

Analysis of the Venn diagram revealed that there is no shared transcripts levels of which changed in response to all 4 stress conditions. There is only one gene common between mild oxidative stress and pH stress groups. This gene (TVN1371) codes for hypothetical protein was induced during pH stress and 0.02 mM oxidative stress.

Similarly, one differentially regulated gene is common between heat shock and mild oxidative stress groups. This gene (TVN0612) product is a flagellar accessory protein FlaH and it was down regulated.

Venn diagram shows that the regulations of the 4 genes under heat shock and two different oxidative stress conditions (0.02 mM  $H_2O_2$  and 0.03 mM  $H_2O_2$  provoked oxidative stress) have changed (Table 3.15). Among these one coding for aldo/keto reductase is significantly up-regulated, and can be critical in dealing with both heat stress and oxidative stress. On the other hand, down regulation of the remaining three genes under oxidative stress might be an indication of impairment of redox potential and carbon metabolism.

**Table 3. 15. Overlapping genes differentially expressed under heat shock and two oxidative stresses**

<b>Gene Symbol</b>	<b>Description</b>	<b>FC for Heat-Shock</b>	<b>FC for Lethal Oxidative Stress</b>	<b>FC for Mild Oxidative Stress</b>
TVN0875	aldo/keto reductase	2.82	12.84	6.33
TVN1278	dehydrogenase	2.38	-3.41	-3.73
TVN1279	ferredoxin-like protein	2.74	-3.61	-2.92
TVN0676	formylmethanofuran dehydrogenase	2.00	-2.58	-2.03

Table 3.16 and Table 3.17 list the differentially expressed genes shared by pH stress and oxidative stress data sets. Expression of genes 22 genes were commonly affected by pH stress and lethal oxidative stress groups. Among these genes, some are related to the electron transfer *i.e.*, Fe-S oxidoreductase (TVN0932), inorganic ion transport *i.e.*, Iron regulated ABC type transporter (TVN1389, TVN1390), and phosphate ABC type transporter (TVN0123), and they all are up regulated. This may suggest that regulations of redox homeostasis and intracellular ionic balance is required under oxidative and pH stress. Furthermore, KEOPS complex encoded by TVN1600 is also found to be induced upon pH and oxidative stress by a factor of 2.88 and 3.97 fold respectively, implying the importance of accurate translation during both stress. Also, transcription level of TVN1392 encoding transcriptional regulator seems to be enhanced during pH and oxidative stress. Its role could be in the control of stress specific gene expression. Genes belonging to functional categories of signaling (TVN0401; GTPase), translation (TVN1247, 30S ribosomal protein S3), lipid metabolism (TVN0363, enoyl CoA hydratase) were repressed in response to the pH and lethal oxidative stress (Table 3.16). When the roles of overlapping genes are considered, the conservation of energy and cell mass appears to be important while cell adapting to diverse stress conditions.

**Table 3. 16. Overlapping genes differentially expressed under pH stress and lethal oxidative stress (0.03 mM H<sub>2</sub>O<sub>2</sub>) data sets**

<b>Gene Symbol</b>	<b>Description</b>	<b>FC for pH Stress</b>	<b>FC for Lethal Oxidative Stress</b>
TVN0784	benzoylformate decarboxylase	-3,10	-2,11
TVN0243	hypothetical protein	2,94	2,82
TVN1389	Iron-regulated ABC-type transporter	4,54	4,67
TVN1084	H/ACA RNA-protein complex component Gar1	2,14	2,37
TVN0896	SAM-dependent methyltransferase	-2,52	-2,29
TVN0932	Fe-S oxidoreductase; K06937	2,71	5,29
TVN0844	hypothetical protein	3,53	-2,32
TVN0401	GTPase; K06883	-2,07	-6,15
TVN1393	aromatic ring hydroxylating enzyme	2,8	3,30
TVN0406	transcription regulator	3,26	-2,04
TVN1391	Iron-regulated ABC transporter	4,69	3,79
TVN0300	hypothetical protein	8,87	-4,91
TVN0992	signal recognition particle Srp54	2,13	-2,51
TVN0940	hypothetical protein	2,16	-2,93
TVN1600	KEOPS complex Cgi121-like subunit	2,88	3,97
TVN1444	protein translocase subunit Sss1	2,1	3,15
TVN1392	transcription regulator	3,22	3,31
TVN1390	Iron-regulated ABC-type	3,97	4,07
TVN0123	phosphate ABC transporter	8,4	2,57
TVN1247	30S ribosomal protein S3	-2,02	-2,67
TVN0363	Enoyl-CoA hydratase	-2.19	-2.50

**Table 3. 17. Overlapping genes differentially expressed under pH stress and two oxidative stress data sets**

<b>Gene Symbol</b>	<b>Description</b>	<b>FC for pH</b>	<b>FC for Lethal Oxidative Stress</b>	<b>FC Mild Oxidative Stress</b>
TVN0932	Fe-S oxidoreductase	2.71	5.29	4.33
TVN0401	GTPase	-2.07	-6.15	-2.30
TVN1600	KEOPS complex Cgi121-like subunit	2.88	3.97	2.20
TVN0363	enoyl-CoA hydratase	-2.19	-2.50	-2.26
TVN0243	hypothetical protein	2.95	2.82	2.88
TVN1444	protein translocase subunit Sss1	2.10	3.15	3.60

On the other hand, 21 differentially expressed genes were found to be commonly expressed under heat shock and lethal oxidative stress. Among these, the genes encoding alcohol dehydrogenase (TVN1284) and alko/keto reductase (TVN0875) could be induced in order to regulate redox balance under both stress conditions (Table 3.18). Also, increased energy demand during heat and oxidative stress might be compensated by inducing genes related to sugar uptake (*e.g.*, permease, TVN0021). On the other hand, 57 % of the overlapping genes were found to be down regulated. According to the functional categorization of these genes, motility (TVN0611; TVN1426) carbohydrate metabolism (TVN0200), pyrimidine metabolism (TVN0802), and transport activity (TVN0226) found to be down regulated, possibly as a result of energy saving and growth retardation. In addition, gene encoding glycosyltransferase was also down regulated in response to heat shock and oxidative stress. Besides, regulation of the some uncharacterized proteins *i.e.*, nucleic acid binding protein (TVN1259 up regulated under heat-shock, but down regulated under oxidative stress) and metal binding protein (TVN0073 down regulated under heat-shock, but up regulated under oxidative stress) was different between pH stress and oxidative stress as listed in Table 3.18.

**Table 3. 18. Overlapping genes differentially expressed under heat shock and lethal oxidative stress groups**

Gene Symbol	Description	FC for Heat-Shock	FC for Lethal Oxidative Stress
TVN0226	Major facilitator superfamily permease	-2.25	-2.96
TVN0073	Metal-binding protein	-2.15	2.59
TVN1426	Flagellin	-4.05	-2.49
TVN0642	Hypothetical protein	-2.31	-2.88
TVN0021	Permease	2.12	2.11
TVN0898	Amino acid transporter	-2.42	-2.16
TVN1260	Acetyl-CoA acetyltransferase	2.28	-2.66
TVN1224	Amino acid transporter	2.07	2.10
TVN0473	NAD(FAD)-dependent dehydrogenase	-2.25	-4.73
TVN0147	Hypothetical protein	-3.07	-2.86
TVN1285	Zn-dependent hydrolase (AttM-related)	3.16	2.77
TVN0875	Aldo/keto reductase	2.07	12.84
TVN0204	Hypothetical protein	3.19	2.29
TVN1284	Alcohol dehydrogenase	2.66	2.60
TVN1405	Hypothetical protein	-2.03	-7.12
TVN0430	Glycosyltransferase	-2.18	-2.43
TVN0200	Phosphoenol pyruvate carboxy kinase	-2.23	-2.53
TVN0611	Flagellar protein G	-2.15	-2.91
TVN0802	Carbamoyl phosphate synthase small subunit	-2.22	-4.20
TVN0624	Transcription regulator	-2.11	-3.33
TVN01259	Nucleic acid binding protein	2.06	-2.42

There was no gene found differentially expressed in common under heat and pH stress. On the other hand, it was revealed that mild and severe oxidative stress groups have 72 transcripts in common. When these oxidative stress groups were compared with respect to the regulation of the genes, it can be seen that both of them exhibit similar gene expression patterns. The overlapping genes between oxidative stress data set shows that nearly 6% of the genes related to the electron transfer and redox balance have enhanced transcription activity. For example, aldo/keto reductase (TVN0875), Fe-S oxidoreductase (TVN0932), and hydrogenase 4 subunits F and B (TVN1444, TVN1458) were found to be up regulated under both oxidative stress conditions.

In addition, some genes involved in transposition were found to be up regulated in both oxidative stress data sets (*e.g.* integrase/recombinase, TVN0137, and transposase, TVN0587).

Another noteworthy result is induced expression of TVN0285 gene encoding arsenite transport permease. This may imply the importance of metal detoxification under oxidative stress. In addition to these, out of 72 shared transcripts, approximately 21 % of them are of hypothetical proteins, which fall into the top category in terms of the number of differentially expressed genes. Further research is necessary to find out if any of these proteins has a critical role in oxidative stress management.

The overlapping genes down regulated in response to two oxidative stress conditions are related to the signaling (*i.e.*, TVN0401, GTPase), cell division (*i.e.*, TVN0027, cell division protein FtsZ), biosynthesis processes (*i.e.*, methionine synthetase, TVN1123; glutamine synthetase, TVN1492; cobalamin sythetase, TVN0495). Highly regulated top 45 genes that are common in two oxidative stress data sets are listed in Table 3.19.

**Table 3. 19. Overlapping genes differentially expressed under mild and lethal oxidative stress groups**

<b>Gene Symbol</b>	<b>Description</b>	<b>FC for Mild Oxidative Stress</b>	<b>FC for Lethal Oxidative Stress</b>
TVN0875	aldo/keto reductase	6.32	12.84
TVN1417	hypothetical protein	3.96	9.27
TVN1053	major facilitator superfamily permease	3.37	6.10
TVN1441	RNA-binding protein	3.90	5.56
TVN1403	HD family phosphatase	3.68	5.39
TVN0933	hypothetical protein	4.14	5.37
TVN0932	Fe-S oxidoreductase	4.32	5.28
TVN0137	integrase/recombinase	3.15	5.16
TVN0697	hypothetical protein	2.77	4.59
TVN0938	metal-dependent transcription regulator	2.45	3.98
TVN1600	KEOPS complex Cgi121-like subunit	2.19	3.97
TVN0835	pyruvate:ferredoxin oxidoreductase. alpha subunit	2.37	3.83
TVN0567	LysR family transcriptional regulator	2.52	3.68
TVN0495	Cobalamin synthetase	-2.15	-2.70
TVN0587	Transposase	2.14	2.15
TVN0285	Arsenite transport permease	2.28	2.90
TVN1458	Hydrogenase 4 subunit B	2.17	2.80
TVN0437	RNA processing exonuclease	3.06	3.55
TVN1245	major facilitator superfamily permease	2.03	3.46
TVN0097	Kef-type K <sup>+</sup> transporter NAD-binding component	2.01	3.44
TVN1455	hydrogenase 4 subunit F	2.54	3.39
TVN1444	protein translocase subunit Sss1	3.59	3.15
TVN0834	2-oxoisovalerate-ferredoxin oxidoreductase. subunit delta (vorD)	2.34	3.11
TVN0687	hypothetical protein	2.54	3.06
TVN1443	nusG; transcription antitermination protein NusG	3.24	3.01
TVN1370	hypothetical protein	2.15	2.99
TVN0698	hypothetical protein	2.74	2.98
TVN0848	aspartate aminotransferase	-4.00	-9.25
TVN1125	5,10-methylenetetrahydrofolate reductase	-3.21	-8.16
TVN0401	GTPase	-2.29	-6.15
TVN0740	metal-dependent carboxypeptidase	-2.71	-5.10

"Table 3.19 (Cont'd)"

Gene Symbol	Description	FC for Mild Oxidative Stress	FC for Lethal Oxidative Stress
TVN0381	hypothetical protein	-2.11	-4.93
TVN0574	SAM-dependent methyltransferase	-2.26	-4.89
TVN0027	cell division protein FtsZ	-2.31	-4.83
TVN1123	methionine synthase	-2.26	-4.66
TVN1124	hypothetical protein	-2.31	-4.45
TVN1240	cation transport ATPase	-3.04	-3.95
TVN0941	hypothetical protein	-3.33	-3.87
TVN1492	glutamine synthetase	-2.14	-3.73
TVN1279	ferredoxin-like protein	-2.92	-3.61
TVN0944	alcohol dehydrogenase	-2.47	-3.55
TVN0998	pyridoxal biosynthesis lyase PdxS	-2.11	-3.49
TVN1278	dehydrogenase	-3.73	-3.41
TVN0015	S-adenosylmethionine synthetase	-2.44	-3.27
TVN0496	aspartate aminotransferase	-2.95	-3.15

### 3.4. Verification of Microarray Results by qRT-PCR

In order to verify the gene expression results obtained from genome wide transcriptional analysis of *Thermoplasma volcanium*, Quantitative Real Time Reverse Transcripton PCR (qRT-PCR) used. Since there is huge data available, some set of genes were selected for qRT-PCR. When selecting genes to be analyzed by qRT-PCR, their functional category, change in their expression levels, and stress type were taken into consideration. The selected genes according to these criteria are: TVN0932 (Fe-S oxidoreductase), TVN1392 (transcription regulator), TVN1466 (AAA family ATPase), TVN1284 (alcohol dehydrogenase), TVN0164 (Phosphoribosylaminoimidazole synthetase), TVN1343 (Acyl-coA dehydrogenase), TVN0875 (Aldo/keto reductase), TVN0570 (TFIIB), TVN1426 (Flagellin), TVN1600 (KEOPS complex), TVN0123(Phosphate ABC transporter permease),TVN0835 (Pyruvate:ferredoxin oxidoreductase,alpha subunit), TVN0167 (Zn dependent hydrolase), TVN1390 (iron regulated ABC type transporter), TVN0830 (Rhodanese), TVN0021( permease), TVN0401(GTPase), and TVN1285 (Zn dependent hydrolase). Differential expression of these genes were investigated by qRT-PCR using total RNA isolated under heat shock (at 68°C), pH stress (pH

5.0) and oxidative stress imposed by 0.03 mM hydrogen peroxide. RT-PCR was performed for each gene per stress condition at least three times. General results for each stress condition are summarized in Table 3.20, 3.21, and 3.22.

### 3.4.1. Absolute Quantification of Expression of TVN0830 Gene Under Heat Shock, pH Stress and Oxidative Stress

qRT-PCR results showed that TVN0830 (encoding rhodanase related protein) gene was found to be up regulated during heat shock and oxidative stress, while down regulated under pH stress. Change in the level of this gene as compared to the control under three different conditions is illustrated in the Figure 3.27. Related amplification and melting curves are given in the Appendix C.



**Figure 3. 27. Changes in the abundance of mRNA level of TVN0830 during heat shock, pH stress, oxidative stress.** Transcript level of up regulated genes is greater than 1 fold; that of down regulated genes is less than 1 fold.

The transcript level of TVN0830 was found to be increased by 1.76 fold in response to the heat shock by qRT-PCR. Its expression was found to be down regulated 2.28-fold as revealed by microarray analysis. In the literature, this inconsistency is explained by differences in the normalization methods used in two techniques, or

RNA quality, or dye biases (Morey *et al.*, 2006). Similarly, results obtained by two methods for pH stress and oxidative stress are quite close (Table 3.21 and 3.22). The difference were found to be insignificant by microarray, and the fold- change by qRT-PCR was <2.0 in both cases.

**Table 3. 20. Analysis of differential expression of selected genes under heat shock by qRT-PCR**

<b>Gene ID</b>	<b>Cp Test (Heat shock)</b>	<b>Cp Control</b>	<b>T<sub>m</sub></b>	<b>FC from RT-PCR</b>	<b>FC from microarray</b>
TVN0830	16.34	17.50	78.30 ±0.11	1.76 ± 0.04	-2.28
TVN1426	13.87	14.86	83.39±0.13	0.68±0.04	-4.04
TVN1285	19.75	20.79	80.53±0.07	1.91± 0.17	3.16
TVN1343	14.77	15.92	83.25±0.12	2.23±0.20	NC
TVN0401	15.49	16.92	77.27±0.16	1.82±0.38	NC
TVN0835	15.07	16.19	82.62±0.17	2.08±0.097	1.41
TVN1390	13.93	14.06	85.92± 0.09	1.41±0.29	NC
TVN1600	15.49	16.58	80.59±0.173	1.79±0.11	-1.47
TVN0021	14.9	15.88	82.11±0.08	1.92±0.15	2.12
TVN0123	15.51	16.46	80.29±0.09	1.64±0.09	-1.96
TVN1392	14.19	15.16	82.62±0.15	1.13±0.24	NC
TVN1466	14.75	15.84	77.92±0.18	1.29±0.02	1.57
TVN1284	14.48	15.87	83.41±0.1	2.26±0.04	2.66
TVN0932	12.80	13.09	78.04±0.22	1.22±0.02	NC
TVN0164	14.57	14.74	83.87±0.134	4.94±0.02	6.33
TVN0167	12.46	16.11	82.32±2.32	6.70±0.47	5.86
TVN0570	16.12	17.79	80.11±0.09	1.38±0.45	NC
TVN0875	18.19	18.29	80.45±0.12	1.28±0.24	2.07

NC: Expression level of genes is not changed significantly.

**Table 3. 21. Analysis of differential expression of selected genes under pH stress by qRT-PCR**

Gene ID	Cp Test (pH stress)	Cp Control	T <sub>m</sub>	FC from RT-PCR	FC from microarray
TVN0830	17.71	17.50	78.35±0.11	0.83±0.07	NC
TVN1426	14.88	14.86	83.64±0.13	0.93±0.06	NC
TVN1285	21.16	20.79	80.33±0.07	0.88± 0.08	2.77
TVN1343	16.61	15.92	83.52±0.12	0.68±0.02	-2.24
TVN0401	17.56	16.92	77.47±0.16	0.81±0.11	-2.069
TVN0835	15.76	16.19	82.64 ±0.17	1.06±0.24	NC
TVN1390	13.34	14.06	85.08± 0.09	1.78±0.46	3.97
TVN1600	15.73	16.58	79.92±0.173	0.96±0.21	2.88
TVN0021	18.92	17.51	82.02±0.14	0.85±0.40	NC
TVN0123	14.65	16.46	80.21±0.09	3.10±0.40	8.44
TVN1392	14.70	15.16	82.92±0.15	1.40±0.07	3.23
TVN1466	15.73	15.84	77.86±0.18	0.87±0.20	NC
TVN1284	16.69	15.87	83.49±0.1	0.89±0.27	NC
TVN0932	12.89	12.20	78.92±0.007	0.80±0.33	2.71
TVN0164	11.89	14.74	83.69±0.134	0.52±0.01	NC
TVN0167	16.91	16.11	81.2±2.32	1.02±0.002	NC
TVN0570	17.71	17.79	80.26±0.09	2.12±0.36	7.42
TVN0875	16.83	18.29	80.11±0.12	1.30±0.007	NC

NC: Expression level of genes is not changed significantly.

**Table 3. 22. Analysis of differential expression of selected genes under oxidative stress (0.03 mM H<sub>2</sub>O<sub>2</sub>) by qRT-PCR**

Gene ID	Cp Test (Oxidative stress)	Cp Control	T <sub>m</sub>	FC from RT-PCR	FC from microarray
TVN0830	16.54	17.50	78.42±0.11	1.50±0.13	NC
TVN1426	14.11	14.86	83.63±0.13	1.64±0.008	- 2.49
TVN1285	21.16	20.79	80.33±0.07	1.57± 0.15	NC
TVN1343	15.23	15.92	83.35±0.12	1.47±0.06	NC
TVN0401	16.43	16.92	77.66±0.16	1.25±0.23	-6.015
TVN0835	14.60	16.19	82.97±0.17	2.20 ± 0.418	3.83
TVN1390	13.13	14.06	85.86± 0.09	4.08 ±0.48	4.06
TVN1600	15.96	16.58	80.63±0.17	2.15±0.72	3.97
TVN0021	17.43	17.51	82.08±0.14	1.40±0.35	2.11
TVN0123	15.62	16.46	80.34±0.09	1.78±0.21	2.57
TVN1392	14.55	15.16	82.92±0.15	1.31±0.15	3.30
TVN1466	14.15	15.84	77.86±0.18	2.22±0.46	14.65
TVN1284	15.56	15.87	83.45±0.1	1.15±0.05	2.59
TVN0932	12.06	13.09	77.66±0.22	1.81±0.098	5.29
TVN0164	15.03	14.74	83.94±0.13	0.79±0.05	NC
TVN0167	16.79	16.11	82.24±2.32	0.61±0.08	NC
TVN0570	17.77	17.79	80.27±0.09	0.92±0.1	NC
TVN0875	18.86	18.29	80.13±0.12	0.90±0.28	12.84

NC: Expression level of genes is not changed significantly.

### 3.4.2. Absolute Quantification of Expression of TVN1426 Gene Under Heat Shock, pH Stress and Oxidative Stress

Transcriptome analysis by microarray revealed that abundance of TVN1426 (flagellin) was decreased by both heat shock (-4.04 fold) and oxidative stress (-2.49 fold), but no significant change was detected in its expression level following pH stress. Results obtained from qRT-PCR indicated that expression of this gene during heat shock was decreased by a factor of 0.68 fold implying a correlation with the result from microarray, although the fold change levels are different (Figure 3.28). Similarly, qRT-PCR result confirmed the result obtained by microarray dataset for pH stress. Expression level of TVN1426 gene was almost unchanged (*i.e.*, 0.93 fold). On the other hand, the results obtained by two techniques are not in agreement for oxidative stress as shown in Table 3.22.

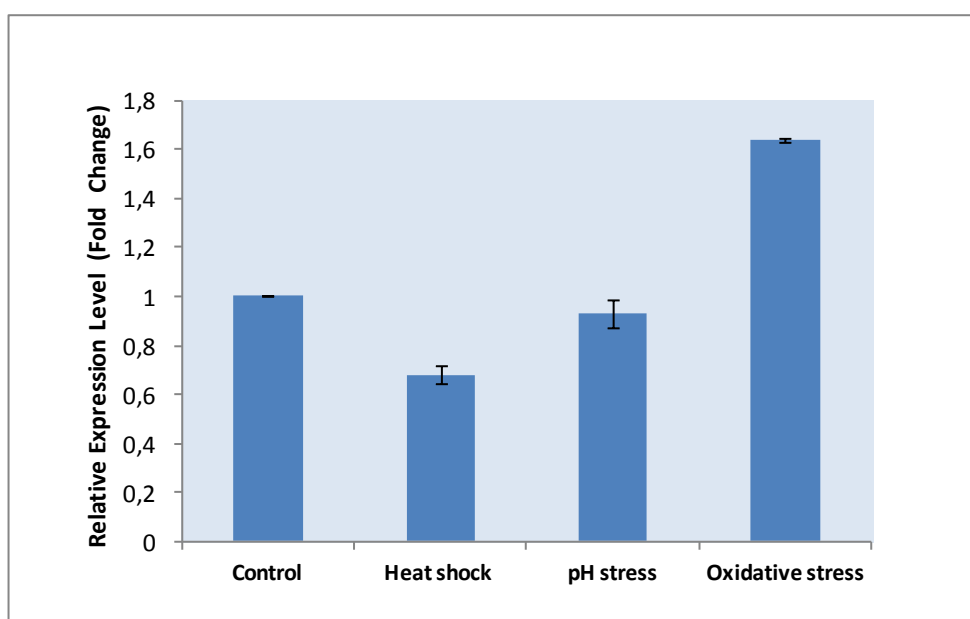


**Figure 3. 28. Changes in the abundance of mRNA level of TVN1426 during heat shock, pH stress, oxidative stress.** Transcript level of up regulated genes is greater than 1 fold; that of down regulated genes is less than 1 fold.

### 3.4.3. Absolute Quantification of Expression of TVN1285 Gene Under Heat Shock, pH Stress and Oxidative Stress

According to the qRT-PCR analysis, Zn dependent hydrolase gene TVN1285 expression was induced during heat shock and oxidative stress, as shown in Figure 3.29. There was a good correlation between the result of microarray and RT-PCR for heat shock data. Gene expression was found to be induced with both techniques (Table 3.20). However, the change in the gene expression levels as determined by two techniques were not in agreement for pH and oxidative stress (Table 3.21 and Table 3.22).

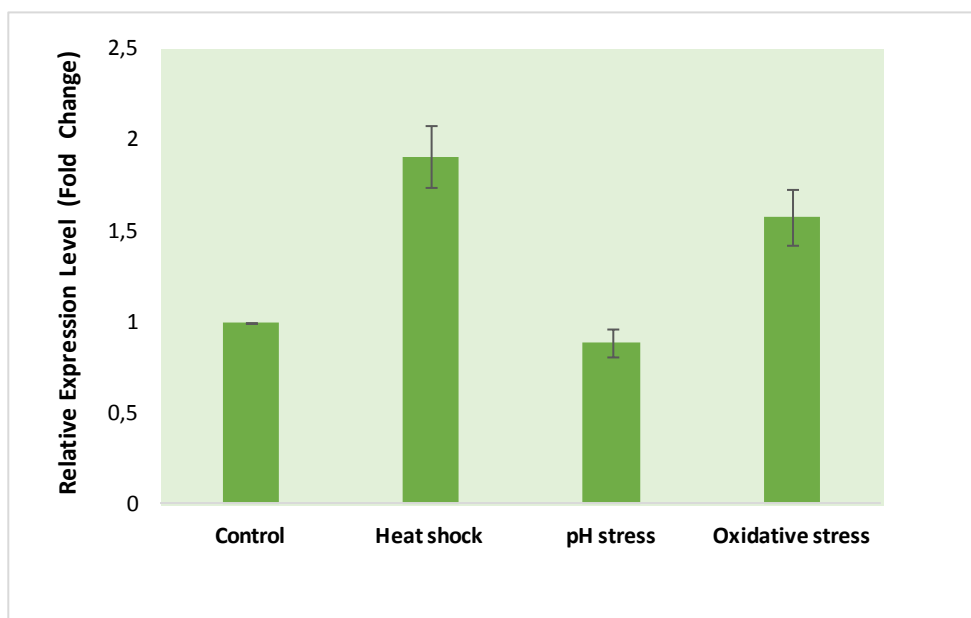
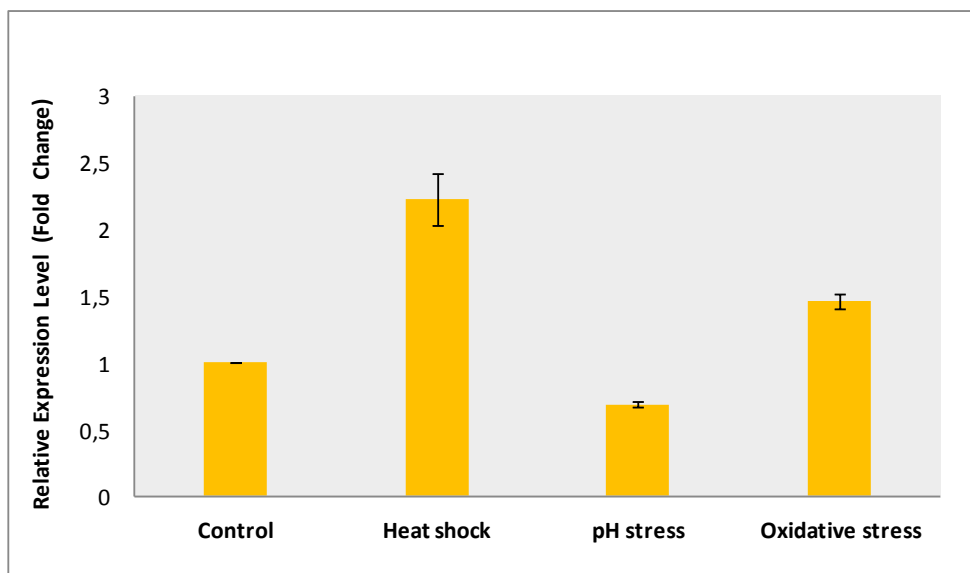


Figure 3. 29. Changes in the abundance of mRNA level of TVN1285 during heat shock, pH stress, oxidative stress. Transcript level of up regulated genes is greater than 1 fold; that of down regulated genes is less than 1 fold.

### 3.4.4. Absolute Quantification of Expression of TVN1343 Gene Under Heat Shock, pH Stress and Oxidative Stress

According to the RT-PCR results, transcript level of TVN1343 encoding Acyl-CoA dehydrogenase was up regulated during heat shock, but down regulated during pH stress as shown in Figure 3.30. Consistent result was obtained for pH stress for this gene with microarray. The change in the expression level of TVN1343 was not

significant as compared to the control as revealed by qRT-PCR (<1.50 fold), and this result is correlated with the microarray result (Table 3.22). However, results obtained by 2 techniques for heat shock data sets are not compatible (Table 3.20).



**Figure 3. 30. Changes in the abundance of mRNA level of TVN1343 during heat shock, pH stress, oxidative stress.** Transcript level of up regulated genes is greater than 1 fold; that of down regulated genes is less than 1 fold.

### 3.4.5. Absolute Quantification of Expression of TVN0401 Gene Under Heat Shock, pH Stress and Oxidative Stress

qRT-PCR experiment results showed that transcript level of TVN0401 gene encoding GTPase up regulated upon oxidative stress and heat shock by a factor of 1.25 and 1.82 fold, respectively (Figure 3.31). The results obtained from microarray experiments revealed strong repression of this gene (6.015- fold) under oxidative stress. Therefore, there is a remarkable disagreement between two results. On the other hand, gene expression profiles of this under pH stress and heat stress were in agreement with microarray when significance cut off was considered (Table 3.20 and 3.22), although their fold -changes are different.

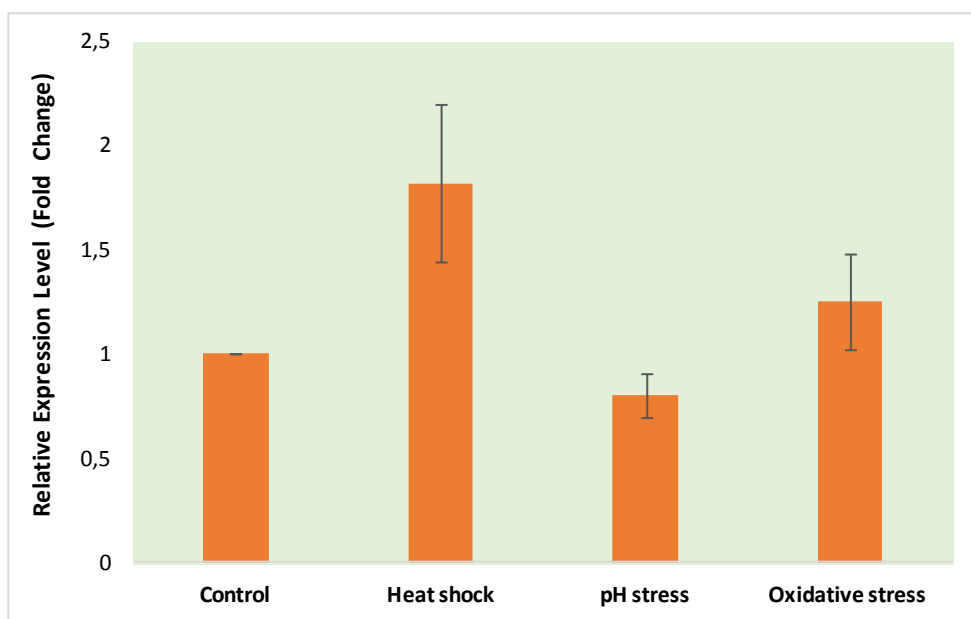


**Figure 3. 31. Changes in the abundance of mRNA level of TVN0401 during heat shock, pH stress, oxidative stress.** Transcript level of up regulated genes is greater than 1 fold; that of down regulated genes is less than 1 fold.

### **3.4.6. Absolute Quantification of Expression of TVN0835 Gene Under Heat Shock, pH Stress and Oxidative Stress**

qRT-PCR results showed that heat shock and oxidative stress increased the expression of the TVN0835 gene (pyruvate: ferredoxin oxidoreductase) by a factor of 2.08 and 2.20 fold, respectively as listed in Table 3.20 and 3.22. However, the mRNA abundance of this gene did not change under pH stress. These results are in agreement with microarray data. Changes in the TVN0835 gene expression in different stress exposed groups relative to the control is shown in Figure 3.32.

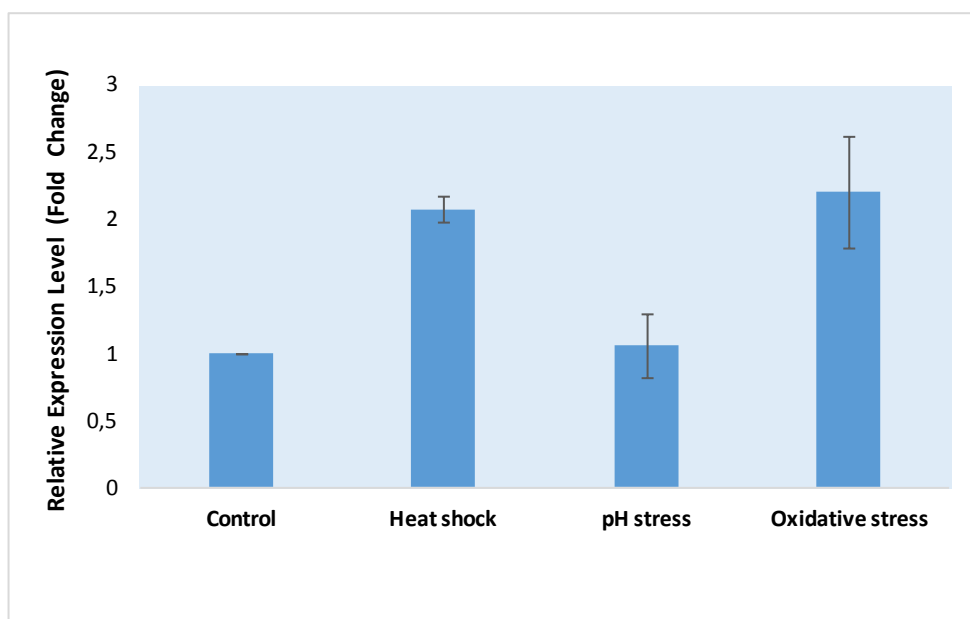


**Figure 3. 32. Changes in the abundance of mRNA level of TVN0835 during heat shock, pH stress, oxidative stress.** Transcript level of up regulated genes is greater than 1 fold; that of down regulated genes is less than 1 fold.

#### **3.4.7. Absolute Quantification of Expression of TVN1390 Gene Under Heat Shock, pH Stress and Oxidative Stress**

Following heat shock, pH stress, and oxidative stress, abundance of transcripts encoding iron regulated ABC type transporter were found to be enhanced as inferred from qRT-PCR data (Figure 3.33). These results are consistent with the results obtained by microarray analysis for pH stress, oxidative stress. (Table 3.21 and 3.22). In qRT-PCR experiment, TVN1390 was found to be up regulated by a factor of 1.41-fold (< 2 fold) in response to the heat-shock, but in microarray, no significant change in its expression level was not detected.

#### **3.4.8. Absolute Quantification of Expression of TVN1600 Gene Under Heat Shock, pH Stress and Oxidative Stress**

According to the qRT-PCR results, oxidative stress caused up regulation of the TVN1600 (KEOPS) by a factor of 2.15 as listed in Table 3.22. This result is in good agreement with microarray data. However, heat shock results and pH results from RT-PCR experiments are contradictory to microarray results (Table 3.20 and 3.21).

Changes in the gene expression in under different stresses relative to the control are shown in Figure 3.34.

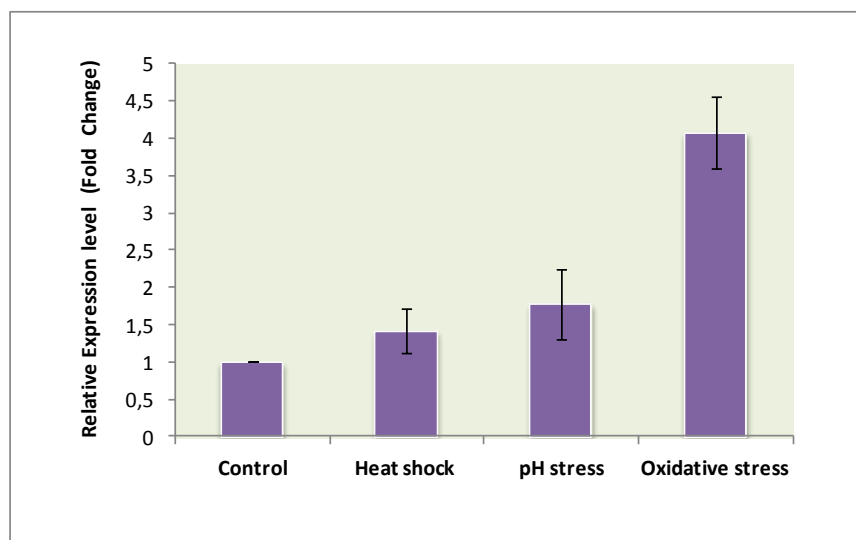


**Figure 3. 33. Changes in the abundance of mRNA level of TVN1390 during heat shock, pH stress, oxidative stress.** Transcript level of up regulated genes is greater than 1 fold; that of down regulated genes is less than 1 fold.

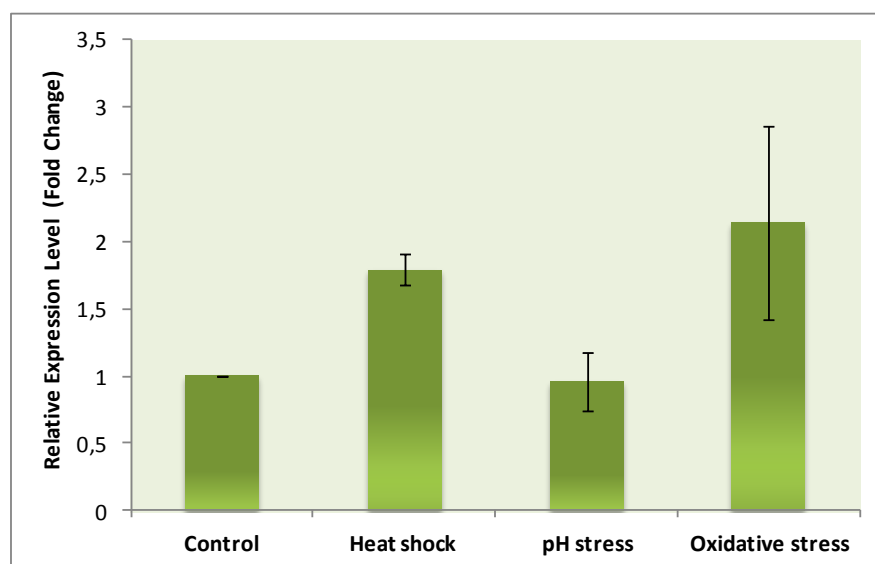


**Figure 3. 34. Changes in the abundance of mRNA level of TVN1600 during heat shock, pH stress, oxidative stress.** Transcript level of up regulated genes is greater than 1 fold; that of down regulated genes is less than 1 fold.

### 3.4.9. Absolute Quantification of Expression of TVN0021 Gene Under Heat Shock, pH Stress and Oxidative Stress

According to the RT-PCR results, transcript levels of TVN0021 encoding permease were increased during heat shock and oxidative stress, while slightly down regulated during pH stress as shown in Figure 3.35. The RT-PCR results are in agreement those of microarray data although there are differences in fold-changes for some stressors (Table 3.20, 3.21, and 3.22).

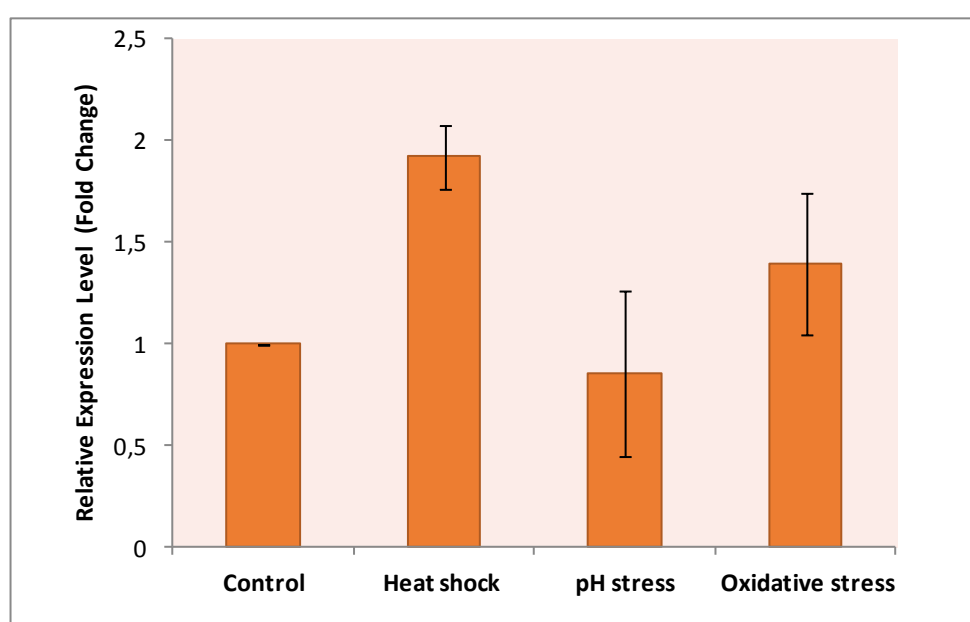


**Figure 3. 35.** Changes in the abundance of mRNA level of TVN0021 during heat shock, pH stress, oxidative stress. Transcript level of up regulated genes is greater than 1 fold; that of down regulated genes is less than 1 fold.

### 3.4.10. Absolute Quantification of Expression of TVN0123 Gene Under Heat Shock, pH Stress and Oxidative Stress

qRT-PCR experiment showed that oxidative stress and pH stress resulted in increase in the mRNA level of TVN0123 gene (phosphate ABC transporter permease) by a factor of 1.78 and 3.10 fold respectively as listed in Table 3.21 and 3.22. These results are in agreement with microarray data, but with some changes in the fold difference values. On the other hand, heat shock results from qRT-PCR experiments are not correlated with the microarray result. Possible reasons for this was mentioned

previously. Changes in the gene expression in under different stresses relative to the control are shown in Figure 3.36.

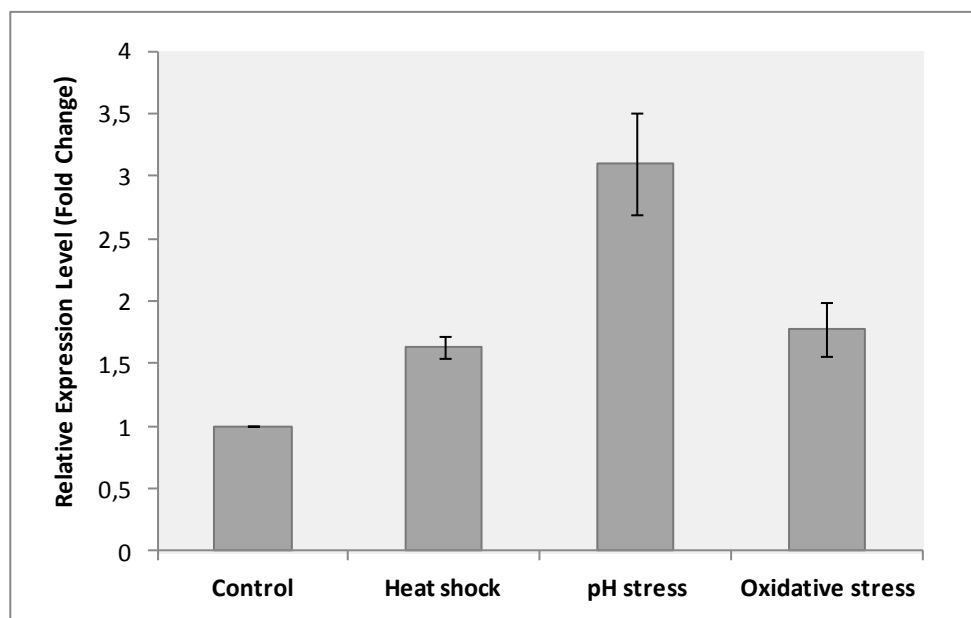


**Figure 3. 36. Changes in the abundance of mRNA level of TVN0123 during heat shock, pH stress, oxidative stress.** Transcript level of up regulated genes is greater than 1 fold; that of down regulated genes is less than 1 fold.

#### **3.4.11. Absolute Quantification of Expression of TVN1392 Gene Under Heat Shock, pH Stress and Oxidative Stress**

According to the results from qRT-PCR experiment, the TVN1392 gene (transcriptional regulator) expression either did not change or slightly up regulated under oxidative stress, heat shock, and pH stress by a factor of 1.31, 1.13 and 1.40 fold, respectively as listed in Table 3.20 - 3.22. This data for three stresses are in good agreement with microarray data. Changes in the gene expression under different stresses relative to the control are shown in Figure 3.37.

#### **3.4.12. Absolute Quantification of Expression of TVN1466 Gene Under Heat Shock, pH Stress and Oxidative Stress**

qRT-PCR results show that transcript level of TVN1466 gene encoding an AAA family ATPase up regulated upon oxidative stress and heat shock by a factor of 2.22 and 1.29 fold, respectively (Figure 3.38). The results obtained from microarray

experiments were in good agreement, but more strong induction of this gene (14.65 fold) under oxidative stress was detected. On the other hand, gene expression level in response to the pH stress seemed to be almost not changed (0.87 fold) as revealed by two method.

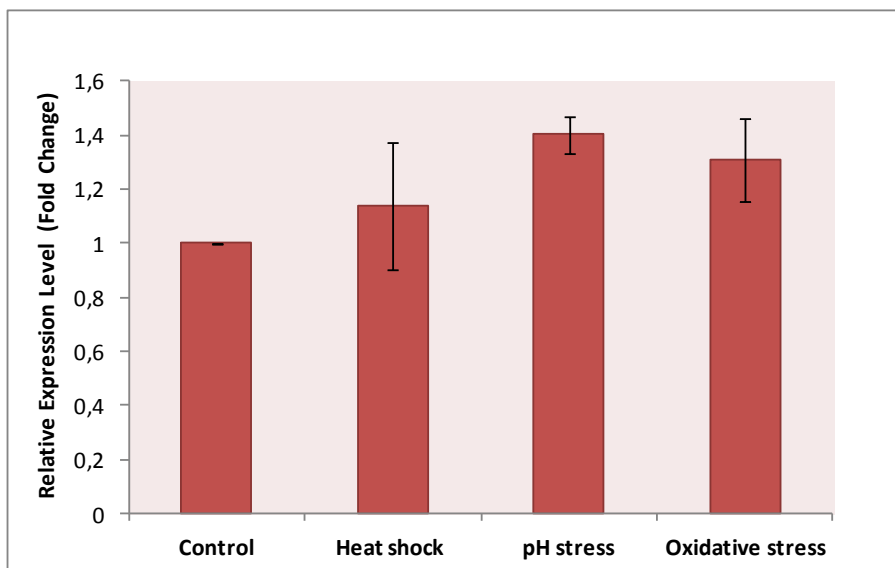


**Figure 3. 37. Changes in the abundance of mRNA level of TVN1392 during heat shock, pH stress, oxidative stress.** Transcript level of up regulated genes is greater than 1 fold; that of down regulated genes is less than 1 fold.

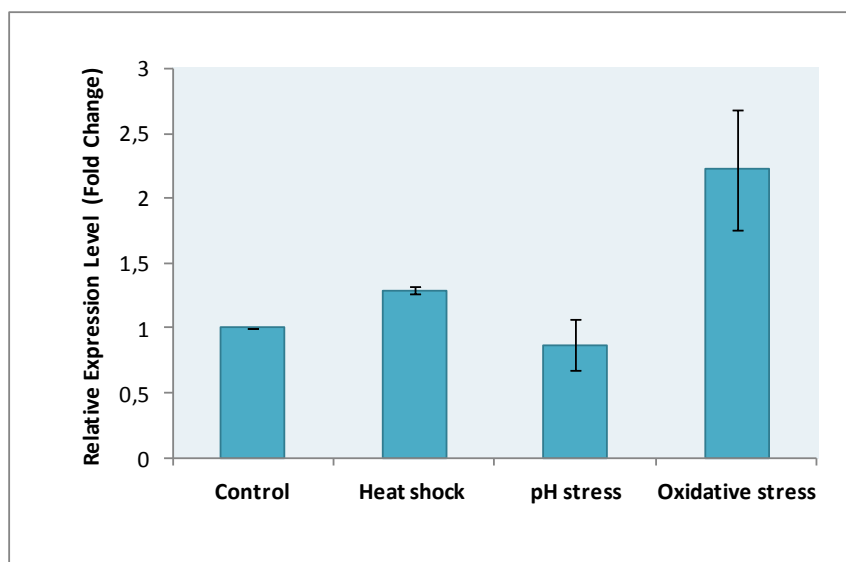


**Figure 3. 38. Changes in the abundance of mRNA level of TVN1466 during heat shock, pH stress, oxidative stress.** Transcript level of up regulated genes is greater than 1 fold; that of down regulated genes is less than 1 fold.

### 3.4.13. Absolute Quantification of Expression of TVN1284 Gene Under Heat Shock, pH Stress and Oxidative Stress

qRT-PCR experiment showed that heat shock resulted in the increased in the transcription activity of TVN1284 (alcohol dehydrogenase) by a factor of 2.26 as listed in Table 3.20. This result is in agreement with microarray data. The change in the expression level was not important under pH stress as revealed by two techniques. On the other hand, oxidative stress results from qRT-PCR experiments is not correlated with microarray result (Table 3.22). Changes in the abundance of mRNA relative to the control under different stresses are shown in Figure 3.39.

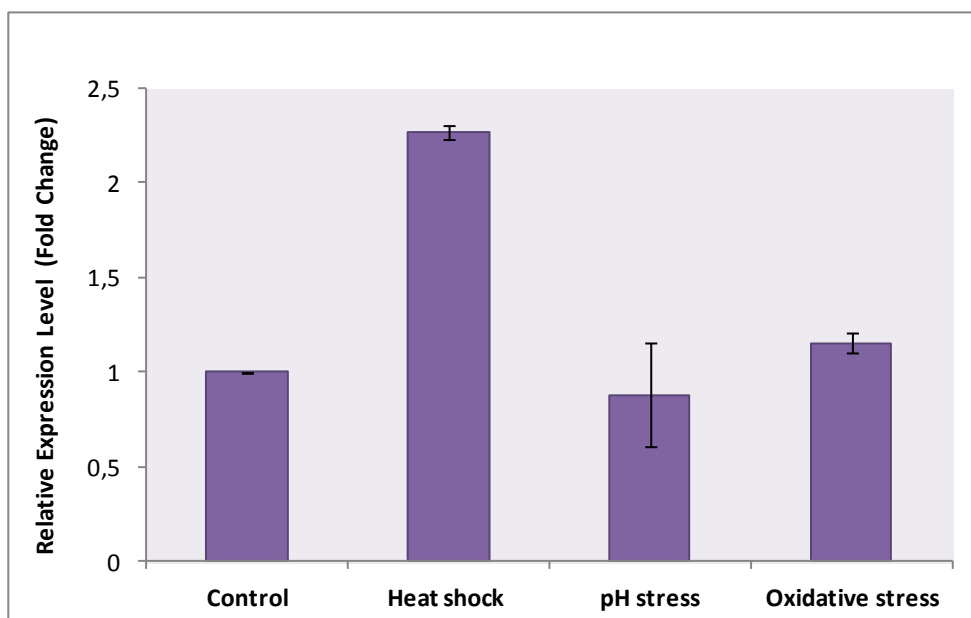
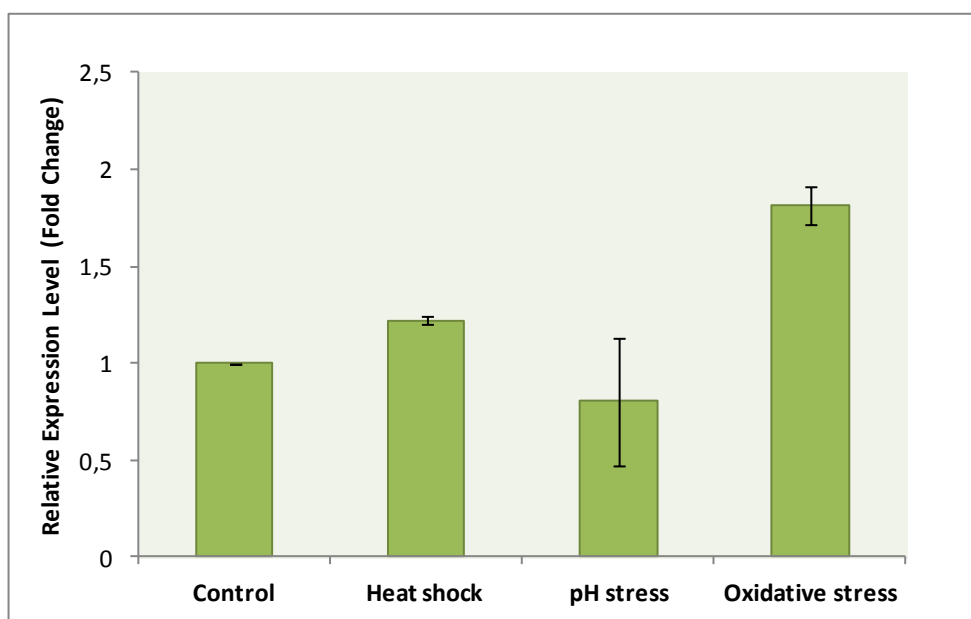


Figure 3. 39. Changes in the abundance of mRNA level of TVN1284 during heat shock, pH stress, oxidative stress. Transcript level of up regulated genes is greater than 1 fold; that of down regulated genes is less than 1 fold.

### 3.4.14. Absolute Quantification of Expression of TVN0932 Gene Under Heat Shock, pH Stress and Oxidative Stress

qRT-PCR experiment showed that oxidative stress resulted in the increase in abundance of the TVN0932 (Fe-S oxidoreductase) mRNA by a factor of 1.81 fold as shown in Table 3.22. Despite fold difference, there was a correlation between microarray data and qRT-PCR data. The expression of the gene under heat-shock did

not changed significantly (1.22-fold), in parallel to the result from microarray analysis. On the other hand, gene expression level in response to the pH stress were seem to be slightly down regulated by a factor of 0.80 fold in qRT-PCR experiment, but in microarray, this expression was seem to be up regulated by a factor of 2.74. Changes in the gene expression in different stress exposed groups relative to the control is shown in Figure 3.40.



**Figure 3. 40. Changes in the abundance of mRNA level of TVN0932 during heat shock, pH stress, oxidative stress.** Transcript level of up regulated genes is greater than 1 fold; that of down regulated genes is less than 1 fold

### **3.4.15. Absolute Quantification of Expression of TVN0164 Gene Under Heat Shock, pH Stress and Oxidative Stress**

Following heat shock abundance of transcripts encoding phosphoribosylaminoimidazole synthetase was found to be enhanced (4.94 fold) which was inferred from qRT-PCR data. This result is consistent with the microarray data. The expression level of this gene in response to the oxidative stress and pH stress seemed to be almost unchanged with both methods. Changes in the gene expression in different stress exposed groups relative to the control is shown in Figure 3.41.

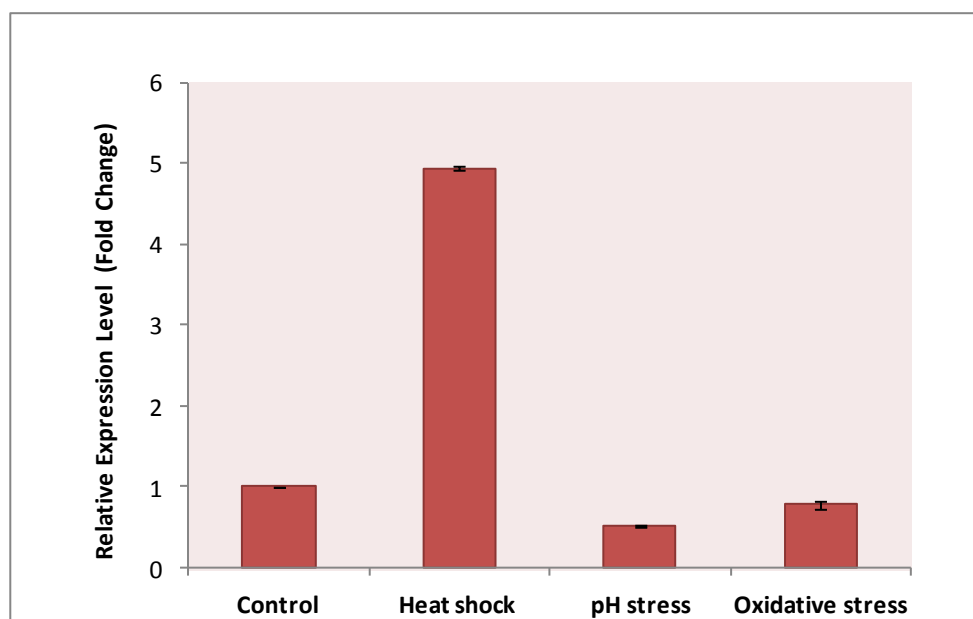


**Figure 3. 41. Changes in the abundance of mRNA level of TVN0164 during heat shock, pH stress, oxidative stress.** Transcript level of up regulated genes is greater than 1 fold; that of down regulated genes is less than 1 fold.

### **3.4.16. Absolute Quantification of Expression of TVN0167 Gene Under Heat Shock, pH Stress and Oxidative Stress**

According to the results from qRT-PCR experiment, heat shock resulted in the up regulation of the TVN0167 gene (Zn dependent hydrolase) by a factor of 6.70 which is in agreement with microarray data (Table 3.20). Also, pH stress and oxidative stress results were found to be well correlated with microarray data which showed almost no change in the expression level as compared to control (Table 3.21 and 3.22). Changes in the gene expression in different stress exposed groups relative to the control are shown in Figure 3.42.

### **3.4.17. Absolute Quantification of Expression of TVN0570 Gene Under Heat Shock, pH Stress and Oxidative Stress**

qRT-PCR results showed that transcript level of TVN0570 encoding TFIIB was enhanced upon pH stress by a factor of 2.12. This result is in good agreement with microarray result, although microarray experiments revealed more strong induction of this gene (7.42 fold) upon pH stress. The gene expression level in response to the

heat stress and oxidative stress did not significantly changed as revealed by two methods (Table 3.20 and 3.22). Changes in the gene expression in different stress exposed groups relative to the control is shown in Figure 3.43.

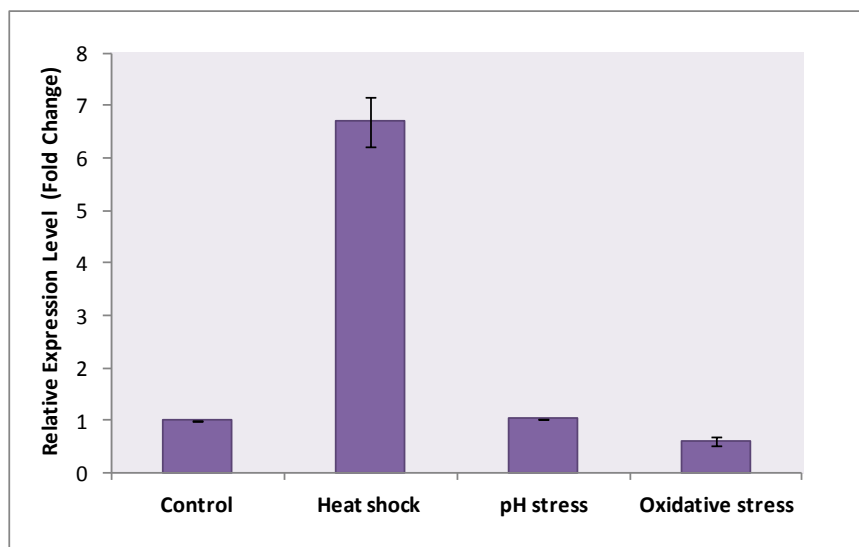


**Figure 3. 42. Changes in the abundance of mRNA level of TVN0167 during heat shock, pH stress, oxidative stress.** Transcript level of up regulated genes is greater than 1 fold; that of down regulated genes is less than 1 fold.

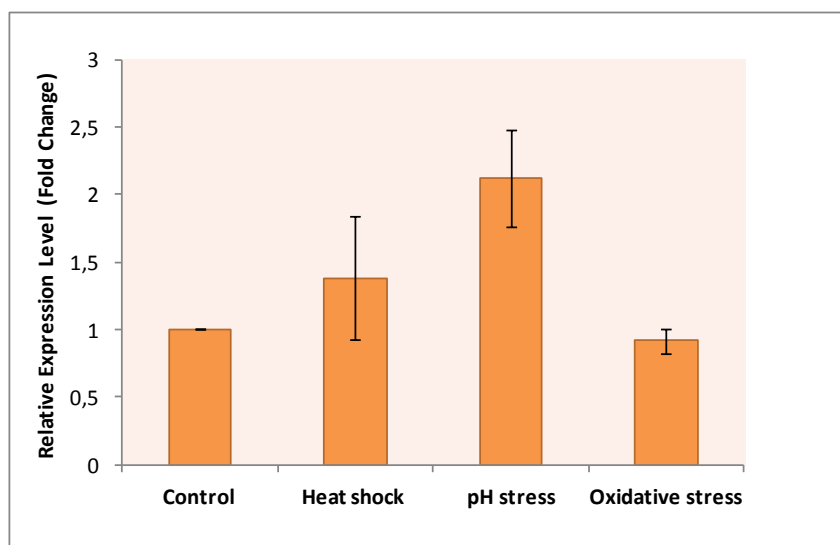


**Figure 3. 43. Changes in the abundance of mRNA level of TVN0570 during heat shock, pH stress, oxidative stress.** Transcript level of up regulated genes is greater than 1 fold; that of down regulated genes is less than 1 fold.

### 3.4.18. Absolute Quantification of Expression of TVN0875 Gene Under Heat Shock, pH Stress and Oxidative Stress

Microarray based transcriptome analysis revealed that gene expression level of TVN0875 gene (aldo/keto reductase) was highly up regulated (about 12.84- fold) upon oxidative stress. On the contrary, results obtained from RT-PCR showed that expression of this gene during oxidative stress was almost not changed. On the other hand, heat shock results were found to be not correlated with microarray result (Table 3.20). As revealed by two method, the expression level of the gene almost did not change under pH stress. Alterations in the gene expressions are shown in Figure 3.44.

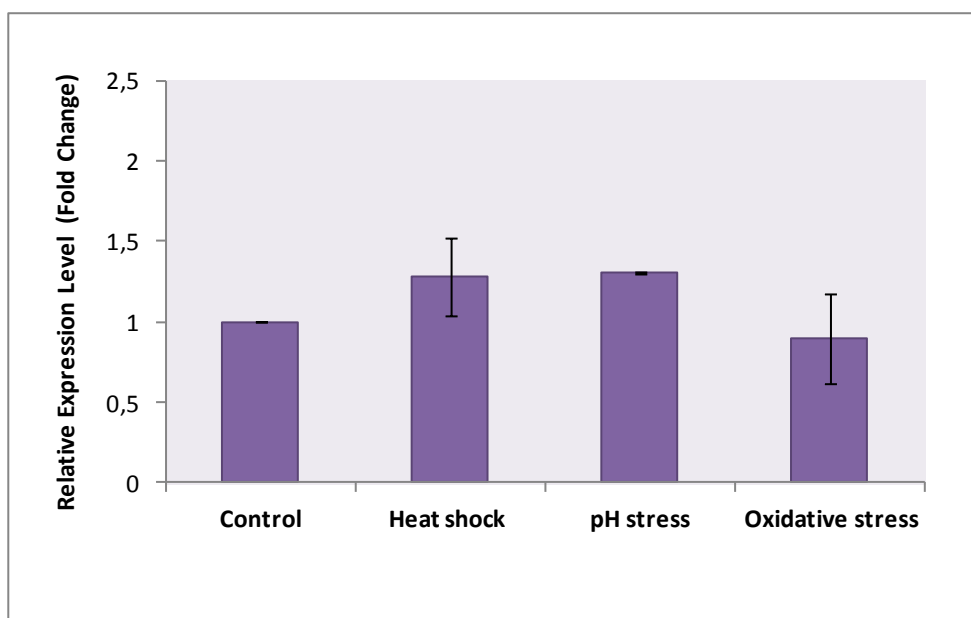


**Figure 3. 44. Changes in the abundance of mRNA level of TVN0875 during heat shock, pH stress, oxidative stress.** Transcript level of up regulated genes is greater than 1 fold; that of down regulated genes is less than 1 fold.

## CHAPTER 4

### CONCLUSION

The microorganisms have developed molecular mechanisms to protect themselves from the damages induced by a variety of stress factors. Among these, the extremophilic archaea have adapted to thrive in habitats that are hostile or even lethal for other life forms. Under suboptimal conditions, these organisms also employ adaptive or inducible strategies to survive. However, in archaea, survival strategies devised under constantly changing environmental conditions have not been clarified yet. Previously, we have investigated gene expression profiling of the thermoacidophilic archaeon *Thermoplasma volcanium* under mild stress conditions by using microarray technology. In this thesis project, as an extension of this afford, transcriptome analysis was performed in the same model organism under severe stress conditions (*i.e.*, heat stress at 68 °C, pH stress at pH 5.0 and oxidative stress at 0.03 mM H<sub>2</sub>O<sub>2</sub> and 0.02 mM H<sub>2</sub>O<sub>2</sub>). The general stress response to three stressors resulted in retardation or complete arrest of cell growth which are accompanied by down regulation of genes involved in essential cellular processes such as translation, transcription, cell motility, and energy metabolism. In addition, some stress specific genes were also activated in response to the heat shock, pH stress and oxidative stress.

The temperature when increased from 60 °C to 68 °C resulted in the significant change (FC  $\geq$ 2.0, cut off value  $p < 0.05$ ) in the expression of 70 genes out of 1,474 annotated expressed *Tpv* genes. The elevated expression of genes encoding heat shock proteins (*e.g.*, molecular chaperones GroEL,  $\alpha$  and  $\beta$  subunits; GrpE, DnaK, and DnaJ) was implicated in the heat-shock specific stress response. Another up-regulated (by a factor of 6.34-fold) gene that can be included into this group codes for phosphoribosylaminoimidazole synthetase. This protein functions in maintenance of thermal stability of proteins upon heat- shock. Modification of the membrane

lipid composition under heat shock should also be associated with the specific response to high temperature. Besides, the genes related to the energy production and conversion, membrane transport system, motility, replication and recombination, lipid metabolism and detoxification were found to be differentially regulated during heat- shock. This result suggest a global transcriptional variation upon stress rather than a specific response to heat- shock.

When the pH of the mid-log culture was up shifted from 2.6 to 5.0 for 1 hour, of the 47 differentially expressed genes, 66% of the genes were up regulated and 34 % of the genes were down regulated. According to the functional analysis of the up regulated genes, pH stress in *T.volcanium* most strongly managed through activation of several transporter genes. The notably induced genes were found to be encode cation transporters (*e.g* phosphate ABC transporters, iron regulated ABC transporters) which have crucial roles in maintance of intracellular pH homeostasis. Another noteworthy observation from microarray analysis was overproduction of transcription initiation factor IIB (7.41 fold), ATP dependent Lon protease, and universal stress protein A (UspA). They should be are critical components of positively regulated mechanisms to survive pH stress for *T.volcanium*.

Thirdly, transcriptional behavior of *Thermoplasma volcanium* when exposed to mild (0.02 mM H<sub>2</sub>O<sub>2</sub>) oxidative stress and lethal (0.03 mM H<sub>2</sub>O<sub>2</sub>) oxidative stress were studied separately. Our transcriptomic results suggested that the most induced genes under oxidative stress take role in electron transfer, redox potential and detoxification of the reactive oxygen species. They may play critical roles in reducing the deleterious effects of the oxidative stress.

The overlapping differentially expressed genes under sub-lethal and lethal oxidative stress are encoding aldo/keto reductase (TVN0875), Fe-S oxidoreductase (TVN0932) and hydrogenase 4 subunits (TVN1444, TVN1458). It is more likely that these proteins have central roles to cope with oxidative stress in *T.volcanium*.

In addition to these, the gene encoding AAA ATPase (TVN1466, 14.65 fold) and the genes for a number of iron-sulfur cluster assembly were strongly induced in response

to the oxidative stress. Over expression of these genes may provide a survival advantage to *T.volcanium* under oxidative stress.

It was also interesting to note that expressions of a number of *Tpv* genes encoding transcriptional factors or regulators were induced by three stressors. They may be involved in expression of the stress specific genes. Similarly, a number of genes related to the carbohydrate metabolism and transport were also activated in response to the three stressors. This might be a strategy used to support increased energy requirements of the cells under stress. From the microarray analysis, it was apparent that hypothetical proteins constituted a significant proportion of the expressed genes under heat shock, pH stress, and oxidative stress. In the future, it will be pertinent to investigate whether these proteins have a role in the stress management.

We have found a good correlation between the results obtained by microarray and qRT-PCR technique.



## REFERENCES

- Agilent GeneSpring GX User Manual. (n.d.). Retrieved January 22, 2015, from Agilent technologies:  
<http://www.chem.agilent.com/cag/bsp/products/gsgx/manuals/genespring-manual.pdf>
- Agilent Microarray Technology. (n.d.). Retrieved February 2, 2015, from <http://www.genomics.agilent.com/article.jsp?pageId=2011>
- Agilent RNA Nano Kit Guide. (2013). Retrieved January 23, 2015, from Agilent Technologies: [http://www.chem.agilent.com/Library/usermanuals/Public/G2938-90034\\_RNA6000Nano\\_KG.pdf](http://www.chem.agilent.com/Library/usermanuals/Public/G2938-90034_RNA6000Nano_KG.pdf)
- Albers, S., Vossenbergh, J., Driessen, A. et al., 2000. Adaptations of the archaeal cell membrane to heat stress. *Frontiers in Bioscience*, 5: 813–820.
- Anitori, R. P., 2012. Extremophiles: Microbiology and Biotechnology. Caister Academic Press, UK.
- Auernik, K.S., Cooper, C.R. & Kelly, R.M., 2008. Life in hot acid: pathway analyses in extremely thermoacidophilic archaea. *Current Opinion in Biotechnology*, 19:445–453.
- Auernik, K.S., Cooper, C.R. & Kelly, R.M., 2008. Life in hot acid: pathway analyses in extremely thermoacidophilic archaea. *Current Opinion in Biotechnology*, 19:445–453.
- Baker-Austin, C. & Dopson, M., 2007. Life in acid: pH homeostasis in acidophiles. *Trends in Microbiology*, 15:165–171.
- Baliga, N. S., Bjork, S. J., Bonneau, R. et al., 2004. Systems level insights into the stress response to UV radiation in the halophilic archaeon Halobacterium NRC-1. *Genome Research*, 14: 1025–1035.
- Blum, P., 2001. Archaea: Ancient Microbes, Extreme Environments and the Origin of Life. Academic Press, Waltham, USA.
- Blum, P., 2008. Archaea: new models for prokaryotic biology. Caister Academic Press, Norfolk, UK.
- Boonyaratanakornkit, B. B., Simpson, A. J., Whitehead, T. A. et al., 2005. Transcriptional profiling of the hyperthermophilic methanarchaeon *Methanococcus jannaschii* in response to lethal heat and non-lethal cold shock. *Environmental Microbiology*, 7: 789–797.

- Booth, I.R., Cash, P. & O'Byrne, C., 2002. Sensing and adapting to acid stress. Antonie van Leeuwenhoek, *International Journal of General and Molecular Microbiology*, 81:33–42.
- Bordo, D., & Bork, P., 2002. The rhodanese/Cdc25 phosphatase superfamily. Sequence-structure-function relations. *EMBO Reports*, 3:741-746.
- Boyd, E. S., Hamilton, T. L., Wang, J. et al., 2013. The role of tetraether lipid composition in the adaptation of thermophilic archaea to acidity. *Frontiers in Microbiology*, 4:1–16.
- Cabiscol, E., Tamarit, J. & Ros, J., 2000. Oxidative stress in bacteria and protein damage by reactive oxygen species. *International Microbiology*, 3: 3–8.
- Calhoun, L.N. & Kwon, Y.M., 2011. Structure, function and regulation of the DNA-binding protein Dps and its role in acid and oxidative stress resistance in *Escherichia coli*: A review. *Journal of Applied Microbiology*, 110: 375–386.
- Cannio, R., Fiorentino, G., Morana, A. et al., 2000. Oxygen: friend or foe? Archaeal superoxide dismutases in the protection of intra- and extracellular oxidative stress. *Frontiers in Bioscience*, 5:768-779.
- Carmel-Harel, O. & Storz, G., 2000. Roles of the glutathione- and thioredoxin-dependent reduction systems in the *Escherichia coli* and *saccharomyces cerevisiae* responses to oxidative stress. *Annual Review of Microbiology*, 54:439–461.
- Cavicchioli, R., 2006. Cold-adapted archaea. *Nature reviews. Microbiology*, 4, pp.331–343.
- Cavicchioli, R., Thomas, T. & Curmi, P.M., 2000. Cold stress response in Archaea. *Extremophiles: life under extreme conditions*, 4: 321–331.
- Coker, J. a, DasSarma, P., Kumar, J. et al., 2007. Transcriptional profiling of the model Archaeon *Halobacterium sp.* NRC-1: responses to changes in salinity and temperature. *Saline Systems*, 3:1-17.
- Conway de Macario, E. & Macario, A.J., 2000. Stressors, stress and survival: overview. *Frontiers in Bioscience*, 5: 780–786.
- Corcelli, A., 2009. The cardiolipin analogues of Archaea. *Biochimica et Biophysica Acta - Biomembranes*, 1788: 2101–2106.
- Cotter, P.D. & Hill, C., 2003. Surviving the Acid Test: Responses of Gram-Positive Bacteria to Low pH. *Microbiology and Molecular Biology Reviews*, 67: 429–453.
- Doldur, F., 2008. Heat Shock Response in *Thermoplasma Volcanium*: Cloning and Differential Expression of Molecular Chaperonin (Thermosome) Genes. MS Thesis, METU.
- Drăghici, S., 2012. Statistics and data analysis for microarrays using R and Bioconductor. CRC Press, Boca Raton, FL.

- n.d., 2010. Automated process for siRNA screening. *Qiagen Gene Expression Newsletter*, 15:1-7
- Eichler, J. & Adams, M.W.W., 2005. Posttranslational protein modification in Archaea. *Microbiology and molecular biology reviews*, 69: 393–425.
- Faguy, D., Bayley, D., Kostyukova, A. et al., 1996. Isolation and characterization of flagella and flagellin proteins from the thermoacidophilic archaea *Thermoplasma volcanium* and *Sulfolobus shibatae*. *Journal of Bacteriology*, 178: 902-905.
- Falciani, F., 2007. Microarray technology through applications. Cromwell Press, UK.
- Feder, M.E. & Hofmann, G.E., 1999. Heat-shock proteins, Molecular chaperones, and the Stress response: Evolutionary and Ecological Physiology. *Annual Review of Physiology*, 61: 243–282.
- Finkel, T. & Holbrook, N.J., 2000. Oxidants, oxidative stress and the biology of ageing. *Nature*, 408: 239–247.
- Foster, P.L., 2007. Stress-Induced Mutagenesis in Bacteria. *Crit Rev Biochem Mol Biol*, 42: 373–397.
- Garrett, R. A., & Klenk, H., 2007. Archaea: evolution, physiology, and molecular biology / edited by Roger A. Garrett and Hans-Peter Klenk. Malden, MA: Blackwell Pub.
- Garrido, C., Paul, C., Seigneuric, R. et al., 2012. The small heat shock proteins family: The long forgotten chaperones. *International Journal of Biochemistry and Cell Biology*, 44: 1588–1592.
- Gèohlmann, H., & Talloen, W., 2009. Gene expression studies using affymetrix microarrays. CRC Press, Ipswich, MA.
- Gerday, C., & Glansdorff, N., 2007. Physiology and biochemistry of extremophiles . ASM Press, Washington, D.C.
- Goodchild, A., Saunders, N. F. W., Ertan, H. et al., 2004. A proteomic determination of cold adaptation in the Antarctic archaeon, *Methanococoides burtonii*. *Molecular Microbiology*, 53: 309–321.
- Gupta, G. N., Srivastava, S., Khare, S. K. et al., 2014. Extremophiles: An Overview of Microorganism from Extreme Environment. *International Journal of Agriculture, Environment and Biotechnology*, 7, pp.371-380.
- Hartl, F.U., Bracher, A. & Hayer-Hartl, M., 2011. Molecular chaperones in protein folding and proteostasis. *Nature*, 475: 324–332.
- Heller, M.J., 2002. DNA microarray technology: devices, systems, and applications. *Annual review of biomedical engineering*, 4:129–153.

- Hengge, R., 2011. The General Stress Response in Gram-Negative Bacteria. In *Bacterial Stress Responses*, 2nd Edition, edited by Gisela Storz and Regine Hengge, 251–89. Washington,DC: ASM Press. doi:10.1016/j.tim.2014.12.006.
- Hengge-Aronis, R., 2002. Recent insights into the general stress response regulatory network in *Escherichia coli*. *Journal of Molecular Microbiology and Biotechnology*, 4: 341–346.
- Hoheisel, J.D., 2006. Microarray technology: beyond transcript profiling and genotype analysis. *Nature Reviews Genetics*, 7: 200–210.
- Hyndman, D., Bauman, D. R., Heredia, V. V. et al., 2003. The aldo-keto reductase superfamily homepage. *Chemico-Biological Interactions* 143: 621–631.
- Ideno, A., Furutani, M., Iba, Y. et al., 2002. FK506 binding protein from the hyperthermophilic archaeon *Pyrococcus horikoshii* suppresses the aggregation of proteins in *Escherichia coli*. *Applied and Environmental Microbiology*, 68: 464–469.
- Ilves, H., Hörak, R. & Kivisaar, M., 2001. Involvement of  $\sigma^S$  in starvation-induced transposition of *Pseudomonas putida* transposon Tn4652. *Journal of Bacteriology*, 183: 5445–5448.
- Iqbal, J. & Qureshi, S. a., 2010. Selective depletion of *Sulfolobus solfataricus* transcription factor E under heat shock conditions. *Journal of Bacteriology*, 192: 2887–2891.
- Irizarry, R. a, Hobbs, B., Collin, F. et al., 2003. Exploration, normalization, and summaries of high density oligonucleotide array probe level data. *Biostatistics*, 4: 249–264.
- Iwasaki, T., 2010. Iron-sulfur world in aerobic and hyperthermoacidophilic archaea *sulfolobus*. *Archaea*, 2010: 1-14.
- Jain, P. & Sinha, S., 2008. Neutrophiles: Acid Challenge and Comparison with Acidophiles. *The Internet Journal of Microbiology*, 7. Doi: 10.5580/1ee7
- Jones, T.H., 2012. Response of *Escherichia Coli* to Environmental Stress. In *Stress Response of Foodborne Microorganisms*, edited by Wong Hin Chung, 293–330. Nova Science Publishers.
- Kawashima, T., Amano, N., Koike, H. et al., 2000. Archaeal adaptation to higher temperatures revealed by genomic sequence of *Thermoplasma volcanium*. *Proceedings of the National Academy of Sciences of the United States of America*, 97: 14257–14262.
- Kocabiyik, S., & Ozel, H., 2007. An Extracellular-Pepstatin Insensitive Acid Protease Produced by *Thermoplasma volcanium*. *Bioresource Technology*, 98: 112–117. doi:10.1016/j.biortech.2005.11.016.

- Kocabiyik, S., & Aygar, S., 2012. Improvement of Protein Stability and Enzyme Recovery under Stress Conditions by Using a Small HSP (Tpv-HSP 14.3) from *Thermoplasma volcanium*. *Process Biochemistry*, 47:1676–83. doi:10.1016/j.procbio.2011.11.014.
- Kohen, R., & Nyska, A., 2002. Oxidation of Biological Systems: Oxidative Stress Phenomena, Antioxidants, Redox Reactions, and Methods for Their Quantification. *Toxicologic Pathology*, 30: 620-650.
- Kregel, K.C., 2002. Heat shock proteins: modifying factors in physiological stress responses and acquired thermotolerance. *Journal of applied physiology*, 92: 2177–2186.
- Krulwich, T. a, Sachs, G. & Padan, E., 2011. Molecular aspects of bacterial pH sensing and homeostasis. *Nature reviews Microbiology*, 9: 330–343.
- Kulaev, I. & Kulakovskaya, T., 2000. Polyphosphate and Phosphate Pump. *Annual Review of Microbiology*, 54: 709–734.
- Kültz, D., 2003. Evolution of the cellular stress proteome: from monophyletic origin to ubiquitous function. *The Journal of experimental biology*, 206: 3119–3124.
- Kültz, D., 2005. Molecular and evolutionary basis of the cellular stress response. *Annual review of physiology*, 67: 225–257.
- Lindquist, S., 1986. The Heat-Shock Response. *Annual Reviews*, 55: 1151–91.
- Lund, P., 2011. Insights into chaperonin function from studies on archaeal thermosomes. *Biochemical Society transactions*, 39: 94–98.
- Luo, H. & Robb, F.T., 2011. Thermophilic protein folding systems. In *Extremophiles handbook*. Springer, 583–599. Doi: 10.1007/978-4-431-53898-1
- Luo, H., Laksanalamai, P. & Robb, F.T., 2009. An exceptionally stable Group II chaperonin from the hyperthermophile *Pyrococcus furiosus*. *Archives of Biochemistry and Biophysics*, 486: 12–18.
- Maaty, W. S., Wiedenheft, B., Tarlykov, P. et al., 2009. Something Old, Something New, Something Borrowed; How the Thermoacidophilic Archaeon *Sulfolobus solfataricus* Responds to Oxidative Stress. *Plos ONE*, 4:1-17.
- Macario, A J., Lange, M., Ahring, B. K. et al., 1999. Stress genes and proteins in the archaea. *Microbiology and Molecular Biology Reviews*, 63: 923–967.
- Manjunath, K., Prasad, S., Kanagaraj, S. et al., 2013. International Journal of Biological Macromolecules Structure of SAICAR synthetase from *Pyrococcus horikoshii* OT3: Insights into thermal stability. *International Journal of Biological Macromolecules*, 53: 7-19.

- Martindale, J.L. & Holbrook, N.J., 2002. Cellular response to oxidative stress: Signaling for suicide and survival. *Journal of Cellular Physiology*, 192: 1–15.
- Maruyama, T. 1 & Furutani, M., 2000. Archaeal peptidyl prolyl cis-trans isomerases (PPIases). *Frontiers in Bioscience*, 5: 821–836.
- Maupin-Furlow, J.A., Heather L, W., Steven J, K. et al., 2000. Proteasomes in the archaea: from structure to function. *Frontiers in bioscience: a journal and virtual library*, 5: 837–865.
- Mèuller, H, & Roeder, T., 2006. Microarrays. Elsevier Academic Press, USA.
- Microarray-Based Gene Expression Analysis Low Input Quick Amp Labeling V6.6. Protocol. (2014). Retrieved January 23, 2015, from Agilent Technologies: [http://www.chem.agilent.com/library/usermanuals/Public/G4140-90040\\_GeneExpression\\_OneColor\\_6.7.pdf](http://www.chem.agilent.com/library/usermanuals/Public/G4140-90040_GeneExpression_OneColor_6.7.pdf)
- Microarray-Based Gene Expression Analysis Low Input Quick Amp Labeling V6.6. Protocol. (2014). Retrieved January 23, 2015, from Agilent Technologies: [http://www.chem.agilent.com/library/usermanuals/Public/G4140-90040\\_GeneExpression\\_OneColor\\_6.7.pdf](http://www.chem.agilent.com/library/usermanuals/Public/G4140-90040_GeneExpression_OneColor_6.7.pdf)
- Mojica, F. J. M., Cisneros, E., Ferrer, C. et al., 1997. Osmotically induced response in representatives of halophilic prokaryotes: The bacterium *Halomonas elongata* and the archaeon *Haloferax volcanii*. *Journal of Bacteriology*, 179: 5471–5481.
- Moran -Reyna, A., & Coker, J., 2014. The effects of extremes of pH on the growth and transcriptomic profiles of three haloarchaea. *F1000Research*, 3: 1-15.
- Morey, J. S., Ryan, J. C., & Van Dolah, F. M., 2006. Microarray validation: factors influencing correlation between oligonucleotide microarrays and real-time PCR. *Biological Procedures Online*, 8: 175–193
- Müller, V., Spanheimer, R., & Santos, H., 2005. Stress response by solute accumulation in archaea. *Current Opinion in Microbiology*, 8: 729–736.
- Nguyen, D. V, Arpat, a B., Wang, N. et al., 2002. DNA microarray experiments: biological and technological aspects. *Biometrics*, 58: 701–717.
- Nordberg, J., & Arnér, E. S., 2001. Reactive oxygen species, antioxidants, and the mammalian thioredoxin system. *Free Radical Biology & Medicine*, 31: 1287-1312.
- Padan, E., Bibi, E., Ito, M. et al., 2005. Alkaline pH homeostasis in bacteria: New insights. *Biochimica et Biophysica Acta - Biomembranes*, 1717: 67–88.
- Pedone, E., Bartolucci, S. & Fiorentino, G., 2004. Sensing and adapting to environmental stress: the archaeal tactic. *Frontiers in bioscience*, 9: 2909–2926.
- Perrochia, L., Guetta, D., Hecker, A. et al., 2013. Functional assignment of KEOPS/EKC complex subunits in the biosynthesis of the universal t6A tRNA modification. *Nucleic Acids Research*, 41: 9484–9499.

- Pflüger, K., Ehrenreich, A., Salmon, K. et al., 2007. Identification of genes involved in salt adaptation in the archaeon *Methanosarcina mazei* Gö1 using genome-wide gene expression profiling. *FEMS Microbiology Letters*, 277: 79–89.
- Pirkkala, L., Nykänen, P. & Sistonen, L., 2001. Roles of the heat shock transcription factors in regulation of the heat shock response and beyond. *The FASEB journal*, 15: 1118–1131.
- Platara, M., Ruiz, A., Serrano, R. et al., 2006. The transcriptional response of the yeast Na<sup>+</sup>-ATPase ENA1 gene to alkaline stress involves three main signaling pathways. *Journal of Biological Chemistry*, 281: 36632–36642.
- Preissler, S. & Deuerling, E., 2012. Ribosome-associated chaperones as key players in proteostasis. *Trends in Biochemical Sciences*, 37: 274–283.
- Reed, C. J., Lewis, H., Trejo, E. et al., 2013. Protein adaptations in archaeal extremophiles. *Archaea*, 2013:1–14.
- Richter, K., Haslbeck, M. & Buchner, J., 2010. The Heat Shock Response: Life on the Verge of Death. *Molecular Cell*, 40: 253–266.
- Rohlin, L., Trent, J. D., Salmon, K., Kim, U. et al., 2005. Heat Shock Response of *Archaeoglobus fulgidus*. *Journal of Bacteriology*, 187: 6046–6057.
- Rothschild, L.J. & Mancinelli, R.L., 2001. Life in extreme environments. *Nature*, 409: 1092–1101.
- Sadhale, P., Verma, J. & Naorem, A., 2007. Basal transcription machinery: Role in regulation of stress response in eukaryotes. *Journal of Biosciences*, 32: 569–578.
- Saibil, H., 2013. Chaperone machines for protein folding, unfolding and disaggregation. *Nature reviews. Molecular cell biology*, 14: 630–42.
- Saito, H. & Kobayashi, H., 2003. Bacterial responses to alkaline stress. *Science progress*, 86: 271–282.
- Salerno, V., Napoli, A., White, M. F. et al., 2003. Transcriptional response to DNA damage in the archaeon *Sulfolobus solfataricus*. *Nucleic Acids Research*, 31: 6127–6138.
- Santoro, M.G., 2000. Heat shock factors and the control of the stress response. *Biochemical Pharmacology*, 59: 55–63.
- Seckbach, J., 2000. Journey to diverse microbial worlds: Adaptation to exotic environments. Kluwer Academic, Dordrecht.
- Seegerer, A., Langworthy, T. A., & Stetter, K. O., 1988. *Thermoplasma acidophilum* and *Thermoplasma volcanium* sp. nov. from Solfatara Fields. *Systematic and Applied Microbiology*, 10: 161–171.

- Shigi, N., 2014. Biosynthesis and functions of sulfur modifications in tRNA. *Frontiers in Genetics*, 5: 1-11.
- Shockley, K., Ward, D., Chhabra, S. et al., 2003. Heat shock response by the hyperthermophilic archaeon *Pyrococcus furiosus*. *Applied and Environmental Microbiology*, 69: 2365-2371.
- Shukla, H.D., 2006. Proteomic analysis of acidic chaperones, and stress proteins in extreme halophile Halobacterium NRC-1: a comparative proteomic approach to study heat shock response. *Proteome science*, 4: 1-11.
- Siddiqui, K. S., & Thomas, T., 2008. Protein adaptation in extremophiles. Nova Biomedical Books, New York.
- Slonczewski, J. L., Fujisawa, M., Dopson, M. et al., 2009. Cytoplasmic pH Measurement and Homeostasis in Bacteria and Archaea. *Advances in Microbial Physiology*, 55: 1-79.
- Smith, D.M., Benaroudj, N. & Goldberg, A., 2006. Proteasomes and their associated ATPases: A destructive combination. *Journal of Structural Biology*, 156: 72-83.
- Söti, C. & Csermely, P., 2007. Protein stress and stress proteins: implications in aging and disease. *Journal of biosciences*, 32: 511-515.
- Strand, K. R., Sun, C., Li, T. et al., 2010. Oxidative stress protection and the repair response to hydrogen peroxide in the hyperthermophilic archaeon *Pyrococcus furiosus* and in related species. *Archives of Microbiology*, 192: 447-459.
- Tachdjian, S. & Kelly, R.M., 2006. Dynamic metabolic adjustments and genome plasticity are implicated in the heat shock response of the extremely thermoacidophilic archaeon *Sulfolobus solfataricus*. *Journal of Bacteriology*, 188: 4553-4559.
- Vabulas, R.M., Raychaudhuri, S., Hartl, H. et al., 2010. Protein Folding in the Cytoplasm and the Heat Shock Response. *Cold Spring Harbour Perspectives in Biology*, 2: 1-18.
- Viladevall, L., Serrano, R., Ruiz, A. et al., 2004. Characterization of the calcium-mediated response to alkaline stress in *Saccharomyces cerevisiae*. *Journal of Biological Chemistry*, 279: 43614-43624.
- Voet, D., & Voet, J., 2011. Biochemistry. J. Wiley & Sons, New York
- Vorob'eva, L.I., Khodzhaev, E.u., Novikova, T.M. et al., 2013. Antistress cross-effects of extracellular metabolites of bacteria, archaea, and yeasts: A review. *Applied Biochemistry and Microbiology*, 49: 323-332.
- Wang, H., Liang, Y., Zhang, B. et al., 2011. Alkaline stress triggers an immediate calcium fluctuation in *Candida albicans* mediated by Rim101p and Crz1p transcription factors. *FEMS Yeast Research*, 11: 430-439.

- Weinberg, M. V., Schut, G. J., Brehm, S. et al., 2005. Cold shock of a hyperthermophilic archaeon: *Pyrococcus furiosus* exhibits multiple responses to a suboptimal growth temperature with a key role for membrane-bound glycoproteins. *Journal of Bacteriology*, 187: 336–348.
- Wiegert, T., Versteeg, S. & Schumann, W., 2001. Alkaline shock induces the *Bacillus subtilis*  $\sigma^w$  regulon. *Molecular Microbiology*, 41: 59–71.
- Williams, E., Lowe, T. M., Savas, J. et al., 2007. Microarray analysis of the hyperthermophilic archaeon *Pyrococcus furiosus* exposed to gamma irradiation. *Extremophiles: Life under Extreme Conditions*, 11: 19–29
- Yasuda, M., Oyaizu, H., Yamagishi, a. et al., 1995. Morphological variation of new *Thermoplasma acidophilum* isolates from Japanese hot springs. *Applied and Environmental Microbiology*, 61: 3482–3485.
- Young, J. C., Agashe, V. R., Siegers, K. et al., 2004. Pathways of chaperone-mediated protein folding in the cytosol. *Nature Reviews Molecular Cell Biology*, 5: 781-791.
- Zhang, W., Culley, D. E., Nie, L. et al., 2006. DNA microarray analysis of anaerobic *Methanosarcina barkeri* reveals responses to heat shock and air exposure. *Journal of Industrial Microbiology and Biotechnology*, 33:784–790.



## APPENDIX A

### BUFFER SOLUTIONS AND COMPOSITIONS

#### **Tris-EDTA (TE) buffer**

- 10 mM Tris-Cl MW: 121.14 gram
- 1mM EDTA MW: 372.24 gram

#### **10 X FA gel buffer (pH = 7.0)**

- 200 mM MOPS M.W 209.26
- 50 mM Sodium acetate anhydrous M.W 82.03
- 10 mM EDTA M.W 372.24
- pH arrangement via NaOH

#### **1X FA gel running buffer**

- 100 mL 10X FA buffer
- 20 mL of 37 % formaldehyde
- Volume completed to 1000 ml with sterile water

#### **5X RNA loading buffer (5 mL)**

- 8  $\mu$ L Bromophenol blue M.W 669.99 g/mol
- 40  $\mu$ L EDTA . pH : 8.0
- 360  $\mu$ L 37 % formaldehyde
- 1 mL 100% glycerol M.W 92.09
- 1542  $\mu$ L formamide M.W 45.04
- 2 mL 10 X FA buffer
- Volume completed to 5 mL with sterile water



## APPENDIX B

### MICROARRAY DATA SETS

**Table B. 1. Up regulated genes upon heat shock**

Gene symbol	Description	Fold change
tvo_TVN0164	phosphoribosylaminoimidazole synthetase	6.3339586
tvo_TVN0167	Zn-dependent hydrolase	5.8601775
tvo_TVN1423	amino acid transporter	3.861244
tvo_TVN0161	hypothetical protein	3.555387
tvo_TVN0204	hypothetical protein	3.1894548
tvo_TVN1285	Zn-dependent hydrolase (AttM-related)	3.1551793
tvo_TVN0721	major facilitator superfamily permease	3.0404258
tvo_TVN1290	hypothetical protein	2.8179464
tvo_TVN0723	integrase/recombinase	2.8006592
tvo_TVN1128	molecular chaperone GroEL	2.74156
tvo_TVN1221	cationic amino acid transporter	2.7195563
tvo_TVN0885	hypothetical protein	2.665708
tvo_TVN1284	alcohol dehydrogenase	2.6638136
tvo_TVN0507	molecular chaperone GroEL	2.5780692
tvo_TVN1309	long-chain-fatty-acid--CoA ligase	2.5688524
tvo_TVN0678	integrase/recombinase	2.559215
tvo_TVN0489	molecular chaperone GrpE (heat shock protein)	2.4555843
tvo_TVN0683	hypothetical protein	2.4191287
tvo_TVN0766	hypothetical protein	2.4040132
tvo_TVN0206	ABC-type sugar transporter. permease component	2.345887
tvo_TVN0692	hypothetical protein; K07497 putative transposase	2.3302224
tvo_TVN1260	acetyl-CoA acetyltransferase	2.2782156
tvo_TVN1199	hypothetical protein	2.2549026
tvo_TVN0809	hypothetical protein	2.167447
tvo_TVN1190	ATP:corrinoid adenosyltransferase	2.162715
tvo_TVN1283	NAD-dependent aldehyde dehydrogenase	2.135254
tvo_TVN1173	hypothetical protein	2.127924
tvo_TVN0021	permease	2.1205702
tvo_TVN0216	major facilitator superfamily permease	2.1122842
tvo_TVN1224	amino acid transporter	2.074074
tvo_TVN0875	aldo/keto reductase	2.0717328
tvo_TVN1259	nucleic-acid-binding protein; K07068	2.0576336
tvo_TVN0670	acyl-CoA dehydrogenase	2.0345519

**Table B. 2. Down regulated genes upon heat shock**

<b>Gene symbol</b>	<b>Description</b>	<b>Fold change</b>
tvo_TVN1426	flagellin; K07325 archaeal flagellin FlaB	-4.0493426
tvo_TVNr03	7S ribosomal RNA	-3.9352822
tvo_TVN1236	single-stranded DNA-binding protein	-3.227925
tvo_TVN0147	hypothetical protein	-3.0724602
tvo_TVN1463	Type III restriction-modification enzyme. helicase subunit	-2.8969014
tvo_TVN0135	hypothetical protein	-2.7173774
tvo_TVN1464	adenine-specific DNA methylase	-2.6193733
tvo_TVN0361	hypothetical protein	-2.5878246
tvo_TVN0948	hypothetical protein	-2.569598
tvo_TVN0436	major facilitator superfamily permease	-2.5529466
tvo_TVN0472	transporter component; K07112	-2.4530427
tvo_TVN0476	transporter component; K07112	-2.4450614
tvo_TVN1422	transcription regulator	-2.433296
tvo_TVN0898	amino acid transporter	-2.422587
tvo_TVN0648	hypothetical protein	-2.4040933
tvo_TVN0642	hypothetical protein	-2.3135843
tvo_TVN1303	RNA helicase	-2.31082
tvo_TVN0830	rhodanese-related protein	-2.2874072
tvo_TVN0473	NAD(FAD)-dependent dehydrogenase	-2.2521586
tvo_TVN0226	major facilitator superfamily permease	-2.2494948
tvo_TVN0200	phosphoenolpyruvate carboxykinase	-2.232282
tvo_TVN0802	carbamoyl phosphate synthase small subunit	-2.2234113
tvo_TVN0430	glycosyltransferase	-2.1772559
tvo_TVN0699	hypothetical protein	-2.155174
tvo_TVN0611	flagellar protein G	-2.1532593
tvo_TVN0073	metal-binding protein containing	-2.148869
tvo_TVN1030	ubiquinone/menaquinone biosynthesis methylase	-2.1472476
tvo_TVN0900	dTDP-4-dehydrorhamnose reductase	-2.1405265
tvo_TVN0624	transcription regulator; K06024 segregation and condensation protein B	-2.109055
tvo_TVN0365	hypothetical protein	-2.1016128
tvo_TVN0255	major facilitator superfamily permease	-2.080928
tvo_TVN0547	cell wall biosynthesis glycosyltransferase	-2.0752919
tvo_TVN1428	GTP:adenosylcobinamide-phosphate guanylyltransferase	-2.0721602
tvo_TVN0869	cell wall biosynthesis glycosyltransferase	-2.0700428
tvo_TVN0546	ABC-type molybdate transporter. ATPase component	-2.0383818
tvo_TVN1405	hypothetical protein	-2.0345418
tvo_TVN1029	hypothetical protein	-2.018691

**Table B. 3. Up regulated genes upon pH stress**

<b>Gene symbol</b>	<b>Description</b>	<b>Fold change</b>
tvo_TVN0679	hypothetical protein	9.259897
tvo_TVN0300	hypothetical protein	8.871412
tvo_TVN0123	phosphate ABC transporter permease	8.444629
tvo_TVN0570	transcription initiation factor IIB	7.4190655
tvo_TVN0743	CoA-binding protein	5.367934
tvo_TVN1391	Iron-regulated ABC transporter ATPase subunit	4.6861687
tvo_TVN1389	iron-regulated ABC-type transporter	4.5355153
tvo_TVN1059	3-oxoacyl-ACP reductase	4.506952
tvo_TVN0502	nucleotide-binding protein (UspA-related)	4.472804
tvo_TVN1390	iron-regulated ABC-type transporter	3.9687636
tvo_TVN0844	hypothetical protein	3.5294735
tvo_TVN0990	lipoate-protein ligase A	3.2776887
tvo_TVN0406	transcription regulator	3.2614088
tvo_TVN1392	transcription regulator	3.2225828
tvo_TVN0243	formate dehydrogenase major subunit	2.947112
tvo_TVN1371	hypothetical protein	2.922826
tvo_TVN1600	KEOPS complex Cgi121-like subunit	2.8798144
tvo_TVN1393	aromatic ring hydroxylating enzyme	2.836307
tvo_TVN0932	Fe-S oxidoreductase	2.7070148
tvo_TVN0601	hypothetical protein	2.430845
tvo_TVN0214	hypothetical protein	2.2701213
tvo_TVN1272	transcription regulator	2.2695997
tvo_TVN0771	nicotinamidase-like amidase	2.2483032
tvo_TVN0494	ATP-dependent protease Lon	2.2447174
tvo_TVN0940	hypothetical protein	2.1615257
tvo_TVN1084	H/ACA RNA-protein complex component Gar1	2.1364763
tvo_TVN0991	lipoate-protein ligase	2.1304774
tvo_TVN0992	signal recognition particle protein Srp54	2.1294687
tvo_TVN1444	protein translocase subunit Sss1	2.0993354
tvo_TVN0961	hypothetical protein	2.0794842
tvo_TVN1238	amino acid transporter	2.0392191

**Table B. 4. Down regulated genes upon pH stress**

<b>Gene symbol</b>	<b>Description</b>	<b>Fold change</b>
tvo_TVN0784	benzoylformate decarboxylase	-3.0975
tvo_TVN1447	transcription regulator (HTH)	-2.8929
tvo_TVN0971	endonuclease IV	-2.5669
tvo_TVN0188	hypothetical protein	-2.5513
tvo_TVN0549	hypothetical protein	-2.5504
tvo_TVN0896	SAM-dependent methyltransferase	-2.5215
tvo_TVN0761	leuS; leucyl-tRNA synthetase	-2.2457
tvo_TVN1343	acyl-CoA dehydrogenase	-2.238
tvo_TVN0363	enoyl-CoA hydratase	-2.188
tvo_TVN1085	GTPase	-2.1628
tvo_TVN0643	hypothetical protein	-2.157
tvo_TVN0401	GTPase	-2.0696
tvo_TVN1088	GMP synthase subunit A	-2.0639
tvo_TVN1243	nicotinate phosphoribosyltransferase	-2.0631
tvo_TVN0555	30S ribosomal protein S8	-2.0578
tvo_TVN1247	30S ribosomal protein S3	-2.015

**Table B. 5. Up regulated genes upon 0.02 mM H<sub>2</sub>O<sub>2</sub>**

<b>Gene symbol</b>	<b>Description</b>	<b>Fold change</b>
tvo_TVN0875	aldo/keto reductase	6.3281455
tvo_TVN0700	hypothetical protein	5.1059875
tvo_TVN0932	Fe-S oxidoreductase	4.3284054
tvo_TVN0933	hypothetical protein	4.143364
tvo_TVN1417	hypothetical protein	3.9640193
tvo_TVN1442	hypothetical protein	3.9221864
tvo_TVN1441	RNA-binding protein	3.903748
tvo_TVN0695	site-specific recombinase. DNA invertase Pin-related	3.6939132
tvo_TVN1403	HD family phosphatase	3.6839373
tvo_TVN1444	protein translocase subunit Sss1	3.5955465
tvo_TVN1053	major facilitator superfamily permease	3.3735802
tvo_TVN1443	nusG; transcription antitermination protein	3.2496445
tvo_TVN0137	integrase/recombinase	3.1511188
tvo_TVN0437	RNA processing exonuclease	3.061458

"Table B.5 (Cont'd)"

<b>Gene symbol</b>	<b>Description</b>	<b>Fold change</b>
tvo_TVN0243	hypothetical protein	2.8777108
tvo_TVN0697	hypothetical protein	2.7734773
tvo_TVN0698	hypothetical protein	2.742115
tvo_TVN0701	hypothetical protein	2.7318938
tvo_TVN0080	hypothetical protein	2.62232
tvo_TVN0687	hypothetical protein	2.5479405
tvo_TVN1455	hydrogenase 4 subunit F	2.5404325
tvo_TVN0466	hypothetical protein	2.5285454
tvo_TVN0567	LysR family transcriptional regulator	2.5227954
tvo_TVN0314	RNA-binding protein	2.5160844
tvo_TVN0938	metal-dependent transcription regulator	2.4585133
tvo_TVN0011	translation initiation factor IF-6	2.4220777
tvo_TVN1178	translation initiation factor IF-1A	2.4130387
tvo_TVN0664	metal-dependent RNase	2.3956275
tvo_TVN0835	pyruvate:ferredoxin oxidoreductase. alpha subunit	2.3744462
tvo_TVN0834	2-oxoisovalerate-ferredoxin oxidoreductase. subunit delta (vorD);	2.3475394
tvo_TVN0136	integrase/recombinase	2.3419678
tvo_TVN1371	hypothetical protein	2.3417232
tvo_TVN0566	molybdopterin biosynthesis protein	2.327552
tvo_TVN0315	rRNA dimethyladenosine transferase	2.296004
tvo_TVN0285	arsenite transport permease	2.278184
tvo_TVN1023	anthranilate synthase component II	2.25591
tvo_TVN0311	pseudouridylate synthase	2.24976
tvo_TVN0696	ATPase AAA	2.233017
tvo_TVN0073	metal-binding protein containing	2.231977
tvo_TVN0063	phosphate permease	2.209709
tvo_TVN1600	KEOPS complex Cgi121-like subunit	2.198748
tvo_TVN1063	hypothetical protein	2.184655
tvo_TVN1458	hydrogenase 4 subunit B	2.16762
tvo_TVN1370	hypothetical protein	2.153594
tvo_TVN0470	thioredoxin reductase	2.150327
tvo_TVN0587	transposase	2.136803
tvo_TVN0589	cysteine synthase; K01738	2.078564
tvo_TVN1245	major facilitator superfamily permease	2.032442
tvo_TVN0097	Kef-type K <sup>+</sup> transporter NAD-binding component	2.011854

**Table B. 6. Repressed genes upon 0.02 mM H<sub>2</sub>O<sub>2</sub>**

<b>Gene symbol</b>	<b>Description</b>	<b>Fold change</b>
TVN0753	hypothetical protein	-2.2827759
TVN0612	flagellar accessory protein FlaH	-2.076817
TVN1316	aroB+ADs- 3-dehydroquinate synthase	-2.283477
TVN1125	5.10-methylenetetrahydrofolate reductase	-3.2116323
TVN0944	alcohol dehydrogenase	-2.477168
TVN0366	Rieske Fe-S protein	-3.1068769
TVN0096	2-phosphosulfolactate phosphatase	-2.1590924
TVN0401	GTPase+ADs- K06883	-2.2990625
TVN0574	SAM-dependent methyltransferase	-2.2659411
TVN1281	electron transfer flavoprotein subunit alpha	-2.4626677
TVN0381	hypothetical protein	-2.1192894
TVN0941	hypothetical protein	-3.3333707
TVN1279	ferredoxin-like protein	-2.9282713
TVN1098	ATPase	-2.1869361
TVN0496	aspartate aminotransferase	-2.9551208
TVN0495	cobS+ADs- cobalamin synthase	-2.1545277
TVN1123	methionine synthase	-2.267367
TVN0360	hypothetical protein	-3.0091798
TVN0160	nucleoid DNA-binding protein (HB-related)	-2.4983897
TVN1240	cation transport ATPase	-3.0452864
TVN1431	hypothetical protein	-2.1600156
TVN0965	inner membrane protein	-2.5695667
TVN0848	aspartate aminotransferase	-4.0065656
TVN0361	hypothetical protein	-2.1305645
TVN1492	glutamine synthetase	-2.1419435
TVN1278	dehydrogenase (flavoprotein)	-3.7301693
TVN0015	S-adenosylmethionine synthetase	-2.446484
TVN1427	transposase	-2.4829118
TVN0610	flagellar protein F	-2.3056114
TVN0998	pyridoxal biosynthesis lyase PdxS	-2.1118498
TVN1124	hypothetical protein	-2.3114514
TVN0740	metal-dependent carboxypeptidase	-2.719139
TVN0027	cell division protein FtsZ	-2.3073041
TVN1432	NAD(FAD)-dependent dehydrogenase	-2.0411212
TVN0676	formylmethanofuran dehydrogenase subunit	-2.0259914
TVN0363	enoyl-CoA hydratase	-2.2628715
TVN1249	hypothetical protein	-2.705495

**Table B. 7. Up regulated genes 0.03 mM H<sub>2</sub>O<sub>2</sub>**

<b>Gene symbol</b>	<b>Description</b>	<b>Fold change</b>
tvo_TVN1466	ATPase AAA	14.650864
tvo_TVN0875	aldo/keto reductase	12.841604
tvo_TVN1417	hypothetical protein	9.275651
tvo_TVN0150	hypothetical protein	8.418194
tvo_TVN1418	hypothetical protein	8.151483
tvo_TVN1053	major facilitator superfamily permease	6.109563
tvo_TVN1130	threonine dehydratase	6.0040436
tvo_TVN1441	RNA-binding protein	5.5618925
tvo_TVN0203	hypothetical protein	5.4854927
tvo_TVN1403	HD family phosphatase	5.3987565
tvo_TVN0933	hypothetical protein	5.374686
tvo_TVN0932	Fe-S oxidoreductase	5.287104
tvo_TVN0137	integrase/recombinase	5.163001
tvo_TVN0241	hypothetical protein	5.1347203
tvo_TVN0688	hypothetical protein	4.7118597
tvo_TVN1389	iron-regulated ABC-type transporter	4.673326
tvo_TVN0697	hypothetical protein	4.594512
tvo_TVN0700	hypothetical protein	4.198791
tvo_TVN0828	Mn <sup>2+</sup> transporter	4.1167827
tvo_TVN1442	hypothetical protein	4.072053
tvo_TVN1390	iron-regulated ABC-type transporter; K09014 Fe-S cluster as	4.068811
tvo_TVN0938	metal-dependent transcription regulator	3.9886093
tvo_TVN1600	KEOPS complex Cgi121-like subunit	3.9740424
tvo_TVN0660	DNA polymerase elongation subunit	3.8360016
tvo_TVN0835	pyruvate:ferredoxin oxidoreductase. alpha subunit	3.8318238
tvo_TVN1391	Iron-regulated ABC transporter ATPase subunit	3.7983294
tvo_TVN0303	phosphate ABC transporter permease	3.7834878
tvo_TVN1442	hypothetical protein	4.072053
tvo_TVN0567	LysR family transcriptional regulator	3.686283
tvo_TVN0437	RNA processing exonuclease	3.5582414
tvo_TVN1245	major facilitator superfamily permease	3.465444
tvo_TVN0097	Kef-type K <sup>+</sup> transporter NAD-binding component	3.443159
tvo_TVN0251	mercuric reductase	3.4413526

"Table B.7 (Cont'd)"

<b>Gene symbol</b>	<b>Description</b>	<b>Fold change</b>
tvo_TVN0834	2-oxoisovalerate-ferredoxin oxidoreductase. subunit delta (vorD)	3.1157918
tvo_TVN1193	hypothetical protein	3.0744157
tvo_TVN0915	enoyl-CoA hydratase	3.0729873
tvo_TVN0687	hypothetical protein	3.0639296
tvo_TVN1443	nusG; transcription antitermination protein	3.010268
tvo_TVN0465	restriction endonuclease S subunit fragment	3.0094273
tvo_TVN1370	hypothetical protein	2.9990945
tvo_TVN0698	hypothetical protein	2.9859536
tvo_TVN0695	site-specific recombinase. DNA invertase Pin-related	2.9302776
tvo_TVN0285	arsenite transport permease	2.8928962
tvo_TVN0315	rRNA dimethyladenosine transferase	2.8842425
tvo_TVN1251	transcription regulator	2.830143
tvo_TVN0243	hypothetical protein	2.8179874
tvo_TVN0599	DNA-binding protein	2.8046572
tvo_TVN1458	hydrogenase 4 subunit B	2.8008573
tvo_TVN0219	multidrug efflux permease	2.79145
tvo_TVN0566	molybdopterin biosynthesis protein	2.7772253
tvo_TVN1285	Zn-dependent hydrolase (AttM-related)	2.7694569
tvo_TVN0696	ATPase AAA	2.7678125
tvo_TVN1455	hydrogenase 4 subunit F	3.3932264
tvo_TVN1392	transcription regulator	3.3048747
tvo_TVN1393	aromatic ring hydroxylating enzyme	3.300864
tvo_TVN1083	tfb; transcription initiation factor IIB	3.2890532
tvo_TVN1143	sugar-binding protein	3.1649313
tvo_TVN1444	protein translocase subunit Sss1	3.1504838

**Table B. 8. Repressed genes upon 0.03 mM H<sub>2</sub>O<sub>2</sub>**

<b>Gene symbol</b>	<b>Description</b>	<b>Fold change</b>
tvo_TVNO848	aspartate aminotransferase	-9.258174
tvo_TVNO1125	5.10-methylenetetrahydrofolate reductase	-8.165158
tvo_TVNO946	hypothetical protein	-7.3729343
tvo_TVNO1405	hypothetical protein	-7.1240463
tvo_TVNO578	FKBP-type peptidylprolyl isomerase	-6.463184
tvo_TVNO860	hypothetical protein	-6.358281
tvo_TVNO401	GTPase	-6.153731
tvo_TVNO1349	chorismate mutase	-5.982682
tvo_TVNO603	transcription regulator (HTH)	-5.7824144
tvo_TVNO911	amino acid transporter	-5.5928216
tvo_TVNO740	metal-dependent carboxypeptidase	-5.103509
tvo_TVNO471	transcription regulator	-4.96975
tvo_TVNO381	hypothetical protein	-4.9362445
tvo_TVNO300	hypothetical protein	-4.916814
tvo_TVNO574	SAM-dependent methyltransferase	-4.8901668
tvo_TVNO1186	transcription regulator	-4.864136
tvo_TVNO027	cell division protein FtsZ	-4.83969
tvo_TVNO1280	electron transfer flavoprotein subunit beta	-4.8060193
tvo_TVNO115	hypothetical protein	-4.7522774
tvo_TVNO473	NAD(FAD)-dependent dehydrogenase	-4.7259564
tvo_TVNO877	Glycosyltransferase	-4.724846
tvo_TVNO890	acylaminoacyl peptidase	-4.678183
tvo_TVNO1123	methionine synthase	-4.664547
tvo_TVNO880	Glycosyltransferase	-4.6234417
tvo_TVNO956	phosphoheptose isomerase	-4.6134067
tvo_TVNO873	SAM-dependent methyltransferase	-4.550658
tvo_TVNO218	amino acid transporter	-4.509412
tvo_TVNO637	acyl-CoA hydrolase	-4.497277
tvo_TVNO910	proline iminopeptidase	-4.4677067
tvo_TVNO1082	phosphoserine phosphatase	-4.459461
tvo_TVNO1124	hypothetical protein	-4.455959
tvo_TVNO657	cell division GTPase	4.4508734
tvo_TVNO201	metal-dependent hydrolase related to alanyl-tRNA synthetase	-4.4407773
tvo_TVNO538	agmatinase	-4.391109
tvo_TVNO171	folate-dependent phosphoribosylglycinamide formyltransferase	-4.3534093
tvo_TVNO655	translation initiation factor IF-2 subunit beta	-4.3215504
tvo_TVNO762	pyruvoyl-dependent arginine decarboxylase	-4.3088894
tvo_TVNO788	hypothetical protein	-4.302997
tvo_TVNO1160	proline/betaine transport permease	-4.2768216
tvo_TVNO209	alpha-mannosidase	-4.2392383
tvo_TVNO802	carbamoyl phosphate synthase small subunit	-4.2049475
tvo_TVNO995	coiled-coil protein	-4.1809916
tvo_TVNO845	nicotinamide-nucleotide adenyltransferase	-4.156954
tvo_TVNO1073	hypothetical protein	-4.135316

"Table B.8 (Cont'd)"

<b>Gene symbol</b>	<b>Description</b>	<b>Fold change</b>
tvo_TVN0913	hypothetical protein	-4.0947676
tvo_TVN1004	Fe-S oxidoreductase	-4.017953
tvo_TVN0945	metal-dependent transcription regulator	-3.98688
tvo_TVN0231	3-hydroxyisobutyrate dehydrogenase	-3.9693232
tvo_TVN1240	cation transport ATPase	-3.9539835
tvo_TVN1090	aspC; aspartyl-tRNA synthetase	-3.943609
tvo_TVN0658	transcription regulator	-3.907418
tvo_TVN1360	metal-dependent amidohydrolase	3.8846166
tvo_TVN0941	hypothetical protein	-3.872039
tvo_TVN1162	transcription regulator (SlyA-related)	-3.854347
tvo_TVN0602	hypothetical protein	-3.8400128
tvo_TVN0355	rpl37e; 50S ribosomal protein L37	-3.8244548
tvo_TVN0899	dTDP-glucose pyrophosphorylase;	-3.8234968
tvo_TVN0812	N-methylhydantoinase A	-3.8154728
tvo_TVN0177	hypothetical protein	-3.809033
tvo_TVN0739	DNA helicase II helicase PcrA	-3.793055
tvo_TVN0498	RNA polymerase II complex ELP3 subunit	-3.7860172
tvo_TVN0865	transposase	-3.7678478
tvo_TVN0656	hypothetical protein	-3.7635126
tvo_TVN0996	asnC; asparaginyl-tRNA synthetase	-3.7428708
tvo_TVN1492	glutamine synthetase	-3.7300346
tvo_TVN1141	glycerol kinase	-3.7286503
tvo_TVN0929	Gluconolactonase	-3.6695998
tvo_TVN1286	hypothetical protein	-3.6468542
tvo_TVN1279	ferredoxin-like protein	-3.6085815
tvo_TVN0997	hypothetical protein	-3.5960584
tvo_TVN0529	dTDP-glucose pyrophosphorylase	-3.5837755
tvo_TVN0944	alcohol dehydrogenase	-3.5533874
tvo_TVN0943	molybdopterin/thiamine biosynthesis dinucleotide-utilizing protein	-3.544516
tvo_TVN1157	oxidoreductase	-3.520339
tvo_TVN0998	pyridoxal biosynthesis lyase PdxS	-3.4956844
tvo_TVN0292	Fe <sup>2+</sup> uptake regulation protein	-3.4735975
tvo_TVN0078	histidinol-phosphate aminotransferase	-3.4601953
tvo_TVN0364	DNA-binding protein	-3.434268
tvo_TVN0493	hypothetical protein	-3.4341488
tvo_TVN0017	enoyl-CoA hydratase	-3.41895
tvo_TVN1278	dehydrogenase	-3.4144826

## APPENDIX C

### AMPLIFICATION AND MELTING CURVES

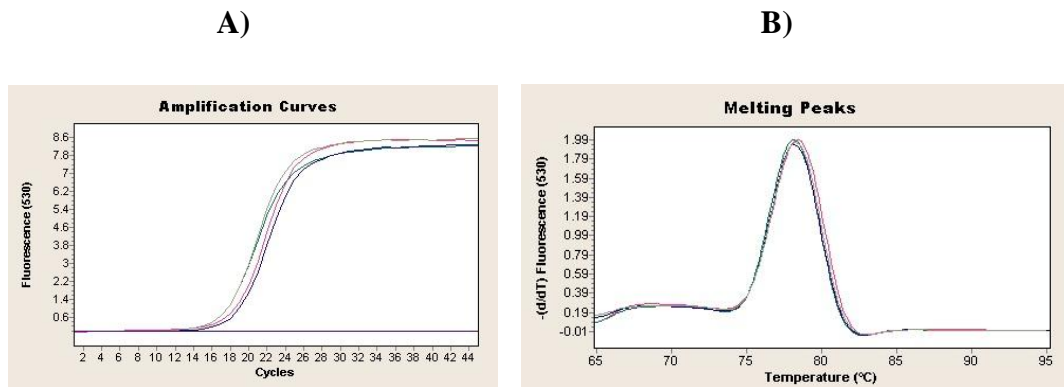


**Figure C. 1. Real time PCR amplification and melting curves for TVN0830 gene under heat shock, pH stress and oxidative stress. Amplification curve (A) and melting curve (B) (green - control, blue-pH stress, grey-oxidative, and pink - heat shock).**

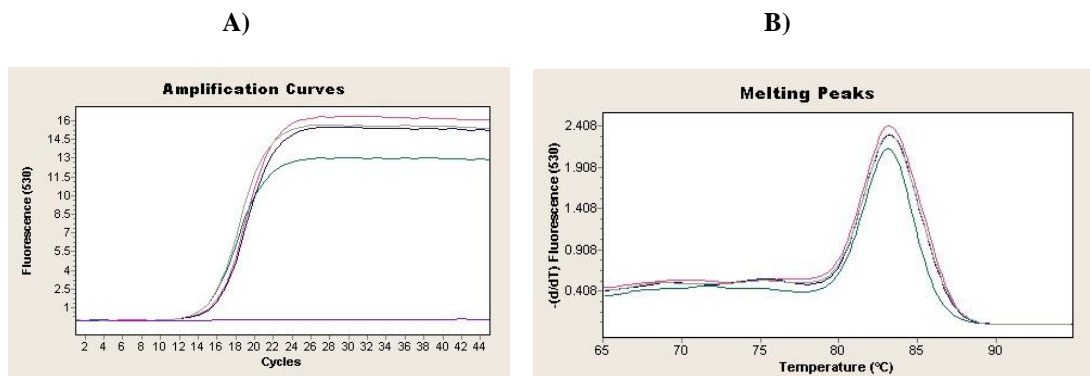


**Figure C. 2 Real time PCR amplification and melting curves for TVN1426 gene under heat shock, pH stress and oxidative stress. Amplification curve (A) and melting curve (B) (grey-control, dark blue - pH stress, light blue-heat shock, and pink - oxidative).**

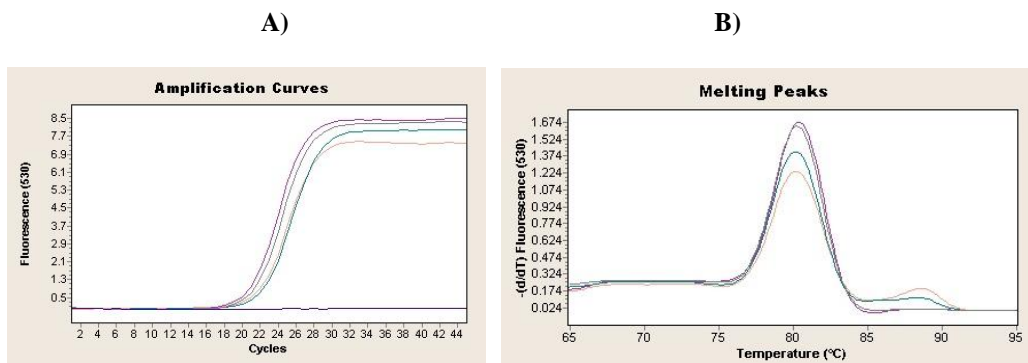


**Figure C. 3. Real time PCR amplification and melting curves for TVN1285 gene under heat shock, pH stress and oxidative stress. Amplification curve (A) and melting curve (B) (blue-control pink- pH stress, purple-heat shock, and grey - oxidative).**

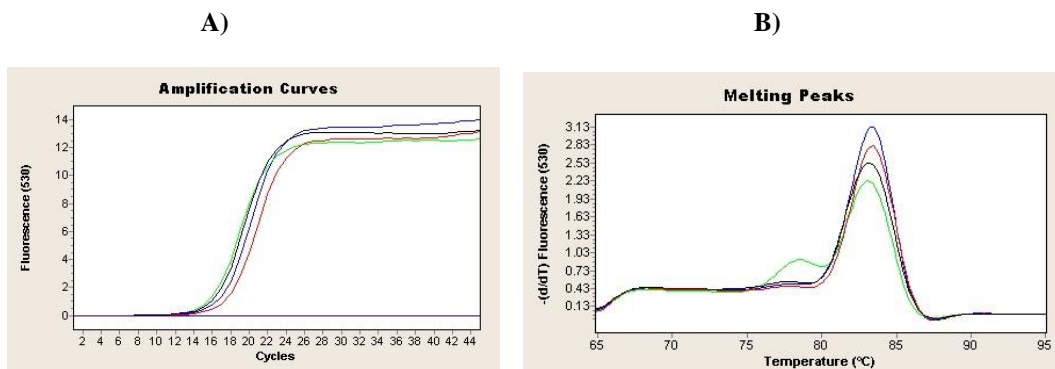


**Figure C. 4. Real time PCR amplification and melting curves for TVN1343 gene under heat shock, pH stress and oxidative stress. Amplification curve (A) and melting curve (B) (green-control, red - pH stress, blue-heat shock, and black - oxidative).**

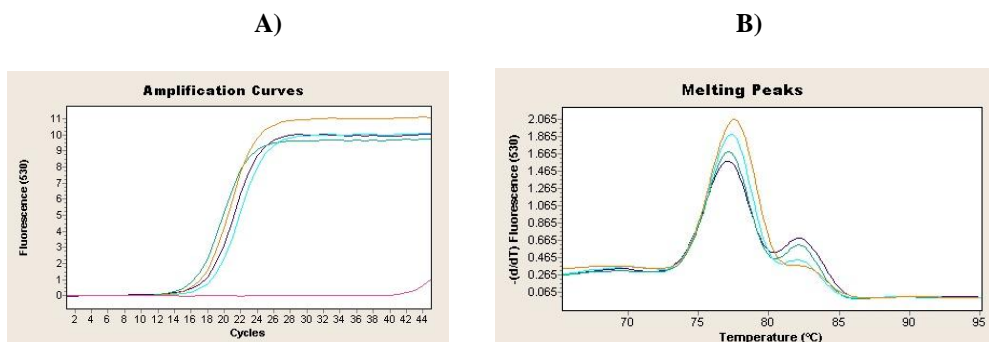


**Figure C. 5. Real time PCR amplification and melting curves for TVN0401 gene under heat shock, pH stress and oxidative stress. Amplification curve (A) and melting curve (B) (light blue-control, green - pH stress, brown- heat shock, and dark blue - oxidative).**

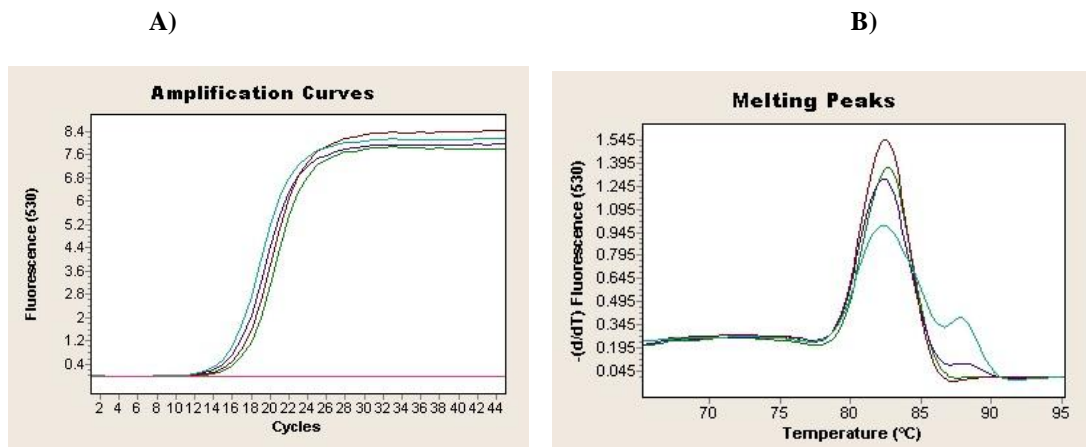


**Figure C. 6. Real time PCR amplification and melting curves for TVN0835 gene under heat shock, pH stress and oxidative stress.** Amplification curve (A) and melting curve (B) (blue- control, green - pH stress, light blue- heat shock, and dark red - oxidative).

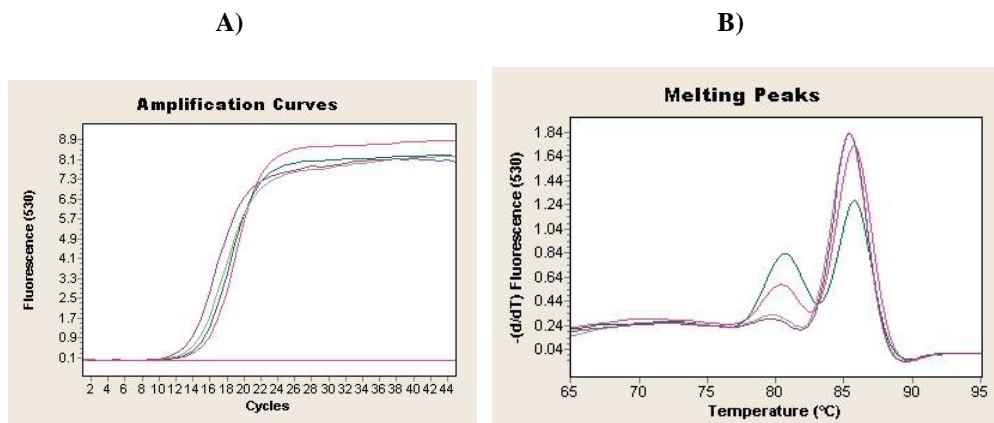


**Figure C. 7. Real time PCR amplification and melting curves for TVN1390 gene under heat shock, pH stress and oxidative stress.** Amplification curve (A) and melting curve (B) (grey- control, green - pH stress, light purple- heat shock, and pink - oxidative).

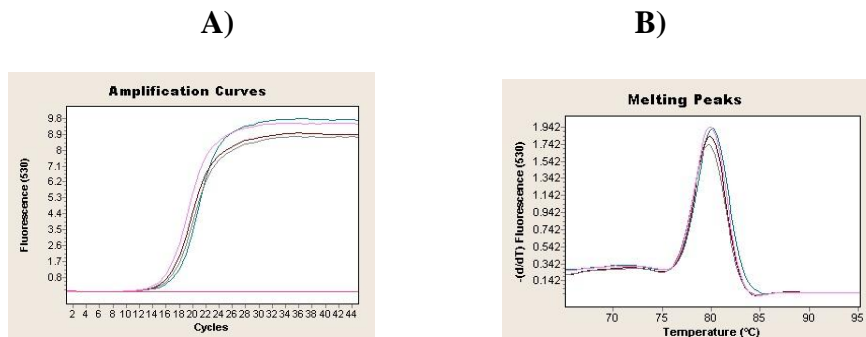


**Figure C. 8. Real time PCR amplification and melting curves for TVN1600 gene under heat shock, pH stress and oxidative stress.** Amplification curve (A) and melting curve (B) (grey- control, green - pH stress, light purple- heat shock, and pink - oxidative).

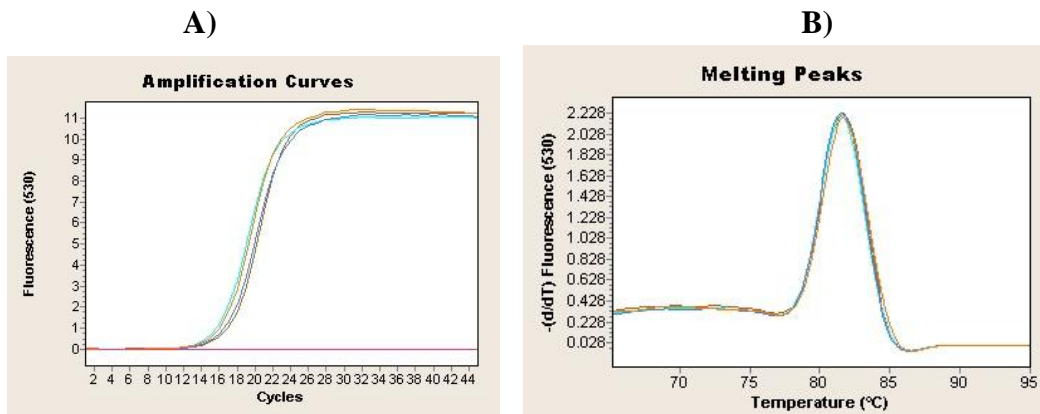


**Figure C. 9.** Real time PCR amplification and melting curves for TVN0021 gene under heat shock, pH stress and oxidative stress. Amplification curve (A) and melting curve (B) (red- control, blue - pH stress, green- heat shock, and yellow - oxidative).

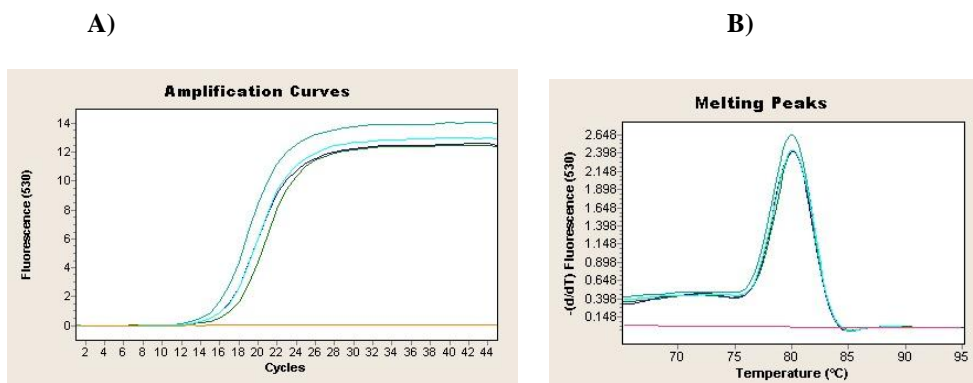


**Figure C. 10.** Real time PCR amplification and melting curves for TVN0123 gene under heat shock, pH stress and oxidative stress. Amplification curve (A) and melting curve (B) (green- control, light green - pH stress, blue - heat shock, and light blue -oxidative).

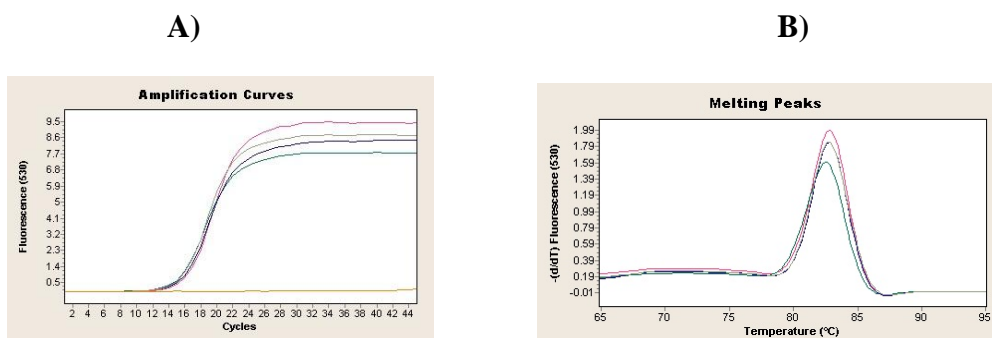


**Figure C. 11.** Real time PCR amplification and melting curves for TVN1392 gene under heat shock, pH stress and oxidative stress. Amplification curve (A) and melting curve (B) (light blue- control, purple - pH stress, grey - heat shock, and pink -oxidative).

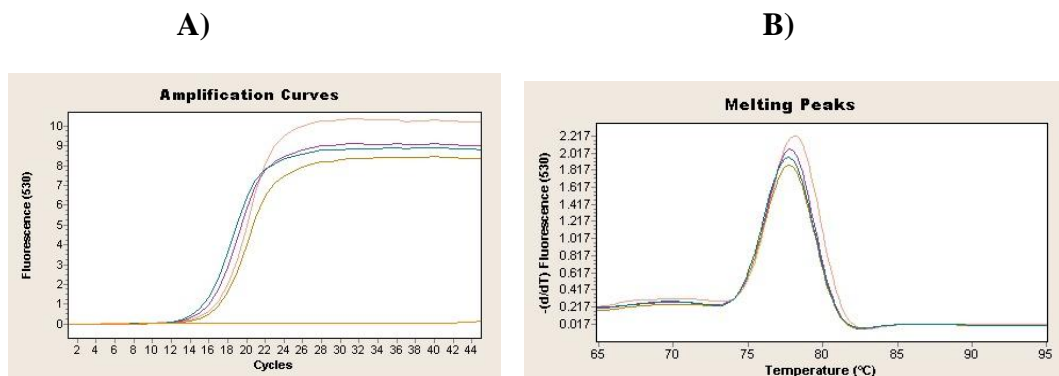


**Figure C. 12. Real time PCR amplification and melting curves for TVN1466 gene under heat shock, pH stress and oxidative stress.** Amplification curve (A) and melting curve (B) (light blue-control, yellow - pH stress, purple - heat shock, and light pink -oxidative).

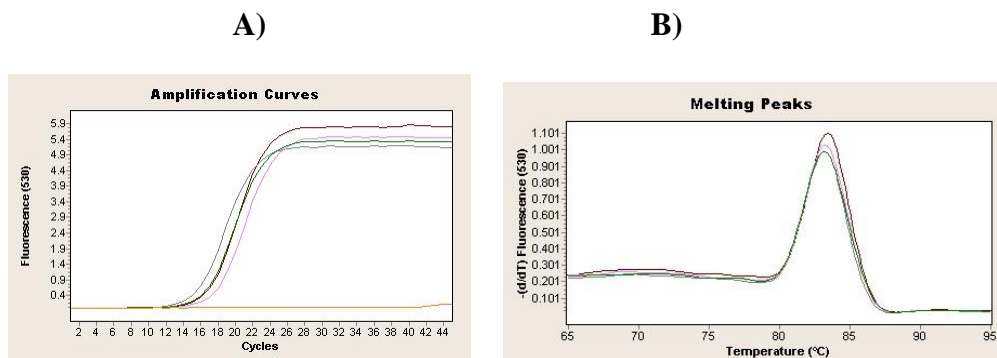


**Figure C. 13. Real time PCR amplification and melting curves for TVN1284 gene under heat shock, pH stress and oxidative stress.** Amplification curve (A) and melting curve (B) (green-control, grey - pH stress, red - heat shock, and light pink -oxidative).

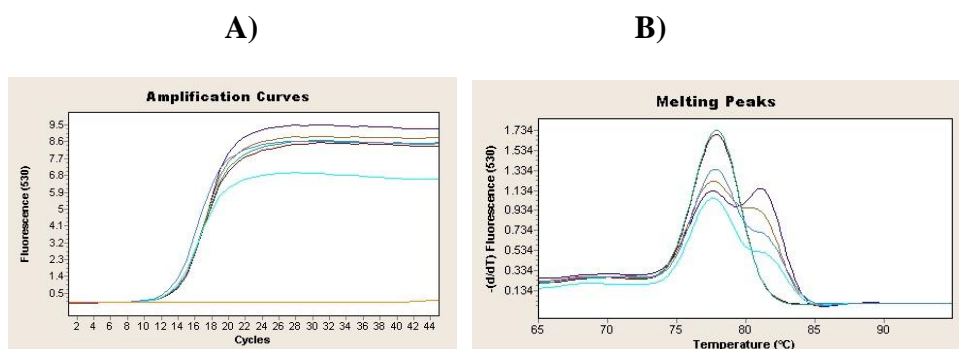


**Figure C. 14. Real time PCR amplification and melting curves for TVN0932 gene under heat shock, pH stress and oxidative stress.** Amplification curve (A) and melting curve (B) (red- control, blue- pH stress, light blue - heat shock, and brown -oxidative).

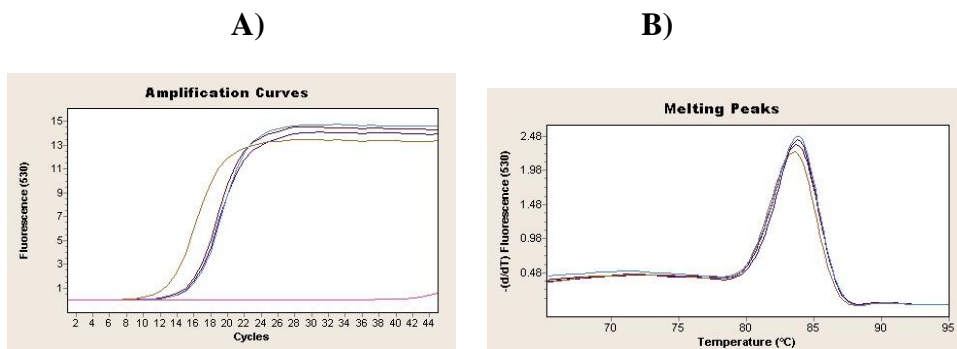


**Figure C. 15. Real time PCR amplification and melting curves for TVN0164 gene under heat shock, pH stress and oxidative stress. Amplification curve (A) and melting curve (B) (dark brown- control, grey- pH stress, light blue - heat shock, and blue -oxidative).**

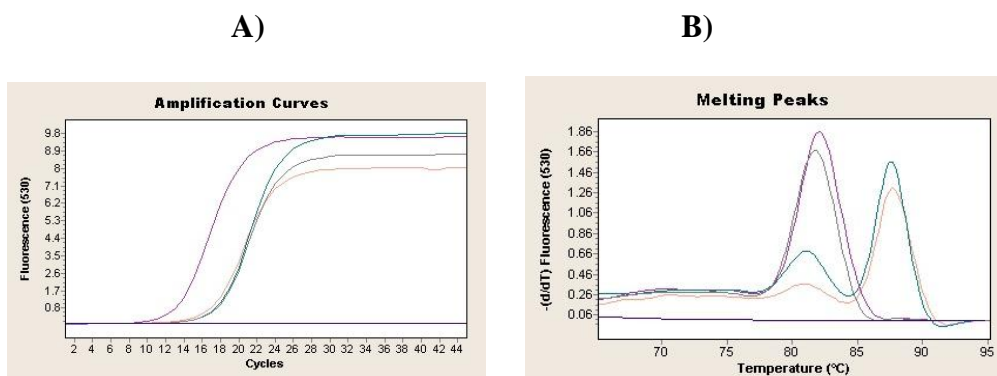


**Figure C. 16. Real time PCR amplification and melting curves for TVN0167 gene under heat shock, pH stress and oxidative stress. Amplification curve (A) and melting curve (B) (blue- control, light pink- pH stress, light purple- heat shock, and grey -oxidative).**

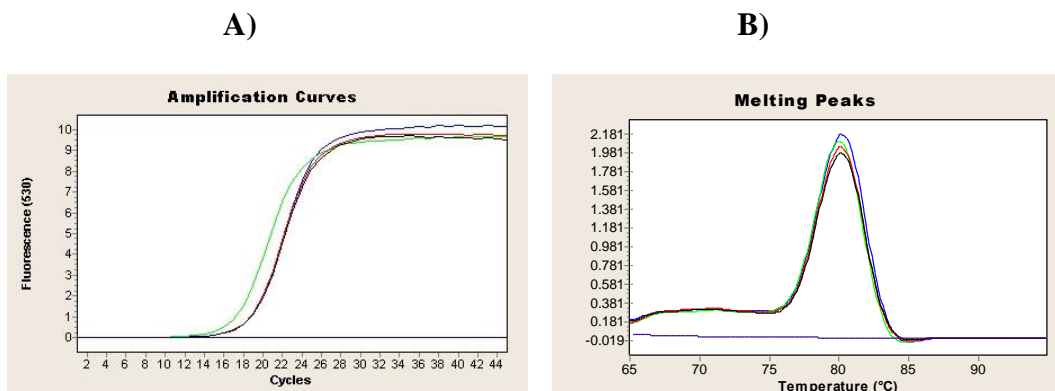


**Figure C. 17. Real time PCR amplification and melting curves for TVN0570 gene under heat shock, pH stress and oxidative stress. Amplification curve (A) and melting curve (B) (red- control, blue- pH stress, yellow- heat shock, and green -oxidative).**

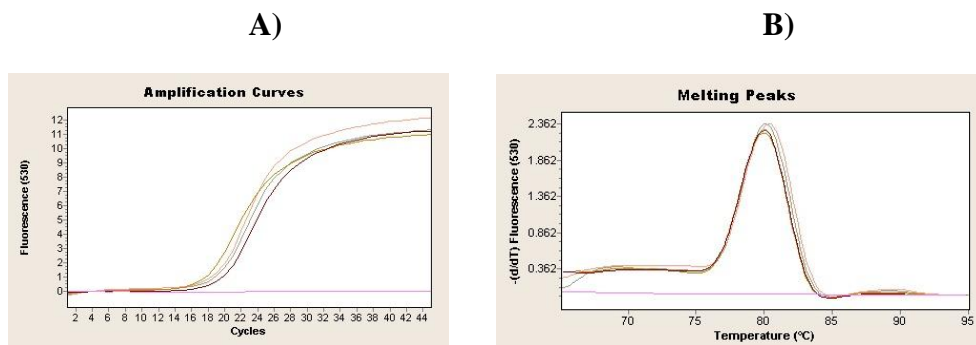


**Figure C. 18. Real time PCR amplification and melting curves for TVN0875 gene under heat shock, pH stress and oxidative stress. Amplification curve (A) and melting curve (B) (red- control, light pink- pH stress, light brown- heat shock, and purple -oxidative).**